Simulation and Modelling Techniques for Noise in Radio Frequency Integrated Circuits

by

Amit Mehrotra

B. Tech. (Indian Institute of Technology, Kanpur) 1994
M. S. (University of California at Berkeley) 1996

A dissertation submitted in partial satisfaction of the
requirements for the degree of
Doctor of Philosophy

in

Engineering-Electrical Engineering and Computer Sciences

in the

GRADUATE DIVISION
of the
UNIVERSITY of CALIFORNIA at BERKELEY

Committee in charge:

Professor Alberto L Sangiovanni-Vincentelli, Chair
Professor Robert K Brayton
Professor J George Shanthikumar

Fall 1999

The dissertation of Amit Mehrotra is approved:

Chair Date

Date

Date

University of California at Berkeley

1999

Simulation and Modelling Techniques for Noise in Radio Frequency Integrated Circuits

Abstract

Simulation and Modelling Techniques for Noise in Radio Frequency Integrated Circuits

by

Amit Mehrotra

Doctor of Philosophy in Engineering-Electrical Engineering and Computer Sciences

University of California at Berkeley

Professor Alberto L Sangiovanni-Vincentelli, Chair

In high speed communications and signal processing applications, random electrical noise that emanates from devices has a direct impact on critical high level specifications, for instance, system bit error rate or signal to noise ratio. Hence, predicting noise in RF systems at the design stage is extremely important. Additionally, with the growing complexity of modern RF systems, a flat transistor-level noise analysis for the entire system is becoming increasingly difficult. Hence accurate modelling at the component level and behavioural level simulation techniques are also becoming increasingly important. In this work, we concentrate on developing noise simulation techniques and mathematically accurate noise models at the component level. These models will also enable behavioural level noise analysis of large RF systems.

The difference between our approach of performing noise analysis for RF circuits and the traditional techniques is that we first concentrate on the noise analysis for oscillators instead of non-oscillatory circuits. As a first step, we develop a new quantitative description of the dynamics of stable nonlinear oscillators in presence of deterministic perturbations. Unlike previous such attempts, this description is not limited to two-dimensional system of equations and does not make any assumptions about the type of nonlinearity. By considering stochastic perturbations in a stochastic differential calculus setting, we obtain a correct mathematical characterization of the noisy oscillator output. We show that the oscillator output is the sum of two stochastic processes: a large signal stochastic process with Brownian motion phase deviation and a small "amplitude" noise process. We further show that

the response of the noisy oscillator is asymptotically wide-sense stationary with Lorentzian power spectral density. We also show that the second order statistics of this output are characterized by a single scalar constant. We present efficient numerical techniques both in time domain and in frequency domain for computing this constant. This approach also determines the relative contribution of the device noise sources to phase noise, which is very useful for oscillator design.

This new way of characterizing the oscillator output has a far-reaching impact on the noise analysis methodology for nonautonomous circuits, which we also investigate. We develop noise analysis techniques for nonautonomous circuits that are driven by a large single-tone periodic signal with phase noise. We formulate this problem as a stochastic differential equation and solve it in presence of white noise sources. We show that the output of a nonlinear nonautonomous circuit, in presence of input signal phase noise which has Brownian motion phase deviation, is asymptotically stationary. We also show that the Lorentzian spectrum of the input signal and the characteristics of the Brownian motion input phase deviation process are preserved at the output. We further show that the input signal phase noise contributes an additional wide-band amplitude noise term that appears as a white noise source modulated by the time derivative of the steady state response.

We also extend this analysis to circuits that are driven by more than one large periodic signal that are corrupted by phase noise. We show that, similar to the one tone case, the output of a nonautonomous circuit driven by two or more large tones is also asymptotically stationary. We show that phase noise of each input signal contributes one additional white noise source that is modulated by derivatives of the steady state response.

These models for autonomous and nonautonomous components of RF circuits will enable one to perform nonlinear noise simulation at the behavioural level for large RF systems. These models can also be used for behavioural level performance optimization and constraint generation for the RF components.

Professor Alberto L Sangiovanni-Vincentelli
Dissertation Committee Chair

To Ma and Pitaji

Contents

List of Figures **vii**

List of Tables **ix**

1 Introduction **1**
1.1 Architecture of an RF Front End . . . 2
1.2 Motivation . . . 6
1.2.1 Noise Sources in RF Transceiver . . . 6
1.2.2 Autonomous versus Nonautonomous Circuits . . . 8
1.3 Thesis Overview . . . 9

2 Overview of Existing Techniques **11**
2.1 Perturbation Analysis of a Nonoscillatory System . . . 11
2.2 Noise Analysis of Nonoscillatory Systems . . . 13
2.2.1 LPTV Approaches and Extensions . . . 14
2.2.2 Time Domain Analysis . . . 15
2.2.3 Our Approach . . . 15
2.3 Oscillator Phase Noise Analysis . . . 16
2.3.1 LTI/LTV Noise Analysis . . . 16
2.3.2 Timing Jitter Analysis . . . 17
2.3.3 Time Domain Noise Analysis . . . 18
2.3.4 Other Approaches . . . 18
2.3.5 Our Approach . . . 19

3 Perturbation Analysis of Stable Oscillators **20**
3.1 Mathematical Preliminaries . . . 20
3.2 Perturbation Analysis Using Linearization . . . 23
3.2.1 Floquet Theory . . . 24
3.2.2 Response to Deterministic Perturbation . . . 28
3.2.3 Response to Stochastic Perturbation . . . 30
3.3 Nonlinear Perturbation Analysis for Phase Deviation . . . 31
3.4 Example . . . 38
3.4.1 The van der Pol Oscillator . . . 38
3.4.2 Forced van der Pol Oscillator Equation . . . 41

3.4.3 Perturbation Analysis of the Forced van der Pol Oscillator 43

4 Noise Analysis of Stable Oscillators 51
4.1 Stochastic Characterization of Phase Deviation 51
4.1.1 Kramers-Moyal Expansion and Fokker-Planck Equation 53
4.1.2 Solution of the Phase Deviation Equation 58
4.2 Spectrum of Oscillator Output with Phase Noise 65
4.3 Phase Noise Characterization for Oscillator 70
4.3.1 Single-Sided Spectral Density and Total Power 70
4.3.2 Spectrum in dBm/Hz 71
4.3.3 Single-Sideband Phase Noise Spectrum in dBc/Hz 71
4.3.4 Timing Jitter 72
4.4 Noise Source Contribution 73
4.5 Numerical Techniques for Phase Noise Characterization 74
4.5.1 Time Domain Technique 74
4.5.2 Frequency Domain Technique 76
4.6 Examples 80
4.6.1 Generic Oscillator 80
4.6.2 LC Tank Oscillator 82
4.6.3 Ring Oscillator 84
4.6.4 Relaxation Oscillator 86

5 Noise Analysis of Nonautonomous Circuits 89
5.1 Mathematical Preliminaries 90
5.2 Cyclostationary Approach 91
5.3 Response of a Noiseless Circuit to Input Signal Phase Noise 92
5.4 Extension to General Noise Analysis 97
5.5 Amplitude Noise Characterization of Oscillators 99
5.6 Modification to Existing Noise Analysis Techniques 101
5.6.1 Time-Domain Technique 103
5.6.2 Frequency-Domain Technique 104
5.6.2.1 Noise Propagation Through Linear Time-Varying System . 104
5.6.2.2 Evaluation of System Transfer Function 108
5.7 Examples 111
5.7.1 Passive Mixer 111
5.7.2 Active Mixer 113

6 Noise Analysis of Circuits with Multitone Inputs 115
6.1 Mathematical Preliminaries 116
6.2 Spectrum of Nonlinear Mixing of Two Tones 117
6.3 Multirate Analysis of Circuits with Multitone Excitations 119
6.4 Noise Analysis of Circuits Driven by Multitone Excitations 125
6.5 Numerical Techniques 132
6.5.1 Propagation of Noise Through a Liner Quasi-Periodic Time Varying System 133

6.5.2 Derivation of the Form of Transfer Function 137
6.6 Examples 140

7 Conclusions and Future Directions **143**
7.1 Conclusions 143
7.2 Noise Models for Circuits Driven by Multitone Excitations 144
7.3 Extensions to Non-White Noise Sources 145
7.4 Behavioural Level Noise Simulation 146

Bibliography **147**

A Definitions and Solution Techniques of SDEs **157**
A.1 Mathematical Preliminaries 157
A.2 Itô Integrals 159
A.3 Stochastic Differential Equations 162

List of Figures

1.1 Block diagram of an RF transceiver front-end . . . 2
1.2 Future high integration RF front-end . . . 5
1.3 Effect of oscillator phase noise on blocking performance . . . 9

2.1 LTI noise analysis of a three stage ring oscillator . . . 16
2.2 Timing jitter analysis of a three stage ring oscillator . . . 17

3.1 Response of an orbitally unstable oscillator . . . 22
3.2 Limit cycle and excursions due to perturbations . . . 32
3.3 Phase deviation $\alpha(\tau)$ of the forced van der Pol oscillator . . . 49
3.4 Exact ($z(\tau)$) and phase shifted ($x_s(\tau+\alpha(\tau))$) response of the forced van der Pol oscillator . . . 50

4.1 Power spectral density of noisy oscillator output . . . 69
4.2 Power spectral density around the first harmonic . . . 70
4.3 Oscillator with a band-pass filter and a comparator . . . 80
4.4 Phase noise characterization for the generic oscillator . . . 81
4.5 Colpitt's Oscillator . . . 83
4.6 $v_1^T(t)D(x_s(t))D^T(x_s(t))v_1(t)$ for the Colpitt's oscillator . . . 83
4.7 Oscillator with on-chip inductor . . . 85
4.8 $v_1^T(t)D(x_s(t))D^T(x_s(t))v_1(t)$ for oscillator with on-chip inductor . . . 86
4.9 Ring oscillator delay cell . . . 87
4.10 Ring-oscillator phase noise performance versus emitter bias current . . . 87

5.1 Block diagram of a mixer with input and output signal frequencies . . . 101
5.2 Four Diode Mixer . . . 111
5.3 Increase of mixer noise figure with phase noise of the local oscillator (LO) signal for the passive mixer with 2% offset in the center tap of the output inductor . . . 112
5.4 Gilbert cell based mixer . . . 113
5.5 Increase of mixer noise figure with phase noise of the local oscillator (LO) signal for the Gilbert cell mixer . . . 114

6.1 $x(t)$ representation of the output of a four diode mixer . . . 125

6.2 $\tilde{x}(t)$ representation of the output of a four diode mixer 126
6.3 Illustration of the AFM method for a box truncation scheme with two incommensurable frequencies 137
6.4 Increase in noise figure due to phase noise in the two input signal for the four diode mixer 141
6.5 Increase in noise figure due to phase noise in the two input signal for the Gilbert cell mixer 141

List of Tables

4.1 Noise source contribution for the Colpitt's oscillator for two different base resistance values 84
4.2 Noise Source Contribution for oscillator with on-chip inductor 85
4.3 Phase noise characterization of the ring oscillator 88

Acknowledgements

Professional Acknowledgements

I am grateful to my research advisor Prof. Alberto Sangiovanni-Vincentelli for the constant support and guidance he provided me throughout this project. His breadth of knowledge has never ceased to amaze me. I am also grateful to Prof. Brayton and Prof. Shanthikumar for providing useful feedback for this dissertation.

The initial part of this work was done when I was interning at Bell Laboratories in the summer of 1997. I am grateful to Alper Demir and Jaijeet Roychowdhury for working with me in that duration. Throughout this project I had very fruitful discussions with Peter Feldmann, Roland Freund, David Long, Edoardo Charbon, Iason Vassiliou, Manolis Terrovitis, Ali Niknejad, Prof. Venkat Anantharam, Prof. James Demmel and Prof. Beresford Parlett. I would like to take this opportunity to express my gratitude to them.

During the course of my stay at Berkeley I had a chance to interact with many distinguished faculty members. The educational and research atmosphere here helped me nurture and sustain my enthusiasm for research in many areas of Electrical Engineering. I had a chance to work with Prof. Robert Brayton, Prof. Richard Newton and Prof. Kurt Keutzer during the NEXSIS project and I thoroughly enjoyed the experience. I also had a chance to work on research projects with Prof. Theodore Van Duzer, Prof. Randy Katz and Prof. Chenming Hu and it turned out to be a learning experience.

I would like to thank my co-authors in various research publications I have undertaken, for putting up with my idiosyncrasies. Shaz Qadeer, Vigyan Singhal and Rajeev Ranjan helped me with my initial publications and helped me gain confidence. I also enjoyed working with Ali Niknejad, Luca Carloni and Wilsin Gosti on various projects.

I would like to take this opportunity to thank Brad Krebs and Judd Reiffin for putting together an exceptional computing environment. Gratitude is also due to Ken Yamaguchi, Philip Chong and Wilsin Gosti for helping me administer my Linux desktop.

Finally I would like to express my sincere gratitude to Prof. Donald Knuth, Leslie Lamport, Prof. Timothy VanZandt and thousands of developers of TEX and LATEX for providing a document preparation system which allowed me to express my ideas succinctly and with clarity. I would also like to thank Linus Torvalds and thousands of developers of Linux, which allowed me to test out my ideas on a desktop without being a burden to other group members. I hope I can contribute to both these noble endeavours in the future.

Personal Acknowledgements

Berkeley provided me a chance to interact with people of diverse social, cultural, ethnic and economic backgrounds. My Berkeley stay has therefore been a learning experience for me in more than one sense of the word. I had known Alok and Shaz from my undergraduate days. Berkeley gave me chance to make new friends: Kaustav, Gurmeet, Luca Carloni, Sriram Rajamani, Marco, Rajeev Murgai, Wilsin, Rizwan, Premal, Tanvi, Ashwin, Pramod just to name a few. Hiking was my favourite hobby and Gurmeet and Ashish gave me very pleasant company while humbling the likes of Mt. Shasta, Mt. Lassen and Half Dome. Edoardo's delicatessen and dinners were always something to look forward to. I will be indebted to Sriram Krishnan for constantly reminding me of my roots, my culture and Hindutva and that I should be proud of it. Amit Narayan constantly amazed me with his ability to judge other people and projects with uncanny accuracy. Andreas Kühlmann's work ethics and outlook towards research have also impressed me a lot.

Finally, I would like to thank Pink Floyd whose music resonated the whole range of human emotions, both positive and not-so-positive (in my case, predominantly later) that one experiences during the course of the initial years of adulthood and provided solace and commiseration in the deepest, darkest moments during my five years of stay at Berkeley.

We do not expect someone (in research) to come in each day and prove four lemmas, two theorems and a corollary before lunch.

– *Ronald L Graham [Ber84]*

Chapter 1

Introduction

With the explosive growth of the communication market in the past few years, mobile personal communication devices have become extremely popular. The primary design effort in this area has been to lower the cost and power dissipation of these systems. Lower power dissipation directly translates into longer battery life, which is very critical for such applications. Another area of interest is to design systems that can conform to multiple standards. This gives rise to interesting challenges in terms of designing different components in this system and the design of entire system itself. Understanding the impact of electronic devices and the underlying process technology limitations on the design of components and the overall system is an important aspect of the design process. These systems are popularly known as radio frequency (RF) or infrared (IR) systems depending on the frequency of operation.

Radio frequency normally refers to the range of frequencies at which the signal is transmitted and received in such a system. Modern RF systems typically operate in 900 MHz to 2.4 GHz frequency range. For IR systems the frequency range is much higher. Design of a complex circuit operating at such frequencies is a challenging problem. In this thesis we address the problem of predicting the performance of RF systems in the presence of *noise*. By noise we mean any undesired signal that corrupts the signal of interest. Noise performance in such systems needs to be predicted both at the individual component level and also at the system level. In this work we address the problem of predicting noise and developing noise models at the component level which can be used in a system level noise simulation technique. We begin by discussing the architecture of a typical present day RF system and also discuss what a future RF system is predicted to look like. We indicate

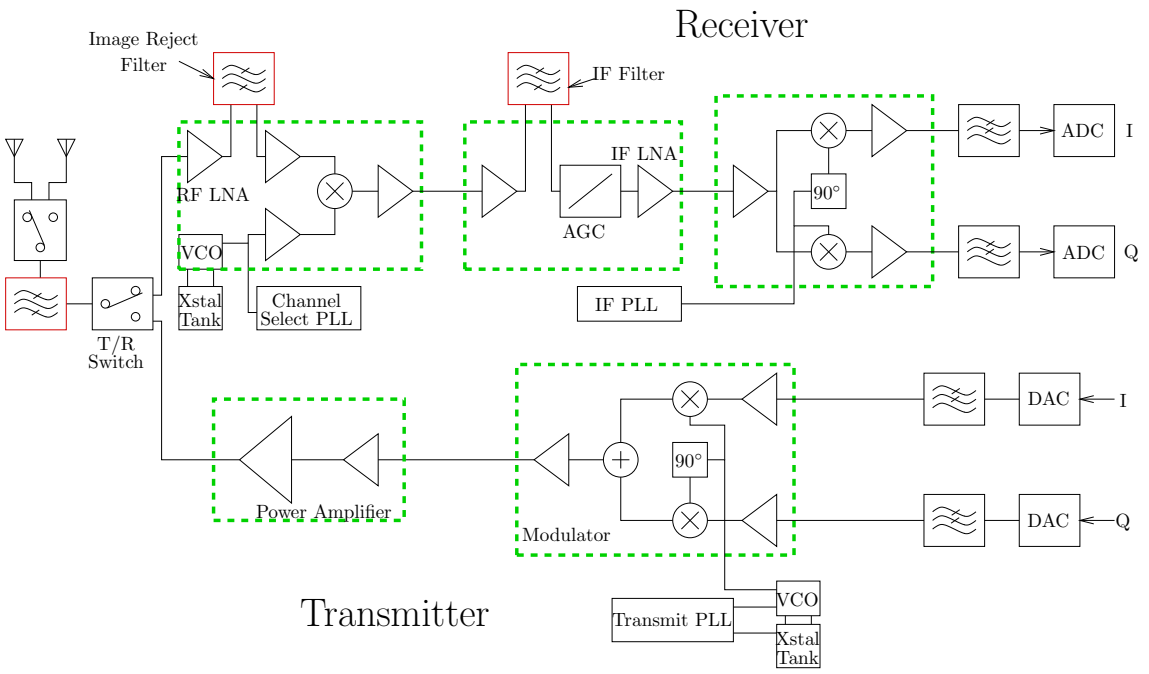

Figure 1.1: Block diagram of an RF transceiver front-end

some of the challenges that are present in designing a complex, multi-standard RF system at very high frequency ranges. We then motivate the problem of performing *noise analysis* in such systems, both at the component level and at the system level. We also provide a brief outline of this thesis.

1.1 Architecture of an RF Front End

The block diagram of the front end of an RF system is given in Figure 1.1 [GM95]. The front end consists of both the transmitter and the receiver part of the RF system. An input signal from the antenna is first filtered using a band-pass filter to reject any out-of-band noise. This signal, which is typically very small (few tens of microwatts to few milliwatts) is amplified by a low noise amplifier (LNA) which typically provides a power gain of about 10dB. This also reduces the noise contribution from subsequent mixing and amplification stages of the receiver. Let the frequency of this received signal be denoted by f_{RF}. The RF signal is frequency-shifted to base band before information can be retrieved from the signal. This frequency-shifting, or *downconversion* typically happens in more

than one stage. This is due to the fact that the frequency of the received signal is of the order of few gigahertz whereas the base band signal has bandwidth of a few kilohertz which makes downconversion in one stage very expensive. Input RF signal is mixed with a large local oscillator signal of frequency f_{LO} and gets downconverted to a fixed intermediate frequency signal f_{IF} where $f_{IF} = |f_{RF} - f_{LO}|$. This allows channel selection filtering and gain control at lower frequencies where high quality factor (Q) filters and variable gain amplifiers can be realized economically [FM99]. By varying the frequency of the local oscillator signal, channels at different frequency band can be downconverted to the same intermediate frequency. By the very nature of the process of downconversion, input signals of frequency $2f_{LO} - f_{RF}$, called the *image* frequency, also get downconverted to the same intermediate frequency. Hence the RF mixer is preceded by a band-pass filter, called the *image-reject* filter, which rejects the signals at the image frequency. This is usually a ceramic filter which is implemented off chip. Since the LNA and the RF mixer operate at RF frequencies, they are implemented on a separate chip using Gallium Arsenide or specialized high speed bipolar technology.

The intermediate frequency signal is amplified and filtered to remove any signal outside the desired band. Since the intermediate frequency of a typical RF system is fixed, the IF filter need not be tunable and hence can be implemented with an extremely sharp cutoff. Surface acoustic wave (SAW) filters are typically used for this purpose. The filtered signal is mixed with the IF local oscillator signal and both the in-phase and quadrature components of the signal get downconverted to base band. These are filtered using a low pass filter to remove any undesired high frequency signal which would be *folded* to base band during the subsequent sampling and digitization. The intermediate frequency range is in few tens of megahertz and typically these circuits are implemented in standard BiCMOS or CMOS technology.

In the transmit path, the in-phase and quadrature signals are upconverted to RF frequency using a transmit phase lock loop (PLL). This signal is amplified using a power amplifier before it drives the antenna. Due to power levels required and frequency of operation, the upconversion mixer and the power amplifier are implemented on separate chips using Gallium Arsenide or specialized high speed bipolar technology.

This architecture usually is implemented in four or five different chips which use several different technologies, ranging from Gallium Arsenide and high speed bipolar to digital CMOS technology. It also consists of some off chip ceramic and SAW filters. This

increases the power consumption and cost of the overall system. Every time an RF signal is driven off chip, the output stage needs to drive the impedance of the lines on a PC board which is typically 50Ω. This incurs extra power dissipation. Hence to increase battery life, the trend in current RF designs is to minimize the number of times high frequency signals need to be driven off chip. This is achieved by integrating more and more components at radio and intermediate frequency of both the transmitter and the receiver on the same silicon die. For designing RF systems which can be used for multiple standards, it is also desirable to digitize the signal at as high a frequency as possible and perform IF downconversion and other signal processing steps in the digital domain. With scaling of digital CMOS technology, the digital portions of RF circuits are getting faster, which also enables intermediate frequency operations to be performed in the digital domain. The block diagram of a future, highly integrated RF transceiver is shown in Figure 1.2 [GM95]. In such an architecture, the number of off chip elements is very small. The main objective is to replace the functions traditionally implemented by high performance, high-Q discrete components with integrated on-chip solutions [RON+98]. For instance, noise and image rejection is performed using active components and channel-select synthesizer is realized using on-chip active and passive components.

A direct consequence of this high integration is that the number of active and passive devices, not just in the RF portion of the system, but also the signal path is increasing. Unlike the digital portion of the system, which can be automatically synthesized using digital synthesis techniques, the RF portion is still designed manually. The increasing number of active and passive devices in this portion causes a dramatic increase in the complexity of the design process and RF front end design is becoming more and more of a bottleneck in the design of the overall communication system. Moreover, high integration typically results in components with inferior performance as compared to their discrete counterparts. For instance, on-chip VCOs which are used in the channel-select synthesizer have much inferior phase noise performance compared to a VCO with high Q off-chip passive elements [ROC+97]. This further exacerbates the design process complexity and leaves little room for over-design.

To enable ease of design at the component level, efficient simulation techniques at the transistor level are required which can effectively handle large circuits with a number of devices operating in their strong nonlinear region. Additionally, in the initial stage of design, transistor level description of the entire system may not be available. Hence compact

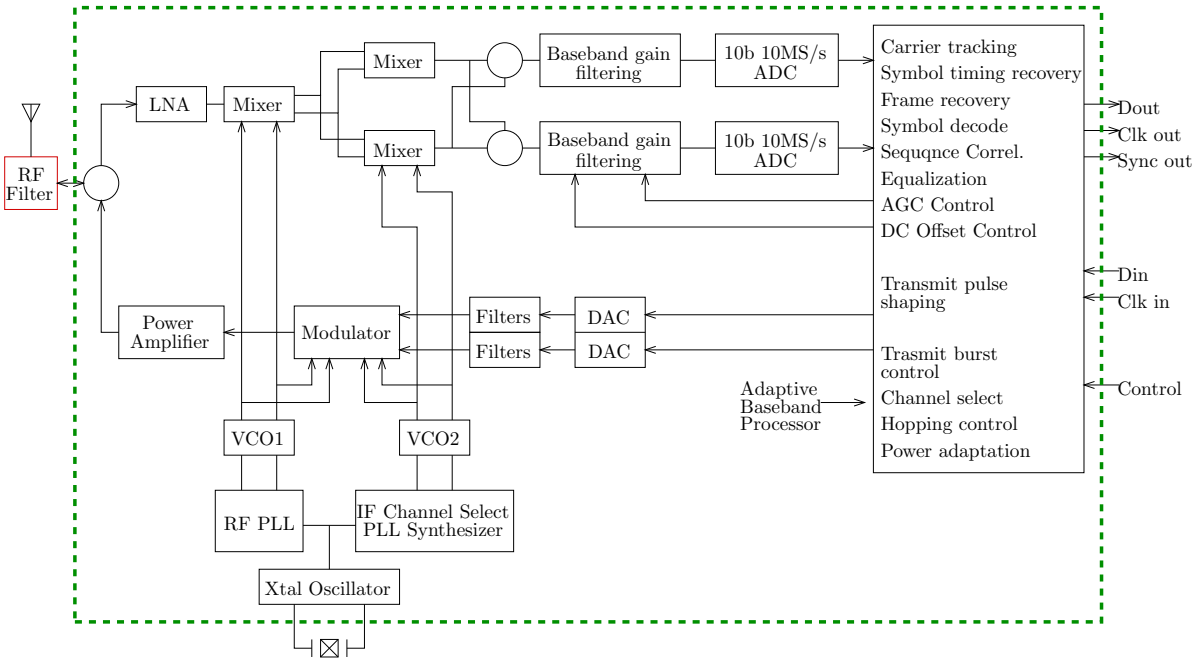

Figure 1.2: Future high integration RF front-end

models of various components, along with behavioural level simulation techniques which use these models, are required. These enable a system designer to quickly evaluate different architectures and choose the one that is best suited for the current set of specifications. The models should therefore be complete, so as to capture all the important effects which have an impact on system performance, and compact so that the behavioural level simulation algorithm does not become excessively slow.

Behavioural level simulation must be able to capture all significant interactions between different components of the system so that the sensitivity of overall system performance to specifications of a particular component performance can be accurately predicted. More importantly, the change required in the specifications of other components of the system, in order to maintain the overall system performance when the specification of one component is changed, must also be predicted accurately. This enables a system designer to investigate various design trade-offs at the behavioural level in a more systematic and meaningful manner. Even at the later stage of a design, when the transistor level netlist for the entire RF system might be available, it is prudent to extract these models from the transistor level description of various components and use a behavioural level simulation

technique using these models.

1.2 Motivation

One of the reasons why RF front-end design is a bottleneck is that noise performance is a very important part of high level specifications of an RF transceiver. Unlike digital circuits where noise is a second order effect, noise in RF circuits directly affects high level system performance such as signal to noise ratio (SNR) or the overall bit error rate (BER). Noise also affects how the system SNR degrades in presence of a large adjacent channel blocker signal. In the transmit path, it affects how much noise power the system is *leaking* into adjacent channels [Pat96].

Roughly speaking *noise* refers to any unwanted change in signals in a circuit. For instance, in a digital circuit, noise refers to any deviation of a signal from a logic zero (which typically is 0V) or a logic one (which typically is the supply voltage V_{DD}). In an RF circuit, noise refers to any unwanted signal coupled into the circuit as well as unwanted signals generated by the devices themselves.

1.2.1 Noise Sources in RF Transceiver

In a highly integrated transceiver, switching signals from digital portions of the circuit can couple into sensitive RF circuit nodes and directly degrade the overall signal to noise ratio. This coupling can happen through power supply lines as well as substrate. However, careful design and layout techniques can minimize the effect of this coupling. By ensuring separate power supply and ground for digital and RF portions of the system, using a large bypass capacitance to remove any unwanted high frequency signals on the supply network and by making the resistance of power supply to the RF portions very low, switching noise coupled through the power supply can be minimized. Several techniques have been proposed in the literature to minimize the amount of coupling from substrate [Gha96]. These usually involve using grounded guard rings around the sensitive RF circuits. For different substrates, different topologies of guard rings can be used to minimize the amount of signal that is coupled through the substrate [Gha96].

Another type of noise that has a detrimental effect on the system performance is electrical noise which is intrinsic to electronic devices that make up the circuit itself. The

discrete nature of charge transfer gives rise to *shot noise* whenever the current crosses a potential barrier. Shot noise is modelled as a zero mean stochastic process.

For a general one-dimensional stochastic process $X(t)$, the *autocorrelation*, as a function of two time variables t and τ, is given by

$$R_{xx}(t,\tau) = \mathbb{E}\left[X(t)X(t+\tau)\right]$$

If $R_{xx}(t,\tau)$ is independent of t, the stochastic process is called *wide-sense stationary*. For a wide-sense stationary stochastic process, the *power spectral density*, i.e., power $S_{xx}(\omega)$ in a unit frequency range at an angular frequency ω is given by

$$S_{xx}(\omega) = \int_{-\infty}^{\infty} R_{xx}(\tau)\exp(-\jmath\omega\tau)\mathrm{d}\tau$$

The spectral density of shot noise is given by

$$S_{xx,shot}(\omega) = 2qI_d \tag{1.1}$$

where q is the electron charge and I_d is the current. The power spectral density is constant for a very large frequency range (few tens of gigahertz) and hence can be modelled as a scaled *white noise source* with power spectral density given in (1.1). White noise is a mathematical idealization of this stochastic process. A white noise process is one which has unit power spectral density for all frequencies.

Nyquist theorem shows that the short circuit current in a resistor, which is in thermodynamic equilibrium, is a zero mean stochastic process. The power spectral density of the output noise, called *thermal noise* is given by

$$S_{xx,thermal}(\omega) = 4kTR \tag{1.2}$$

where k is the Boltzmann's constant, T is equilibrium temperature and R is the resistance. The power spectral density is constant for a very large frequency range before dropping to zero. Hence this noise process is also modelled as a scaled white noise process.

Another source of noise in devices is the *flicker* or $1/f$ noise. The physical origin of this noise is due to random capture and release of charge by surface impurities. Due to this noise generation method, noise power spectral density is typically much larger for lower frequencies than higher frequencies. The noise power spectral density for this process is given by

$$S_{xx,flicker}(\omega) \propto \frac{1}{\omega^b} \tag{1.3}$$

where b is 1 for typical flicker noise processes and ω is the angular frequency. This type of noise represents a problem for noise modelling since the integrated noise power in any finite band of frequencies around $\omega = 0$ is infinite which is clearly unphysical [Wei93]. A popular model of flicker noise is a stochastic process whose spectral density flattens out at a finite and small frequency. This can be modelled as a series of filtered white noise processes [MK82]. We will postpone further discussion of modelling flicker noise for now.

In this work we address the problem of analyzing the effect of electrical noise in RF circuits. Specifically we address the problem of noise analysis in presence of additive white noise sources. We use the mathematical idealization of a white noise source and formulate the problem of noise analysis in nonlinear RF circuits as solutions of appropriate stochastic differential equations. Given the specific nature of these stochastic differential equations, we enumerate various properties of the solutions and develop compact and accurate mathematical models for RF components.

1.2.2 Autonomous versus Nonautonomous Circuits

For the purpose of noise analysis, we divide components present in a typical RF system into two broad categories, autonomous and nonautonomous circuits. Autonomous circuits are those which have no inputs (except for DC power supplies) and produce a (usually) periodic output. Typical examples of such circuits in an RF front-end are oscillators. Nonautonomous circuits on the other hand will produce an interesting output only if supplied with one or more inputs. Typical examples of such components in an RF front end are mixers, filters, amplifiers etc.

Noise in autonomous oscillators is an important topic of investigation in itself. A noiseless oscillator is supposed to provide a perfect time reference to the circuit. However since the oscillator output is corrupted by noise, it is not perfectly periodic and it is said to have *phase noise*. Predicting phase noise in oscillators which are present in an RF system is extremely important because it critically affects the overall system noise performance [Nez98, Tom98, HKK98, VV83, Rob82]. Consider the frequency plot shown in Figure 1.3. The desired channel that needs to be down-converted is showed as a solid arrow. Due to phase noise in the local oscillator, the oscillator output spectrum is not a delta function, but is spread around the frequency of oscillation. If an adjacent channel is also transmitting at the same time (shown as broken arrow), since the noisy oscillator

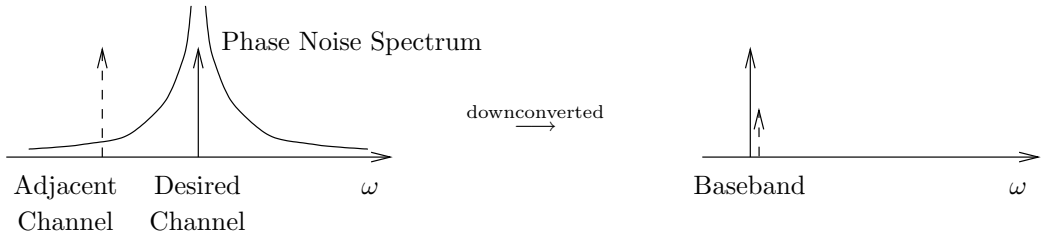

Figure 1.3: Effect of oscillator phase noise on blocking performance

output power spectral density is nonzero at this adjacent channel frequency, the adjacent channel also gets down-converted to base band, thereby directly degrading the overall SNR of the system. Similarly in the transmit path, phase noise in local oscillator output causes the upconverted signal to have finite energy outside the desired channel. Hence predicting oscillator output noise is an important problem in its own right.

1.3 Thesis Overview

This dissertation is organized in the following manner: In Chapter 2 we present a mathematical framework for performing noise analysis for RF circuits, both autonomous and nonautonomous. We classify some of the existing noise analysis techniques in this framework. We observe that traditional noise analysis of RF circuits is based on linear perturbation analysis. We then show that this analysis cannot be carried over to oscillatory circuits since linear perturbation analysis is not valid for autonomous system of equations (Chapter 3). We develop a new perturbation analysis technique for oscillatory system of equations that is valid for deterministic perturbations. We obtain a nonlinear differential equation for phase error of oscillators. For white noise perturbations, this differential equation becomes a *stochastic differential equation* (Chapter 4). We use standard techniques from stochastic differential equation theory to obtain a second order characterization of phase error and oscillator output as a stochastic process. The new oscillator phase noise characterization forces us to revisit the traditional noise analysis techniques for nonautonomous circuits which are driven by periodic signal which are derived from *real* oscillators and hence have phase noise. We address this problem in Chapter 5. We extend this analysis (Chapter 6) to nonautonomous circuits which are driven by more than one large periodic signals with incommensurable frequencies. We conclude (Chapter 7) by pointing

out some future directions where we believe this research can be extended.

Chapter 2

Overview of Existing Techniques

In this chapter we review some of the existing noise analysis techniques for autonomous and nonautonomous circuits. We begin by describing a general framework of noise analysis of nonautonomous circuits. We review some of the existing noise analysis techniques based on this framework. We then review existing noise analysis techniques for oscillators. We conclude by briefly describing our approach and contrasting them against existing techniques.

2.1 Perturbation Analysis of a Nonoscillatory System

The behaviour of a nonlinear electronic circuit can be described by the following system of differential equations

$$\frac{\mathrm{d}q(x(t))}{\mathrm{d}t} + f(x(t)) + b(t) = 0 \tag{2.1}$$

In this equation $x(\cdot) : \mathbb{R} \rightarrow \mathbb{R}^n$ represents a vector of state variables which, for an electronic circuit, are node voltages and branch currents of voltage sources and inductors. $q(\cdot) : \mathbb{R}^n \rightarrow \mathbb{R}^n$ represents the nonlinear charge and flux storage elements in the circuit, $f(\cdot) : \mathbb{R}^n \rightarrow \mathbb{R}^n$ represents memoryless nonlinearities in the circuit and $b(\cdot) : \mathbb{R} \rightarrow \mathbb{R}^n$ represents inputs to the nonautonomous circuit. RF circuits are usually analyzed for their steady-state response for one or more periodic inputs. For the purpose of our analysis we assume that $b(t)$ is a large periodic signal with period T. By large we imply that the application of $b(t)$ causes the circuit operating point to change appreciably as a function of time. We assume that the steady-state response of this circuit is given by $x_s(t)$, i.e., $x_s(t)$ satisfies (2.1). Since

the circuit is nonautonomous, $x_s(t)$ is also periodic with period T. Now we assume that the circuit equations are perturbed by a perturbation term $D(x)b(t)$. $D(\cdot) : \mathbb{R}^n \rightarrow \mathbb{R}^{n\times p}$ is state dependent modulation term and $b(\cdot) : \mathbb{R} \rightarrow \mathbb{R}^p$ is the state independent (but time dependent) perturbation term. I.e., the perturbed system of equations is given by

$$\frac{\mathrm{d}q(x(t))}{\mathrm{d}t} + f(x(t)) + b(t) + D(x)b(t) = 0 \tag{2.2}$$

Let $z(t)$ be the solution of (2.2). Linear perturbation analysis proceeds by assuming that the response $z(t)$ can be represented as

$$z(t) = x_s(t) + x_p(t) \tag{2.3}$$

and for *small* perturbation term $D(x)b(t)$, the deviation term $x_p(t)$ is small and bounded for all t. Substituting the form of the solution (2.3) in (2.2) we have

$$\frac{\mathrm{d}q(x_s(t) + x_p(t))}{\mathrm{d}t} + f(x_s(t) + x_p(t)) + b(t) + D(x_s(t) + x_p(t))b(t) = 0 \tag{2.4}$$

Since $x_p(t)$ is assumed to be small, the nonlinear functions q and f can be linearized around the periodic steady-state solution $x_s(t)$ and (2.4) can be written as

$$\frac{\mathrm{d}}{\mathrm{d}t}\left(q(x_s(t)) + \left.\frac{\mathrm{d}q(x)}{\mathrm{d}x}\right|_{x_s(t)} x_p(t)\right) + f(x_s(t)) + \left.\frac{\mathrm{d}f(x)}{\mathrm{d}x}\right|_{x_s(t)} x_p(t) + b(t) + D(x_s(t))b(t) = 0$$

Here we have ignored $x_p(t)$ in the argument of $D(\cdot)$. We use only the zeroth order Taylor series term $B(x_s)b(t)$ which captures the modulation of the perturbation sources with the large signal steady state and ignore the first order term in the expansion of $B(x)b(t)$ around $x_s(t)$, i.e.,

$$\left.\frac{\mathrm{d}D(x)}{\mathrm{d}x}\right|_{x_s(t)} x_p(t)b(t)$$

This term is a high-order effect that captures the modulation of the perturbation sources with themselves and can be neglected for all practical purposes. Since $x_s(t)$ is the solution of (2.1), we obtain

$$\frac{\mathrm{d}}{\mathrm{d}t}(C(t)x_p(t)) + G(t)x_p(t) + D(x_s(t))b(t) = 0 \tag{2.5}$$

where

$$C(t) = \left.\frac{\mathrm{d}q(x)}{\mathrm{d}x}\right|_{x_s(t)}$$

and

$$G(t) = \left.\frac{\mathrm{d}f(x)}{\mathrm{d}x}\right|_{x_s(t)}$$

and $C(t)$ and $G(t)$ are T-periodic. (2.5) can be rewritten as

$$C(t)\dot{x}_p(t) + A(t)x_p(t) + D(x_s(t))b(t) = 0 \tag{2.6}$$

where $A(t) = G(t) + \dot{C}(t)$. For a typical circuit, $C(t)$ need not be full rank and hence not all entries of $x_p(t)$ are independent of each other. (2.6) is a differential equation that is linear in $x_p(t)$ and the coefficient matrices $A(t)$ and $C(t)$ are T-periodic. Hence the homogeneous part of (2.6) describes a linear periodic time varying (LPTV) transfer function $h(t_1, t_2)$. Once $h(t_1, t_2)$ is obtained, the output $x_p(t)$ can be obtained by the following convolution integral

$$x_p(t) = \int_{-\infty}^{\infty} h(t, s)D(x_s(s))b(s)\mathrm{d}s$$

2.2 Noise Analysis of Nonoscillatory Systems

For stochastic perturbations, specifically for white noise perturbations $b(t) = \xi(t)$, (2.6) is a stochastic differential equation and $x_p(t)$ is now a stochastic process. (2.6) is written in the stochastic differential form as follows [Øks98]

$$C(t)\mathrm{d}x_p(t) + A(t)x_p(t)\mathrm{d}t + D(x_s(t))\mathrm{d}B(t) = 0 \tag{2.7}$$

where $B(t)$ is a p-dimensional Brownian motion process. It can be shown that this linear differential equation has a solution of the form

$$x_p(t) = \int_{-\infty}^{\infty} h(t, s)D(x_s(s))\mathrm{d}B(s)$$

where the integral in the above equation is to be interpreted as a stochastic integral [Øks98]. Hence

$$\begin{aligned}
\mathbb{E}\left[x_p(t_1)x_p^T(t_2)\right] &= \mathbb{E}\left[\int_{-\infty}^{\infty} h(t_1, s_1)D(x_s(s_1))\mathrm{d}B(s_1)\int_{-\infty}^{\infty} \mathrm{d}B^T(s_2)D^T(x_s(s_2))h^T(t_2, s_2)\right] \\
&= \int_{-\infty}^{\infty}\int_{-\infty}^{\infty} h(t_1, s_1)D(x_s(s_1))\mathbb{E}\left[\mathrm{d}B(s_1)\mathrm{d}B^T(s_2)\right]D^T(x_s(s_2))h^T(t_2, s_2) \\
&= \int_{-\infty}^{\infty} h(t_1, s)D(x_s(s))D^T(x_s(s))h^T(t_2, s)\mathrm{d}s
\end{aligned}$$

Existing noise analysis techniques take advantage of the fact that the transfer function is linear periodic time varying and hence satisfies the relation

$$h(t_1, t_2) = h(t_1 + T, t_2 + T)$$

This implies that for stationary input noise (i.e., the second order statistics do not change with time) or cyclostationary input noise (i.e., the second order statistics are periodic with the *same* period T), the output noise is also cyclostationary. Noise statistics for one period are directly computed from (2.7). There are several techniques proposed in the literature which perform this computation either in time domain or in frequency domain.

2.2.1 LPTV Approaches and Extensions

Noise analysis of nonlinear RF components driven by one or more periodic signals, has been a focus of attention of several researchers. One of the earliest efforts was concentrated on noise analysis of millimeter wave mixers [HK77]. Earlier works concentrated on extending traditional linear time invariant noise analysis techniques to weakly nonlinear circuits [RPP88]. Target circuits for these approaches were almost invariably high frequency mixers [RMC89]. Efforts were made later to extend this noise analysis to strongly nonlinear components present in RF front ends [HKW91, Hud92] and with arbitrary topologies [RM92]. Earlier efforts concentrated on microwave circuits which were predominantly linear with very few nonlinear elements [OTS91, RMM92b, RMM92a, RMM94b, RMM94a, RMM95, RMC98]. Since then, techniques have been suggested to speed up Newton iteration and the solution of the underlying large linear system of equations using iterative linear algebra techniques [RFL98]. These techniques can also address the problem of noise analysis of nonautonomous circuits driven by two or more large periodic signals [RMM94b, RMM94a, RFL98]. Though frequency domain techniques, usually based on harmonic balance, are more popular for RF circuits, several time domain techniques have also been suggested [Hul92, HM93, TKW96]. All these techniques usually concentrate on analyzing noise performance of nonlinear nonautonomous circuits assuming perfect LO input. The underlying assumption is that a noisy oscillator output can be viewed as a deterministic, large, perfectly periodic signal with additive amplitude and phase noise. With this assumption, input signal noise can be absorbed in the circuit and can be viewed as a circuit noise source [RMMN92]. However, as we will see in Chapter 3, this representation

is not valid for real oscillator output. Therefore we need to revisit the problem of noise analysis of nonautonomous circuits in presence of input signal phase noise.

2.2.2 Time Domain Analysis

In [DLSV96], a technique for numerically solving (2.7) as a stochastic differential equation is presented. No assumption is made about the nature of inputs. From (2.7), an ordinary differential equation for the variance $\mathbb{E}\left[x(t)x^T(t)\right]$ and the autocorrelation $\mathbb{E}\left[x(t_1)x^T(t_2)\right]$ is derived. These equations are solved numerically using transient simulation algorithm in SPICE. Circuit noise sources are modelled as white noise processes. This technique is used to compute output noise of a bipolar active mixer (along with several other circuits). Since input to the mixer is assumed to be perfectly periodic, the output noise variance is calculated to be periodically varying with time. However, no provision has been made to account for input signal phase noise in the simulation algorithm. Several other time domain noise analysis techniques have also been proposed which use different numerical integration techniques for stochastic differential equations [SD98, Dob93].

2.2.3 Our Approach

Existing techniques for noise simulation for nonautonomous circuits do not take into account the effect of input signal phase noise. If the input signal is noiseless and perfectly periodic, the output noise is cyclostationary as would be predicted by these existing techniques. However, the input signal is derived from a *real* signal source (oscillator) and therefore has phase noise. A noisy periodic signal does not provide a perfect time reference. Therefore noise in a circuit driven by such a signal cannot be cyclostationary. Cyclostationarity of output noise implies that its statistics vary *perfectly* periodically with time, i.e., provide a perfect time reference.

We formulate the problem of performing noise analysis of nonautonomous circuits driven by large periodic signals with phase noise as the solution of a stochastic differential equation. We show that

- The output of nonlinear nonautonomous systems in the presence of period input with Brownian motion phase deviation, is asymptotically wide sense stationary.
- The Lorentzian spectrum of the input signal and the characteristics of the Brownian motion input phase deviation process are preserved at the output.

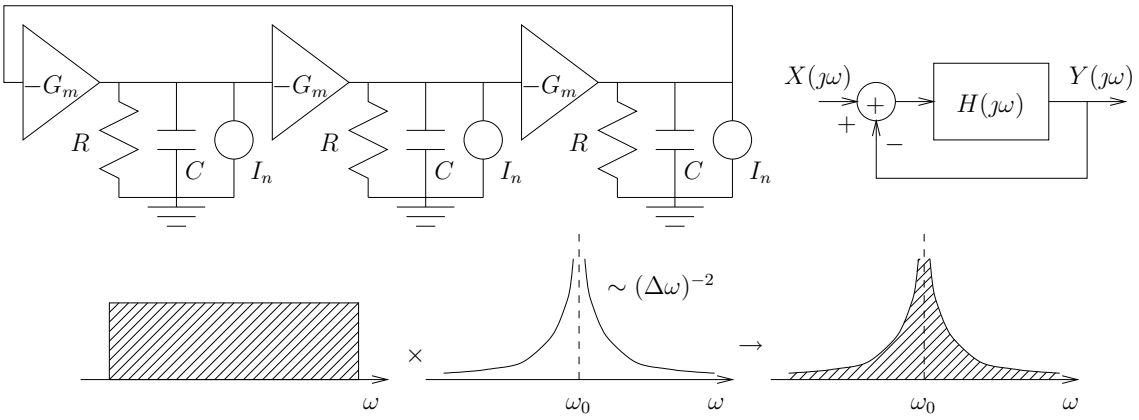

Figure 2.1: LTI noise analysis of a three stage ring oscillator

- Noisy input is shown to contribute a wide-band amplitude noise term at the output of the nonlinear circuit. This appears as a white noise source modulated by the time derivative of the steady-state response of the system.

2.3 Oscillator Phase Noise Analysis

We now review some of the techniques proposed in the literature for performing noise analysis of oscillators. Most of the approaches try to extend the LPTV noise analysis techniques of nonautonomous circuits to oscillators. A few techniques take advantage of the fact that phase uncertainty in an oscillator output is equivalent to uncertainty in timing and predict the time uncertainty directly at specific instances (such as zero crossings of the output). Some very sophisticated techniques for predicting spectral dispersions in lasers have been proposed in optics literature and we give a brief overview of those as well.

2.3.1 LTI/LTV Noise Analysis

We first investigate what happens if linear perturbation analysis based noise analysis is applied to oscillators. Consider a three stage ring oscillator shown in Figure 2.1. Each stage of the oscillator consists of a linear gain $-G_m$, output resistance R, input capacitance of the next stage C and noise source I_n. Traditional linear perturbation analysis based noise analysis proceeds by first computing the open loop transfer function $H(\jmath\omega)$. For stable oscillators it can shown that the resulting closed loop transfer is proportional to

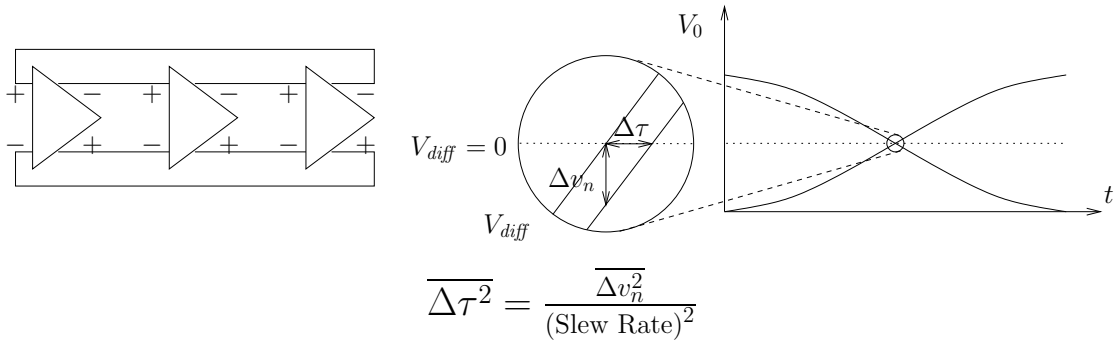

Figure 2.2: Timing jitter analysis of a three stage ring oscillator

$1/(\Delta\omega)^2$ [Raz96] where $\Delta\omega$ is the offset frequency from the frequency of oscillation. For input white noise source I_n, the closed loop transfer function modulates the output noise process and the spectrum of the output noise is also proportional to $1/(\Delta\omega)^2$. These investigations aim to provide insight into frequency domain properties of phase noise in order to develop rules for designing practical oscillators [Lee66, Sau77, Rob82, RC95, AKR94].

To account for nonlinearities in high Q oscillator, attempts to improve on LTI analysis have concentrated on borrowing linear time-varying (LTV) analysis methods from forced nonoscillatory systems [Haf66, Kur68, ABR76]. Several works on computational methods for general oscillators using LTV analysis are also available [RMMN93, RCMC94, OT97, DSG97, HL98]. These techniques can be used to compute the noise power spectral density at an offset frequency. However, at the oscillation frequency, these techniques predicts infinite noise power spectral density. Moreover, the total integrated noise power spectral density in a finite band around the frequency of oscillation is also infinite. Nonlinear effects such as frequency upconversion due to nonlinear operation of the circuit have also been specifically addressed in [Ohi93, VLPG96, Raz96, Poo97, FAOR95, SS85, Che91]. Specialized techniques for special type of oscillators have also been proposed [CHG95, DTS98a, DTS98b, YL97, AM97]. [Swe72] proposed a noise analysis technique for Gunn oscillators while [Sjö72] proposed a noise analysis technique for Read oscillators.

2.3.2 Timing Jitter Analysis

The same circuit as in Figure 2.1 can also be analyzed in time domain. A noiseless oscillator output provides a perfect periodic time reference with period T. If the first zero

crossing of the oscillator output is synchronized to $t = 0$, then a noiseless oscillator output will have a zero crossing at time $t = kT$, $k \in \mathbb{Z}^+$. Since a real oscillator output is corrupted by noise, zero crossings will not exactly be at time $t = kT$. The variance of zero crossing time is known as *cycle to cycle jitter*. Consider the three stage ring oscillator in Figure 2.2. Variance in zero crossing is computed by calculating the voltage noise at the zero crossing instance and dividing it by the square of the slew rate at that time. There are techniques proposed in the literature [WKG94, McN97] which compute the voltage variance assuming idealized models of specific kinds of delay cells that are used in the ring oscillator. Similar techniques [AM83] are proposed for oscillators with regenerative switching (or relaxation oscillator). The mechanisms of such oscillators suggest the fundamental intuition that timing or phase errors increase with time. These technique become extremely involved if realistic models for delay cells are used. It is also not clear how to extend these techniques to compute phase noise in nonswitching (harmonic) oscillators.

2.3.3 Time Domain Noise Analysis

Demir et. al. [DSV96] used their time domain non-Monte Carlo noise simulation algorithm [DLSV96] to compute the noise in an oscillator output. The noise simulation technique is also based on linear perturbation analysis. They concluded that the envelop of the variance of output noise power keeps increasing unbounded with time. This result, in some sense, is the time domain equivalent interpretation of the result derived in Section 2.3 which predict infinite integrated power of oscillator output noise. The reason why both these techniques show this unphysical result is because they are based on linear perturbation analysis which is not valid for oscillators.

2.3.4 Other Approaches

More sophisticated analysis techniques exist in optics. Here, stochastic analysis is common and it is well known that that phase error in oscillators, due to white noise sources, is described by a Brownian motion process. Although justifications of this fact are often based on approximations, precise descriptions of phase noise have been obtained for certain systems. In the seminal work of Lax [Lax67], an equation describing the growth of phase fluctuations with time is obtained for pumped lasers. The fact that a Brownian motion phase error process leads to Lorentzian output power spectrum is also well established [FV88,

VV83]. However, a general theory is not available in this field as well.

There are a few approaches which are based on nonlinear analysis of the oscillator dynamics [Dek87, Gol89]. Possibly the most general and rigorous treatment of phase noise has been that of [Kär90]. Using several novel methods, the oscillator response is decomposed into phase and amplitude variation and a nonlinear differential equation for phase error is obtained. By solving a linear, small time approximation to this equation with stochastic inputs, a Lorentzian spectrum due to white noise is obtained. In spite of these advances, certain gaps remain, particularly with respect to the derivation and solution of the differential equation governing phase error.

2.3.5 Our Approach

Our approach for oscillator phase noise analysis can be summarized as follows:

- As a first step, we develop a new quantitative description of the dynamics of stable nonlinear oscillators in presence of deterministic perturbations which is not limited to two-dimensional system of equations and does not make any assumptions about the type of nonlinearity.
- By considering stochastic perturbations in a stochastic differential calculus setting, we obtain a correct mathematical characterization of the noisy oscillator output.
- We show that the oscillator output is represented as the sum of two stochastic processes: a large signal output with Brownian motion phase deviation and a small "amplitude" noise process.
- We further show that the response of the noisy oscillator is asymptomatically wide-sense stationary with Lorentzian power spectral density.

Chapter 3

Perturbation Analysis of Stable Oscillators

As pointed out in Chapter 2, noise analysis in electrical circuits is based on perturbation analysis. It is well known that linear perturbation analysis is not valid for oscillatory circuits. In order to develop a noise analysis technique for oscillators we first need to develop a rigorous perturbation analysis technique. In this chapter we first show that traditional linear perturbation analysis is not valid for oscillators. This also helps us introduce the notations which we use when we describe our perturbation analysis technique. We show that this incorrect linearization leads to nonphysical results such as infinite oscillator output phase noise power in presence of white noise. We then describe our perturbation analysis technique in detail. This analysis is not limited to any specific type electrical oscillator. In fact this analysis is valid for *any* autonomous system of equations with oscillatory solution. We also demonstrate our technique with an example.

3.1 Mathematical Preliminaries

The dynamics of any autonomous system without undesired perturbations can be described by a system of differential equations:[1]

$$\dot{x} = f(x) \tag{3.1}$$

[1]For notational simplicity, we use the state equation formulation to describe the dynamics of an autonomous system. The results we present can be easily extended to mixed differential-algebraic formulation given by $\frac{\mathrm{d}q(x)}{\mathrm{d}t} + f(x) = 0$.

where $x \in \mathbb{R}^n$ and $f(\cdot) : \mathbb{R}^n \to \mathbb{R}^n$. We assume that $f(\cdot)$ satisfies the conditions of the Picard-Lindelőf existence and uniqueness theorem for initial value problems [Far94]. We assume that solution of (3.1), $x_s(t)$ is periodic with period T and describes an *asymptotically orbitally stable* limit cycle in the n-dimensional solution space. We explain the concept of asymptotic orbital stability below [Far94].

Since $x_s(t)$ is a solution of (3.1), $x_s(t-t_0)$ is also a nonconstant T-periodic solution for arbitrary $t_0 \in \mathbb{R}$. The initial values $x_s(0)$ and $x_s(-t_0)$ can be arbitrarily close (if $|t_0|$ is small enough), and still $x_s(t) - x_s(t-t_0)$ does not tend to zero as t tends to infinity. Let the *path* γ of the T-periodic solution $x_s(t)$ be

$$\gamma = \{x \in \mathbb{R} : x = x_s(t), t \in \mathbb{R}_+\}$$

We note that $x_s(t)$ and $x_s(t-t_0)$ have the same path γ.

Definition 3.1 (Orbital Stability) *The solution $x_s(t)$ of (3.1) is said to be* orbitally stable *if for every $\epsilon > 0$, there exists a $\delta(\epsilon)$ such that if the distance of the initial value $x(0) = x_0$ from the path γ of $x_s(t)$ is less than $\delta(\epsilon)$, i.e., $\mathrm{dist}(x_0, \gamma) < \delta(\epsilon)$, then the solution $\phi(t, x_0)$ of (3.1) that assumes the value x_0 at $t = 0$ satisfies*

$$\mathrm{dist}(\phi(t, x_0), \gamma) < \epsilon$$

for $t \geq 0$.

For instance, the system of equations which describes an unstable limit cycle is not orbitally stable, since for any initial condition not on the limit cycle, the solution will diverge away from it. Consider the differential equation

$$\begin{bmatrix} \dot{x}_1 \\ \dot{x}_2 \end{bmatrix} = \begin{bmatrix} x_2 \\ 2(x_1^2 - 1)x_2 + x_1 \end{bmatrix}$$

The response of the oscillator describes an unstable limit cycle (or path γ) in the phase plane (x_1-x_2 plane) as shown in Figure 3.1. Hence for any initial condition *outside* the region enclosed by the limit cycle, the phase plane trajectory diverges away. Similarly for any initial condition inside the limit cycle, the phase plane trajectory goes to zero.

If the solution $x_s(t)$ is orbitally stable, then each solution with the same path γ, i.e., every solution $x_s(t+\alpha)$ for $\alpha \in \mathbb{R}$, is also orbitally stable.

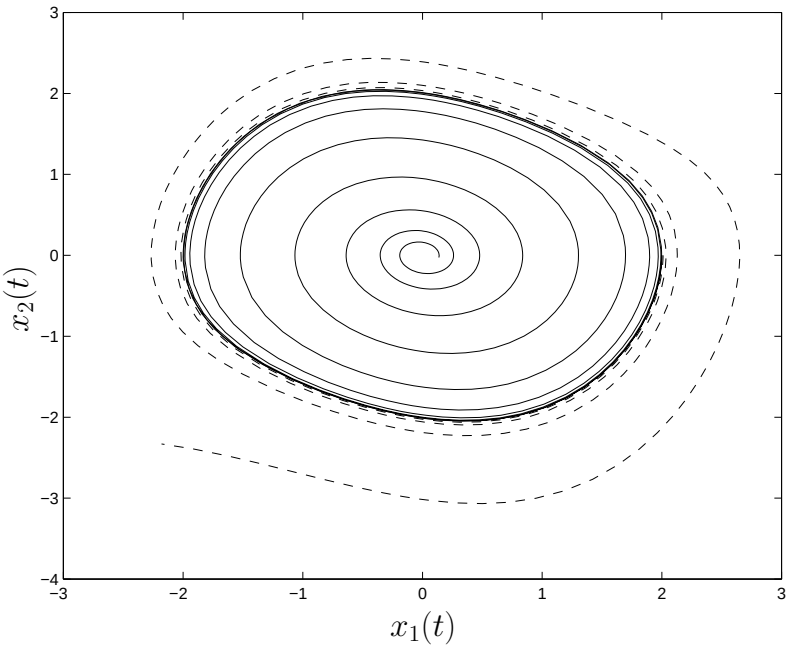

Figure 3.1: Response of an orbitally unstable oscillator

Definition 3.2 (Asymptotic Orbital Stability) *The solution* $x_s(t)$ *of* (3.1) *is said to be* asymptotically orbitally stable *if it is orbitally stable, and if a* $\delta > 0$ *exists such that* $\text{dist}(x_0, \gamma) < \delta$ *implies*

$$\text{dist}(\phi(t, x_0), \gamma) \to 0 \quad as \quad t \to \infty$$

Definition 3.3 (Asymptotic Phase Property) *The solution* $x_s(t)$ *is said to have the* asymptotic phase property *if a* $\delta > 0$ *exists such that to each initial value* x_0 *satisfying* $\text{dist}(x_0, \gamma) < \delta$ *there corresponds an* asymptotic phase $\alpha(x_0) \in \mathbb{R}$ *with the property*

$$\lim_{t \to \infty} |\phi(t, x_0) - x_s(t + \alpha(x_0))| = 0$$

A lossless LC tank with a finite energy stored in the tank is not an asymptotically orbitally stable system. The response of the oscillator describes a closed orbit in two-dimensional state space (formed by the capacitor voltage and inductor current). However, if the oscillator is perturbed by a small instantaneous change in the system energy, the system moves to a new limit cycle and never returns to its original limit cycle. Hence

this is not an asymptotically orbitally stable system. For the autonomous systems we are dealing in this work, we assume that there exists a nontrivial periodic solution $x_s(t)$ which is asymptotically orbitally stable, and has the asymptotic phase property.

We are interested in the response of such systems to a small state-dependent perturbation of the form $D(x)b(t)$ where $D(\cdot) : \mathbb{R}^n \to \mathbb{R}^{n\times p}$ and $b(\cdot) : \mathbb{R} \to \mathbb{R}^p$. I.e., the perturbed system is described by

$$\dot{x} = f(x) + D(x)b(t) \tag{3.2}$$

Let the exact solution of the perturbed system in (3.2) be $z(t)$.

3.2 Perturbation Analysis Using Linearization

The traditional approach to analyzing perturbed nonlinear systems is to linearize about the unperturbed solution under the assumption that the resultant deviation, i.e., the difference between the solutions of the perturbed and unperturbed systems, will be small. Let this deviation be $w(t)$, i.e.,

$$z(t) = x_s(t) + w(t)$$

Substituting this expression in (3.2) we obtain

$$\dot{x}_s(t) + \dot{w}(t) = f(x_s(t) + w(t)) + D(x_s(t) + w(t))b(t)$$

We assume that for "small" perturbations $D(x)b(t)$ the resulting deviation $w(t)$ will be small. Hence, in the above expression we can approximate $f(x_s(t) + w(t))$ by its first order Taylor series expansion and replace $D(x_s(t) + w(t))b(t)$ with $D(x_s(t))b(t)$. Using these approximations and observing that $x_s(t)$ satisfies (3.1), we obtain

$$\begin{aligned} \dot{w}(t) &\approx \left.\frac{\partial f(x)}{\partial x}\right|_{x_s(t)} w(t) + D(x_s(t))b(t) \\ &= J(t)w(t) + D(x_s(t))b(t) \end{aligned} \tag{3.3}$$

where the Jacobian

$$J(t) = \left.\frac{\partial f(x)}{\partial x}\right|_{x_s(t)}$$

$J : \mathbb{R} \to \mathbb{R}^{n\times n}$ is T-periodic. We would like to solve for $w(t)$ in (3.3) to see if our assumption that it is small is indeed justified. (3.3) describes a linear periodically time-varying system

of equations governing the dynamics of $w(t)$. For solving this equation we will use results from Floquet theory [Far94, Gri90] which we describe below.

3.2.1 Floquet Theory

The homogeneous system of differential equations corresponding to (3.3) is given by

$$\dot{w} = J(t)w \tag{3.4}$$

We begin by making the following observations:

Remark 3.1

- *The conditions of the Picard-Lindelőf existence and uniqueness theorem [Far94] for initial value problems are trivially satisfied by (3.3) and (3.4). Hence, there exist unique solutions to (3.3) and (3.4) given an initial condition $w(t_0) = w_0$.*
- *It can be shown that the set of real solutions of (3.4) form an n-dimensional linear space.*
- *Let $w_1(t, t_0), \ldots, w_n(t, t_0)$ be n linearly independent solutions of (3.4). Then,*

  $$W(t, t_0) = [w_1(t, t_0), \ldots, w_n(t, t_0)]$$

  is called a fundamental matrix. *The fundamental matrix satisfies*

  $$\frac{\mathrm{d}W(t, t_0)}{\mathrm{d}t} = J(t)W(t, t_0)$$

  If $W(t_0, t_0) = I$, the $n \times n$ identity matrix then $W(t, t_0)$ is called the principal fundamental matrix, *or* the state transition matrix *for (3.4), denoted by $\Phi(t, t_0)$.*
- *Any solution of (3.4) can be expressed as $W(t, t_0)c$ where $c \neq 0$ is a constant vector. In particular, for $w(t_0) = x_0$, the solution of (3.4) is given by $\Phi(t, t_0)x_0$.*
- *If $\tilde{W}(t, t_0)$ is another fundamental matrix for (3.4) then $\tilde{W}(t, t_0) = W(t, t_0)C$ where C is a nonsingular constant matrix.*
- *The solution w of (3.3) satisfying the initial condition $w(t_0) = w_0$ is given by*

  $$w(t, t_0, x_0) = \Phi(t, t_0)x_0 + \int_{t_0}^{t} \Phi(t, s)D(x_s(s))b(s)\mathrm{d}s$$

In the above observations we have not used the fact that the entries of $J(t)$ are periodic. Since for the case of a periodic oscillator, $J(t)$ is T-periodic, $J(t+T) = J(t)$ for all $t \in \mathbb{R}$. Let $W(t, t_0)$ be a fundamental matrix for (3.4). We further observe that:

Remark 3.2

- *If $W(t, t_0)$ is a fundamental matrix then for $W(t+T, t_0)$, we have*

$$\begin{aligned}\dot{W}(t+T, t_0) &= J(t+T)W(t+T, t_0) \\ &= J(t)W(t+T, t_0)\end{aligned}$$

  hence $W(t+T, t_0)$ is also a fundamental matrix. Then,

$$W(t+T, t_0) = W(t, t_0)B$$

  where B is a nonsingular matrix and

$$B = W^{-1}(t_0, t_0)W(t_0+T, t_0)$$

  Since the columns of W are linearly independent, the inverse in the above expression exists.

- *Even though B is not unique, it can be shown that any other B will have the same eigenvalues.*

- *The (unique) eigenvalues of B, $\lambda_1, \ldots, \lambda_n$, are called the* characteristic multipliers *of the equation (3.4) and the* characteristic (Floquet) exponents *$\mu_1, \ldots, \mu_n$ are defined as*

$$\lambda_i = \exp(\mu_i T)$$

Assumption 3.1 *We assume that B has distinct eigenvalues and it is diagonalizable*[2].

Now we state a result due to Floquet (1883):

Theorem 3.1 (Floquet) *Let B be diagonalized as*

$$B = \Xi\Lambda\Xi^{-1}$$

[2]The extension to nondiagonalizable matrices is straightforward.

where $\Lambda = \text{diag}[\lambda_1, \ldots, \lambda_n]$. *Let*

$$D = \text{diag}[\mu_1, \ldots, \mu_n]$$

where μ_i *is defined as* $\lambda_i = \exp(\mu_i T)$. *Then, the state transition matrix of the system* (3.4), *as a function of two variables,* t *and* $s = t_0$, *can be written in the form*

$$\Phi(t, s) = U(t) \exp(D(t - s))V(s) \tag{3.5}$$

where $U(t)$ *and* $V(t)$ *are both* T*-periodic and nonsingular, and satisfy*

$$U(t) = V^{-1}(t)$$

for all t.

Proof: We have

$$\begin{aligned} W(t + T, s) &= W(t, s)B \\ &= W(t, s)\Xi\Lambda\Xi^{-1} \end{aligned}$$

and hence

$$W(t + T, s)\Xi = W(t, s)\Xi\Lambda \tag{3.6}$$

Let $Y(t, s) = W(t, s)\Xi$. Using this relation, (3.6) reduces to

$$\begin{aligned} Y(t + T, s) &= Y(t, s)\Lambda \\ &= Y(t, s) \exp(DT) \end{aligned}$$

Since $W(t, s)$ is nonsingular, $Y(t, s)$ is also a fundamental matrix of (3.4). For a given s let

$$U(t) = Y(t, s) \exp(-D(t - s))$$

and $V(t) = U^{-1}(t)$. We observe that

$$\begin{aligned} U(t + T) &= Y(t + T, s) \exp(-D(t + T - s)) \\ &= Y(t, s) \exp(DT) \exp(-D(t + T - s)) \\ &= Y(t, s) \exp(-D(t - s)) \\ &= U(t) \end{aligned}$$

i.e., $U(t)$ is T-periodic. Here we used the fact that for scalar s and t

$$\exp(Ds) \exp(Dt) = \exp(Dt) \exp(Ds) = \exp(D(t + s))$$

Hence both $U(t)$ and $V(t)$ are T-periodic. Let

$$\Phi(t,s) = U(t)\exp(D(t-s))V(s)$$

We note that $\Phi(s,s) = I$ and $\Phi(t,s)$ satisfies (3.4), hence $\Phi(t,s)$ is the state transition matrix of (3.4). ∎

Remark 3.3

- *The state transition matrix $\Phi(t,s)$ can be written as*

$$\begin{aligned}\Phi(t,s) &= \begin{bmatrix} u_1(t) & \dots & u_n(t)\end{bmatrix}\begin{bmatrix} e^{\mu_1(t-s)} & & \\ & \ddots & \\ & & e^{\mu_n(t-s)}\end{bmatrix}\begin{bmatrix} v_1^T(s) \\ \vdots \\ v_n^T(s)\end{bmatrix} \\ &= \sum_{i=1}^{n} \exp\left(\mu_i(t-s)\right)u_i(t)v_i^T(s)\end{aligned}$$

  where $u_i(t)$ are the columns of $U(t)$, and $v_i^T(t)$ are the rows of $V(t) = U^{-1}(t)$.

- *With this representation of the state transition matrix, the solutions of the homogeneous system (3.4) and the inhomogeneous system (3.3) with a periodic coefficient matrix are given by*

$$w_H(t) = \sum_{i=1}^{n} \exp\left(\mu_i(t-t_0)\right)u_i(t)v_i^T(t_0)x(t_0)$$

  and

$$w_{IH}(t) = w_H(t) + \sum_{i=1}^{n} u_i(t)\int_{t_0}^{t} \exp\left(\mu_i(t-s)\right)v_i^T(s)b(s)\mathrm{d}s$$

- *For any i, $w(t) = u_i(t)\exp(\mu_i t)$ is a solution of (3.4) with the initial condition $w(t_0) = u_i(t_0)\exp(\mu_i t_0)$. Similarly, $w(t) = v_i(t)\exp(-\mu_i t)$ is a solution of the* adjoint system

$$\dot{w} = -J^T(t)w$$

  with the initial condition $w(t_0) = v_i(t_0)\exp(-\mu_i t_0)$.

- *We have*

$$\begin{aligned}\Phi(T,0) &= \sum_{i=1}^{n} \exp\left(\mu_i T\right)u_i(T)v_i^T(0) \\ &= \sum_{i=1}^{n} \exp\left(\mu_i T\right)u_i(0)v_i^T(0)\end{aligned}$$

From the above, $u_i(0)$ are the eigenvectors of $\Phi(T,0)$ with corresponding eigenvalues $\exp(\mu_i T)$, and $v_i(0)$ are the eigenvectors of $\Phi(T,0)^T$ corresponding to the same eigenvalues.

3.2.2 Response to Deterministic Perturbation

We now use the results of Floquet Theory to obtain a solution $w(t)$ of (3.3). The state transition matrix of (3.4), the homogeneous part of (3.3), is given by (3.5) which is repeated here

$$\Phi(t,s) = U(t)\exp(D(t-s))V(s)$$

Here $U(t)$ is a T-periodic nonsingular matrix, $V(t) = U^{-1}(t)$ and $D = \text{diag}[\mu_1, \ldots, \mu_n]$ where where μ_i are the Floquet (characteristic) exponents and $\exp(\mu_i T)$ are the characteristic multipliers.

Remark 3.4 *Let $u_i(t)$ be the columns of $U(t)$ and $v_i^T(t)$ be the rows of $V(t) = U^{-1}(t)$. Then $\{u_1(t), u_2(t), \ldots, u_n(t)\}$ and $\{v_1(t), v_2(t), \ldots, v_n(t)\}$ both span $\mathbb{R}^n$ and satisfy the* bi-orthogonality conditions *$v_i^T(t)\,u_j(t) = \delta_{ij}$ for every t. In general, $U(t)$ itself is not an orthogonal matrix.*

Let us first consider the homogeneous part of (3.3), the solution of which is given by

$$\begin{aligned} w_H(t) &= U(t)\exp(Dt)V(0)w(0) \\ &= \sum_{i=1}^{n} u_i(t)\exp(\mu_i t)v_i^T(0)w(0) \end{aligned}$$

where $w(0)$ is the initial condition. Next, we will show that one of the terms in the summation in the above equation does not decay with t.

Lemma 3.2

- *The time-derivative of the periodic solution $x_s(t)$ of (3.1), i.e., $\dot{x}_s(t)$, is a solution of the homogeneous part of (3.3).*
- *The unperturbed oscillator (3.1) has a nontrivial T-periodic solution $x_s(t)$ if and only if the number 1 is a characteristic multiplier of the homogeneous part of (3.3), or equivalently, one of the Floquet exponents satisfies $\exp(\mu_i T) = 1$.*

Proof: Since $x_s(t)$ is a nontrivial periodic solution of (3.1), it satisfies

$$\dot{x}_s(t) = f(x_s(t))$$

Taking the time derivative of both sides of this equation, we have

$$\ddot{x}_s = \left.\frac{\partial f}{\partial x}\right|_{x_s(t)} \dot{x}_s$$

Hence, $\dot{x}_s(t)$ satisfies $\dot{w} = J(t)w$, the homogeneous part of (3.3). Thus,

$$\dot{x}_s(t) = \sum_{i=1}^{n} u_i(t) \exp(\mu_i t) v_i^T(0) \dot{x}_s(0)$$

Since $\dot{x}_s(t)$ is periodic, it follows that at least one of the Floquet exponents satisfies $\exp(\mu_i T) = 1$. ∎

Remark 3.5 *One can show that if* 1 *is a characteristic multiplier, and the remaining* $n-1$ *Floquet exponents satisfy* $|\exp(\mu_i T)| < 1$, $i = 2, \ldots, n$, *then the periodic solution* $x_s(t)$ *of* (3.1) *is asymptotically orbitally stable and it has the asymptotic phase property [Far94]. This is a sufficient condition for asymptotic orbital stability, not a necessary one. We assume that this sufficient condition is satisfied by the system and the periodic solution* $x_s(t)$. *Moreover, if any of the Floquet exponents satisfy* $|\exp(\mu_i T)| > 1$, *then the solution* $x_s(t)$ *is orbitally* unstable.

Without loss of generality, we choose $\mu_1 = 0$ and $u_1(t) = \dot{x}_s(t)$.

Remark 3.6 *With* $u_1(t) = \dot{x}_s(t)$, *we have*

$$v_1^T(t)\, \dot{x}_s(t) = 1$$

and

$$v_1^T(t)\, u_j(t) = 0 \quad j = 2, \ldots, n$$

$v_1(t)$ *will play an important role in the rest of our treatment.*

Next, we obtain the particular solution of (3.3), given by

$$\begin{aligned} w_P(t) &= \int_0^t U(t) \exp(D(t-r)) V(r) D(x_s(r)) b(r) \mathrm{d}r \\ &= \sum_{i=1}^{n} u_i(t) \int_0^t \exp(\mu_i(t-r)) v_i^T(r) D(x_s(r)) b(r) \mathrm{d}r \end{aligned}$$

Since $\exp(\mu_1 T) = 1$, the first term in the above summation is given by

$$u_1(t) \int_0^t v_1^T(r) D(x_s(r)) b(r) \mathrm{d}r$$

If the integrand has a nonzero average value, then the deviation $w(t)$ in (3.3) will grow unbounded. Hence, the assumption that $w(t)$ is small becomes invalid and the linearization based perturbation analysis is inconsistent.

Before we present our perturbation analysis technique for stable oscillators, we will show that noise analysis of oscillators based on linear perturbation analysis is also invalid and it leads to nonphysical results such as infinite total integrated noise power.

3.2.3 Response to Stochastic Perturbation

Now, we consider the case where the perturbation $b(t)$ is a vector of uncorrelated white noise sources $\xi(t)$, i.e.,

$$\mathbb{E}\left[\xi(t_1)\xi^T(t_2)\right] = I\delta(t_1 - t_2)$$

where $\mathbb{E}[\cdot]$ denotes the probabilistic *expectation* operator and I is $p \times p$ identity matrix. We now find the expression of the autocorrelation matrix

$$K(t) = \mathbb{E}\left[w(t)w^T(t)\right]$$

of the solution of (3.3) for $K(0) = 0$. We have

$$\begin{aligned}
K(t) &= \mathbb{E}\left[w(t)w^T(t)\right] \\
&= \mathbb{E}\left[\int_0^t \Phi(t,s_1) D(x_s(s_1)) \xi(s_1) \mathrm{d}s_1 \int_0^t \xi^T(s_2) D^T(x_s(s_2)) \Phi^T(t,s_2) \mathrm{d}s_2\right] \\
&= \int_0^t \int_0^t \Phi(t,s_1) D(x_s(s_1)) \mathbb{E}\left[\xi(s_1)\xi^T(s_2)\right] D^T(x_s(s_2)) \Phi^T(t,s_2) \mathrm{d}s_1 \mathrm{d}s_2 \\
&= \int_0^t \int_0^t \Phi(t,s_1) D(x_s(s_1)) \delta(s_1 - s_2) D^T(x_s(s_2)) \Phi^T(t,s_2) \mathrm{d}s_1 \mathrm{d}s_2
\end{aligned}$$

i.e.,

$$K(t) = \int_0^t \Phi(t,s) D(x_s(s)) D^T(x_s(s)) \Phi(t,s)^T \mathrm{d}s \tag{3.7}$$

If we substitute

$$\Phi(t,s) = \sum_{i=1}^{n} \exp\left(\mu_i(t-s)\right) u_i(t) v_i^T(s)$$

in (3.7) we obtain

$$K(t) = \sum_{i=1}^{n} \sum_{j=1}^{n} u_i(t) u_j^T(t) \left[\int_0^t \exp((\mu_i + \mu_j)t) v_i^T(s) D(x_s(s)) D^T(x_s(s)) v_j(s) \mathrm{d}s \right]$$

Since $\exp(\mu_1 T) = 1$, the term in the summation above for $i = j = 1$ is given by

$$u_1(t) u_1^T(t) \left[\int_0^t v_1^T(s) D(x_s(s)) D^T(x_s(s)) v_1(s) \mathrm{d}s \right]$$

The integrand $v_1^T(s) D(x_s(s)) D^T(x_s(s)) v_1(s)$ is a nonnegative scalar that is periodic in s since $D(x_s(s)) D^T(x_s(s))$ is a positive semi-definite matrix. This scalar has a positive average value, hence this term grows unbounded with t. Thus, the assumption that the deviation $w(t)$ stays small is also invalid for the stochastic perturbation case, because the variances of the entries of $w(t)$ can grow unbounded. The notion of "staying small" is quite different for a stochastic process than the one for a deterministic function. For instance, a Gaussian random variable can take arbitrarily large values with nonzero probability even when its variance is "small". We say that a stochastic process is "bounded" when its variance is bounded, even though some of its sample paths (representing a nonzero probability) can grow unbounded.

3.3 Nonlinear Perturbation Analysis for Phase Deviation

As seen in the previous section, traditional perturbation techniques do not suffice for analyzing oscillators. In this section, we develop a novel nonlinear perturbation analysis suitable for oscillators. Before we present the mathematical details we will explain the intuition behind our approach. Consider the unperturbed oscillator output which describes a stable limit cycle. When a perturbation is applied to the oscillator, this periodicity is lost. For stable oscillators, however, the perturbed trajectory remains within a small band around the unperturbed trajectory as shown in Figure 3.2.

The proximity of the perturbed and unperturbed trajectories in the phase plane does not imply that the time-domain waveforms are also close to each other. At a given time t, the unperturbed oscillator output $x_s(t)$ and the perturbed oscillator output $z(t)$, can be far from each other as illustrated in Figure 3.2. This further indicates that the linear perturbation analysis which concludes that the deviation $w(t) = z(t) - x_s(t)$ grows unbounded is incorrect, since $w(t)$ is bounded by the diameter of the limit cycle. This

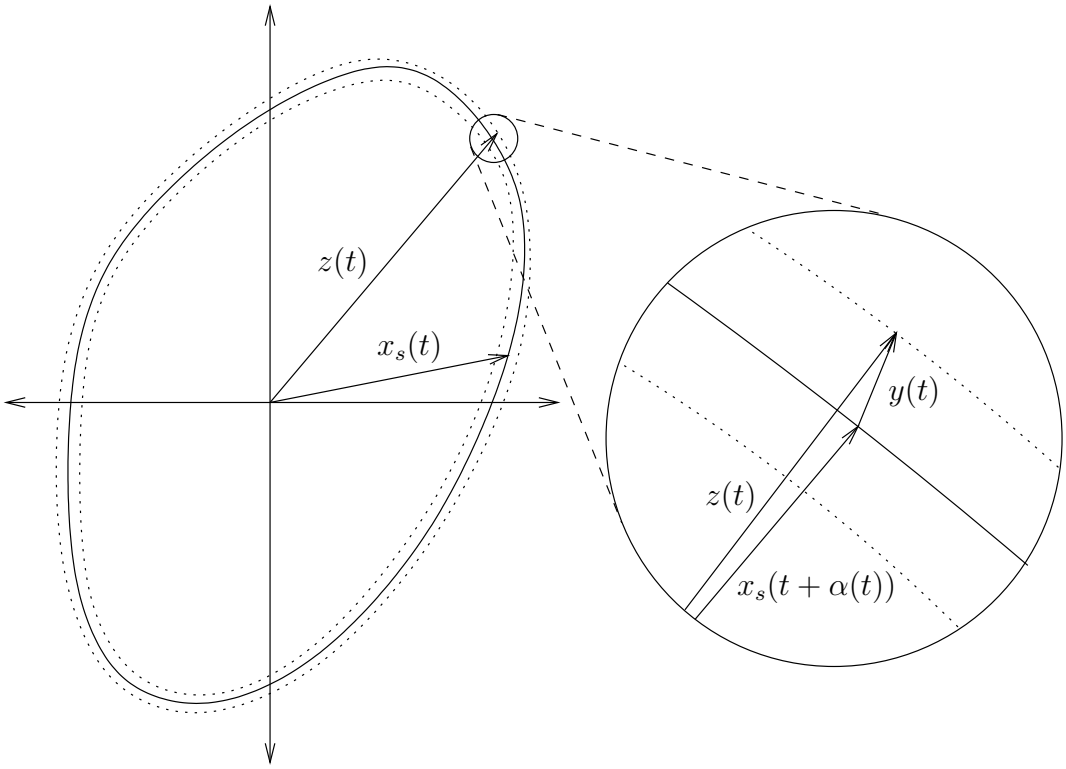

Figure 3.2: Limit cycle and excursions due to perturbations

also suggests that the perturbed oscillator response *does* remain close to the unperturbed response which has been suitably time shifted ($\alpha(t)$ in Figure 3.2). Hence the perturbed oscillator response can be decomposed in two components, time shift along the limit cycle $x_s(t+\alpha(t))$ and deviation away from the limit cycle $y(t)$. In our approach, we find a nonlinear differential equation governing the phase shift $\alpha(t)$ such that the deviation away from the limit cycle, $y(t) = z(t) - x_s(t+\alpha(t))$ stays small and bounded for all times. We call $y(t)$ orbital or amplitude deviation and $x_s(t+\alpha(t))$, phase deviation.

The new analysis proceeds along the following lines:

1. We rewrite (3.2) with the (small) perturbation $D(x)b(t)$ split into two small parts $b_1(x,t)$ and $\tilde{b}(x,t)$:

$$\dot{x} = f(x) + b_1(x,t) + \tilde{b}(x,t) \tag{3.8}$$

2. We choose the first perturbation term $b_1(x,t)$ in such a way that its effect is to create only *phase errors* to the unperturbed solution. In other words, we show that the

equation

$$\dot{x} = f(x) + b_1(x,t) \tag{3.9}$$

is solved by

$$x_p(t) = x_s(t + \alpha(t))$$

for a certain function $\alpha(t)$, called the *phase error*. It will be seen that $\alpha(t)$ can grow unboundedly large with time even though the perturbation $b_1(x,t)$ remains small.

3. We then treat the remaining term $\tilde{b}(x,t)$ as a small perturbation to (3.9), and perform a consistent traditional perturbation analysis in which the resultant deviations from $x_p(t)$ remain small. I.e., we show that

$$z(t) = x_s(t + \alpha(t)) + y(t)$$

solves (3.8) for a certain $y(t)$ that *remains small* for all t. $y(t)$ will be called the *orbital deviation*. It should be pointed out that we will indeed perform a linearized perturbation analysis for the orbital deviation $y(t)$. However in this case we prove that this linear analysis is correct and consistent by showing that the orbital deviation indeed stays small for small perturbations. In the traditional linear perturbation analysis presented in Section 3.2.2, the response deviation for the system does not stay small for small perturbations, hence is not valid. Even though the perturbation analysis for the orbital deviation is linear, we derive a *nonlinear* equation for the phase deviation, hence we perform a *nonlinear perturbation analysis* for the overall deviation, i.e., the phase deviation and the orbital deviation.

We start by defining $\alpha(t)$ concretely through a differential equation.

Definition 3.4 *Let $\alpha(t)$ be defined by*

$$\frac{\mathrm{d}\alpha(t)}{\mathrm{d}t} = v_1^T(t + \alpha(t)) D\big(x_s(t + \alpha(t))\big) b(t) \quad \alpha(0) = 0 \tag{3.10}$$

where $v_1(t)$ is the Floquet basis vector as defined in Section 3.2.2.

Remark 3.7 *The existence and uniqueness theorem for ordinary differential equations guarantees that $\alpha(t)$ exists and is unique.*

Remark 3.8 *$\alpha(t)$ can grow unbounded even if $b(t)$ remains small. For example, consider the case where $b(t)$ is a small positive constant $\epsilon \ll 1$, $D \equiv 1$, and $v_1(t)$ is a constant k. Then $\alpha(t) = k\epsilon t$.*

Having defined $\alpha(t)$, we are in a position to split $D(x)b(t)$ into $b_1(x,t)$ and $\tilde{b}(x,t)$. We consider the bi-orthogonal Floquet eigenvectors $\{u_i(t)\}$ and $\{v_i(t)\}$. Since $\{u_i(t)\}$ are linearly independent for all t, they span the n-dimensional space for all t. In particular they span this space for time $t+\alpha(t)$. We find the projection of the perturbation term $D(x)b(t)$ along the directions $\{u_i(t+\alpha(t))\}$. We call $b_1(x,t)$, the component along the direction $u_1(t+\alpha(t))$.

Definition 3.5 *Let*

$$b_1(x,t) = c_1(x,t)u_1(t+\alpha(t)) \tag{3.11}$$

and

$$\begin{aligned} \tilde{b}(x,t) &= D(x)b(t) - b_1(x,t) \\ &= \sum_{i=2}^{n} c_i(x,t)u_i(t+\alpha(t)) \end{aligned} \tag{3.12}$$

where the scalars $c_i(x,t)$ are given by

$$c_i(x,t) = v_i^T(t+\alpha(t))D(x)b(t)$$

Lemma 3.3 *$x_p(t) = x_s(t+\alpha(t))$ solves (3.9) (which is repeated here)*

$$\dot{x} = f(x) + b_1(x,t)$$

Proof: Substituting $x_s(t+\alpha(t))$ in (3.9) and using $\dot{x}_s(t) = u_1(t)$ we obtain

$$\dot{x}_s(t+\alpha(t))(1+\dot{\alpha}(t)) = f\big(x_s(t+\alpha(t))\big) + v_1^T(t+\alpha(t))D\big(x_s(t+\alpha(t))\big)b(t)u_1(t+\alpha(t))$$

Since $x_s(t)$ satisfies $\dot{x} = f(x)$ for all time, in particular time $t+\alpha(t)$, the above expression simplifies to

$$\dot{\alpha}(t)u_1(t+\alpha(t)) = v_1^T(t+\alpha(t))D\big(x_s(t+\alpha(t))\big)b(t)u_1(t+\alpha(t))$$

or

$$\dot{\alpha}(t) = v_1^T(t+\alpha(t))D\big(x_s(t+\alpha(t))\big)b(t)$$

$\alpha(t)$ and $c_1(t)$ are scalars while $u_1(t)$ and $v_1(t)$ are vectors. In the above reduction we have used the fact that for any t, all the entries of $\dot{x}_s(t)$ and hence $u_1(t)$ cannot be simultaneously zero otherwise the oscillator will cease to oscillate. ∎

With Lemma 3.3, we have shown that the $b_1(x,t)$ component causes deviations only along the limit cycle, i.e., phase deviations. Next, we show that the remaining perturbation component $\tilde{b}(x,t)$ perturbs $x_p(t)$ only by a small amount $y(t)$, provided $b(t)$ is small. We first make the following useful observation.

Lemma 3.4 *For $b(t)$ sufficiently small, the mapping $t \mapsto t+\alpha(t)$ is invertible.*

Proof: It suffices to show that $s(t) = t+\alpha(t)$ is strictly monotonic. The time derivative of this function is $1+\dot{\alpha}(t)$. Now

$$\dot{\alpha}(t) = v_1^T(t+\alpha(t))D\big(x_s(t+\alpha(t))\big)b(t)$$

The terms $v_1^T(\cdot)$ and $D(x_s(\cdot))$ are both bounded because they are periodic with t. Hence $|\dot{\alpha}(t)|$ can be made less than 1 if $b(t)$ is small enough. Since the derivative of the mapping will then be strictly greater than 0, the mapping will be invertible. ∎

Definition 3.6 *Let $b(t)$ be small enough that $s(t) = t+\alpha(t)$ is invertible. Then define $\hat{b}(\cdot)$ by:*

$$\hat{b}(s(t)) = b(t)$$

Definition 3.7 *Define*

$$y(t) = \sum_{i=2}^{n} u_i(s) \int_0^s \exp\left(\mu_i(s-r)\right) v_i^T(r) D(x_s(r)) \hat{b}(r) \mathrm{d}r$$

where $s = t+\alpha(t)$.

Remark 3.9 *In the above definition of $y(t)$ the index of the summation starts from 2. Since $|\exp(\mu_i T)| < 1, i \geq 2$ (due to asymptotic orbital stability), this implies that $y(t)$ is within a constant factor of $b(t)$, hence small and bounded for all t.*

Theorem 3.5 *If $b(t)$ is small (implying that $y(t)$ in Definition 3.7 is also small), then*

$$z(t) = x_p(t) + y(t)$$

solves (3.8) to first order in $y(t)$.

Proof: Consider (3.9) perturbed by $\tilde{b}(x,t)$ to obtain (3.8). Assume the solution to be $z(t) = x_p(t) + y(t)$. Then we have:

$$\dot{x}_p(t) + \dot{y}(t) = f\left(x_p(t) + y(t)\right) + b_1(x_p(t) + y(t), t) + \tilde{b}(x_p(t) + y(t), t)$$

Ignoring higher order terms in $b(t)$ and $y(t)$, and using Lemma 3.3 we have

$$\dot{y}(t) \approx \left.\frac{\partial f}{\partial x}\right|_{x_p(t)} y(t) + \tilde{b}(x_p(t), t)$$

or equivalently

$$\dot{y}(t) \approx J(t + \alpha(t))y(t) + \tilde{b}\big(x_s(t + \alpha(t)), t\big)$$

with

$$J(x) = \left.\frac{\partial f}{\partial x}\right|_{x_s(t)}$$

Now we define $s(t) = t + \alpha(t)$, and apply Lemma 3.4 to invert $s(t)$ in order to define

$$\hat{y}(s) = y(t) \tag{3.13}$$

and

$$\hat{b}(x_s(s(t)), s(t)) = \tilde{b}\big(x_s(s(t)), t\big) = D\big(x_s(s(t))\big)b(t) = D\big(x_s(s(t))\big)\hat{b}(s(t)) \tag{3.14}$$

Now we substitute $z(t) = y(t) + x_p(t)$ in (3.2) and come up with a differential equation for $y(t)$. We again assume that $||y(t)|| \ll ||x_p(t)||$. We observe that

$$\begin{aligned}\dot{x}_s(t + \alpha(t))(1 + \dot{\alpha}(t)) + \dot{y}(t) &= f(x_p(t) + y(t)) + D(x_s(t + \alpha(t)) + y(t))b(t) \\ &\approx f(x_p(t)) + \left.\frac{\partial f(x)}{\partial x}\right|_{x_s(t+\alpha(t))} y(t) \\ &\quad + D\big(x_s(t + \alpha(t))\big)b(t) + \left.\frac{\partial D(x)}{\partial x}\right|_{x_s(t+\alpha(t))} y(t)b(t)\end{aligned} \tag{3.15}$$

Since

$$\left.\frac{\partial D}{\partial x}\right|_{x_s(t+\alpha(t))} y(t)b(t)$$

is linear in both $y(t)$ and $b(t)$, it can be written as $M\big(x_s(t+\alpha(t)),b(t)\big)y(t)$ for some $M(\cdot)$. Moreover, since $M(\cdot)$ is linear in $b(t)$, it is small when $b(t)$ is small. Specifically, we can make $M\big(x_s(t+\alpha(t)),b(t)\big) \ll \frac{\partial f}{\partial x}\big(x_s(t+\alpha(t))\big)$ and hence this term can be ignored in (3.15) which is rewritten as

$$\begin{aligned}
\frac{\mathrm{d}y(t)}{\mathrm{d}t} &= \left.\frac{\partial f(x)}{\partial x}\right|_{x_p(t)} y(t) + D\big(x_s(t+\alpha(t))\big)b(t) \\
&\quad - v_1^T(t+\alpha(t))D\big(x_s(t+\alpha(t))\big)b(t)u_1(t+\alpha(t)) \\
\Rightarrow \quad \frac{\mathrm{d}y(t)}{\mathrm{d}t} &= \left.\frac{\partial f(x)}{\partial x}\right|_{x_p(t)} y(t) + \tilde{b}\big(x_s(t+\alpha(t)),t\big) \\
\Rightarrow \quad \frac{\mathrm{d}\hat{y}(s)}{\mathrm{d}s}\left(1+\frac{\mathrm{d}\alpha}{\mathrm{d}t}\right) &= \left.\frac{\partial f(x)}{\partial x}\right|_{x_s(s)} \hat{y}(s) + \hat{b}(x_s(s),s)
\end{aligned}$$

From (3.10), we conclude that $\dot{\alpha}$ is bounded to within a constant multiple of $b(t)$, hence $|\dot{\alpha}| \ll 1$ if $|b(t)| \ll 1$. Hence we can approximate $1+\dot{\alpha}$ by 1 to obtain

$$\frac{\mathrm{d}\hat{y}(s)}{\mathrm{d}s} \approx J(x_s(s))\hat{y}(s) + \hat{b}(x_s(s),s)$$

The above equation is of the same form as (3.3), hence its solution is of the form

$$\hat{y}(s) = \sum_{i=1}^{n} u_i(s) \int_0^s \exp\left(\mu_i(s-r)\right) v_i^T(r)\hat{b}(x_s(r),r)\mathrm{d}r$$

Consider the $i=1$ term of the above expression. Since $\mu_1 = 0$, the integrand equals the $v_1^T(r)\hat{b}(x_s(r),r)$. From its definition in (3.14), it is clear that $\hat{b}$, expressed in the basis $\{u_i(\cdot)\}$, contains no u_1 component. Therefore, by bi-orthogonality of $\{u_i(\cdot)\}$ and $\{v_i(\cdot)\}$, $v_1^T(r)\hat{b}(x_s(r),r)$ is identically zero, hence the $i=1$ term vanishes. The expression for $y(t)$ then becomes

$$y(t) = \hat{y}(\hat{t}) = \sum_{i=2}^{n} u_i(s) \int_0^s \exp\left(\mu_i(s-r)\right) v_i^T(r)\hat{b}(x_s(r),r)\mathrm{d}r$$

or equivalently

$$y(t) = \sum_{i=2}^{n} u_i(s) \int_0^{\hat{t}} \exp\left(\mu_i(\hat{t}-r)\right) v_i^T(r)D(x_s(r))\hat{b}(r)\mathrm{d}r$$

■

Hence we see that the perturbed oscillator output can be decomposed into a phase deviation term $x_s(t+\alpha(t))$ and the amplitude deviation term $y(t)$. We will use these results to develop phase noise characterization for oscillators.

3.4 Example

We conclude this chapter by demonstrating our perturbation analysis technique. We perform a perturbation analysis of probably the most celebrated oscillator in literature; the van der Pol oscillator [vdP22]. The reason for this choice is that we can analytically compute the approximate response of the free running and forced (which in our case would be perturbed) van der Pol oscillator. We need this to compute the Floquet eigenvectors needed for our analysis. This example is somewhat contrived since this oscillator is traditionally analyzed by treating the weak nonlinearity as a perturbation term. In our case however, we treat the forcing term as the perturbation term.

3.4.1 The van der Pol Oscillator

The van der Pol oscillator equation is given by

$$\ddot{x} + \mu(x^2 - 1)\dot{x} + \omega_0^2 x = 0$$

We use the Lindstedt-Poincaré method to calculate the response of the oscillator [Hag81, NM79]. In order to calculate the angular frequency ω, we introduce normalized time $\tau = \omega t$. Then the above equation changes to

$$\omega^2 x'' + \mu\omega(x^2 - 1)x' + \omega_0^2 x = 0 \tag{3.16}$$

where the primes indicate derivative with respect to τ. We assume that ω and $x(\tau)$ can be expanded in terms of the power series of μ, i.e.,

$$\begin{aligned} \omega &= \omega_0 + \mu\omega_1 + \mu^2\omega_2 + \mu^3\omega_3 + \dots \\ x(\tau) &= x_0(\tau) + \mu x_1(\tau) + \mu^2 x_2(\tau) + \mu^3 x_3(\tau) + \dots \end{aligned} \tag{3.17}$$

Substituting this in (3.16) we have

$$\begin{aligned} &[\omega_0^2 + 2\mu\omega_0\omega_1 + \mu^2(\omega_1^2 + 2\omega_0\omega_1) + \mu^3(2\omega_1\omega_2 + 2\omega_0\omega_3) + \dots](x_0'' + \mu x_1'' + \mu^2 x_2'' + \dots) \\ &+ \mu(\omega_0 + \mu\omega_1 + \mu^3\omega_3 + \mu^2\omega_2 + \dots)[x_0^2 - 1 + 2\mu x_0 x_1 + \mu^2(x_1^2 + 2x_0x_2) + \mu^3(2x_1x_2 \\ &+ 2x_0x_3) + \dots](x_0' + \mu x_1' + \mu^2 x_2' + \mu^3 x_3') + \omega_0^2(x_0 + \mu x_1 + \mu^2 x_2 + \mu^3 x_3 + \dots) = 0 \end{aligned}$$

Collecting the coefficients of various powers of μ and equating them to zero we have

$$\mu^0: \quad \omega_0^2 x_0'' + \omega_0^2 x_0 = 0 \tag{3.18}$$

$$\mu^1: \quad \omega_0^2 x_1'' + 2\omega_0\omega_1 x_0'' + \omega_0(x_0^2 - 1)x_0' + \omega_0^2 x_1 = 0 \tag{3.19}$$

$$\mu^2: \quad \begin{aligned} &\omega_0^2 x_2'' + 2\omega_0\omega_1 x_1'' + (\omega_1^2 + 2\omega_0\omega_2)x_0'' + \omega_0(x_0^2 - 1)x_1' + 2\omega_0 x_0 x_1 x_0' \\ &+\omega_1(x_0^2 - 1)x_0' + \omega_0^2 x_2 = 0 \end{aligned} \tag{3.20}$$

$$\mu^3: \quad \begin{aligned} &\omega_0^2 x_3'' + 2\omega_0\omega_1 x_2'' + (\omega_1^2 + 2\omega_0\omega_2)x_1'' + (2\omega_1\omega_2 + 2\omega_0\omega_3)x_0'' + \omega_0(x_0^2 - 1)x_2' \\ &+2\omega_0 x_0 x_1 x_1' + \omega_0(x_1^2 + 2x_0 x_2)x_0' + \omega_1(x_0^2 - 1)x_1' + 2\omega_1 x_0 x_1 x_0' \\ &+\omega_2(x_0^2 - 1)x_0' + \omega_0^2 x_3 = 0 \end{aligned} \tag{3.21}$$

(3.18) has a general solution of the form

$$x_0(\tau) = A_0 \cos\tau + B_0 \sin\tau$$

where A_0 and B_0 are arbitrary constants. Since (3.16) is autonomous and since only the periodic solution is of interest, we choose $x'(0) = 0$, and satisfy this condition by choosing $x_i'(0) = 0$ for all i. This implies $B_0 = 0$ and

$$x_0(\tau) = A_0 \cos\tau \tag{3.22}$$

Rearranging (3.19), we have

$$x_1'' + x_1 = -2\frac{\omega_1}{\omega_0}x_0'' - \frac{1}{\omega_0}(x_0^2 - 1)x_0'$$

Substituting the value of x_0 from (3.22) in the above equation we have

$$\begin{aligned} x_1'' + x_1 &= 2A_0\frac{\omega_1}{\omega_0}\cos\tau + \frac{1}{\omega_0}(A_0^2\cos^2\tau - 1)A_0\sin\tau \\ &= 2A_0\frac{\omega_1}{\omega_0}\cos\tau + \frac{A_0}{\omega_0}\left(\frac{A_0^2}{4} - 1\right)\sin\tau + \frac{A_0^3}{4\omega_0}\sin 3\tau \end{aligned}$$

For the above equation to have periodic solution, the coefficients of $\sin\tau$ and $\cos\tau$ should be zero, i.e.,

$$2A_0\frac{\omega_1}{\omega_0} = 0 \quad \text{and} \quad \frac{A_0}{\omega_0}\left(1 - \frac{1}{4}A_0^2\right) = 0$$

which has a nontrivial solution $A_0 = 2$ and $\omega_1 = 0$. I.e., (3.22) becomes

$$x_0(\tau) = 2\cos\tau \tag{3.23}$$

and equation for x_1 becomes

$$x_1'' + x_1 = \frac{2}{\omega_0}\sin 3\tau$$

The above equation has a general solution of the form

$$x_1(\tau) = A_1\cos\tau + B_1\sin\tau - \frac{1}{4\omega_0}\sin 3\tau$$

where A_1 and B_1 are constants yet to be determined. Requiring $x_1'(0) = 0$ we obtain $B_1 = 3/(4\omega_0)$, i.e.,

$$x_1(\tau) = A_1\cos\tau + \frac{3}{4\omega_0}\sin\tau - \frac{1}{4\omega_0}\sin 3\tau \tag{3.24}$$

Using the fact that $\omega_1 = 0$ and the form of $x_0(\tau)$ and $x_1(\tau)$ ((3.23) and (3.24)), (3.20) is rewritten as

$$\begin{aligned} x_2'' + x_2 &= -2\frac{\omega_2}{\omega_0}x_0'' - \frac{1}{\omega_0}(x_0^2 - 1)x_1' - \frac{2}{\omega_0}x_0x_1x_0' \\ &= \left(\frac{4\omega_2}{\omega_0} + \frac{1}{4\omega_0^2}\right)\cos\tau + \frac{2A_1}{\omega_0}\sin\tau + \frac{3A_1}{\omega_0}\sin 3\tau - \frac{3}{2\omega_0^2}\cos 3\tau + \frac{5}{4\omega_0^2}\cos 5\tau \end{aligned}$$

The assumed periodicity of the solution requires that the coefficients of $\cos\tau$ and $\sin\tau$ be zero, i.e., $\omega_2 = -1/(16\omega_0)$ and $A_1 = 0$. Hence the equation governing x_2 becomes

$$x_2'' + x_2 = -\frac{3}{2\omega_0^2}\cos 3\tau + \frac{5}{4\omega_0^2}\cos 5\tau$$

which has a solution

$$x_2(\tau) = A_2\cos\tau + B_2\sin\tau + \frac{3}{16\omega_0^2}\cos 3\tau - \frac{5}{96\omega_0^2}\cos 5\tau$$

where A_2 and B_2 are constants yet to be determined. Since $x_2'(0) = 0$, $B_2 = 0$.

Using $\omega_1 = 0$ and $\omega_2 = -1/(16\omega_0)$, (3.21) is rewritten as

$$\begin{aligned} x_3'' + x_3 &= \frac{1}{8\omega_0^2}x_1'' - 2\frac{\omega_3}{\omega_0}x_0'' - \frac{1}{\omega_0}(x_0^2 - 1)x_2' - \frac{2}{\omega_0}x_0x_1x_1' - \frac{1}{\omega_0}(x_1^2 + 2x_0x_2)x_0' \\ &\quad + \frac{1}{16\omega_0^3}(x_0^2 - 1)x_0' \\ &= \left(\frac{1}{4\omega_0^3} + \frac{2A_2}{\omega_0}\right)\sin\tau + \frac{4\omega_3}{\omega_0}\cos\tau + \left(\frac{3A_2}{\omega_0} - \frac{9}{32\omega_0^3}\right)\sin 3\tau + \frac{35}{24\omega_0^3}\sin 5\tau \\ &\quad - \frac{7}{12\omega_0^3}\sin 7\tau \end{aligned}$$

The coefficients of $\sin\tau$ and $\cos\tau$ are zero hence $A_2 = -1/(8\omega_0^2)$ and $\omega_3 = 0$.

Hence we conclude that

$$\omega = \omega_0 \left(1 - \frac{\mu^2}{16\omega_0^2}\right) + \dots \tag{3.25}$$

and the solution $x(\tau)$ of (3.16) is

$$x(\tau) = \left(2 - \frac{\mu^2}{8\omega_0^2}\right)\cos\tau + \frac{3\mu}{4\omega_0}\sin\tau - \frac{\mu}{4\omega_0}\sin 3\tau + \frac{5\mu^2}{16\omega_0^2}\cos 3\tau - \frac{5\mu^2}{96\omega_0^2}\cos 5\tau + \dots \tag{3.26}$$

Assuming that the nonlinearity is small, i.e., μ is small, terms of the order of μ^3 and above have been neglected in the above expansion.

3.4.2 Forced van der Pol Oscillator Equation

Next we find the solution of the forced van der Pol oscillator. We assume that this oscillator is forced by a *small* forcing signal $K\cos\gamma t$ where γ and ω are incommensurable and that $K \ll 1$. Then the forced van der Pol oscillator equation becomes

$$\ddot{x} + \mu(x^2 - 1)\dot{x} + \omega_0^2 x + K\cos\gamma t = 0$$

Introducing $\tau = \omega t$ we rewrite the above equation as

$$\omega^2 x'' + \mu\omega(x^2 - 1)x' + \omega_0^2 x + K\cos\beta\tau = 0 \tag{3.27}$$

where $\beta = \frac{\gamma}{\omega}$. Assuming the same form of ω and $x(\tau)$ as in (3.17), substituting it in (3.27) and equating the coefficients of various powers of μ we find that the equations governing x_i, $i > 0$ are the same as (3.19)–(3.21). However, since the solution of the equation for x_0 changes with the introduction of the perturbation term, $x_i(\tau)$s also need to recomputed. The equation for x_0 changes to

$$\omega_0^2 x_0'' + \omega_0^2 x_0 + K\cos\beta\tau = 0$$

which has a solution

$$x_0(\tau) = C_0\cos\tau + D_0\sin\tau + \frac{K}{\omega_0^2(\beta^2 - 1)}\cos\beta\tau$$

where C_0 and D_0 are constants yet to be determined. Requiring as before that $x_i'(0) = 0$ we have $D_0 = 0$.

The equation governing $x_1(\tau)$ is written as

$$\begin{aligned}
x_1'' + x_1 &= -2\frac{\omega_1}{\omega_0}x_0'' - \frac{1}{\omega_0}(x_0^2-1)x_0' \\
&= \frac{2C_0\omega_1}{\omega_0}\cos\tau + \left(-\frac{C_0}{\omega_0} + \frac{C_0^3}{4\omega_0} + \frac{K^2C_0}{2\omega_0^5(\beta^2-1)^2}\right)\sin\tau + \frac{C_0^3}{4\omega_0}\sin 3\tau \\
&\quad + \frac{2K\beta^2\omega_1}{\omega_0^3(\beta^2-1)}\cos\beta\tau + \frac{K\beta}{\omega_0^3(\beta^2-1)}\left(-1 + \frac{C_0^2}{2} + \frac{K^2}{4\omega_0^4(\beta^2-1)^2}\right)\sin\beta\tau \\
&\quad + \frac{K^2C_0(2\beta+1)}{4\omega_0^5(\beta^2-1)^2}\sin(2\beta+1)\tau + \frac{K^2D_0(2\beta-1)}{4\omega_0^5(\beta^2-1)^2}\sin(2\beta-1)\tau \\
&\quad + \frac{K^3\beta}{4\omega_0^7(\beta^2-1)^3}\sin 3\beta\tau + \frac{C_0^2K(\beta-2)}{4\omega_0^3(\beta^2-1)}\sin(\beta-2)\tau + \frac{C_0^2K(\beta+2)}{4\omega_0^3(\beta^2-1)}\sin(2+\beta)\tau
\end{aligned}$$

In the above expansion we have used the fact that β and 1 are incommensurable and hence no terms involving sine and cosine of $\beta\tau$, or any multiples thereof, contribute to $\cos\tau$ or $\sin\tau$. Requiring that the coefficients of $\cos\tau$ and $\sin\tau$ vanish, we have $\omega_1 = 0$ and

$$C_0 = 2\sqrt{1 - \frac{K^2}{2\omega_0^4(\beta^2-1)^2}} \tag{3.28}$$

Even though we assumed $K \ll 1$, in general we cannot ignore the K^2 term in (3.28) since $K/(\beta^2-1)$ need not necessarily be small. The equation for x_1 is given by

$$\begin{aligned}
x_1'' + x_1 &= \frac{C_0^3}{4\omega_0}\sin 3\tau + \frac{K\beta}{\omega_0^3(\beta^2-1)}\left(1 - \frac{3K^2}{4\omega_0^4(\beta^2-1)^2}\right)\sin\beta\tau + \frac{K^3\beta}{4\omega_0^7(\beta^2-1)^3}\sin 3\beta\tau \\
&\quad + \frac{K^2C_0(2\beta+1)}{4\omega_0^5(\beta^2-1)^2}\sin(2\beta+1)\tau + \frac{K^2C_0(2\beta-1)}{4\omega_0^5(\beta^2-1)^2}\sin(2\beta-1)\tau \\
&\quad + \frac{C_0^2K(\beta-2)}{4\omega_0^3(\beta^2-1)}\sin(\beta-2)\tau + \frac{C_0^2K(\beta+2)}{4\omega_0^3(\beta^2-1)}\sin(2+\beta)\tau
\end{aligned}$$

The solution to this equation is given by

$$\begin{aligned}
x_1 &= C_1\cos\tau + D_1\sin\tau - \frac{C_0^3}{32\omega_0}\sin 3\tau - \frac{K\beta}{\omega_0^3(\beta^2-1)^2}\left(1 - \frac{3K^2}{4\omega_0^4(\beta^2-1)^2}\right)\sin\beta\tau \\
&\quad - \frac{K^3\beta}{4\omega_0^7(\beta^2-1)^3(9\beta^2-1)}\sin 3\beta\tau - \frac{K^2C_0(2\beta+1)}{16\omega_0^5(\beta^2-1)^2\beta(\beta+1)}\sin(2\beta+1)\tau \\
&\quad - \frac{K^2C_0(2\beta-1)}{16\omega_0^5(\beta^2-1)^2\beta(\beta-1)}\sin(2\beta-1)\tau - \frac{C_0^2K(\beta-2)}{4\omega_0^3(\beta^2-1)(\beta-)(\beta-1)}\sin(\beta-2)\tau \\
&\quad - \frac{C_0^2K(\beta+2)}{4\omega_0^3(\beta^2-1)(\beta+3)(\beta+1)}\sin(2+\beta)\tau
\end{aligned}$$

where C_1 and D_1 are constants yet to be determined. Requiring that $x_1'(0) = 0$, we have

$$D_1 = \frac{3C_0^3}{32\omega_0} + \frac{K\beta^2}{\omega_0^3(\beta^2-1)^2} + \frac{K^2C_0(4\beta-3)}{8\omega_0^5(\beta^2-1)^3} + \frac{C_0^2K\beta(\beta^2-5)}{2\omega_0^3(\beta^2-1)^2(\beta^2-9)} \tag{3.29}$$

The equation governing x_2 is written as

$$\begin{aligned}
x_2'' + x_2 &= -2\frac{\omega_2}{\omega_0}x_0'' - \frac{1}{\omega_0}(x_0^2-1)x_1' - \frac{2}{\omega_0}x_0x_1x_0' \\
&= C_1\left(\frac{2}{\omega_0} + \frac{K^2}{\omega_0^5(\beta^2-1)^2}\right)\sin\tau - \Big[4\beta^{12}\omega_0^8 + 64\omega_0^9\omega_2\beta^{12} - 896\omega_0^9\omega_2\beta^10 - 56\beta^{10}\omega_0^8 \\
&\quad + 220\beta^8\omega_0^8 - 4K^2\beta^8\omega_0^4 + 3520\omega_0^9\omega_2\beta^8 - 16K^2\omega_0^4\beta^6 - 400\omega_0^8\beta^6 - 6400\omega_0^9\omega_2\beta^6 \\
&\quad + K^4\beta^4 + 380\omega_0^8\beta^4 + 200K^2\omega_0^4 + 6080\omega_0^9\omega_2\beta^4 + 21K^4\beta^2 - 2944\omega_0^9\omega_2\beta^2 \\
&\quad - 184\omega_0^8\beta^2 - 336K^2\omega_0^4\beta^2 + 156K^2\omega_0^4 + 36\omega_0^8 - 78K^4 + 576\omega_0^9\omega_2\Big] \\
&\quad \frac{C_0}{32(\beta^2-1)(\beta^2-1)^4}\cos\tau + \ldots
\end{aligned}$$

In the last expansion, only the coefficients of $\sin\tau$ and $\cos\tau$ have been retained. Since these coefficients should be zero, we conclude that $C_1 = 0$ and

$$\omega_2 = -\frac{1}{16\omega_0} - \frac{K^2(\beta^4+4\beta^2-39)}{16\omega_0^5(\beta^2-9)(\beta^2-1)^3} + \frac{K^4(\beta^4+21\beta^2-78)}{64\omega_0^9(\beta^2-9)(\beta^2-1)^5}$$

Hence the response of the forced van der Pol oscillator is given by

$$\begin{aligned}
x(\tau) &= C_0\cos\tau + \mu D_1\sin\tau - \frac{\mu C_0^3}{32\omega_0}\sin 3\tau - \frac{\mu K\beta}{\omega_0^3(\beta^2-1)^2}\left(1 - \frac{3K^2}{4\omega_0^4(\beta^2-1)^2}\right)\sin\beta\tau \\
&\quad - \frac{\mu K^3\beta}{4\omega_0^7(\beta^2-1)^3(9\beta^2-1)}\sin 3\beta\tau - \frac{\mu K^2C_0(2\beta+1)}{16\omega_0^5(\beta^2-1)^2\beta(\beta+1)}\sin(2\beta+1)\tau \\
&\quad - \frac{\mu K^2C_0(2\beta-1)}{16\omega_0^5(\beta^2-1)^2\beta(\beta-1)}\sin(2\beta-1)\tau - \frac{\mu C_0^2K(\beta-2)}{4\omega_0^3(\beta^2-1)(\beta-3)(\beta-1)}\sin(\beta-2)\tau \\
&\quad - \frac{\mu C_0^2K(\beta+2)}{4\omega_0^3(\beta^2-1)(\beta+3)(\beta+1)}\sin(2+\beta)\tau
\end{aligned} \tag{3.30}$$

where C_0 and D_1 are defined by (3.28) and (3.29) and

$$\omega = \omega_0 - \frac{\mu^2}{16\omega_0} - \frac{\mu^2K^2(\beta^4+4\beta^2-39)}{16\omega_0^5(\beta^2-9)(\beta^2-1)^3} + \frac{\mu^2K^4(\beta^4+21\beta^2-78)}{64\omega_0^9(\beta^2-9)(\beta^2-1)^5}$$

We now carry out a perturbation analysis of the forced van der Pol oscillator and obtain the phase error term $\alpha(t)$ and compare the phase shifted steady-state solution with (3.30).

3.4.3 Perturbation Analysis of the Forced van der Pol Oscillator

In order to perform a perturbation analysis of the van der Pol oscillator as described in Section 3.3, we rewrite (3.16) in form (3.1) by introducing two variables, $y_1(\tau) = x(\tau)$

and $y_2(\tau) = x'(\tau)$ as

$$y' = \begin{bmatrix} y_1' \\ y_2' \end{bmatrix} = \begin{bmatrix} y_2 \\ -\frac{\mu}{\omega}(y_1^2 - 1)y_2 - \frac{\omega_0^2}{\omega^2} y_1 \end{bmatrix}$$

The steady-state solution of this equation can obtained from (3.26) as

$$\begin{bmatrix} y_1(\tau) \\ y_2(\tau) \end{bmatrix} = \begin{bmatrix} \left(2 - \frac{\mu^2}{8\omega_0^2}\right)\cos\tau + \frac{3\mu}{4\omega_0}\sin\tau - \frac{\mu}{4\omega_0}\sin 3\tau + \frac{3\mu^2}{16\omega_0^2}\cos 3\tau - \frac{5\mu^2}{96\omega_0^2}\cos 5\tau + \dots \\ -\left(2 - \frac{\mu^2}{8\omega_0^2}\right)\sin\tau + \frac{3\mu}{4\omega_0}\cos\tau - \frac{3\mu}{4\omega_0}\cos 3\tau - \frac{9\mu^2}{16\omega_0^2}\sin 3\tau + \frac{25\mu^2}{96\omega_0^2}\sin 5\tau + \dots \end{bmatrix} \tag{3.31}$$

This solution is periodic (in τ) with period 2π. The Jacobian for this system of equations is given by

$$J(\tau) = \begin{bmatrix} 0 & 1 \\ -2\frac{\mu}{\omega}y_1 y_2 - \frac{\omega_0^2}{\omega^2} & -\frac{\mu}{\omega}(y_1^2 - 1) \end{bmatrix}$$

Since $y_1(\tau)$ and $y_2(\tau)$ are periodic, $J(\tau)$ is also periodic. To compute $v_1(\tau)$ (see Remark 3.6), we need to find the solution of

$$v' = -J^T(\tau)v$$

from $\tau = 0$ to $\tau = 2\pi$ subject to the initial condition $v_1(0)$ such that $v_1^T(0)u_1(0) = 1$. $v_1(0)$ is obtained by finding the eigenvector of $\Phi^T(2\pi, 0)$ corresponding to the eigenvalue 1, where $\Phi(\tau, \sigma)$ is the state transition matrix of the system of equations

$$u' = J(\tau)u \tag{3.32}$$

which has one of the solutions as $u_1(\tau) = y'(\tau)$. We first make the following useful observations.

Lemma 3.6 *Let*

$$W(\tau, \sigma) = \det \Phi(\tau, \sigma)$$

If $W(\sigma, \sigma) \neq 0$ *then*

$$W(\tau, \sigma) = W(\sigma, \sigma) \exp\left(\int_\sigma^\tau \mathrm{tr} J(t) \mathrm{d}t\right)$$

where $\mathrm{tr}J(t)$ *denotes the trace of the matrix* $J(t)$.

Proof: [Gri90] ∎

Lemma 3.7 *Let B be defined as in Section 3.2.1, i.e.,*

$$B = \Phi^{-1}(\tau, \sigma)\Phi(\tau + 2\pi, \sigma)$$

Then B is given by

$$\det B = \exp\left(\int_0^{2\pi} \mathrm{tr} J(\tau)\mathrm{d}\tau\right) \tag{3.33}$$

Proof: [Gri90] ∎

Let $\Phi(\tau, 0)$ be given by

$$\Phi(\tau, 0) = \begin{bmatrix} \phi_{11}(\tau) & \phi_{12}(\tau) \\ \phi_{21}(\tau) & \phi_{22}(\tau) \end{bmatrix}$$

where

$$\begin{bmatrix} \phi_{11}(\tau) \\ \phi_{21}(\tau) \end{bmatrix} \quad \text{and} \quad \begin{bmatrix} \phi_{12}(\tau) \\ \phi_{22}(\tau) \end{bmatrix}$$

are linearly independent solution of (3.32) such that $\phi_{11}(0) = 1$, $\phi_{21}(0) = 0$, $\phi_{12}(0) = 0$ and $\phi_{22}(0) = 1$. Therefore, the matrix B is given by

$$B = \begin{bmatrix} \phi_{11}(2\pi) & \phi_{12}(2\pi) \\ \phi_{21}(2\pi) & \phi_{22}(2\pi) \end{bmatrix}$$

The characteristic multipliers ρ of (3.32) are the eigenvalues of B and hence are given by

$$\rho^2 - (\phi_{11}(2\pi) + \phi_{22}(2\pi))\rho + \det B = 0$$

By Lemma 3.7 we have

$$\begin{aligned}
\det B &= \exp\left(\int_0^{2\pi} \mathrm{tr} J(\tau)\mathrm{d}\tau\right) \\
&= \exp\left(\int_0^{2\pi} -\frac{\mu}{\omega}(y_1^2 - 1)\mathrm{d}\tau\right) \\
&= \exp\left[-\frac{\pi\mu}{\omega}\left(4 + \frac{\mu^2}{2\omega_0^2} + \frac{9\mu^2}{16\omega_0^2} + \frac{\mu^2}{16\omega_0^2} - 2\right)\right] \\
&= \exp\left[-\frac{2\mu\pi}{\omega_0}\left(1 + \frac{9\mu^2}{16\omega_0^2}\right)\left(1 - \frac{\mu^2}{16\omega_0^2}\right)^{-1}\right] \\
&= \exp\left[-\frac{2\mu\pi}{\omega_0}\left(1 + \frac{5\mu^2}{8\omega_0^2}\right)\right]
\end{aligned}$$

where we have neglected the terms corresponding to μ^4. Since (3.16) has a periodic solution, the time derivative of the steady-state solution is a solution for (3.32) and 1 is a characteristic multiplier. Also since $y_1'(0) = 0$, we have

$$\rho_2 = 1 \quad \text{and} \quad \rho_1 = \exp\left[-\frac{\pi\mu}{\omega_0}\left(2 + \frac{5\mu^2}{4\omega_0^2}\right)\right]$$

For positive μ and ω, $\rho_1 < 1$ and hence the oscillator is asymptotically orbitally stable.

Since $y_1'(0) = 0$, and $y'(\tau)$ is a periodic solution of (3.32) with period 2π, $\phi_{12}(2\pi) = 0$ and $\phi_{22}(2\pi) = 1$. Moreover since

$$\phi_{11}(2\pi) + \phi_{22}(2\pi) = \rho_1 + \rho_2$$

we have

$$\phi_{11}(2\pi) = \exp\left[-\frac{\pi\mu}{\omega_0}\left(2 + \frac{5\mu^2}{4\omega_0^2}\right)\right] = \rho_1$$

Hence B is of the form

$$B = \begin{bmatrix} \phi_{11}(2\pi) & 0 \\ \phi_{21}(2\pi) & 1 \end{bmatrix} = \begin{bmatrix} \frac{\phi_{11}(2\pi)-1}{\sqrt{(\phi_{11}(2\pi)-1)^2+\phi_{21}^2(2\pi)}} & 0 \\ \frac{\phi_{21}(2\pi)}{\sqrt{(\phi_{11}(2\pi)-1)^2+\phi_{21}^2(2\pi)}} & 1 \end{bmatrix} \begin{bmatrix} \phi_{11}(2\pi) & 0 \\ 0 & 1 \end{bmatrix} \begin{bmatrix} \frac{\sqrt{(\phi_{11}(2\pi)-1)^2+\phi_{22}^2(2\pi)}}{\phi_{11}(2\pi)-1} & 0 \\ -\frac{\phi_{21}(2\pi)}{\phi_{11}(2\pi)-1} & 1 \end{bmatrix}$$

and

$$v_1(0) = \frac{1}{-2 - \frac{25\mu^2}{96\omega_0^2}} \begin{bmatrix} -\frac{\phi_{21}(2\pi)}{\phi_{11}(2\pi)-1} \\ 1 \end{bmatrix}$$

We will not explicitly determine the first component of $v_1(0)$ but obtain it by asserting the periodicity of the solutions of $v' = -J^T(\tau)v$. This equation is rewritten as

$$\begin{bmatrix} v_{11}' \\ v_{21}' \end{bmatrix} = \begin{bmatrix} 0 & 2\frac{\mu}{\omega}y_1y_2 + \frac{\omega_0^2}{\omega^2} \\ -1 & \frac{\mu}{\omega}(y_1^2 - 1) \end{bmatrix} \begin{bmatrix} v_{11} \\ v_{21} \end{bmatrix}$$

or

$$v_{11}' = \left(2\frac{\mu}{\omega}y_1y_2 + \frac{\omega_0^2}{\omega^2}\right)v_{21} \tag{3.34}$$

$$v_{21}' = -v_{11} + \frac{\mu}{\omega}(y_1^2 - 1)v_{21} \tag{3.35}$$

Differentiating (3.35) and substituting for v_{11}' from (3.34) we have

$$\begin{aligned} v_{21}'' &= -v_{11}' + \frac{\mu}{\omega}(y_1^2 - 1)v_{21}' + 2\frac{\mu}{\omega}y_1y_1'v_{21} \\ &= -2\frac{\mu}{\omega}y_1y_2v_{21} - \frac{\omega_0^2}{\omega^2}v_{21} + \frac{\mu}{\omega}(y_1^2 - 1)v_{21}' + 2\frac{\mu}{\omega}y_1y_2v_{21} \end{aligned}$$

i.e.,

$$\omega^2 v_{21}'' - \mu\omega(y_1^2 - 1)v_{21}' + \omega_0^2 v_{21} = 0 \tag{3.36}$$

We know that this equation has a periodic solution with period 2π since (3.16) describes an asymptotically orbitally stable oscillator. We assume that the solution of (3.36) is of the form

$$v_{21}(\tau) = v_{21,0}(\tau) + \mu v_{21,1}(\tau) + \mu^2 v_{21,2}(\tau) + \mu^3 v_{21,3}(\tau) + \dots$$

Substituting this expression and the value of $y_1(\tau)$ in (3.36) we have

$$\begin{aligned}
&\omega_0^2\left(1 - \frac{\mu^2}{8\omega_0^2}\right)(v_{21,0}'' + \mu v_{21,1}'' + \mu^2 v_{21,2}'' + \mu^3 v_{21,3}'') - \mu\omega_0\left(1 - \frac{\mu^2}{16\omega_0^2}\right)\left(4\cos^2\tau - 1\right.\\
&+ \frac{3\mu}{\omega_0}\sin\tau\cos\tau - \frac{\mu}{\omega_0}\sin 3\tau\cos\tau - \frac{\mu^2}{2\omega_0^2}\cos^2\tau + \frac{9\mu^2}{16\omega_0^2}\sin^2\tau + \frac{\mu^2}{16\omega_0^2}\sin^2 3\tau\\
&\left.- \frac{3\mu^2}{8\omega_0^2}\sin\tau\sin 3\tau + \frac{3\mu^2}{4\omega_0^2}\cos\tau\cos 3\tau - \frac{5\mu^2}{24\omega_0^2}\cos\tau\cos 5\tau\right)(v_{21,0}' + \mu v_{21,1}' + \mu^2 v_{21,2}'\\
&+ \mu^3 v_{21,3}') + \omega_0^2(v_{21,0} + \mu v_{21,1} + \mu^2 v_{21,2} + \mu^3 v_{21,3}) = 0
\end{aligned}$$

In the above expansion, only terms up to the power of μ^3 have been considered. Equating the coefficient of μ^0 to zero we have

$$\omega_0^2 v_{21,0}'' + \omega_0^2 v_{21,0} = 0$$

which has a solution

$$v_{21,0}(\tau) = A_0\cos\tau + B_0\sin\tau$$

where A_0 and B_0 are constants. Since $u(0)v^T(0) = 1$ and from (3.31) we know that

$$u(0) = \begin{bmatrix} y_1'(0) \\ y_2'(0) \end{bmatrix} = \begin{bmatrix} 0 \\ -2 - \frac{25\mu^2}{96\omega_0^2} \end{bmatrix}$$

Therefore

$$v_{21}(0) = \frac{1}{-2 - \frac{25\mu^2}{96\omega_0^2}} \approx -\frac{1}{2}\left(1 - \frac{25\mu^2}{192\omega_0^2}\right)$$

and we have $v_{21,0}(0) = -1/2$ and $v_{21,1}(0) = 0$ and

$$v_{21,2}(0) = \frac{25}{384\omega_0^2}$$

This implies $A_0 = -1/2$. Equating the coefficients of μ to zero we have

$$\omega_0^2 v_{21,1}'' - \omega_0(4\cos^2\tau - 1)v_{21,0}' + \omega_0^2 v_{21,1} = 0$$

or equivalently

$$v_{21,1}'' + v_{21,1} = \frac{1}{2\omega_0}\sin 3\tau - \frac{2B_0}{\omega_0}\cos\tau - \frac{B_0}{\omega_0}\cos 3\tau$$

For this equation to have a periodic solution the coefficient of $\cos\tau$ term should be zero, i.e., $B_0 = 0$. The equation governing $v_{21,1}$ becomes

$$v_{21,1}'' + v_{21,1} = \frac{1}{2\omega_0}\sin 3\tau$$

which has a solution

$$v_{21,1}(\tau) = A_1\cos\tau + B_1\sin\tau - \frac{1}{16\omega_0}\sin 3\tau$$

where A_1 and B_1 are constants yet to be determined. Requiring that $v_{21,1}(\tau) = 0$, we have $A_1 = 0$. Equating the coefficient of μ^2 to zero we have

$$\omega_0^2 v_{21,2}'' - \frac{1}{8}v_{21,0}'' + \omega_0^2 v_{21,2} - (3\sin\tau\cos\tau - \sin 3\tau\cos\tau)v_{21,0}' - \omega_0(4\cos^2\tau - 1)v_{21,1}' = 0$$

or equivalently

$$\begin{aligned} v_{21,2}'' + v_{21,2} &= \frac{1}{16\omega_0^2}\cos\tau + \frac{1}{\omega_0}(4\cos^2\tau - 1)\left(B_1\cos\tau - \frac{3}{16\omega_0}\cos 3\tau\right) \\ &\quad + \frac{1}{2\omega_0^2}\cos\tau\sin\tau(3\sin\tau - \sin 3\tau) \\ &= \left(\frac{2B_1}{\omega_0} + \frac{1}{8\omega_0^2}\right)\cos\tau + \left(\frac{B_1}{\omega_0} - \frac{9}{16\omega_0^2}\right)\cos 3\tau - \frac{1}{16\omega_0^2}\cos 5\tau \end{aligned}$$

Since the coefficient of $\cos\tau$ should be zero for $v_{21}(\tau)$ to have a periodic solution, $B_1 = -1/(16\omega_0)$ and the above equation reduces to

$$v_{21,2}'' + v_{21,2} = -\frac{5}{8\omega_0^2}\cos 3\tau - \frac{1}{16\omega_0^2}\cos 5\tau$$

which has a solution

$$v_{21,2}(\tau) = A_2\cos\tau + B_2\sin\tau + \frac{5}{64\omega_0^2}\cos 3\tau + \frac{1}{384\omega_0^2}\cos 5\tau$$

Requiring that $v_{21,2}(0) = 25/(384\omega_0^2)$ we have $A_2 = -1/(64\omega_0^2)$. Equating the coefficient of μ^3 to zero equating the coefficient of $\cos\tau$ to zero we have $B_2 = 0$. Hence $v_{21}(\tau)$ is given by

$$v_{21}(\tau) = -\left(\frac{1}{2} + \frac{\mu^2}{64\omega_0^2}\right)\cos\tau - \frac{\mu}{16\omega_0}\sin\tau - \frac{\mu}{16\omega_0}\sin 3\tau + \frac{5\mu^2}{64\omega_0^2}\cos 3\tau + \frac{\mu^2}{384\omega_0^2}\cos 5\tau$$

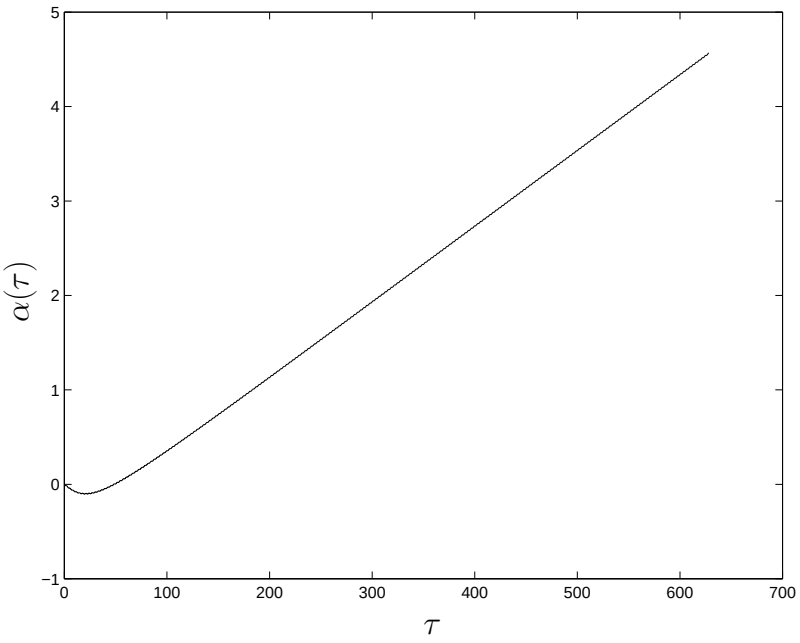

Figure 3.3: Phase deviation $\alpha(\tau)$ of the forced van der Pol oscillator

For the forced van der Pol oscillator, we have the forcing term as the perturbation term for the purpose our analysis. From (3.10) we have

$$\begin{aligned}\alpha' &= v_1^T(\tau+\alpha(\tau))D(x_s(\tau+\alpha(\tau))b(\tau)\\ &= \begin{bmatrix} v_{11}(\tau+\alpha(\tau)) & v_{21}(\tau+\alpha(\tau))\end{bmatrix}\begin{bmatrix}0\\ -K\cos\beta\tau\end{bmatrix}\\ &= -Kv_{21}(\tau+\alpha(\tau))\cos\beta\tau\end{aligned}$$

The variation of $\alpha(\tau)$ for $\omega_0 = 1$, $\mu = 0.2$, $\beta = \pi/3$ and $K = 0.1$ is shown in Figure 3.3. We see that this phase deviation keeps increasing without bounds. Figure 3.4 shows the forced oscillator response $z(\tau)$ and the steady-state response phase shifted by the amount $\alpha(\tau)$. We see that the two waveforms differ in amplitude but not in phase even for large τ.

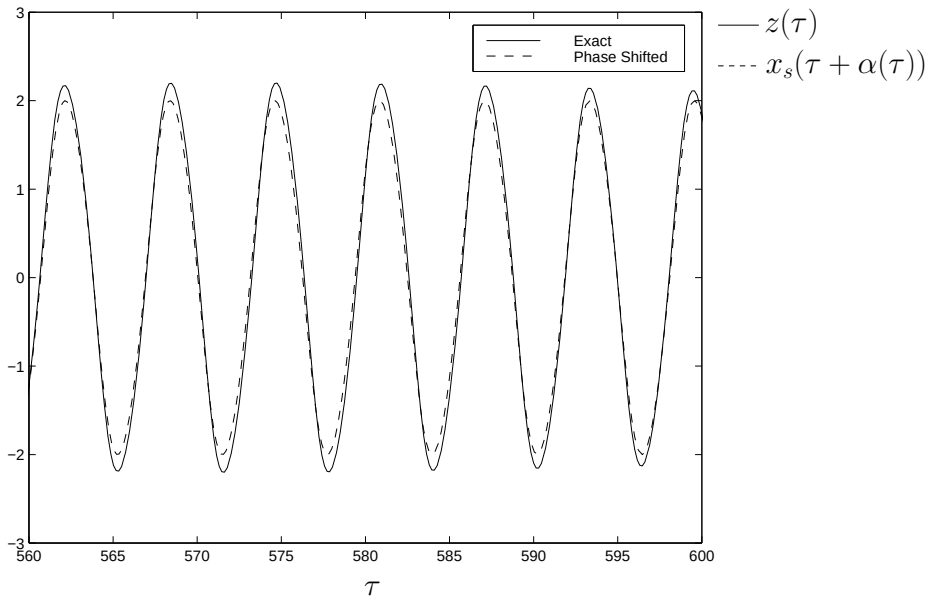

Figure 3.4: Exact ($z(\tau)$) and phase shifted ($x_s(\tau + \alpha(\tau))$) response of the forced van der Pol oscillator

Chapter 4

Noise Analysis of Stable Oscillators

In Chapter 3 we developed a new perturbation analysis technique suitable for stable oscillators. We showed that it is not mathematically consistent to view the perturbed oscillator response as the sum of pure tones (unperturbed oscillator response) and a small deviation. Rather, the perturbed oscillator output should be viewed as a sum of two signals: unperturbed oscillator output phase shifted by $\alpha(t)$ along the limit cycle (Definition 3.4) and a small deviation away from the limit cycle. In case of stochastic perturbations, the oscillator output is a stochastic process which can also be viewed as a sum of two stochastic processes: phase noise and amplitude noise process. Since phase noise is the dominant effect in the oscillator response we will not concentrate on amplitude noise at present. We begin by obtaining a stochastic characterization of the phase deviation $\alpha(t)$ which we use to obtain the time domain and frequency domain characterization of the output of noisy oscillator. We give efficient numerical techniques, both in time and frequency domain for characterization of the output of a noisy oscillator. We conclude this chapter with some examples of electrical circuits which have been analyzed with this technique.

4.1 Stochastic Characterization of Phase Deviation

In the previous chapter we saw that an oscillatory system of equation

$$\dot{x} = f(x)$$

describes an asymptotically orbitally stable limit cycle and has a T-periodic steady-state solution $x_s(t)$. When this system of equations is perturbed by a small perturbation term

$D(x)b(t)$, the resulting oscillator output can be approximated by phase shifting the unperturbed response by an amount $\alpha(t)$ given by

$$\frac{\mathrm{d}\alpha(t)}{\mathrm{d}t} = v_1^T(t+\alpha(t))D\big(x_s(t+\alpha(t))\big)b(t)$$

We now characterize the phase deviation α when the perturbation $b(t)$ is a vector of uncorrelated white noise sources $\xi(t)$, i.e.,

$$\frac{\mathrm{d}\alpha(t)}{\mathrm{d}t} = v_1^T(t+\alpha(t))D\big(x_s(t+\alpha(t))\big)\xi(t) \tag{4.1}$$

The extension to correlated noise sources is trivial. We consider uncorrelated noise sources for notational simplicity. Moreover, various noise sources in electronic devices usually have independent physical origin, and hence they are modelled as uncorrelated stochastic processes. Since the input to this equation is now a stochastic process, the output $\alpha(t)$ is also a stochastic process and we need to treat (3.10) as a stochastic differential equation [Øks98, Arn74, Gar83] since the rules of ordinary calculus are no longer applicable.

The stochastic process α is a family $\{\alpha(t) : t \in \mathbb{R}_+\}$ of random variables indexed by time t and taking values in $\mathbb{R}$. Evaluation of the random variable $\alpha(t)$ at some time t yields a number in $\mathbb{R}$, and an evaluation of α for all $t \in \mathbb{R}_+$ is called a *realization* or *sample path* of the stochastic process α. The "complete" collection of the sample paths of the stochastic process α is called the *ensemble*. The $\alpha(t)$s (for different values of t) are not independent in general. If $t = [t_1, t_2, \ldots, t_n]$ is a vector taking values in $\mathbb{R}_+$, then the vector

$$[\alpha(t_1), \alpha(t_2), \ldots, \alpha(t_n)]$$

has the joint distribution function $F_d(\eta, t) : \mathbb{R}^n \to [0, 1]$ given by

$$F_d(\eta, t) = \mathbb{P}\left[\alpha(t_1) \leq \eta_1, \ldots, \alpha(t_n) \leq \eta_n\right]$$

where $\mathbb{P}[\cdot]$ denotes the *probability measure*. The collection $\{F(\eta, t)\}$, as t ranges over all vectors of members of $\mathbb{R}_+$ of any finite length, is called the collection of *finite-dimensional distributions* (FDDs) of α. In general, the knowledge of the FDDs of a process α does *not* yield "complete" information about the properties of its sample paths [GS92]. Nevertheless, the FDDs provide more than adequate information to calculate the second-order (e.g., spectral) properties of a stochastic process, since they capture the *correlation* information between $\alpha(t_1)$ and $\alpha(t_2)$ for all $t_1, t_2 \in \mathbb{R}_+$.

In this section, we will employ the following procedure to find an adequate probabilistic characterization of the phase deviation α for our purposes:

1. We first calculate the time-varying *probability density function* (PDF) $p_\alpha(\eta, t)$ of α defined as

$$p_\alpha(\eta, t) = \frac{\partial \mathbb{P}\left[\alpha(t) \leq \eta\right]}{\partial \eta} \quad t \geq 0$$

   and show that it becomes the PDF of a Gaussian random variable asymptotically with t. A Gaussian PDF is completely characterized by the mean and the variance of the random variable. We show that, asymptotically with t, $\alpha(t)$ becomes a Gaussian random variable with a constant (as a function of t) mean m and a variance that is linearly increasing with time, i.e., ct for some constants m and c. The fact that $\alpha(t)$ is a Gaussian random variable for every t does not imply that α is a Gaussian stochastic process. α is a Gaussian process if its FDDs are multivariate Gaussian distributions. Individually Gaussian random variables are not necessarily jointly Gaussian. In this step, we only calculate the time-varying PDF of $\alpha(t)$ which is only a partial characterization of its FDDs [GS92].

2. The time-varying PDF $p_\alpha(\eta, t)$ does not provide any correlation information between $\alpha(t)$ and $\alpha(t+\tau)$ that is needed for the evaluation of its spectral characteristics. We then calculate this correlation to be

$$\mathbb{E}\left[\alpha(t)\alpha(t+\tau)\right] = m^2 + c\min(t, t+\tau)$$

3. We then show that $\alpha(t_1)$ and $\alpha(t_2)$ become *jointly* Gaussian asymptotically with time, which does not follow immediately from the fact that they are individually Gaussian.

Starting with the stochastic differential equation (3.10) for α, one can derive a partial differential equation, known as the *Fokker-Planck equation* [Gar83, Ris96], for the time-varying PDF $p_\alpha(\eta, t)$. We outline this derivation next.

4.1.1 Kramers-Moyal Expansion and Fokker-Planck Equation

The probability density functions $p_\alpha(\eta, t+\Delta t)$ and $p_\alpha(\eta, t)$ are related by

$$p_\alpha(\eta, t+\Delta t) = \int p(\eta, t+\Delta t|\bar{\eta}, t) p_\alpha(\bar{\eta}, t) \mathrm{d}\bar{\eta}$$

where $p(\eta, t+\Delta t|\bar{\eta}, t)$ is the transition probability density function. We express $p(\eta, t+\Delta t|\bar{\eta}, t)$ in terms of its moments. The i^{th} moment of $p(\eta, t+\Delta t|\bar{\eta}, t)$ is given by

$$\begin{aligned} M_i(\bar{\eta}, t, \Delta t) &= \mathbb{E}\left[(\alpha(t+\Delta t)-\alpha(t))^i\right]\big|_{\alpha(t)=\bar{\eta}} \\ &= \int (\eta-\bar{\eta})^i p(\eta, t+\Delta t|\bar{\eta}, t)\mathrm{d}\eta \end{aligned}$$

The characteristic function of $p(\eta, t+\Delta t|\bar{\eta}, t)$ is given by

$$\begin{aligned} C(\omega, \bar{\eta}, t, \Delta t) &= \int_{-\infty}^{\infty} \exp(\jmath\omega(\eta-\bar{\eta}))p(\eta, t+\Delta t|\bar{\eta}, t)\mathrm{d}\eta \\ &= 1+\sum_{i=1}^{\infty}\frac{(\jmath\omega)^i M_i(\bar{\eta}, t, \Delta t)}{i!} \end{aligned}$$

The probability density function can thus be expressed in terms of its moments as

$$\begin{aligned} p(\eta, t+\Delta t|\bar{\eta}, t) &= \frac{1}{2\pi}\int_{-\infty}^{\infty}\exp(-\jmath\omega(\eta-\bar{\eta}))C(\omega, \bar{\eta}, t, \Delta t)\mathrm{d}\omega \\ &= \frac{1}{2\pi}\int_{-\infty}^{\infty}\exp(-\jmath\omega(\eta-\bar{\eta}))\left(1+\sum_{i=1}^{\infty}\frac{(\jmath\omega)^i M_i(\bar{\eta}, t, \Delta t)}{i!}\right)\mathrm{d}\omega \end{aligned} \tag{4.2}$$

For small Δt the moments can be expanded in a Taylor series as

$$\frac{M_i(\bar{\eta}, t, \Delta t)}{i!} = D^{(i)}(\bar{\eta}, t)\Delta t + O\big((\Delta t)^2\big)$$

where $D^{(i)}(\bar{\eta}, t)$ are called the *Kramers-Moyal* expansion coefficients and are given by

$$D^{(i)}(\bar{\eta}, t) = \frac{1}{i!}\lim_{\Delta t\to 0}\frac{\mathbb{E}\left[(\alpha(t+\Delta t)-\alpha(t))^i\right]}{\Delta t}\bigg|_{\alpha(t)=\bar{\eta}} \tag{4.3}$$

Hence (4.2) can be re-expressed as

$$p(\eta, t+\Delta t|\bar{\eta}, t) = \frac{1}{2\pi}\int_{-\infty}^{\infty}\exp(-\jmath\omega(\eta-\bar{\eta}))\left[1+\sum_{i=1}^{\infty}(\jmath\omega)^i\left(D^{(i)}(\bar{\eta}, t)\Delta t + O((\Delta t)^2)\right)\right]\mathrm{d}\omega$$

and $p_\alpha(\eta, t+\Delta t)$ is given by

$$\begin{aligned} p_\alpha(\eta, t+\Delta t) &= \int p(\eta, t+\Delta t|\bar{\eta}, t)p_\alpha(\bar{\eta}, t)\mathrm{d}\bar{\eta} \\ &= \int \frac{1}{2\pi}\int_{-\infty}^{\infty}\exp(-\jmath\omega(\eta-\bar{\eta}))\left[1+\sum_{i=1}^{\infty}(\jmath\omega)^i\left(D^{(i)}(\bar{\eta}, t)\Delta t + O((\Delta t)^2)\right)\right] \\ &\quad \mathrm{d}\omega p_\alpha(\bar{\eta}, t)\mathrm{d}\bar{\eta} \\ &= \frac{1}{2\pi}\int_{-\infty}^{\infty}\exp(-\jmath\omega\eta)\int\exp(\jmath\omega\bar{\eta})\left[1+\sum_{i=1}^{\infty}(\jmath\omega)^i\left(D^{(i)}(\bar{\eta}, t)\Delta t + O((\Delta t)^2)\right)\right] \\ &\quad \mathrm{d}\bar{\eta}p_\alpha(\bar{\eta}, t)\mathrm{d}\omega \end{aligned} \tag{4.4}$$

The first term of the summation in (4.4) is

$$\frac{1}{2\pi}\int_{-\infty}^{\infty}\exp(-\jmath\omega\eta)\int\exp(\jmath\omega\bar{\eta})p_\alpha(\bar{\eta},t)\mathrm{d}\bar{\eta}\mathrm{d}\omega$$

The inner integral is

$$\mathcal{F}(p_\alpha(\eta,t))$$

while the outer integral is

$$\mathcal{F}^{-1}(\mathcal{F}(p_\alpha(\eta,t)))$$

where $\mathcal{F}(f)$ represents the Fourier transform of f and $\mathcal{F}^{-1}$ represents the inverse Fourier transform. Hence

$$\frac{1}{2\pi}\int_{-\infty}^{\infty}\exp(-\jmath\omega\eta)\int\exp(\jmath\omega\bar{\eta})p_\alpha(\bar{\eta},t)\mathrm{d}\bar{\eta}\mathrm{d}\omega = p_\alpha(\eta,t)$$

Taking this term to the left hand side of (4.4), dividing throughout with Δt and taking the limit as $\Delta t \to 0$, we obtain

$$\begin{aligned}\frac{\partial p_\alpha(\eta,t)}{\partial t} &= \lim_{\Delta t\to 0}\frac{p_\alpha(\eta,t+\Delta t)-p_\alpha(\eta,t)}{\Delta t}\\ &= \sum_{i=1}^{\infty}\int_{-\infty}^{\infty}\frac{1}{2\pi}\exp(-\jmath\omega\eta)(\jmath\omega)^i\int\exp(\jmath\omega\bar{\eta})D^{(i)}(\bar{\eta},t)p_\alpha(\bar{\eta},t)\mathrm{d}\bar{\eta}\mathrm{d}\omega\end{aligned}$$

Yet again, the inner integral in the summation is

$$\mathcal{F}(D^{(i)}(\eta,t)p_\alpha(\eta,t))$$

and the outer integral is

$$\mathcal{F}^{-1}((\jmath\omega)^i\mathcal{F}\big(D^{(i)}(\eta,t)p_\alpha(\eta,t)\big))$$

which is the i^{th} derivative of $(-1)^iD^{(i)}(\eta,t)p_\alpha(\eta,t)$ with respect to η. Hence we obtain

$$\frac{\partial p_\alpha(\eta,t)}{\partial t} = \sum_{i=1}^{\infty}\frac{\partial^i}{\partial\eta^i}(-1)^iD^{(i)}(\eta,t)p_\alpha(\eta,t) \tag{4.5}$$

where $D^{(i)}(\eta,t)$ satisfy (4.3).

Let the random process $\alpha(t)$ satisfy the following nonlinear differential equation

$$\dot{\alpha} = h(\alpha,t) + g^T(\alpha,t)\xi(t) \tag{4.6}$$

where $\xi(t)$ is a vector of uncorrelated zero mean Gaussian white noise processes. By integrating both sides from t to $t+\Delta t$ the above equation can be written in equivalent integral from as

$$\alpha(t+\Delta t) - \alpha(t) = \int_t^{t+\Delta t} \left(h(\alpha(t_1), t_1) + g^T(\alpha(t_1), t_1)\xi(t_1)\right) \mathrm{d}t_1 \tag{4.7}$$

Expanding h and g in Taylor series we obtain

$$h(\alpha(t_1), t_1) = h(\eta, t_1) + h'(\eta, t_1)(\alpha(t_1) - \eta) + \dots$$

and

$$g^T(\alpha(t_1), t_1) = g^T(\eta, t_1) + g^{T'}(\eta, t_1)(\alpha(t_1) - \eta) + \dots$$

where

$$h'(\eta, t_1) \triangleq \frac{\partial h(\eta, t_1)}{\partial \eta} = \left.\frac{\partial h(\alpha(t_1), t_1)}{\partial \alpha(t_1)}\right|_{\alpha(t)=\eta}$$

Substituting this in (4.7) we obtain

$$\begin{aligned}\alpha(t+\Delta t) - \alpha(t) = &\int_t^{t+\Delta t} h(\eta, t_1)\mathrm{d}t_1 + \int_t^{t+\Delta t} h'(\eta, t_1)(\alpha(t_1) - \alpha(t))\mathrm{d}t_1 + \dots \\ &+ \int_t^{t+\Delta t} g^T(\eta, t_1)\xi(t_1)\mathrm{d}t_1 + \int_t^{t+\Delta t} (\alpha(t_1) - \alpha(t))g^{T'}(\eta, t_1)\xi(t_1)\mathrm{d}t_1 + \dots\end{aligned}$$

For $\alpha(t_1) - \alpha(t)$ in the integrand on the right hand side we re-substitute the same expression as of $\alpha(t+\Delta t) - \alpha(t)$ in the above equation to obtain

$$\begin{aligned}\alpha(t+\Delta t) - \alpha(t) = &\int_t^{t+\Delta t} h(\eta, t_1)\mathrm{d}t_1 + \int_t^{t+\Delta t} h'(\eta, t_1) \int_t^{t_1} h(\eta, t_2)\mathrm{d}t_2\mathrm{d}t_1 \\ &+ \int_t^{t+\Delta t} h'(\eta, t_1) \int_t^{t_1} g^T(\eta, t_2)\xi(t_2)\mathrm{d}t_2\mathrm{d}t_1 + \dots \\ &+ \int_t^{t+\Delta t} g^T(\eta, t_1)\xi(t_1)\mathrm{d}t_1 + \int_t^{t+\Delta t} \int_t^{t_1} h(\eta, t_2)g^{T'}(\eta, t_1)\xi(t_1)\mathrm{d}t_2\mathrm{d}t_1 \\ &+ \int_t^{t+\Delta t} \int_t^{t_1} g^T(\eta, t_2)\xi(t_2)\xi^T(t_1)g'(\eta, t_1)\mathrm{d}t_2\mathrm{d}t_1 + \dots\end{aligned} \tag{4.8}$$

Here we have used the fact that $g^{T'}(\eta, t_1)\xi(t_1) = \xi^T(t_1)g'(\eta, t_1)$. By repeated iteration, only the white noise sources and the known functions $g(\eta, t)$ and $h(\eta, t)$ remain on the right hand side (since that this computation is being performed for a given η). Hence this expression

can be used to evaluate $D^{(i)}$s. Taking the expected value of (4.8) on both sides and using $\mathbb{E}[\xi(t)] = 0]$ and $\mathbb{E}\left[\xi(t)\xi^T(t_1)\right] = I\delta(t-t_1)$ where I is the identity matrix and $\delta(t)$ is the unit impulse we obtain

$$\mathbb{E}\left[\alpha(t+\Delta t) - \alpha(t)\right]|_{\alpha(t)=\eta} = \int_t^{t+\Delta t} h(\eta, t_1)\mathrm{d}t_1 + \int_t^{t+\Delta t} h'(\eta, t_1)\int_t^{t_1} h(\eta, t_2)\mathrm{d}t_2\mathrm{d}t_1 + \ldots$$
$$+ \int_t^{t+\Delta t}\int_t^{t_1} g^T(\eta, t_2)\delta(t_2 - t_1)Ig'(\eta, t_1)\mathrm{d}t_2\mathrm{d}t_1 + \ldots$$

In evaluating the last integral we have to find the value of $\int_{-t}^{0}\delta(\Delta t)\mathrm{d}\Delta t$. A delta function can be defined as the limit of a rectangle of width ϵ and height $1/\epsilon$ in the interval $[-\lambda\epsilon, (1-\lambda)\epsilon]$ as $\epsilon \to 0$. For any value of λ in the interval $[0, 1]$, in the limit $\epsilon \to 0$, the rectangle tends to a delta function. However, the integral $\int_{-t}^{0}\delta(\Delta t)\mathrm{d}\Delta t$ will differ depending on which value of λ is chosen. A physical interpretation would be to take $\lambda = 0.5$ which corresponds to Stratonovich's definition of the *stochastic integral* (Section A.2). This states that, in order to evaluate a stochastic integral of the form

$$\int_S^T f(t)\xi(t)\mathrm{d}t = \int_S^T f(t)\mathrm{d}B(t)$$

in the interval $[S, T]$ (where $B(t)$ is the Brownian motion process) as a limit of

$$\sum_{j=0}^{n} f(t_j^*)[B(t_{j+1}) - B(t_j)] \quad t_j^* \in [t_j, t_{j+1}]$$

as $n \to \infty$, one should choose t_j^* as the mid-point of the interval $[t_j, t_{j+1}]$. Unlike the case of an ordinary Riemann-Stieljes integral, the choice of t_j^* makes a difference in the evaluation of the limit [Øks98], thereby subjecting the stochastic integral to multiple interpretations. Another interpretation is to take t_j^* as the left end point t_j of $[t_j, t_{j+1}]$ which corresponds to Itô's definition of the stochastic integral (also known as Itô integral) and $\lambda = 0$. This property of the Itô integral of "not looking into the future" (more formally, the Itô integrals are *martingales*, see Appendix A Definition A.7) simplifies proofs immensely and hence is preferred in the literature. We will postpone the selection of λ value as of now and assume that $\int_{-t}^{0}\delta(\Delta t)\mathrm{d}\Delta t = \lambda$. Therefore

$$\int_t^{t_1} g^T(\eta, t_2)\delta(t_2 - t_1)I\mathrm{d}t_2 = g^T(\eta, t_1)\int_t^{t_1}\delta(t_2 - t_1)\mathrm{d}t_2 = \lambda g^T(\eta, t_1)$$

and hence

$$\mathbb{E}\left[\alpha(t+\Delta t) - \alpha(t)\right]|_{\alpha(t)=\eta} = \int_t^{t+\Delta t} h(\eta, t_1)\mathrm{d}t_1 + \int_t^{t+\Delta t} h'(\eta, t_1)\int_t^{t_1} h(\eta, t_2)\mathrm{d}t_2\mathrm{d}t_1 + \ldots$$
$$+ \lambda\int_t^{t+\Delta t} g^T(\eta, t_1)g'(\eta, t_1)\mathrm{d}t_1 + \ldots$$

Dividing both sides by Δt and taking the limit $\Delta t \to 0$ we obtain

$$D^{(1)} = h(\eta, t) + \lambda g^T(\eta, t) g'(\eta, t)$$

All the other terms in the expansion involve double or more integrals. These contribute terms in $\mathbb{E}\left[\alpha(t+\Delta t) - \alpha(t)\right]$ which are $O((\Delta t)^2)$ or higher which vanish as $\Delta t \to 0$. We can use similar arguments to show that

$$D^{(2)}(\eta, t) = \frac{1}{2} \lim_{\Delta t \to 0} \int_t^{t+\Delta t} \int_t^{t+\Delta t} g(\eta, t_1) g(\eta, t_2) \delta(t_1 - t_2) \mathrm{d}t_1 \mathrm{d}t_2 = \frac{1}{2} g^T(\eta, t) g(\eta, t)$$

and that $D^{(i)} = 0$ for $i > 2$. Hence the differential equation governing the probability density function $p_\alpha(\eta)$ can be written as

$$\begin{aligned} \frac{\partial p_\alpha(\eta, t)}{\partial t} = &- \frac{\partial}{\partial \eta} \left(h(\eta, t) p_\alpha(\eta, t) + \lambda p_\alpha(\eta, t) \frac{\partial g^T(\eta, t)}{\partial \eta} g(\eta, t) \right) \\ &+ \frac{1}{2} \frac{\partial^2}{\partial \eta^2} \left(g^T(\eta, t) g(\eta, t) p_\alpha(\eta, t) \right) \end{aligned}$$

(3.10) is in the same form as (4.6) except that $h(\eta, t)$ is zero, $g^T(\eta, t) = v_1^T(t + \eta(t)) D\big(x_s(t + \eta(t))\big)$ and $\xi(t) = b(t)$. Hence the corresponding Fokker-Planck equation for α can be written as

$$\frac{\partial p_\alpha(\eta, t)}{\partial t} = - \frac{\partial}{\partial \eta} \left(\lambda p_\alpha(\eta, t) \frac{\partial g^T(\eta, t)}{\partial \eta} g(\eta, t) \right) + \frac{1}{2} \frac{\partial^2}{\partial \eta^2} \left(g^T(\eta, t) g(\eta, t) p_\alpha(\eta, t) \right)$$

where

$$g^T(\eta, t) = v^T(\eta + t) = v_1^T(t + \eta(t)) D\big(x_s(t + \eta(t))\big)$$

4.1.2 Solution of the Phase Deviation Equation

The Fokker-Planck equation for $\alpha(t)$ takes the form

$$\frac{\partial p_\alpha(\eta, t)}{\partial t} = - \frac{\partial}{\partial \eta} \left(\lambda p_\alpha(\eta, t) \frac{\partial v^T(t + \eta)}{\partial \eta} v(t + \eta) \right) + \frac{1}{2} \frac{\partial^2}{\partial \eta^2} \left(v^T(t + \eta) v(t + \eta) p_\alpha(\eta, t) \right) \tag{4.9}$$

where

$$v^T(t) = v_1^T(t) D(x_s(t))$$

and $0 \leq \lambda \leq 1$ depends on the definition of the stochastic integral [Gar83, Øks98] used to interpret the stochastic differential equation in (4.1). We would like to solve (4.9) for

$p_\alpha(\eta, t)$. It turns out that $p_\alpha(\eta, t)$ becomes a *Gaussian* PDF asymptotically with *linearly* increasing variance. We show this by first solving for the *characteristic function* $F(\omega, t)$ of $\alpha(t)$, which is defined by

$$F(\omega, t) = \mathbb{E}\left[\exp\left(\jmath\omega\alpha(t)\right)\right] = \int_{-\infty}^{\infty} \exp\left(\jmath\omega\eta\right) p_\alpha(\eta, t)\mathrm{d}\eta$$

Since both $v_1^T(\cdot)$ and $D(x_s(\cdot))$ are T-periodic in their arguments, $v^T(\cdot)$ is also periodic in its argument with period T. Hence we can expand $v^T(t)$ into its Fourier series:

$$v^T(t) = \sum_{i=-\infty}^{\infty} V_i^T \exp(\jmath i\omega_0 t) \quad \omega_0 = \frac{2\pi}{T}$$

Lemma 4.1 *The characteristic function of $\alpha(t)$, $F(\omega, t)$, satisfies*

$$\frac{\partial F(\omega, t)}{\partial t} = \sum_{i=-\infty}^{\infty} \sum_{k=-\infty}^{\infty} V_i^T V_k^* \exp(\jmath\omega_0(i-k)t) \left(-\lambda\omega_0 i\omega - \frac{1}{2}\omega^2\right) F(\omega_0(i-k) + \omega, t) \tag{4.10}$$

where $*$ denotes complex conjugation.

Proof: Let $h(\eta)$ be a smooth function. For notational simplicity we will drop the explicit dependence of $p_\alpha(\eta, t)$, $h(\eta)$ and $v^T(t+\eta)$ on η and t from now on. Then from (4.9) we have

$$\int_{-\infty}^{\infty} \frac{\partial p_\alpha}{\partial t} h\mathrm{d}\eta = \int_{-\infty}^{\infty} -\frac{\partial}{\partial\eta}\left(\lambda p_\alpha \frac{\partial v^T}{\partial\eta} v\right) h\mathrm{d}\eta + \int_{-\infty}^{\infty} \frac{1}{2}\frac{\partial^2\left(v^T v p_\alpha\right)}{\partial\eta^2} h\mathrm{d}\eta$$

The term on the left hand side is the time derivative of $\mathbb{E}\left[h(\alpha(t))\right]$. Integrating the first term on the right hand side by parts we get

$$\int_{-\infty}^{\infty} -\frac{\partial}{\partial\eta}\left(\lambda p_\alpha \frac{\partial v^T}{\partial\eta} v\right) h\mathrm{d}\eta = -\left.\lambda p_\alpha \frac{\partial v^T}{\partial\eta} v h\right|_{-\infty}^{\infty} + \int_{-\infty}^{\infty} \lambda \frac{\mathrm{d}h}{\mathrm{d}\eta} p_\alpha \frac{\partial v^T}{\partial\eta} v\mathrm{d}\eta$$

The first term above, on the right hand side, is zero at both the limits, because the PDF of a well-defined random variable should be zero at $\pm\infty$. The second term can be written as an expectation, i.e.,

$$\int_{-\infty}^{\infty} \lambda \frac{\mathrm{d}h}{\mathrm{d}\eta} p_\alpha \frac{\partial v^T}{\partial\eta} v\mathrm{d}\eta = \mathbb{E}\left[\lambda \frac{\mathrm{d}h}{\mathrm{d}\alpha}\frac{\partial v^T}{\partial\alpha} v\right]$$

Similarly (using integration by parts twice) it can be shown that

$$\int_{-\infty}^{\infty} \frac{1}{2} \frac{\partial^2 \left(v^T v p_\alpha\right)}{\partial \alpha^2} h \mathrm{d}\eta = \frac{1}{2} \mathbb{E}\left[\frac{\mathrm{d}^2 h}{\mathrm{d}\alpha^2} v^T v\right]$$

Hence

$$\frac{\mathrm{d}\mathbb{E}\left[h\right]}{\mathrm{d}t} = \mathbb{E}\left[\lambda \frac{\mathrm{d}h}{\mathrm{d}\alpha} \frac{\partial v^T}{\partial \alpha} v\right] + \frac{1}{2} \mathbb{E}\left[\frac{\mathrm{d}^2 h}{\mathrm{d}\alpha^2} v^T v\right]$$

We now substitute $h(\alpha) = \exp(\jmath\omega\alpha)$ and the Fourier series representation of v to obtain a differential equation for the characteristic function. The left hand side term is the time derivative of the characteristic function $F(\omega, t)$ of $\alpha(t)$.

$$\begin{aligned}
\frac{\partial F(\omega,t)}{\partial t} &= \mathbb{E}\left[\jmath\omega\lambda \frac{\partial v^T}{\partial \alpha} v \exp(\jmath\omega\alpha) + \frac{1}{2}(\jmath\omega)^2 v^T v \exp(\jmath\omega\alpha)\right] \\
&= \sum_{i=-\infty}^{\infty} \sum_{k=-\infty}^{\infty} V_i^T V_k^* \exp(\jmath\omega_0(i-k)t) \\
&\qquad \mathbb{E}\left[\left(-\lambda\omega_0 i\omega - \frac{1}{2}\omega^2\right) \exp(\jmath\omega_0(i-k)\alpha + \jmath\omega\alpha)\right] \\
&= \sum_{i=-\infty}^{\infty} \sum_{k=-\infty}^{\infty} V_i^T V_k^* \exp(\jmath\omega_0(i-k)t) \left(-\lambda\omega_0 i\omega - \frac{1}{2}\omega^2\right) F(\omega_0(i-k)+\omega, t)
\end{aligned}$$

■

Theorem 4.2 *The differential equation for $F(\omega, t)$, (4.10) has a solution that becomes the characteristic function of a Gaussian random variable asymptotically with time and*

$$\lim_{t\to\infty} F(\omega, t) = \exp\left(\jmath\omega\mu(t) - \frac{\omega^2\sigma^2(t)}{2}\right) \tag{4.11}$$

solves (4.10), where $\mu(t) = m$ is a constant, and $\sigma^2(t) = ct$ where

$$c = \frac{1}{T}\int_0^T v^T(t) v(t) \mathrm{d}t. \tag{4.12}$$

The variance of this Gaussian random variable increases linearly with time, exactly as in a Wiener process.

Proof: The characteristic function of a Gaussian random variable with mean $\mu(t)$ and variance $\sigma^2(t)$ is given by $\exp(\jmath\omega\mu(t) - 1/2\omega^2\sigma^2(t))$ [GS92]. Substituting this expression in (4.10) for the characteristic function we obtain

$$\begin{aligned}
&\left(\jmath\omega\frac{\mathrm{d}\mu}{\mathrm{d}t} - \frac{\omega^2}{2}\frac{\mathrm{d}\sigma^2}{\mathrm{d}t}\right) \exp\left(\jmath\omega\mu - \frac{1}{2}\omega^2\sigma^2\right) \\
&= \sum_{i=-\infty}^{\infty} \sum_{k=-\infty}^{\infty} V_i^T V_k^* \exp(\jmath\omega_0(i-k)t) \left(-\lambda\omega_0 i\omega - \frac{1}{2}\omega^2\right) \exp\left(\jmath(\omega+\omega_0(i-k))\mu\right) \\
&\qquad \exp\left(-\frac{1}{2}(\omega+\omega_0(i-k))^2\sigma^2\right)
\end{aligned}$$

where we dropped the explicit dependence of $\mu(t)$ and $\sigma^2(t)$ on t. This equation is rewritten as

$$\left(\jmath\omega\frac{\mathrm{d}\mu}{\mathrm{d}t}-\frac{\omega^2}{2}\frac{\mathrm{d}\sigma^2}{\mathrm{d}t}\right)=\sum_{i=-\infty}^{\infty}\sum_{k=-\infty}^{\infty}V_i^TV_k^*\exp(\jmath\omega_0(i-k)(t+\mu))\left(-\lambda\omega_0i\omega-\frac{1}{2}\omega^2\right)\exp(-\omega\omega_0(i-k)\sigma^2)\exp\left(-\frac{1}{2}\omega_0^2(i-k)^2\sigma^2\right) \tag{4.13}$$

This equation should be valid for all values of ω. Hence the coefficients of the same powers of ω on both sides should be equal. Expanding $\exp(-\omega\omega_0(i-k)\sigma^2)$ in a power series and equating the coefficients of ω on both sides we obtain

$$\jmath\frac{\mathrm{d}\mu}{\mathrm{d}t}=\sum_{i=-\infty}^{\infty}\sum_{k=-\infty}^{\infty}V_i^TV_k^*\exp(\jmath\omega_0(i-k)t)\exp(\jmath\omega_0(i-k)\mu)\exp\left(-\frac{1}{2}\omega_0^2(i-k)^2\sigma^2\right)(-\lambda\omega_0i)$$

or

$$\frac{\mathrm{d}\mu}{\mathrm{d}t}=\sum_{i=-\infty}^{\infty}\sum_{k=-\infty}^{\infty}\jmath\lambda\omega_0iV_i^TV_k^*\exp(\jmath\omega_0(i-k)t)\exp(\jmath\omega_0(i-k)\mu)\exp\left(-\frac{1}{2}\omega_0^2(i-k)^2\sigma^2\right) \tag{4.14}$$

For large t and hence large σ^2 (to be verified, see below), $\exp(-1/2\omega_0^2(i-k)^2\sigma^2)$ becomes vanishingly small for all $i\neq k$. For $i=k$ (4.14) becomes

$$\begin{aligned}\frac{\mathrm{d}\mu}{\mathrm{d}t}&=\sum_{i=-\infty}^{\infty}\jmath\lambda\omega_0iV_i^TV_i^*\\&=\frac{\lambda}{T}\int_0^T\frac{\mathrm{d}v^T(t)}{\mathrm{d}t}v(t)\mathrm{d}t\\&=\frac{\lambda}{2T}\int_0^T\frac{\mathrm{d}v^T(t)v(t)}{\mathrm{d}t}\mathrm{d}t\\&=\frac{\lambda}{2T}\,v^T(t)v(t)\big|_0^T\\&=0\end{aligned}$$

In evaluating the above integral we used the fact that $v(t)$ and hence $v^T(t)v(t)$ is T-periodic. Hence asymptotically, the mean $\mu(t)$ becomes a constant.

Equating the coefficients of ω^2 on both sides of (4.13) we obtain

$$\frac{\mathrm{d}\sigma^2}{\mathrm{d}t}=\sum_{i=-\infty}^{\infty}\sum_{k=-\infty}^{\infty}(1-2\lambda\omega_0^2i(i-k)\sigma^2)V_i^TV_k^*\exp(\jmath\omega_0(i-k)t)\exp(\jmath\omega_0(i-k)\mu)\exp\left(-\frac{1}{2}\omega_0^2(i-k)^2\sigma^2\right) \tag{4.15}$$

Using the same arguments as above we conclude that for large t, only the $i = k$ terms contribute to the summation. Thus

$$\begin{aligned}\frac{\mathrm{d}\sigma^2}{\mathrm{d}t} &= \sum_{i=-\infty}^{\infty} V_i^T V_i^* \\ &= \frac{1}{T}\int_0^T v^T(t)v(t)\mathrm{d}t = c\end{aligned}$$

which is the time average of $v^T(t)v(t)$. This shows that asymptotically the variance is growing linearly with t (which verifies our assumption above that it becomes large for large t) and the slope is the time average of $v^T(t)v(t)$. The differential equations (4.14) and (4.15) for $\sigma^2(t)$ and $\mu(t)$ form a pair of coupled differential equations and can be solved numerically to obtain the final value m to which $\mu(t)$ settles.

Now, we examine the coefficients of ω^n in (4.13) for $n > 2$. Equating the coefficients of ω^n, $n > 2$ on both sides of (4.13), we obtain

$$\begin{aligned}0 = \sum_{i=-\infty}^{\infty}\sum_{k=-\infty}^{\infty} &\left(-\lambda\omega_0 i\frac{(-\omega_0(i-k)\sigma^2)^{n-1}}{(n-1)!} - \frac{1}{2}\frac{(-\omega_0(i-k)\sigma^2)^{n-2}}{(n-2)!}\right) V_i^T V_k^* \\ &\exp(\jmath\omega_0(i-k)t)\exp(\jmath\omega_0(i-k)\mu)\exp\left(-\frac{1}{2}\omega_0^2(i-k)^2\sigma^2\right)\end{aligned} \tag{4.16}$$

For large t, $\sigma^2(t)$ becomes large (increasing linearly with t), hence $\exp(-1/2\omega_0^2(i-k)^2\sigma^2)$ becomes vanishingly small for all $i \neq k$. For $i = k$, the right hand side of the above equation is identically zero. Hence, (4.16) becomes consistent asymptotically in time with $\mu(t) = m$ and $\sigma^2(t) = ct$. Thus, the characteristic function of the Gaussian distribution with mean $\mu(t) = m$ and variance $\sigma^2(t) = ct$ asymptotically satisfies (4.10). ∎

Lemma 4.3 *The second order statistics of α are governed by*

$$\mathbb{E}\left[\alpha(t)\alpha(t+\tau)\right] = \begin{cases} \mathbb{E}\left[\alpha^2(t)\right] & \text{if} \quad \tau \geq 0 \\ \mathbb{E}\left[\alpha^2(t+\tau)\right] & \text{if} \quad \tau < 0 \end{cases}$$

Proof: The proof is trivial if we interpret (3.10) using Itô's definition of the stochastic integral [Arn74, Øks98] (corresponding to $\lambda = 0$ in (4.9)). Using the integral form of (3.10) that defines α, one can write for $\tau \geq 0$.

$$\begin{aligned}\alpha(t+\tau) &= \alpha(t) + (\alpha(t+\tau) - \alpha(t)) \\ &= \alpha(t) + \zeta(t,\tau)\end{aligned}$$

where $\zeta(t,\tau)$ is uncorrelated with $\alpha(t)$.

For general λ we observe that given $\tau \geq 0$,

$$\begin{aligned}
\mathbb{E}\left[\alpha(t)\alpha(t+\tau)\right] &= \mathbb{E}\left[\int_0^t \int_0^{t+\tau} v^T(t_1+\alpha(t_1))\xi(t_1)v^T(t_2+\alpha(t_2))\xi(t_2)\mathrm{d}t_2\mathrm{d}t_1\right] \\
&= \mathbb{E}\left[\int_0^t \int_0^{t} v^T(t_1+\alpha(t_1))\xi(t_1)v^T(t_2+\alpha(t_2))\xi(t_2)\mathrm{d}t_1\mathrm{d}t_2\right] \\
&\quad + \mathbb{E}\left[\int_0^t \int_t^{t+\tau} v^T(t_1+\alpha(t_1))v(t_2+\alpha(t_2))\xi^T(t_1)\xi(t_2)\mathrm{d}t_2\mathrm{d}t_1\right] \\
&= \mathbb{E}\left[\alpha^2(t)\right] + \mathbb{E}\left[\int_0^t \int_t^{t+\tau} v^T(t_1+\alpha(t_1))v(t_2+\alpha(t_2))\xi^T(t_1)\xi(t_2)\mathrm{d}t_2\mathrm{d}t_1\right] \\
&= \mathbb{E}\left[\alpha^2(t)\right] + \int_0^t \int_t^{t+\tau} \mathbb{E}\left[v^T(t_1+\alpha(t_1))v(t_2+\alpha(t_2))\xi^T(t_1)\xi(t_2)\right]\mathrm{d}t_2\mathrm{d}t_1
\end{aligned} \tag{4.17}$$

We define $r_{12} = v^T(t_1+\alpha(t_1))v(t_2+\alpha(t_2))$ as a random process which is correlated with both $\xi(t_1)$ and $\xi(t_2)$. However, v is periodic in it's argument hence we can find a scalar M such that $-M \leq r_{12} \leq M$. We use this fact to bound the above expectation. We define $p_{R_{12},\Xi_1,\Xi_2}(r_{12},\xi_1,\xi_2)$ as the joint probability density function of the three random variables r_{12}, $\xi_1 \triangleq \xi(t_1)$ and $\xi_2 \triangleq \xi(t_2)$. Using this we obtain

$$\mathbb{E}\left[r_{12}\xi_1^T\xi_2\right] = \iiint r_{12}\xi_1^T\xi_2 p_{R_{12},\Xi_1,\Xi_2}(r_{12},\xi_1,\xi_2)\mathrm{d}r_{12}\mathrm{d}\xi_1\mathrm{d}\xi_2$$

Since $-M \leq r_{12} \leq M$, we have

$$\begin{aligned}
&-M\iiint \xi_1^T\xi_2 p_{R_{12},\Xi_1,\Xi_2}(r_{12},\xi_1,\xi_2)\mathrm{d}r_{12}\mathrm{d}\xi_1\mathrm{d}\xi_2 \leq \mathbb{E}\left[r_{12}\xi_1^T\xi_2\right] \leq \\
&M\iiint \xi_1^T\xi_2 p_{R_{12},\Xi_1,\Xi_2}(r_{12},\xi_1,\xi_2)\mathrm{d}r_{12}\mathrm{d}\xi_1\mathrm{d}\xi_2
\end{aligned}$$

or

$$\begin{aligned}
&-M\iint \xi_1^T\xi_2 p_{\Xi_1,\Xi_2}(\xi_1,\xi_2)\mathrm{d}\xi_1\mathrm{d}\xi_2 \leq \mathbb{E}\left[r_{12}\xi_1^T\xi_2\right] \leq \\
&M\iint \xi_1^T\xi_2 p_{\Xi_1,\Xi_2}(\xi_1,\xi_2)\mathrm{d}\xi_1\mathrm{d}\xi_2
\end{aligned}$$

or

$$-Mn\delta(t_1-t_2) \leq \iiint r_{12}\xi_1^T\xi_2 p_{R_{12},\Xi_1,\Xi_2}(r_{12},\xi_1,\xi_2)\mathrm{d}r_{12}\mathrm{d}\xi_1\mathrm{d}\xi_2 \leq Mn\delta(t_1-t_2)$$

where n is the size of $\xi(t_1)$ and $\xi(t_2)$. Hence

$$\begin{aligned}
-Mn\int_0^t \int_t^{t+\tau} \delta(t_1-t_2)\mathrm{d}t_2\mathrm{d}t_1 &\leq \int_0^t \int_t^{t+\tau} \mathbb{E}\left[v^T(t_1+\alpha(t_1))v(t_2+\alpha(t_2))\xi^T(t_1)\xi(t_2)\right]\mathrm{d}t_2\mathrm{d}t_1 \\
&\leq Mn\int_0^t \int_t^{t+\tau} \delta(t_1-t_2)\mathrm{d}t_2\mathrm{d}t_1
\end{aligned}$$

Evaluation of the above integrals also depends on the particular definition of δ function being used. Let us define $f_1(t)$ as a rectangular box of height $1/\epsilon$ between $[-\lambda\epsilon, (1-\lambda)\epsilon]$ and zero elsewhere. For any $0 \leq \lambda \leq 1$, as $\epsilon \to 0$, $f_1(t) \to \delta(t)$. We evaluate the above integral using this $f_1(t)$ and later take the limit $\epsilon \to 0$. In the above integral, t_2 varies from t to $t+\tau$ and t_1 varies from 0 to t.

$$\begin{aligned}\int_0^t \int_t^{t+\tau} \delta(t_1 - t_2)\mathrm{d}t_2\mathrm{d}t_1 &= \lim_{\epsilon\to 0} \int_0^t \int_t^{t+\tau} f_1(t_1 - t_2)\mathrm{d}t_2\mathrm{d}t_1 \\ &= \lim_{\epsilon\to 0} \int_0^t f_2(t_1)\mathrm{d}t_1\end{aligned}$$

Where

$$f_1(t_2) = \begin{cases} 0 & t_2 < -\lambda\epsilon \\ \frac{1}{\epsilon} & -\lambda\epsilon \leq t_2 \leq (1-\lambda)\epsilon \\ 0 & t_2 > (1-\lambda)\epsilon \end{cases}$$

and

$$f_2(t_1) = \begin{cases} 0 & t_1 \leq t - \epsilon(1-\lambda) \\ \frac{t_1 - t + \epsilon(1-\lambda)}{\epsilon} & t - \epsilon(1-\lambda) \leq t_1 \leq t + \lambda\epsilon \\ 1 & t + \lambda\epsilon \leq t_1 \leq t + \tau - \epsilon(1-\lambda) \\ \frac{t+\tau-t_1-\epsilon\lambda}{\epsilon} & t + \tau - \epsilon(1-\lambda) \leq t_1 \leq t + \tau + \lambda\epsilon \\ 0 & t + \tau + \lambda\epsilon \leq t_1 \end{cases}$$

Therefore

$$\begin{aligned}\int_0^t \int_t^{t+\tau} \delta(t_1 - t_2)\mathrm{d}t_2\mathrm{d}t_1 &= \lim_{\epsilon\to 0} \int_0^t f_2(t_1)\mathrm{d}t_1 \\ &= \lim_{\epsilon\to 0} \frac{1}{2}\epsilon(1-\lambda)^2 \\ &= 0\end{aligned}$$

Hence the second integral in (4.17) is identically zero and $\mathbb{E}\left[\alpha(t)\alpha(t+\tau)\right] = \mathbb{E}\left[\alpha^2(t)\right]$. ∎

Corollary 4.4 *Asymptotically with t*

$$\mathbb{E}\left[\alpha(t)\alpha(t+\tau)\right] = m^2 + c\min(t, t+\tau)$$

Proof: Follows trivially from Lemma 4.3 ∎

Definition 4.1 *Two real valued random variables Ψ_1 and Ψ_2 are called* jointly *Gaussian if for all $a_1, a_2 \in \mathbb{R}$, the real random variable $a_1\Psi_1 + a_2\Psi_2$ is Gaussian.*

Theorem 4.5 *Asymptotically with time,* $\alpha(t_1)$ *and* $\alpha(t_2)$ *become* jointly *Gaussian.*

Sketch of Proof: The proof is trivial if we interpret (3.10) using Itô's definition of the stochastic integral [Arn74] (corresponding to $\lambda = 0$ in (4.9)), as in the proof of Lemma 4.3. The proof is more involved for $0 < \lambda \leq 1$. In this case, we prove this result by showing that the *cumulants* of $a_1\alpha(t_1) + a_2\alpha(t_2)$ (for any $a_1, a_2 \in \mathbb{R}$) vanish for order higher than 2. The *cumulants* of a random variable Ψ are defined as the coefficients in the Taylor series expansion of its *cumulant generating function* which is, in turn, defined by

$$K_\psi = \log \mathbb{E}\left[\exp\left(\theta\Psi\right)\right] = \sum_{i=1}^{\infty} \frac{1}{i!} k_i(\Psi)\theta^i$$

where $k_i(\Psi)$ is the i^{th} order cumulant [GS92]. A random variable is Gaussian if and only if its cumulants of order higher than 2 vanish [Gar83]. In the proof, we also use the fact that $\alpha(t_1)$ and $\alpha(t_2)$ become *individually* Gaussian asymptotically with t. ∎

The stochastic characterization of the phase deviation α that we obtained in this section can be summarized by Lemma 4.3, Corollary 4.4 and Theorem 4.5. These do not completely specify the FDDs of α as a stochastic process. However, they provide adequate information for a practical characterization of the effect of phase deviation α on the signal generated by an autonomous oscillator, e.g., its spectral properties, as we will see in Section 4.2 and Section 4.3.

4.2 Spectrum of Oscillator Output with Phase Noise

Having obtained the asymptotic stochastic characterization of α, we now compute the power spectral density (PSD) of $x_s(t + \alpha(t))$ where $x_s(t)$ is the steady-state response of (3.1). We first obtain an expression for the nonstationary autocorrelation function $R(t, \tau)$ of $x_s(t + \alpha(t))$. Next, we demonstrate that the autocorrelation becomes independent of t asymptotically. This implies our main result, that the autocorrelation of the oscillator output with phase noise contains no nontrivial cyclostationary components. This confirms the intuitive expectation that a noisy autonomous system cannot have periodic cyclostationary variations because it has no perfect time reference. Finally, we show that the PSD of the stationary component is a summation of Lorentzian spectra, and that a single scalar constant, namely c in (4.12), is sufficient to characterize it.

We start by calculating the autocorrelation function of $x_s(t+\alpha(t))$, given by

$$R(t,\tau) = \mathbb{E}\left[x_s(t+\alpha(t))\, x_s^*(t+\tau+\alpha(t+\tau))\right] \tag{4.18}$$

Definition 4.2 *Let X_i to be the Fourier coefficients of $x_s(t)$:*

$$x_s(t) = \sum_{i=-\infty}^{\infty} X_i \exp\left(\jmath i\omega_0 t\right)$$

The following simple Lemma establishes the basic form of the autocorrelation:

Lemma 4.6 *The autocorrelation of the oscillator output $x_s(t+\alpha(t))$ is given by*

$$R(t,\tau) = \sum_{i=-\infty}^{\infty}\sum_{k=-\infty}^{\infty} X_i X_k^* \exp\left(\jmath(i-k)\omega_0 t\right)\exp\left(-\jmath k\omega_0\tau\right)\mathbb{E}\left[\exp\left(\jmath\omega_0\beta_{ik}(t,\tau)\right)\right] \tag{4.19}$$

where

$$\beta_{ik}(t,\tau) = i\alpha(t) - k\alpha(t+\tau)$$

and $\omega_0 = 1/T$.

Proof: Follows directly from (4.18) and Definition 4.2. ∎

To evaluate the expectation in the above Lemma, it is useful to first consider the statistics of $\beta_{ik}(t,\tau)$.

Lemma 4.7 *The statistics of $\beta_{i,k}(t,\tau)$ satisfy the following equations:*

$$\lim_{t\to\infty}\mathbb{E}\left[\beta_{ik}(t,\tau)\right] = (i-k)m \tag{4.20}$$

$$\lim_{t\to\infty}\mathbb{E}\left[\left(\beta_{ik}(t,\tau)\right)^2\right] - \left(\mathbb{E}\left[\beta_{ik}(t,\tau)\right]\right)^2 = (i-k)^2 ct + k^2 c\tau - 2ikc\min(0,\tau) \tag{4.21}$$

where m and c are defined in Theorem 4.2. Also, $\beta_{ik}(t,\tau)$ becomes Gaussian asymptotically with t.

Proof: From Theorem 4.2 we observe that

$$\lim_{t\to\infty}\mathbb{E}\left[\beta_{ik}(t,\tau)\right] = i\lim_{t\to\infty}\mathbb{E}\left[\alpha(t)\right] - k\lim_{t\to\infty}\mathbb{E}\left[\alpha(t+\tau)\right] = (i-k)m$$

Using Corollary 4.4 we have

$$\begin{aligned}\lim_{t\to\infty}\mathbb{E}\left[\beta_{ik}^2(t,\tau)\right] &= i^2\lim_{t\to\infty}\mathbb{E}\left[\alpha^2(t)\right]+k^2\lim_{t\to\infty}\mathbb{E}\left[\alpha^2(t+\tau)\right]-2ik\lim_{t\to\infty}\mathbb{E}\left[\alpha(t)\alpha(t+\tau)\right]\\ &= i^2(m^2+ct)+k^2(m^2+c(t+\tau))-2ik(m^2+c\min(t,t+\tau))\\ &= (i-k)^2(m^2+ct)+k^2c\tau-2ikc\min(0,\tau)\end{aligned}$$

This implies that

$$\lim_{t\to\infty}\mathbb{E}\left[\left(\beta_{ik}(t,\tau)\right)^2\right]-\left(\mathbb{E}\left[\beta_{ik}(t,\tau)\right]\right)^2=(i-k)^2ct+k^2c\tau-2ikc\min(0,\tau)$$

The fact that $\beta_{ik}(t,\tau)$ is asymptotically Gaussian follows directly from Theorem 4.5. ∎

Using the asymptotically Gaussian nature of $\beta_{ik}(t,\tau)$, we are now able to obtain a form for the expectation in (4.19).

Lemma 4.8 *If $c>0$, the characteristic function of $\beta_{ik}(t,\tau)$ is asymptotically independent of t and has the following form:*

$$\lim_{t\to\infty}\mathbb{E}\left[\exp\left(\jmath\omega_0\beta_{ik}(t,\tau)\right)\right]=\begin{cases}0 & \text{if } i\neq k\\ \exp\left(-\frac{1}{2}\omega_0^2k^2c|\tau|\right) & \text{if } i=k\end{cases}\tag{4.22}$$

Proof: Using Lemma 4.7 and the form of the characteristic function of a Gaussian random variable [GS92] we have

$$\begin{aligned}\lim_{t\to\infty}\mathbb{E}\left[\exp\left(\jmath\omega_0\beta_{ik}(t,\tau)\right)\right] =& \exp(\jmath\omega_0(i-k)m)\\ &\exp\left(-\frac{1}{2}\omega_0^2((i-k)^2ct+k^2c\tau-2ikc\min(0,\tau))\right)\end{aligned}$$

Taking the asymptotic limit of this expression, we observe that only for $i=k$ the above limit has a nontrivial value. ∎

Using the second order statistics of $\beta_{i,k}(t,\tau)$ we can now obtain the second order statistics of $x_s(t+\alpha(t))$ as follows:

Lemma 4.9 *The autocorrelation $R(t,\tau)$ given by (4.19) satisfies*

$$\lim_{t\to\infty}R(t,\tau)=\sum_{i=-\infty}^{\infty}X_iX_i^*\exp\left(-\jmath i\omega_0\tau\right)\exp\left(-\frac{1}{2}\omega_0^2i^2c|\tau|\right)\tag{4.23}$$

Proof: The result is obtained by substituting (4.22) in (4.19). ∎

The spectrum of $x_s(t+\alpha(t))$ can now be determined as follows:

Theorem 4.10 *The spectrum of $x_s(t+\alpha(t))$ is determined by the asymptotic behaviour of $R(t,\tau)$ as $t \to \infty$. All nontrivial cyclostationary components are zero, while the stationary component of the spectrum is given by:*

$$S(\omega) = \sum_{i=-\infty}^{\infty} X_i X_i^* \frac{\omega_0^2 i^2 c}{\frac{1}{4}\omega_0^4 i^4 c^2 + (\omega + i\omega_0)^2} \tag{4.24}$$

There is also a term $X_0\, X_0^*\, \delta(\omega)$ due to the DC part of $x_s(t)$, which is omitted in (4.24).

Proof: It can be shown that the cyclostationary component [Gar90] of the autocorrelation at any frequency ω_{cyc} is given by:

$$R_{\omega_{cyc}}(\tau) = \lim_{T\to\infty} \frac{1}{T} \int_0^T R(t,\tau)\, \exp\left(\jmath\omega_{cyc} t\right) \mathrm{d}t$$

This expression is determined by the asymptotic form of $R(t,\tau)$ as a function of t, given in (4.23). Because this becomes independent of t, the above limit is identically zero for all $\omega_{cyc} \neq 0$, whereas for $\omega_{cyc} = 0$ (the stationary component), it reduces to (4.23). The result is obtained by taking the Fourier transform of (4.23). ∎

Hence we conclude that the output of a noisy oscillator $x_s(t + \alpha(t))$ is a large stochastic process which is wide-sense stationary. The power spectral density of the output consists of a series of Lorentzians centered around the harmonics of the oscillator.

These results have important implications. The noisy oscillator output cannot be viewed as a deterministic periodic signal along with additive noise. We conclude that it should be viewed as a sum of two stochastic processes: a large signal output process with stochastic phase error which behaves like Brownian motion and a small amplitude noise process. Among other implications, this requires us to revisit the noise analysis techniques for nonautonomous circuits which we motivate and present in the next two chapters.

The Lorentzian shape of the output spectrum implies that the power spectral density at the carrier frequency and its harmonics has a finite value. Integrating the power spectral density we observe that

$$\begin{aligned}\int_{-\infty}^{\infty} S(\omega)\mathrm{d}\omega &= \int_{-\infty}^{\infty} \sum_{i=-\infty}^{\infty} X_i X_i^* \frac{\omega_0^2 i^2 c}{\frac{1}{4}\omega_0^4 i^4 c^2 + (\omega + i\omega_0)^2}\mathrm{d}\omega \\ &= \sum_{i=-\infty}^{\infty} X_i X_i^*\end{aligned}$$

i.e., the total carrier power is preserved despite spectral spreading due to noise. This result is physically consistent since adding a stochastic phase error $\alpha(t)$ to the oscillator

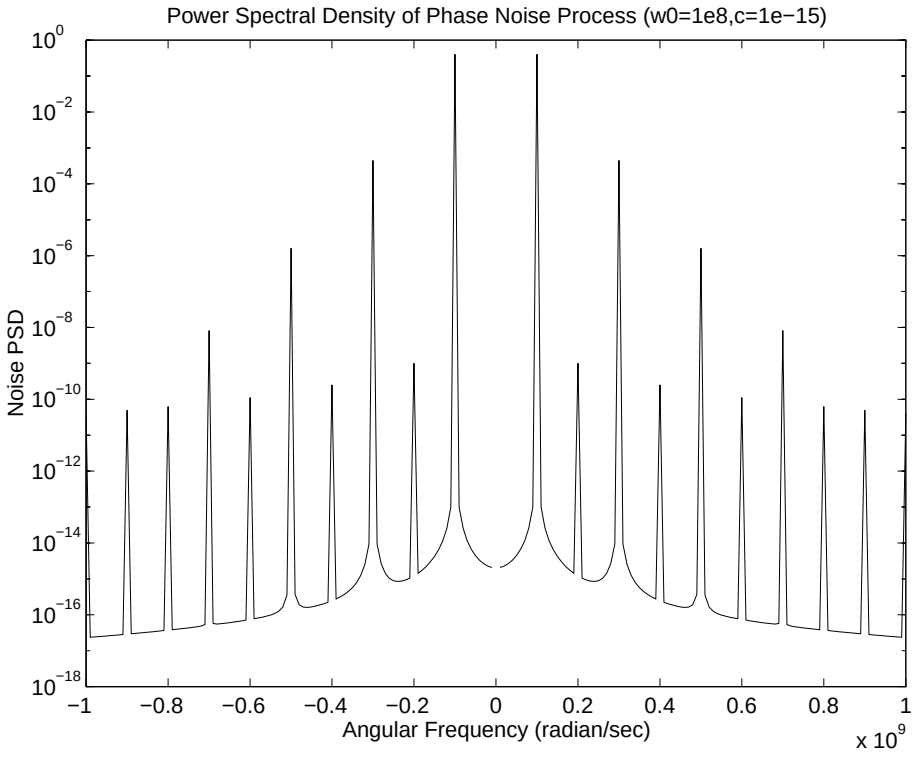

Figure 4.1: Power spectral density of noisy oscillator output

steady-state response should not change the total integrated power. Previous analyses based on linear time-invariant (LTI) or linear time-varying (LTV) concepts erroneously predict infinite noise power density at the carrier, as well as infinite total integrated power. That the oscillator output is stationary is surprising at first sight, since oscillators are nonlinear systems with periodic swings, hence it might be expected that output noise power would change periodically as in forced systems. However, it must be remembered that while forced systems are supplied with an external time reference (through the forcing), oscillators are not. Cyclostationarity in the oscillator's output would, by definition, imply a perfect time reference. Hence the stationarity result reflects the fundamental fact that noisy autonomous systems cannot provide a perfect time reference.

The power spectral density as calculated in (4.24) is shown in Figure 4.1 for $\omega_0 = 1 \times 10^8$ rad/sec and $c = 1 \times 10^{-15}$ sec. It consists of peaks at the harmonics of the oscillator which rapidly decay away from the harmonics. Figure 4.2 shows the power spectral density as a function of offset frequency around the first harmonic. We observe that the PSD does

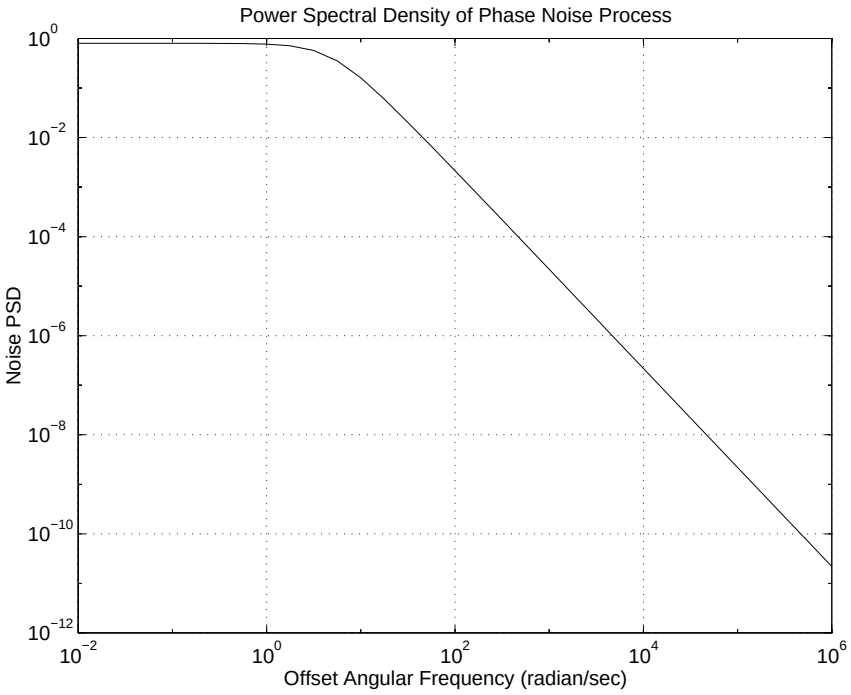

Figure 4.2: Power spectral density around the first harmonic

not blow up to infinity at $\Delta\omega \to 0$ but flattens out to a finite value.

4.3 Phase Noise Characterization for Oscillator

In this section, we discuss several popular characterizations of phase noise that are used in the design of electronic oscillators, and how they can easily be obtained from the stochastic characterization we obtained in Section 4.1 and Section 4.2.

4.3.1 Single-Sided Spectral Density and Total Power

The PSD $S(\omega)$ in (4.24) (defined for $-\infty < \omega < \infty$, hence called a double-sided density) is a real and even function of ω, because the periodic steady-state $x_s(t)$ is real hence its Fourier series coefficients X_i in Definition 4.2 satisfy $X_i = X_{-i}^*$. The *single-sided* spectral density (defined for $0 \le f < \infty$) is given by

$$S_{ss}(f) = 2S(2\pi f) = 2\sum_{i=-\infty}^{\infty} X_i X_i^* \frac{f_0^2 i^2 c}{\pi^2 f_0^4 i^4 c^2 + (f + i f_0)^2} \tag{4.25}$$

where we substituted $\omega = 2\pi f$ and $\omega_0 = 2\pi f_0$. The *total power* (i.e., the integral of the PSD over the range of the frequencies it is defined for) in $S_{ss}(f)$ is the same as in $S(2\pi f)$, which is

$$P_{tot} = \text{Total power in } S_{ss}(f) = \int_0^\infty S_{ss}(f)\mathrm{d}f = \sum_{i=1}^{\infty} 2\,|X_i|^2 \tag{4.26}$$

The total power in the periodic signal $x_s(t)$ (without phase noise) is also equal to the expression in (4.26) (excluding the power in the DC part), as can be easily seen from the Fourier expansion in Definition 4.2.

The phase deviation $\alpha(t)$ does *not* change the total power in the periodic signal $x_s(t)$, but it alters the power density in frequency, i.e., the power spectral density. For the perfect periodic signal $x_s(t)$, the power spectral density has δ functions located at discrete frequencies (i.e., the harmonics). The phase deviation $\alpha(t)$ *spreads* the power in these δ functions in the form given in (4.25), which can be experimentally observed with a spectrum analyzer.

4.3.2 Spectrum in dBm/Hz

For electrical oscillators, the state variable in the oscillator that is observed as the output is usually a *voltage* or a *current*. The spectrum in (4.25) is expressed as a function of frequency (f in Hz), then the PSD is in units of volts^2/Hz and amps^2/Hz for a voltage and a current state variable respectively. Then, the spectral density of the expected power dissipated in a 1Ω resistor (with the voltage (current) output of the oscillator as the voltage across (current through) the resistor) is equal to the PSD in (4.25) (in watts/Hz), which is usually expressed in dBw/Hz as defined by

$$S_{dBw}(f) = 10\log_{10}\left(S_{ss}(f) \text{ in watts/Hz}\right) \tag{4.27}$$

This expected power is the same as the time-average power, assuming that the stochastic process $x_s(t+\alpha(t))$ is ergodic [Gar90]. If $S_{ss}(f)$ is in miliwatts/Hz, then the PSD in dBm/Hz is given by

$$S_{dBm}(f) = 10\log_{10}\left(S_{ss}(f) \text{ miliwatts/Hz}\right) \tag{4.28}$$

4.3.3 Single-Sideband Phase Noise Spectrum in dBc/Hz

In practice, we are usually interested in the PSD around the first harmonic, i.e., $S_{ss}(f)$ for f around f_0. The *single-sideband* phase noise $\mathcal{L}(f_m)$ (in dBc/Hz) that is very

widely used in practice is defined as

$$\mathcal{L}(f_m) = 10 \log_{10} \left(\frac{S_{ss}(f_o + f_m)}{2|X_1|^2} \right) \tag{4.29}$$

For "small" values of c, and for $0 \leq f_m \ll f_0$, (4.29) can be approximated as

$$\mathcal{L}(f_m) \approx 10 \log_{10} \left(\frac{f_0^2 c}{\pi^2 f_0^4 c^2 + f_m^2} \right) \tag{4.30}$$

Furthermore, for $\pi f_0^2 c \ll f_m \ll f_0$, $\mathcal{L}(f_m)$ can be approximated by

$$\mathcal{L}(f_m) \approx 10 \log_{10} \left(\left(\frac{f_0}{f_m} \right)^2 c \right) \tag{4.31}$$

Notice that the approximation of $\mathcal{L}(f_m)$ in (4.31) blows up as $f_m \to 0$. For $0 \leq f_m < \pi f_0^2 c$, (4.31) is not accurate, in which case the approximation in (4.30) should be used.

4.3.4 Timing Jitter

In some applications, such as clock generation and recovery, one is interested in a characterization of the phase/time deviation $\alpha(t)$ itself rather than the spectrum of $x_s(t+\alpha(t))$ that was calculated in Section 4.2. In these applications, an oscillator generates a square-wave like waveform to be used as a clock. The effect of the phase deviation $\alpha(t)$ on such a waveform is to create uncertainty *jitter* in the *zero-crossing* or *transition* times. In Section 4.1, we found out that $\alpha(t)$ (for an autonomous oscillator) becomes a Gaussian random variable with a linearly increasing variance

$$\sigma^2(t) = ct$$

Let us take one of the transitions (i.e., edges) of a clock signal as a reference (i.e., trigger) transition and synchronize it with $t = 0$. If the clock signal is perfectly periodic, then one will see transitions exactly at $t_k = kT$, $k = 1, 2, \ldots$ where T is the period. For a clock signal with a phase deviation $\alpha(t)$ that has a linearly increasing variance as above, the timing of the k^{th} transition t_k will have a variance (i.e., mean-square error)

$$\mathbb{E}\left[(t_k - kT)^2\right] = ckT \tag{4.32}$$

The spectral dispersion caused by $\alpha(t)$ in an oscillation signal can be observed with a spectrum analyzer. Similarly, one can observe the timing jitter caused by $\alpha(t)$ using a

sampling oscilloscope. McNeill [McN97] experimentally observed the linearly increasing variance for the timing of the transitions of a clock signal generated by an autonomous oscillator, as predicted by our theory. Moreover, c (in $\sec^2$Hz) in (4.32) exactly quantifies the rate of increase of timing jitter with respect to a reference transition. Another useful figure of merit is the *cycle-to-cycle* timing jitter, i.e., the timing jitter in one clock cycle, which has a variance cT.

4.4 Noise Source Contribution

The scalar constant c appears in all of the characterizations we discussed above. It is given by

$$c = \frac{1}{T}\int_0^T v_1^T(\tau)D(x_s(\tau))D^T(x_s(\tau))v_1(\tau)\mathrm{d}\tau \tag{4.33}$$

where $D(\cdot) : \mathbb{R}^n \to \mathbb{R}^{n\times p}$ represents the *modulation* of the intensities of the noise sources with the large-signal state. (4.33) can be rewritten as

$$c = \sum_{i=1}^{p}\frac{1}{T}\int_0^T [v_1^T(\tau)\, D_i(\tau)]^2\,\mathrm{d}\tau = \sum_{i=1}^{p} c_i$$

where p is the number of the noise sources, i.e., the column dimension of $D(x_s(\cdot))$, and $D_i(\cdot)$ is the i^{th} column of $D(x_s(\cdot))$ which maps the i^{th} noise source to the equations of the system. Hence,

$$c_i = \frac{1}{T}\int_0^T [v_1^T(\tau)D_i(\tau)]^2\mathrm{d}\tau$$

represents the contribution of the ith noise source to c. Thus, the ratio

$$\frac{c_i}{c = \sum_{i=1}^{p} c_i} \tag{4.34}$$

can be used as a *figure of merit* representing the contribution of the i^{th} noise source to phase noise/timing jitter.

One can also define

$$c_s^{(k)} = \frac{1}{T}\int_0^T [v_1^T(\tau)\, e_k]^2\mathrm{d}\tau \tag{4.35}$$

(where $1 \le k \le n$ and e_k is the k^{th} unit vector) as the *phase noise/timing jitter sensitivity* of the k^{th} equation (i.e., node), because e_k represents a unit intensity noise source added to the k^{th} equation (i.e., connected to the k^{th} node) in (3.1).

4.5 Numerical Techniques for Phase Noise Characterization

From Section 4.1, Section 4.2 and Section 4.3 we observe that for various phase noise characterizations of an oscillator, one needs to calculate the steady-state periodic solution $x_s(t)$, and the periodic vector $v_1(t)$ in (4.33). $x_s(t)$ is available from the steady-state analysis of the circuit. We outline two methods, one in time domain and one in frequency domain, for computing the periodic vector $v_1(t)$.

4.5.1 Time Domain Technique

The procedure for calculating $v_1(t)$ in the time domain is as follows:

1. The large signal periodic steady-state solution $x_s(t)$ is computed for $0 \leq t \leq T$ by numerically integrating (3.1), either using transient simulation or possibly using a technique such as the shooting method [KWSV90] to directly compute the steady-state response of the oscillator.

2. The state transition matrix $\Phi(T, 0)$ is computed (see Section 3.2.1) by numerically integrating

$$\dot{Y} = J(t)Y \quad Y(0) = I_n$$

from 0 to T, where the Jacobian $J(t)$ is defined in (3.3). We recall that

$$\Phi(T, 0) = Y(T)$$

3. $u_1(0)$ is computed using

$$u_1(0) = \dot{x}_s(0)$$

$u_1(0)$ is an eigenvector of $\Phi(T, 0)$ corresponding to the eigenvalue 1.

4. $v_1(0)$ is an eigenvector of $\Phi^T(T, 0)$ corresponding to the eigenvalue 1. To compute $v_1(0)$, first compute an eigenvector of $\Phi^T(T, 0)$ corresponding to the eigenvalue 1, then scale this eigenvector so that

$$v_1(0)^T u_1(0) = 1 \tag{4.36}$$

is satisfied.

5. The periodic vector $v_1(t)$ is computed for $0 \leq t \leq T$ by numerically solving the adjoint system

$$\dot{y} = -J^T(t)y \tag{4.37}$$

using $v_1(0) = v_1(T)$ as the initial condition. $v_1(t)$ is a periodic steady-state solution of (4.37) corresponding to the Floquet exponent that is equal to 0, i.e., $\mu_1 = 0$. Since J is the Jacobian of an asymptotically orbitally stable oscillator, it is not possible to calculate $v_1(t)$ by numerically integrating (4.37) *forward* in time, because the numerical errors in computing the solution and the numerical errors in the initial condition $v_1(0)$ will excite the modes of the solution of (4.37) that grow without bound. However, one can integrate (4.37) *backwards* in time with the "initial" condition $v_1(T) = v_1(0)$ to calculate $v_1(t)$ for $0 \leq t \leq T$ in a numerically stable way.

6. Then, c is calculated using (4.33).

We implemented the above algorithm partly in SPICE and partly in MATLAB. Transient simulation of the oscillator circuit is performed in SPICE till steady-state is reached. The circuit is then simulated for one period with very small time step. The circuit matrices that are generated during this step are handed over to MATLAB where noise analysis is performed. In implementing the above algorithm, one can increase the efficiency by saving LU factored matrices that needs to be calculated in Step 2 and reuse them in Step 5. If the periodic steady-state $x_s(t)$ of the oscillator is calculated using the shooting method [KWSV90] in Step 1, then the state transition matrix $\Phi(T, 0)$ of the linear time varying system, obtained by linearizing the nonlinear oscillator circuit around the periodic steady-state, is already available. It can be shown that the *Jacobian* of the nonlinear system of equations that is solved in the shooting method, using Newton's method to calculate the initial condition that results in the periodic steady-state solution, is equal to $\Phi(T, 0) - I$ [AT72a, AT72b].

Moreover, one can avoid calculating $\Phi(T, 0)$ explicitly, and use iterative methods both for the shooting method, and at Step 4 to calculate the eigenvector of $\Phi^T(T, 0)$ that corresponds to the eigenvalue 1. For high-Q oscillators, the iterative methods can run into problems, because $\Phi(T, 0)$ may have several other eigenvalues which are close to 1. In our implementation, we explicitly calculate $\Phi(T, 0)$ and perform a full eigenvalue/eigenvector calculation. We select all the eigenvectors corresponding the eigenvalues which are close to

1 and use the following relation to determine the correct eigenvalue

$$\begin{aligned} v_i(0)^T u_1(0) &= v_i(0)\dot{x}_s(0) \\ &= \begin{cases} 1 & i = 1 \\ 0 & i \neq 1 \end{cases} \end{aligned}$$

We first calculate $\dot{x}_s(t)$ from the steady-state response of the oscillator. We then calculate the inner product with $v_i(0)$'s whose corresponding eigenvalues are close to 1. Due to numerical errors in determining the period and integration, the inner product is not exactly zero but the desired eigenvalue is easily identified. Full eigenvector/eigenvalue decomposition also allows us to investigate the properties of the state transition matrix for various oscillator circuits. Even with a full eigenvalue/eigenvector calculation for $\Phi(T, 0)$, the phase noise characterization algorithm discussed above is still very efficient. The phase noise characterization comes almost for free once the periodic steady-state solution $x_s(t)$ is computed.

4.5.2 Frequency Domain Technique

Here we outline how we can calculate $v_1(t)$ using a frequency domain technique such as harmonic balance. We consider (3.4)

$$\dot{w} = J(t)w$$

This describes a linear periodic time varying system of equation and represents an LPTV transfer function $h(t, s) = \Phi(t, s)$ where $\Phi(t, s)$ is the state transition matrix of $\dot{w} = Jw$. $h(t, s)$ is periodic in both it's arguments with period T, i.e.,

$$h(t + T, s + T) = h(t, s)$$

The periodicity of h implies that it can be expanded in a Fourier series [RFL98]

$$h(t, s) = \sum_{i=-\infty}^{\infty} h_i(t - s) \exp(\jmath i\omega_0 t) \quad \omega_0 = \frac{2\pi}{T} \tag{4.38}$$

h_i are referred to as *harmonic impulse response* of the LPTV system. The Fourier transform of h_i, $H_i(\omega)$ is defined as

$$H_i(\omega) = \int_{-\infty}^{\infty} h_i(t) \exp(-\jmath\omega t) \mathrm{d}t \tag{4.39}$$

A harmonic balance technique for solving $\dot{x} = f(x)$ typically yields a *harmonic balance conversion matrix* which is defined as follows.

Definition 4.3 ([RFL98]) *The harmonic balance conversion matrix is defined in terms of H_is as*

$$\mathcal{H}(\omega) = \begin{bmatrix} \vdots & \vdots & \vdots & \vdots & \vdots & \\ \cdots & H_0(\omega+2\omega_0) & H_1(\omega+\omega_0) & H_2(\omega) & H_3(\omega-\omega_0) & H_4(\omega-2\omega_0) & \cdots \\ \cdots & H_{-1}(\omega+2\omega_0) & H_0(\omega+\omega_0) & H_1(\omega) & H_2(\omega-\omega_0) & H_3(\omega-2\omega_0) & \cdots \\ \cdots & H_{-2}(\omega+2\omega_0) & H_{-1}(\omega+\omega_0) & H_0(\omega) & H_1(\omega-\omega_0) & H_2(\omega-2\omega_0) & \cdots \\ \cdots & H_{-3}(\omega+2\omega_0) & H_{-2}(\omega+\omega_0) & H_{-1}(\omega) & H_0(\omega-\omega_0) & H_1(\omega-2\omega_0) & \cdots \\ \cdots & H_{-4}(\omega+2\omega_0) & H_{-3}(\omega+\omega_0) & H_{-2}(\omega) & H_{-1}(\omega-\omega_0) & H_0(\omega-2\omega_0) & \cdots \\ & \vdots & \vdots & \vdots & \vdots & \vdots & \end{bmatrix}$$

Definition 4.4 *We define the matrices U_i and V_i to be the Fourier components of $U(t)$ and $V(t)$, i.e.,*

$$U(t) = \sum_{i=-\infty}^{\infty} U_i e^{j\omega_0 it} \tag{4.40}$$

$$V(t) = \sum_{i=-\infty}^{\infty} V_i e^{j\omega_0 it} \tag{4.41}$$

Definition 4.5 *We define the block-Toeplitz matrices $\mathcal{U}$ and $\mathcal{V}$ as follows:*

$$\mathcal{U} = \begin{bmatrix} \ddots & & & & & \\ & U_0 & U_1 & U_2 & \dots & \dots \\ & U_{-1} & U_0 & U_1 & U_2 & \dots \\ & U_{-2} & U_{-1} & U_0 & U_1 & U_2 \\ & \dots & U_{-2} & U_{-1} & U_0 & U_1 \\ & \dots & \dots & U_{-2} & U_{-1} & U_0 \\ & & & & & \ddots \end{bmatrix} \tag{4.42}$$

$$\mathcal{V} = \begin{bmatrix} \ddots & & & & & \\ & V_0 & V_1 & V_2 & \dots & \dots \\ & V_{-1} & V_0 & V_1 & V_2 & \dots \\ & V_{-2} & V_{-1} & V_0 & V_1 & V_2 \\ & \dots & V_{-2} & V_{-1} & V_0 & V_1 \\ & \dots & \dots & V_{-2} & V_{-1} & V_0 \\ & & & & & \ddots \end{bmatrix} \tag{4.43}$$

Lemma 4.11 *$\mathcal{U}$ and $\mathcal{V}$ are both invertible, since*

$$\mathcal{UV} = \begin{bmatrix} \ddots & & & & & & \\ & I & & & & & \\ & & I & & & & \\ & & & I & & & \\ & & & & I & & \\ & & & & & I & \\ & & & & & & \ddots \end{bmatrix}$$

Proof: Follows from the bi-orthonormality of $U(t)$ and $V(t)$. ∎

Definition 4.6 *Let*

$$D_k(\omega) = \begin{bmatrix} \jmath(\omega + k\omega_0) - \mu_0 & & \\ & \ddots & \\ & & \jmath(\omega + k\omega_0) - \mu_n \end{bmatrix}$$

We note that D_k is strictly diagonal.

Remark 4.1 *We observe that $D_k(\omega)$ is singular for $\omega = -k\omega_0$, if the oscillator is asymptotically orbitally stable.*

Definition 4.7 *Let*

$$\mathcal{D}(\omega) = \begin{bmatrix} \ddots & & & & & & & \\ & D_2(\omega) & & & & & & \\ & & D_1(\omega) & & & & & \\ & & & D_0(\omega) & & & & \\ & & & & D_{-1}(\omega) & & & \\ & & & & & D_{-2}(\omega) & & \\ & & & & & & \ddots \end{bmatrix}$$

$\mathcal{D}$ is also strictly diagonal.

Remark 4.2 *$\mathcal{D}(\omega)$ is singular for $\omega = k\omega_0$, $k \in \mathbb{Z}$ if the oscillator is asymptotically orbitally stable.*

Theorem 4.12 *The frequency-domain conversion matrix $\mathcal{H}(\omega)$ of the oscillator is related to $\mathcal{U}$, $\mathcal{D}(\omega)$ and $\mathcal{V}$ by:*

$$\mathcal{H}(\omega) = \mathcal{U}\mathcal{D}^{-1}(\omega)\mathcal{V}$$

Proof: We know that the transfer function $h(t,s)$ is the state transition matrix $\Phi(t,s)$. Hence for $\tau > 0$

$$\begin{aligned}\Phi(t,t-\tau) &= U(t)\exp(D\tau)V(t-\tau)\\ &= \sum_{k=-\infty}^{\infty}\sum_{l=-\infty}^{\infty} U_k \exp(D\tau)V_l \exp(\jmath\omega_0(kt+lt-l\tau))\end{aligned}$$

The coefficient of $\exp(\jmath\omega_0 it)$ in the above expression is given by

$$h_i(\tau) = \sum_{k=-\infty}^{\infty} U_k \exp(D\tau)V_{i-k}\exp(-\jmath\omega_0(i-k)\tau)$$

and hence

$$\begin{aligned}H_i(\omega) &= \int_{-\infty}^{\infty}\sum_{k=-\infty}^{\infty} U_k \exp(D\tau)V_{i-k}\exp(-\jmath\omega_0(i-k)\tau)\exp(\jmath\omega\tau)\mathrm{d}\tau\\ &= -\sum_{k=-\infty}^{\infty} U_k[D-\jmath(\omega_0(i-k)-\omega)I]^{-1}V_{i-k}\end{aligned}$$

where we have used the fact that $\phi(t,t-\tau)$ is defined for $\tau \geq 0$ only. The result follows immediately from the above form of $H_i(\omega)$. ∎

Theorem 4.13 *$\mathcal{H}^{-1}(0)$ is a singular matrix (with rank-deficiency one) and the null space of its transpose is spanned by the Fourier components of $v_1(t)$, i.e.,*

$$\begin{aligned}\ker\left(\mathcal{H}^{-T}(0)\right) &= \begin{bmatrix}1 & 0 & \cdots & 0\end{bmatrix}\begin{bmatrix}\cdots & V_{-2} & V_{-1} & V_0 & V_1 & V_2 & \cdots\end{bmatrix}\\ &= \begin{bmatrix}\cdots & V_{1,-2}^T & V_{1,-1}^T & V_{1,0}^T & V_{1,1}^T & V_{1,2}^T & \cdots\end{bmatrix}\end{aligned}$$

where $V_{1,i}$ are the Fourier coefficients of $k\,v_1^T(t)$, for some nonzero scalar k, i.e.,

$$kv_1^T(t) = \sum_{i=-\infty}^{\infty} V_{1,i}^T\, e^{\jmath\omega_0 it}$$

Sketch of Proof: The proof follows from the fact that $v_1(t)$ is the eigenvector of $\Phi^T(t,0)$ corresponding to eigenvalue 1. ∎

$\mathcal{H}^{-T}(0)$ is simply the transpose of the Harmonic Balance Jacobian matrix of the oscillator at solution. Its null space can be found efficiently even for large circuits by using

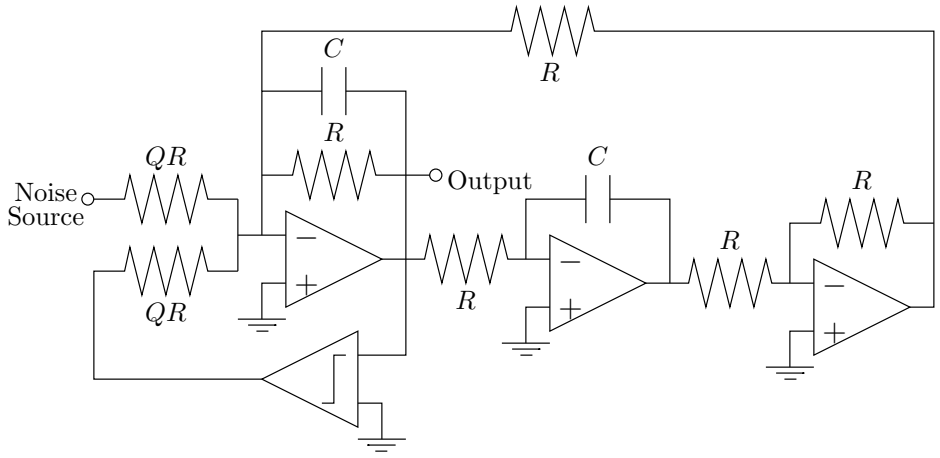

Figure 4.3: Oscillator with a band-pass filter and a comparator

iterative linear algebra techniques [RFL98]. Hence a scaled version of $v_1^T(t)$ can be found easily. The scaling constant k can be found by applying $v_1^T(t)u_1(t) = 1$, $u_1(t)$ having first been obtained by differentiating the large-signal steady-state solution of the oscillator.

4.6 Examples

We apply these characterization techniques to electrical oscillators. There are three distinct kinds of electrical oscillators with three very different oscillation mechanisms. The LC oscillator consists of a unstable feedback amplifier with frequency selection provided by the LC tank circuit. A ring oscillator consists of a number of delay stages connected in a ring. The frequency of oscillation is set by the number of stages and the delay of each stage. A relaxation oscillator uses regenerative switching to produce the output waveform. The signal generation mechanism for all these oscillators is very different but our analysis is valid for all these oscillators.

4.6.1 Generic Oscillator

This oscillator (Figure 4.3) consists of a Tow-Thomas second-order bandpass filter and a comparator [DTS98a]. If the OpAmps are considered to be ideal, it can be shown that this oscillator is equivalent (in the sense of the differential equations that describe it) to a parallel RLC circuit in parallel with a nonlinear voltage-controlled current source

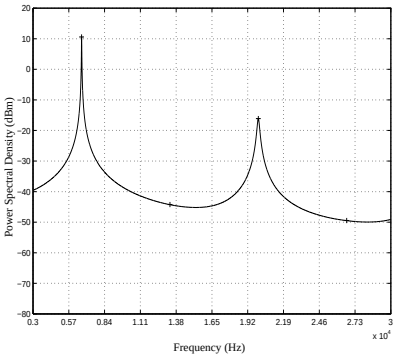

(a) Computed PSD (4 harmonics)

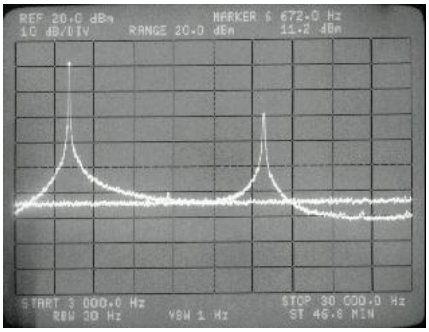

(b) Spectrum analyzer measured PSD [DTS98a]

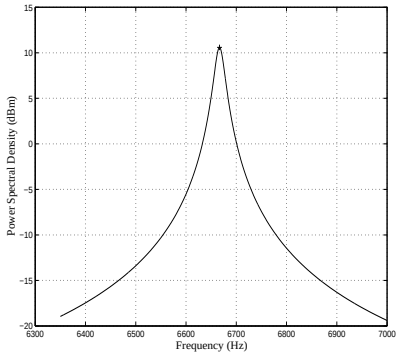

(c) Computed PSD (first harmonic)

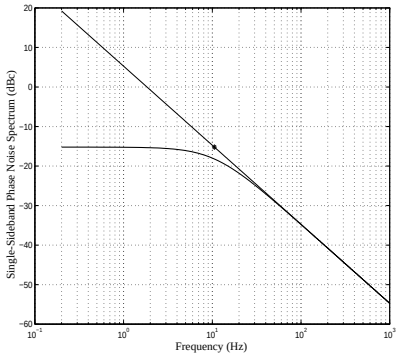

(d) $\mathcal{L}(f_m)$ computed with (4.30) and (4.31)

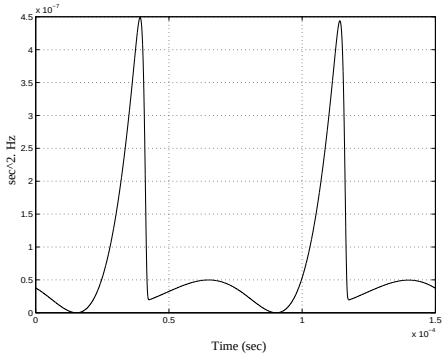

(e) $(v_1^T(t)D)^2$

Figure 4.4: Phase noise characterization for the generic oscillator

(or equivalently a series RLC circuit in series with a nonlinear current-controlled voltage source) as in Figure 4.3. In [DTS98a], authors bread-boarded this circuit with an external white noise source (intensity of which was chosen such that its effect is much larger than the other internal noise sources), and measured the PSD of the output with a spectrum analyzer. For $Q = 1$ and $f_o = 6.66$ KHz, we performed a phase noise characterization of this oscillator using the numerical methods in Section 4.5, and computed the periodic oscillation waveform $x_s(t)$ for the output and $c = 7.56\times10^{-8}$ sec^{2}Hz. Figure 4.4(a) shows the PSD of the oscillator output computed using (4.25), and Figure 4.4(b) shows the spectrum analyzer measurement. Figure 4.4(c) shows an expanded version of the PSD around the first harmonic. The single-sideband phase noise spectrum using both (4.30) and (4.31) is in Figure 4.4(d). (4.31) can not predict the PSD accurately below the cut-off frequency $f_c = \pi f_0^2 c = 10.56$ Hz (marked with a $*$ in Figure 4.4(d)) of the Lorentzian. The oscillator model that was simulated has two state variables and a single stationary noise source. Figure 4.4(e) shows a plot of the periodic nonnegative scalar

$$v_1^T(t)D(x_s(t))D^T(x_s(t))v_1(t) = (v_1^T(t)D)^2$$

where D is independent of t since the noise source is stationary. c is the time average of this scalar that is periodic in time.

4.6.2 LC Tank Oscillator

A Colpitt's oscillator with an off-chip inductor is shown in Figure 4.5. This oscillator is designed to oscillate at 1.05 GHz. We computed $c = 9.00 \times 10^{-19}$ sec^{2}Hz which corresponds to $\mathcal{L}(f_m) = -100$ dBc/Hz at $f_m = 100$ KHz using (4.31). The simplified circuit had 11 state variables and 8 noise sources. We generated a noise source contribution report (Table 4.1) and found that 85% of the contribution to c is from the noise in base spreading resistor r_b of the transistor. A decrease in this value (due to sizing of transistor) by a factor of 5 causes the value of c to be reduced to 4.38×10^{-19} sec^{2}Hz. We also plot $v_1^T(t)D(x_s(t))D^T(x_s(t))v_1(t)$ as a function of time for one period of oscillation(Figure 4.6). We see that this value peaks at a time equal to half the period of oscillation. This also is useful feedback to the designers as it can be used to further improve the noise performance of this oscillator.

A simplified schematic of a 4.7 GHz oscillator with on-chip inductor is shown in Figure 4.7 [Kin98]. This oscillator is fabricated in a standard digital 0.35 μ CMOS process

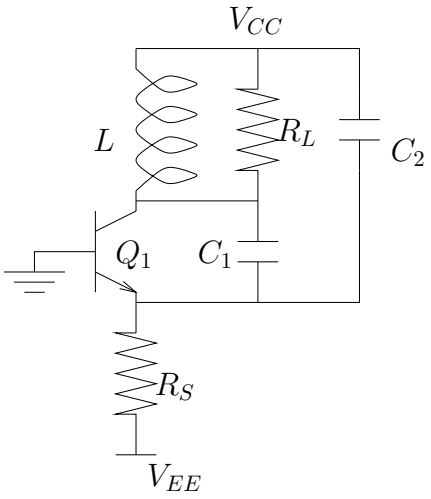

Figure 4.5: Colpitt's Oscillator

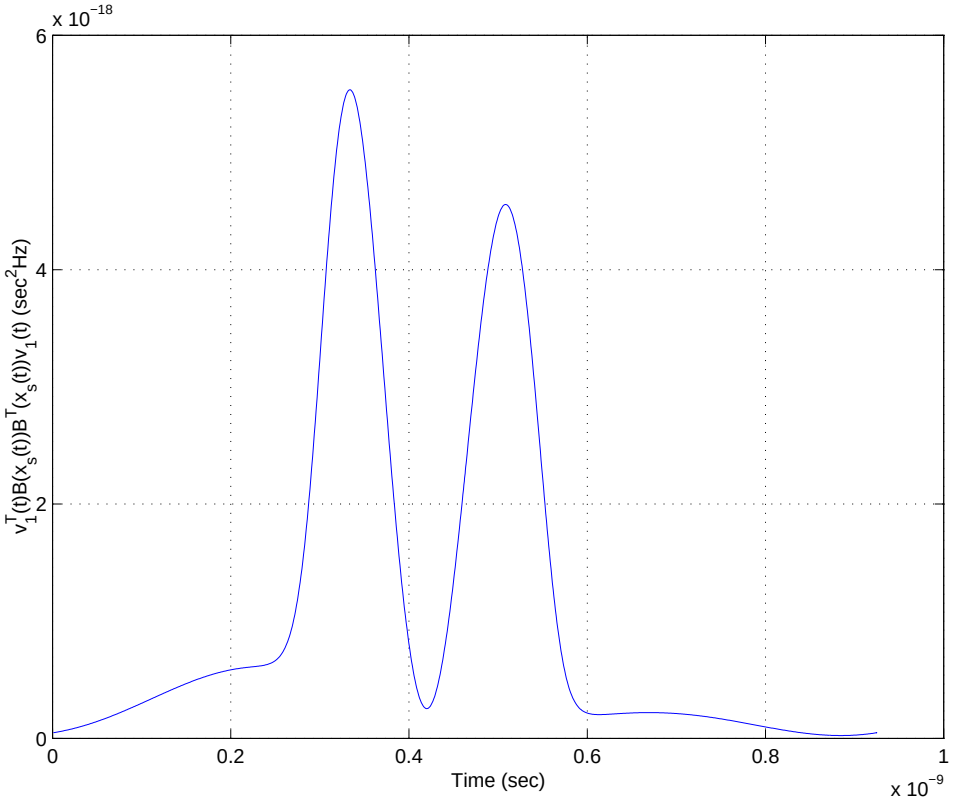

Figure 4.6: $v_1^T(t)D(x_s(t))D^T(x_s(t))v_1(t)$ for the Colpitt's oscillator

and uses transistor parasitics for tank capacitors in the oscillator. We computed $c = 5.12 \times 10^{-19}$ sec^{2}Hz which corresponds to $\mathcal{L}(f_m) = -89.3$ dBc/Hz at $f_m = 100$ KHz using (4.31). The author in [Kin98] reported a measured value of -90 dBc/Hz at 100KHz offset. There were 20 state variables and 28 noise sources in the simulated circuit. We generated a noise source contribution report for this oscillator using (4.34), which is shown in Table 4.2. We find that apart from the transistors, M1 and M2, inductor losses also contribute significantly towards oscillator phase noise. $v_1(t)D(x_s(t))^T D(x_s(t))v_1^T(t)$ is plotted as a function of time in Figure 4.8.

4.6.3 Ring Oscillator

The ring oscillator circuit is a three stage oscillator with fully differential ECL buffer delay cells (differential pairs followed by emitter followers) as shown in Figure 4.9 [McN97]. [McN97] and [WKG94] use analytical techniques to characterize the timing jitter/phase noise performance of ring oscillators with ECL type delay cells. [McN97] does the analysis for a bipolar ring oscillator, and [WKG94] does it for a CMOS one. Since they use analytical techniques, they use a simplified model of the circuit and make several approximations in their analysis. [McN97] and [WKG94] use time domain Monte Carlo noise simulations to verify the results of their analytical results. They obtain qualitative and some quantitative results, and offer guidelines for the design of low phase noise ring oscillators with ECL type delay cells. However, their results are only valid for their specific oscillator circuits. We compare their results with the results we obtain for the above ring oscillator using the general phase noise characterization methodology we have proposed which makes it possible to analyze a complicated oscillator circuit without simplifications. We performed several phase noise characterizations of the bipolar ring oscillator. The circuit consists of 91

Noise Source	$\frac{c_i}{c}$	
	$r_b = 25\ \Omega$	$r_b = 5\ \Omega$
Q_1 Base resistor	85.4%	59.8%
R_L	10.4%	26.4%
Rs	3.5%	12.3%
Others	0.7%	1.5%

Table 4.1: Noise source contribution for the Colpitt's oscillator for two different base resistance values

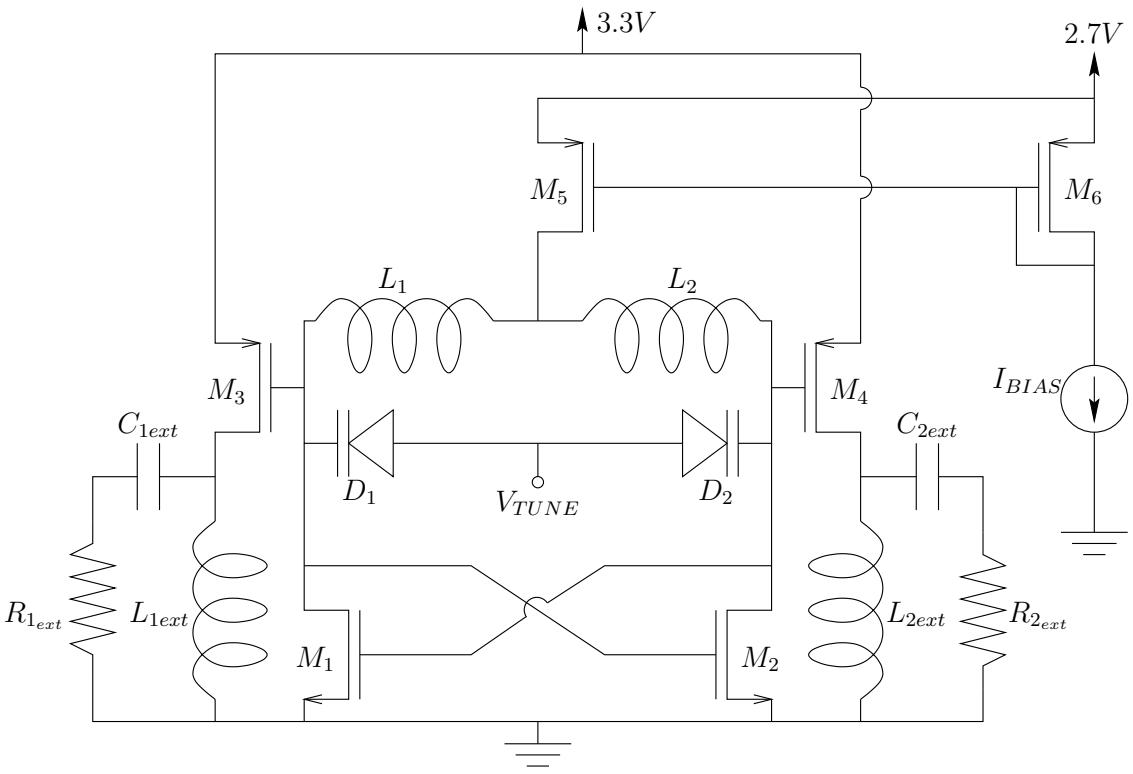

Figure 4.7: Oscillator with on-chip inductor

Noise sources of	$\frac{c_i}{c=\sum_{i=1}^{p} c_i} \times 100$
M1 and M2	57.6 %
Inductor losses	38.5 %
Others	3.9 %

Table 4.2: Noise Source Contribution for oscillator with on-chip inductor

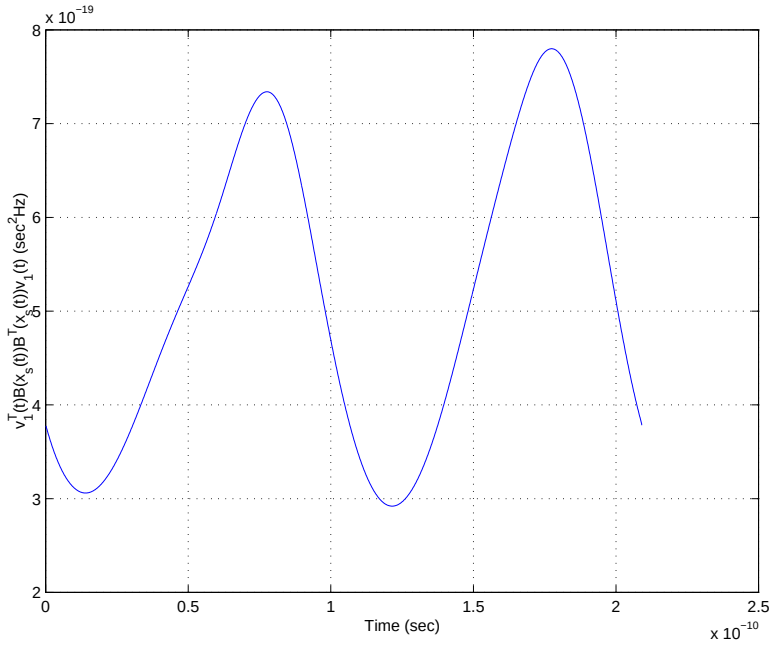

Figure 4.8: $v_1^T(t)D(x_s(t))D^T(x_s(t))v_1(t)$ for oscillator with on-chip inductor

state variables and 121 noise sources. The results are shown in Table 4.3, where R_c is the collector load resistance for the differential pair (DP) in the delay cell, r_b is the zero bias base resistance for the BJTs in the DP, I_{EE} is the tail bias current for the DP, and f_o is the oscillation frequency for the three stage ring oscillator. The changes in R_c and r_b affect the oscillation frequency, unlike the changes in I_{EE}. Figure 4.10 shows a plot of $(2\pi f_o)^2\, c$ versus I_{EE} using the data from Table 4.3. This prediction of the dependence of phase noise/timing jitter performance on the tail bias current is in agreement with the analysis and experimental results presented in [McN97] and [WKG94] for ring oscillators with ECL type delay cells. Larger values for $(2\pi f_o)^2\, c$ indicate *worse* phase noise performance.

4.6.4 Relaxation Oscillator

The relaxation oscillator is a VCO that is based on the emitter-coupled multivibrator circuit [GM93]. [AM83] analyzes the process of jitter production for this circuit by describing the circuit behaviour with a single first-order stochastic differential equation based on a simplified model for the circuit, and lumping all of the noise sources into a single stationary current noise source. [AM83] arrives at intuitive qualitative results for

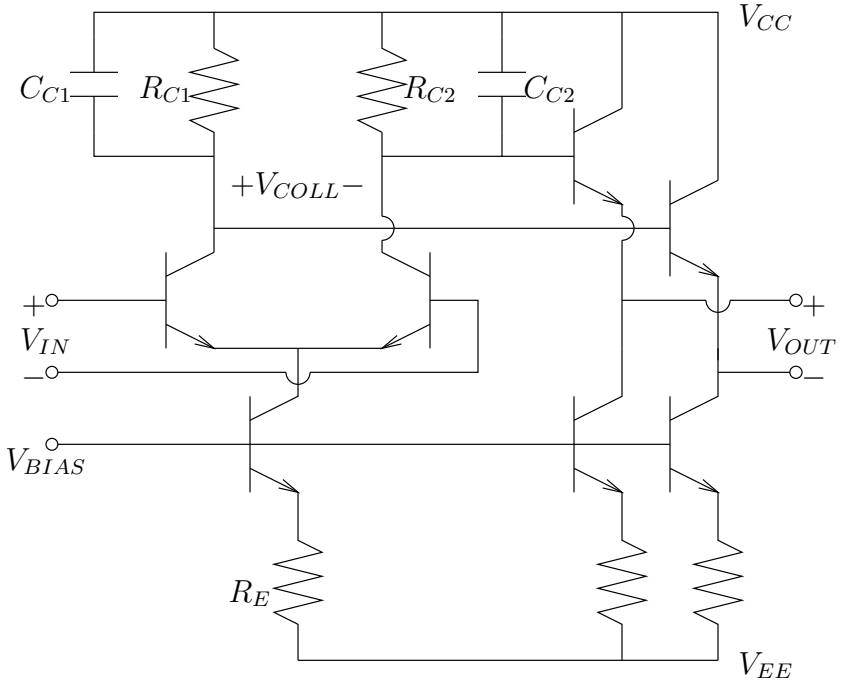

Figure 4.9: Ring oscillator delay cell

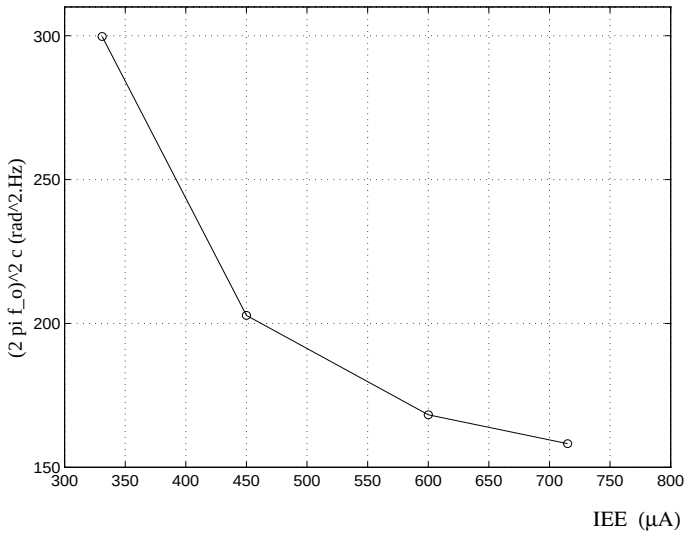

Figure 4.10: Ring-oscillator phase noise performance versus emitter bias current

R_c (Ω)	r_b (Ω)	I_{EE} (μA)	f_o (MHz)	c ($\text{sec}^2.\text{Hz} \times 10^{-15}$)
500	58	331	167.7	0.269
2000	58	331	74	0.149
500	1650	331	94.6	0.686
500	58	450	169.5	0.182
500	58	600	169.7	0.151
500	58	715	167.7	0.142

Table 4.3: Phase noise characterization of the ring oscillator

low jitter relaxation oscillator design. A relaxation oscillator operates in a highly nonlinear fashion due to regenerative switchings. The analysis of the process of jitter production is not analytically tractable without reverting to simplifications.

For this oscillator, using the numerical methods described in Section 4.5, we obtain

$$f_o = 0.89 \text{ MHz} \quad (2\pi f_o)^2 c = 0.83 \text{ rad}^2\text{Hz}$$

which corresponds to

$$\frac{\sqrt{cT}}{T} = 153.2 \text{ ppm RMS}$$

cycle-to-cycle timing jitter, where ppm is *parts per million* and RMS is *root-mean-square*. This circuit contained 37 noise sources and 47 state variables.

Chapter 5

Noise Analysis of Nonautonomous Circuits

In the previous chapter we developed a noise simulation and characterization technique for oscillators. We found that a mathematically consistent way of representing the output of a noisy oscillator is to view it as a sum of two stochastic processes: a small amplitude noise process and a large signal output process which is the noiseless oscillator response phase shifted by a Brownian motion process. This new way of characterizing the oscillator output has far reaching impact on the methodology of performing noise simulation for circuits driven by these oscillators. The "traditional" approach for this is to view the oscillator output as a deterministic signal with some additive noise, classified as phase noise and amplitude noise. Therefore, for traditional noise analysis of nonautonomous circuits, it is assumed that the input signal noise can be viewed as a circuit noise source. Since the circuit is driven by a periodic input signal, the circuit response is also periodic. Traditional noise analysis techniques linearize the circuit equations around the periodic response and solve the resulting linear periodic time varying (LPTV) system of equations. Since the circuit is driven by a large periodic signal, the circuit noise statistics and the output noise statistics are also periodically time varying.

However, given our new way of characterizing the oscillator output, we need to reexamine the noise analysis methodology for nonautonomous circuits as well. The principal difference is that the circuit is driven by a large signal wide-sense stationary stochastic process instead of a deterministic periodic signal. In this chapter we address the problem

of noise analysis for nonautonomous circuits driven by a periodic input signal which has phase noise. We first briefly describe the traditional noise analysis techniques for circuits in presence of deterministic periodic signals. We then analyze a noiseless nonlinear circuit which is driven by a periodic input signal with phase noise and show that general noise analysis is an extension of this case. We then suggest modifications to the existing noise analysis techniques, both in time and frequency domain. We conclude this chapter with some examples.

5.1 Mathematical Preliminaries

The dynamics of a unperturbed nonautonomous system can be described by the following system of differential equations

$$\dot{x} = f(x) + b_0(t) \tag{5.1}$$

where $x \in \mathbb{R}^n$ is a vector of state variables, $f(x) : \mathbb{R}^n \to \mathbb{R}^n$ and $b_0(t) : \mathbb{R} \to \mathbb{R}^n$ is deterministic T-periodic input. We make a distinction between forced and nonautonomous circuits. A nonautonomous circuit is one which does not produce any output of interest without an input stimulus. A forced circuit, on the other hand, has a large forcing input signal. However, the equations of a forced circuit can also be oscillatory and then the response of the system is a forced oscillation. In the following exposition, we are interested only in nonautonomous circuits. For sake of simplicity, we use the state equation formulation to describe the system. These results and techniques can be extended to the mixed differential-algebraic equation formulation (for instance, as in modified nodal analysis (MNA)) of the form $\frac{\mathrm{d}q(x)}{\mathrm{d}t} + f(x) = 0$ in a straightforward manner. We assume that this equation satisfies the Cauchy-Peano existence and uniqueness theorem for the initial value problem [Gri90]. We further assume that the system is stable in the sense that in the absence of $b_0(t)$, the steady-state solution of this equation is 0. We assume that the steady-state solution of this system (in presence of $b_0(t)$) is given by $x_s(t)$, which is also periodic with period T. This assumption is justified for almost all nonautonomous RF components except for frequency dividers where the output is periodic with a larger period T'. The analysis we present here is therefore not immediately applicable for frequency dividers.

We are interested in the response of this system in the presence of noise, both in the form of circuit intrinsic noise $D(x)\xi(t)$ and phase noise in the input signal of the

form $b_0(t+\alpha(t))$. $D(\cdot):\mathbb{R}^n \to \mathbb{R}^{n\times p}$ describes the connectivity and modulation of the circuit noise sources, $\xi(\cdot):\mathbb{R}\to\mathbb{R}^p$ are circuit white noise sources and $\alpha(\cdot):\mathbb{R}\to\mathbb{R}$ is the phase deviation process of the input signal which is a scaled Brownian motion process, i.e., of the form $\sqrt{c}B(t)$ where c is the rate of increase of the variance (see Section 4.4 and (4.33)). Hence the behaviour of the nonautonomous circuit along with noise is governed by the following differential equation.

$$\dot{x} = f(x) + b_0(t+\alpha(t)) + D(x)\xi(t) \tag{5.2}$$

Since $\alpha(t)$ and $\xi(t)$ are stochastic processes, $x(t)$ in general will also be a stochastic process and the above equation should be treated as a stochastic differential equation. One approach of solving this would be to construct a Fokker-Planck equation as we did in Chapter 4 for (4.1). (4.1) is a stochastic differential equation of one variable $\alpha(t)$. For $x(t)$ we need to find the Fokker-Planck equation governing the joint probability density function of all n components of $x(t)$. This analysis becomes intractable very quickly. Instead, we rewrite (5.2) in the following form

$$\mathrm{d}x = f(x)\mathrm{d}t + b_0(t+\alpha(t))\mathrm{d}t + D(x)\mathrm{d}B_p(t) \tag{5.3}$$

where $B_p(t)$ is a p-dimensional Brownian motion independent of $\alpha(t)$.

(5.3) is not in the standard stochastic differential equation form. For this we define $x_1(t) = x(t)$ and $x_2 = cB(t)$ where $B(t)$ is a Brownian motion process uncorrelated with any of the components of $B_p(t)$. Using this we rewrite (5.3) as

$$\begin{bmatrix}\dot{x}_1(t)\\ \dot{x}_2(t)\end{bmatrix} = \begin{bmatrix}f(x_1)+b_0(t+x_2(t))\\ 0\end{bmatrix}\mathrm{d}t + \begin{bmatrix}D(x_1)\mathrm{d}B_p(t)\\ \sqrt{c}\mathrm{d}B(t)\end{bmatrix}$$

However, it turns out that solving (5.3) directly is easier.

5.2 Cyclostationary Approach

We begin with a brief description of classical cyclostationary noise analysis. We consider (5.3) but with ideal periodic input signal $b_0(t)$, i.e.,

$$\mathrm{d}x = f(x)\mathrm{d}t + b_0(t)\mathrm{d}t + D(x)\mathrm{d}B_p(t) \tag{5.4}$$

The traditional approach assumes that the perturbed response of this system is $x_s(t)+y(t)$ where $y(t)$ is the small stochastic deviation of the response of the system. Substituting this in (5.4) we have

$$\mathrm{d}x_s(t) + \mathrm{d}y(t) = f(x_s(t)+y(t))\mathrm{d}t + b_0(t)\mathrm{d}t + D\left(x_s(t)+y(t)\right)\mathrm{d}B_p(t)$$

Linearizing $f(x_s(t)+y(t))$ around $x_s(t)$, ignoring $y(t)$ in the argument of $B(\cdot)$ and using that fact that $x_s(t)$ satisfies (5.1), the above equation reduces to

$$\mathrm{d}y(t) \approx \left.\frac{\mathrm{d}f}{\mathrm{d}x}\right|_{x_s(t)} y(t)\mathrm{d}t + D(x_s(t))\mathrm{d}B_p(t) \tag{5.5}$$

where

$$\left.\frac{\mathrm{d}f}{\mathrm{d}x}\right|_{x_s(t)} = J(t)$$

is the Jacobian of $f(x)$ evaluated at $x_s(t)$. Since $x_s(t)$ is T-periodic, it follows that $J(t)$ is also T-periodic. Hence (5.5) describes a linear periodic time-varying system of equations governing $y(t)$. Since the input signal $b_0(t)$ is T-periodic, the modulation term $D(x_s(t))$ is also periodic and hence circuit noise sources statistics are cyclostationary. This means that the deviation process $y(t)$ is also cyclostationary. The time-varying statistics of $y(t)$ are usually computed by considering the periodic time-varying noise as an input to a linear periodically time-varying system corresponding to

$$\frac{\mathrm{d}y}{\mathrm{d}t} = J(t)y$$

which is computed directly from the steady-state response of the circuit [TKW96, RFL98].

5.3 Response of a Noiseless Circuit to Input Signal Phase Noise

We now introduce our approach to solving (5.3). To illustrate the basic principles of our approach we will assume that the nonlinear circuit itself is noiseless, i.e., $D(x) = 0$. We will relax this assumption later. As indicated earlier, the additive amplitude noise component of the input signal can also be absorbed in the circuit equations so we will only consider an input signal which has phase deviation but no amplitude noise, i.e., of the form $b_0(t+\alpha(t))$. Hence (5.2) reduces to

$$\dot{x} = f(x) + b_0(t+\alpha(t))$$

or equivalently,

$$\mathrm{d}x = f(x)\mathrm{d}t + b_0(t + \alpha(t))\mathrm{d}t \tag{5.6}$$

where, as before, $\alpha(t) = \sqrt{c}B(t)$. Assuming that c is small, i.e., the input signal phase noise is small and the system is stable, the response of the system can be assumed to be of the form

$$x_s(t + \alpha(t)) + y_1(t)$$

where $y_1(t)$ is assumed to be small. By choosing the response to be of this form, we are assuming that the circuit is able to follow any variations in input frequency. This is a valid assumption if input signal phase noise (i.e., c) is assumed to be small which means that the variation in frequency is small. Further we assume that the circuit is nonautonomous. For practical circuits, there will also be a small change in the amplitude of the response with the frequency variation which we absorb in $y_1(t)$. We will substitute this form of solution in (5.6) and solve for $y_1(t)$. We first make the following useful observations.

Definition 5.1 *Let*

$$s(t) = t + \alpha(t) \tag{5.7}$$

Definition 5.2 (One-dimensional Itô Process [Øks98]) *A one-dimensional Itô process is a stochastic process $X(t)$, on the underlying probability space, of the form*

$$X(t) = X(0) + \int_0^t u(\tau, \omega)\mathrm{d}\tau + \int_0^t u(\tau, \omega)\mathrm{d}B(\tau) \tag{5.8}$$

where $\omega \in \Omega$ and Ω is the sample space of the underlying probability space and $u(t, \omega)$ and $v(t, \omega)$ are stochastic processes. Further v is such that $v \in \mathcal{W}_{\mathcal{H}}$ and

$$\mathbb{P}\left[\int_0^t v(\tau, \omega)^2\mathrm{d}\tau < \infty \quad \forall t \geq 0\right] = 1$$

(See Appendix A Definition A.8 for the definition of $\mathcal{W}_{\mathcal{H}}$). We also assume that u is $\mathcal{H}_t$-adapted (see Appendix A Definition A.3) and

$$\mathbb{P}\left[\int_0^t |u(\tau, \omega)|\mathrm{d}\tau < \infty \quad \forall t \geq 0\right] = 1$$

Here $\mathcal{H}_t$ is an increasing family of σ-algebras such that $B(t)$ is a martingale (see Appendix A Definition A.7) with respect to $\mathcal{H}_t$.

Lemma 5.1 *$s(t)$ as defined in (5.7) is an Itô process.*

Proof: We have

$$\begin{aligned} \mathrm{d}s(t) &= \mathrm{d}t + \mathrm{d}\alpha(t) \\ &= \mathrm{d}t + \sqrt{c}\mathrm{d}B(t) \end{aligned}$$

According to (5.8), $u(t,\omega) \equiv 1$ and $v(t,\omega) \equiv \sqrt{c}$ trivially satisfy the conditions of Definition 5.2. ∎

The advantage of proving $s(t)$ to be an Itô process is that we can use the following result to evaluate $\mathrm{d}x_s(t+\alpha(t))$.

Lemma 5.2 (The Itô Formula [Øks98]) *Let $X(t)$ be an Itô process given by*

$$\mathrm{d}X(t) = u\mathrm{d}t + u\mathrm{d}B(t)$$

Let $g(t,x)$ be twice continuously differentiable on $\mathbb{R}_+ \times \mathbb{R}$. Then

$$Y(t) = g(t, X(t))$$

is also an Itô process and

$$\mathrm{d}Y(t) = \frac{\partial g}{\partial t}(t, X(t))\mathrm{d}t + \frac{\partial g}{\partial x}(t, X(t))\mathrm{d}X(t) + \frac{1}{2}\frac{\partial^2 g}{\partial x^2}(t, X(t))(\mathrm{d}X(t))^2$$

where

$$(\mathrm{d}X(t))^2 = \mathrm{d}X(t)\mathrm{d}X(t)$$

is computed according to the rules

$$\mathrm{d}t\mathrm{d}t = \mathrm{d}t\mathrm{d}B(t) = 0$$

and

$$\mathrm{d}B(t)\mathrm{d}B(t) = \mathrm{d}t$$

We assume that $x_s(t)$ is twice differentiable with respect to its argument. Let

$$\dot{x}_s(t) = \frac{\mathrm{d}x_s}{\mathrm{d}t}(t)$$

and

$$\ddot{x}_s(t) = \frac{\mathrm{d}^2 x_s}{\mathrm{d}t^2}(t)$$

Then using the result of Lemma 5.2 we have

$$\begin{aligned}
\mathrm{d}x_s(t+\alpha(t)) &= \mathrm{d}x_s(s(t)) \\
&= \dot{x}_s(s(t))\mathrm{d}s(t) + \frac{1}{2}\ddot{x}_s(s(t))[\mathrm{d}s(t)]^2 \\
&= \dot{x}_s(s(t))\big(\mathrm{d}t + \sqrt{c}\mathrm{d}B(t)\big) + \frac{1}{2}\ddot{x}_s(s(t))\big(\mathrm{d}t + \sqrt{c}\mathrm{d}B(t)\big)^2 \\
&= \Big(\dot{x}_s(s(t)) + \frac{c}{2}\ddot{x}_s(s(t))\Big)\,\mathrm{d}t + \sqrt{c}\dot{x}_s(s(t))\mathrm{d}B(t)
\end{aligned}$$

The term $\frac{c}{2}\ddot{x}_s(s(t))\mathrm{d}t$ in the above expansion is due to the fact that $\mathrm{d}B(t)$ is of the order of $\sqrt{\mathrm{d}t}$. Substituting this expression in (5.6) and linearizing $f(x)$ around $x_s(s(t))$ we obtain

$$\begin{aligned}
\mathrm{d}y_1(t) + \dot{x}_s(s(t))(\mathrm{d}t + \sqrt{c}\mathrm{d}B(t)) + \frac{c}{2}\ddot{x}_s(s(t))\mathrm{d}t \approx f\big(x_s(s(t))\big)\mathrm{d}t + \left.\frac{\mathrm{d}f}{\mathrm{d}x}\right|_{x_s(s(t))} y_1(t)\mathrm{d}t \\
+ b_0(s(t))\mathrm{d}t
\end{aligned}$$

Since $x_s(t)$ is the steady-state solution of (5.1),

$$\frac{\mathrm{d}x_s}{\mathrm{d}t}(s(t)) = f\big(x_s(s(t))\big) + b_0(s(t))$$

and hence

$$\mathrm{d}y_1(t) = J(s(t))y_1(t)\mathrm{d}t + M_1(s(t))\mathrm{d}B(t) + M_2(s(t))\mathrm{d}t \tag{5.9}$$

where $M_1(t) = -\sqrt{c}\dot{x}_s(t)$ and $M_2(t) = -0.5c\ddot{x}_s(t)$ are also T-periodic.

Remark 5.1

- *The term $M_1(s(t))\mathrm{d}B(t)$ represents a white noise source modulated by the time derivative of the steady-state response of the nonlinear circuit. This means that phase noise in the input signal also appears as a circuit white noise source and contributes to time-varying wide-band noise at the output of the circuit.*
- *The periodic coefficients J, M_1 and M_2 are evaluated at $s(t) = t + \alpha(t)$ and* not *at t.*
- *(5.9) is a stochastic differential equation which is linear in $y_1(t)$ and the terms*

  $$M_1(s(t))\mathrm{d}B(t) \text{ and } M_2(s(t))\mathrm{d}t$$

  represent two inputs to this linear system. Hence $y_1(t)$ can be represented as $y_{11}(t) + y_{12}(t)$ where $y_{11}(t)$ satisfies

  $$\mathrm{d}y_{11}(t) = J(s(t))y_{11}(t)\mathrm{d}t + M_1(s(t))\mathrm{d}B(t) \tag{5.10}$$

and $y_{12}(t)$ *satisfies*

$$\mathrm{d}y_{12}(t) = J(s(t))y_{12}(t)\mathrm{d}t + M_2(s(t))\mathrm{d}t \tag{5.11}$$

To solve (5.10) we make the following useful observations:

Definition 5.3 *Define* $U(t)$ *as*

$$U(t) = \sqrt{c}B(t) \mod T$$

Lemma 5.3 *The solution of* (5.10) *is the same as the solution of*

$$\mathrm{d}y_{11}(t) = J(t+U(t))y_{11}(t)\mathrm{d}t + M_1(t+U(t))\mathrm{d}B(t)$$

Proof: Follows from the fact that $J(t)$ and $M_1(t)$ are T-periodic. ∎

Lemma 5.4 *Asymptotically* $U(t)$ *is a random process which is uniformly distributed between 0 and* T *for every* t*.*

Sketch of Proof: This follows from the fact that the variance of a Brownian motion grows unbounded with t. ∎

Definition 5.4 *Define* $r = t + U(t)$ *and* $z_{11}(r) = y_{11}(t)$*.*

Then using the fact that c is small and Lemma 5.4, it follows that (5.10) is equivalent to the following equation

$$\mathrm{d}z_{11}(r) = J(r)z_{11}(r)\mathrm{d}r + M_1(r)\mathrm{d}B(r)$$

This equation is in the exact same form as (5.5). Using the same arguments as in Section 5.2 we can conclude that $z_{11}(r)$ is a cyclostationary process. Moreover, since $J(\cdot)$ is the Jacobian of a stable system, if $M_1(r)w(r)$ is small, $z_{11}(r)$ is small for all r. Hence the above analysis is consistent.

Using the fact that $y_{11}(t) = z_{11}(r) = z_{11}(t+U(t))$ and $U(t)$ is uniformly distributed between 0 and T for all t, we conclude that

Theorem 5.5

- $y_{11}(t)$ *is wide-sense stationary*

- *The autocorrelation* $\mathbb{E}\left[y_{11}(t)y_{11}^T(t+\tau)\right]$, *where* $y_{11}(t)$ *is the solution of*

$$\mathrm{d}y_{11}(t) = J(t+\alpha(t))y_{11}(t)\mathrm{d}t + M_1(t+\alpha(t))\mathrm{d}B(t)$$

is the stationary component of $\mathbb{E}\left[z_{11}(t)z_{11}^T(t+\tau)\right]$ *where* $z_{11}(t)$ *is the solution of*

$$\mathrm{d}z_{11} = J(t)z_{11}(t)\mathrm{d}t + M_1(t)\mathrm{d}B(t)$$

Proof: [Pap91] ∎

Hence we can compute $y_{11}(t)$ by considering the stationary component of $z_{11}(r)$ which can be computed using existing noise analysis techniques for nonautonomous circuits.

Next we consider (5.11). Defining $z_{12}(s(t)) = y_{12}(t)$ as for $z_{11}(s(t))$ we conclude that $z_{12}(s)$ satisfies the following differential equation

$$\mathrm{d}z_{12} = J(s)z_{12}(s)\mathrm{d}s + M_2(s)\mathrm{d}s$$

The above equation is linear in $z_{12}(s)$ with a *deterministic* periodic input $M_2(s)$ (in the argument s). If c is small, $M_2(s)$ will be small and the response $z_{12}(s)$ will also be small and periodic. Hence the solution of (5.11) is of the form

$$y_{12}(t) = z_{12}(t+\alpha(t))$$

where z_{12} is periodic in it's argument. This term is the small amplitude variation term that we had indicated when we chose the particular form of the solution of (5.9). Using similar arguments as in Section 4.2 we conclude that $y_{12}(t) = z_{12}(t+\alpha(t))$ is a wide-sense stationary stochastic process with a noise spectrum which is very similar to the spectrum of $x_s(t+\alpha(t))$ except that it is much smaller in magnitude. Hence this typically contributes to noise power outside the frequency band of interest.

5.4 Extension to General Noise Analysis

We now extend this result to the general noise analysis case where we also consider circuit noise sources. We now consider (5.3)

$$\mathrm{d}x = f(x)\mathrm{d}t + b_0(t+\alpha(t))\mathrm{d}t + D(x)\mathrm{d}B_p(t)$$

We assume that the response of the circuit is of the form

$$x_s(t+\alpha(t)) + y_0(t)$$

Proceeding exactly as in Section 5.3, we conclude that $y_0(t) = y_{01}(t) + y_{02}(t)$ where $y_{01}(t)$ satisfies

$$\mathrm{d}y_{01}(t) = J(s(t))y_{01}(t)\mathrm{d}t + M_1(s(t))\mathrm{d}B(t) + M_0(s(t))\mathrm{d}B_p(t) \tag{5.12}$$

where $B(t)$ and $B_p(t)$ are uncorrelated and $M_0(t) = D(x_s(t))$. $y_{02}(t)$ is still given by (5.11). (5.12) can be rewritten as

$$\mathrm{d}y_{01}(t) = J(s(t))y_{01}(t)\mathrm{d}t + M(s(t))\mathrm{d}B_{p+1}(t)$$

where

$$M(t) = \begin{bmatrix} M_1(t) & M_0(t) \end{bmatrix}$$

and

$$B_{p+1}(t) = \begin{bmatrix} B(t) \\ B_p(t) \end{bmatrix}$$

Hence it follows that

Corollary 5.6

- *$y_{01}(t)$ is wide-sense stationary*
- *The autocorrelation $\mathbb{E}\left[y_{01}(t)y_{01}^T(t+\tau)\right]$, where $y_{01}(t)$ is the solution of*

$$\mathrm{d}y_{01}(t) = J(t+\alpha(t))y_{01}(t)\mathrm{d}t + M(t+\alpha(t))\mathrm{d}B_{p+1}(t)$$

is the stationary component of $\mathbb{E}\left[z_{01}(t)z_{01}^T(t+\tau)\right]$ where $z_{01}(t)$ is the solution of

$$\mathrm{d}z_{01} = J(t)z_{01}(t)\mathrm{d}t + M(t)\mathrm{d}B_{p+1}(t) \tag{5.13}$$

Therefore, we conclude that the output of a nonautonomous circuit driven by a oscillatory (periodic) signal with Brownian motion phase deviation $\alpha(t)$ is given by

$$x_s(t+\alpha(t)) + y_{01}(t) + y_{02}(t)$$

$x_s(t+\alpha(t))$ is the steady-state response of the circuit phase shifted by $\alpha(t)$ and $y_{02}(t) \equiv z_{02}(t+\alpha(t))$ is an additional small amplitude variation. Both $x_s(t)$ and $z_{02}(t)$ are deterministic, periodic functions but $x_s(t+\alpha(t))$ and $y_{02}(t)$ are stochastic processes since $\alpha(t)$

is Brownian motion. The spectrum of both these processes consists of Lorentzians centered around the frequency of oscillation of the input signal. On the other hand $y_{01}(t)$ is a small wide-band amplitude noise process which is evaluated using (5.12).

The fact that the output noise of the nonautonomous circuit is stationary is surprising at first glance. If the input signal is perfectly periodic then the output noise is indeed cyclostationary. However, in presence of a noisy input signal, which, by definition cannot provide perfectly periodic time reference, the output noise cannot be cyclostationary. Another way of intuitively understanding this result is to view the nonautonomous circuit as a part of the oscillator circuit which is generating the periodic input waveform. Then the analysis which we presented in Chapter 4 is valid for this composite oscillator circuit as well. Hence the output noise for this circuit has to be wide-sense stationary. For the case of oscillator output noise, we were interested in the noise spectral density close to the frequency of oscillation where the phase noise term dominates. For the case of nonautonomous circuits, we are usually interested in noise spectral density well away from the frequency of oscillation and hence we need to compute the amplitude noise. We revisit this fact in more detail in Section 5.6.

Remark 5.2

The above analysis makes the assumption that the input signal phase noise are uncorrelated with the circuit noise sources and noise coming from any other input port. Consider the case when the LNA in the receiver path is driven by a small desired signal and a large blocker. The blocker acts as an LO for the nonlinearities present in the LNA. Hence the LNA output consists of a large in-band blocker along with LNA output noise which is correlated to the blocker. Noise analysis of subsequent blocks will have to take this correlation into account until the in-band power of the blocker drops below the noise floor. This problem can be finessed by analyzing the cascade of circuit blocks till the in-band power of the blocker is negligible. This does increase the circuit size but if efficient algorithms coupled with iterative linear solvers are used, the running time increases almost linearly (actually $O(n \log n)$).

5.5 Amplitude Noise Characterization of Oscillators

The analysis presented in Section 5.4 can be used to evaluate amplitude noise response of oscillators as well. From Section 3.3 the deviation away from the limit cycle

$(y(t))$ is given by

$$\frac{\mathrm{d}y}{\mathrm{d}t} = J(t+\alpha(t))y(t) + \tilde{b}(x_s(t+\alpha(t)),t) \tag{5.14}$$

where

$$\tilde{b}(x,t) = \sum_{i=2}^{n} c_i(x,t)u_i(t+\alpha(t))$$

and

$$c_i(x,t) = v_i^T(t+\alpha(t))D(x)b(t)$$

$\alpha(t)$ is the phase deviation of the oscillator response and is governed by the following differential equation:

$$\frac{\mathrm{d}\alpha}{\mathrm{d}t} = v_1^T(t+\alpha(t))D\big(x_s(t+\alpha(t))\big)b(t) \quad \alpha(0)=0$$

Here $\{u_i(t)\}$ and $\{v_i(t)\}$ are bi-orthonormal Floquet basis vectors, which span the n-dimensional space at every t. Therefore, (5.14) can be rewritten as

$$\frac{\mathrm{d}y}{\mathrm{d}t} = J(t+\alpha(t))y(t) + \sum_{i=2}^{n} u_i(t+\alpha(t))v_i^T(t+\alpha(t))D\big(x_s(t+\alpha(t))\big)b(t)$$

For white noise perturbations $\xi(t) = b(t)$, this equation is rewritten as

$$\mathrm{d}y = J(t+\alpha(t))y(t)\mathrm{d}t + \sum_{i=2}^{n} M_{oi}(t+\alpha(t))\mathrm{d}B_p(t)$$

where

$$M_{oi}(t) = u_i(t)v_i^T(t)D(x_s(t))$$

and we have written $\mathrm{d}B_p(t)$ instead of $\xi(t)\mathrm{d}t$. This equation is in the same form as (5.12). Hence we can solve this equation using the analysis presented in Section 5.4. We can also conclude that the amplitude noise process of a noisy oscillator output is also a wide-sense stationary process. Amplitude noise power spectral density is typically much smaller compared to the noise spectral density of the large signal oscillator output $x_s(t+\alpha(t))$ for frequency ranges of interest and hence is typically not considered.

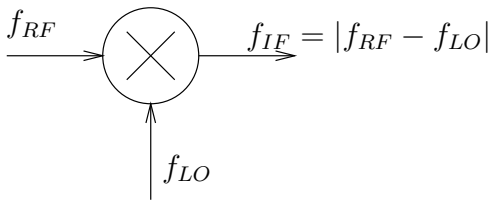

Figure 5.1: Block diagram of a mixer with input and output signal frequencies

5.6 Modification to Existing Noise Analysis Techniques

As pointed out in Section 5.4, the output of a nonautonomous circuit is given by

$$x_s(t + \alpha(t)) + y_{01}(t) + y_{02}(t)$$

The spectrum of $x_s(t+\alpha(t))+y_{02}(t)$ consists of Lorentzians centered around the harmonics of the frequency of the input signal. The noise power spectral density rapidly diminishes away from these harmonics. For typical application of these circuits, we are interested in the noise power spectral density well away from the frequency of the large input signal. Consider a mixer driven by a large LO signal with frequency f_{LO} (Figure 5.1). The RF signal frequency is usually present in a small frequency band centered around frequency f_{RF}. The output (IF) signal is centered around a frequency $|f_{RF} - f_{LO}|$. The IF signal frequency is typically much smaller than either RF or LO (typically $\frac{1}{4}$ or $\frac{1}{5}$ of f_{LO}). Around the IF frequency, the power spectral density of $x_s(t + \alpha(t)) + y_{02}(t)$ is of the order of $X_1^2 c$ which is much smaller than the noise spectral density of $y_{01}(t)$. Hence we will only describe techniques for solving (5.12) for $y_{01}(t)$. As pointed out in Corollary 5.6, the autocorrelation $\mathbb{E}\left[y_{01}(t)y_{01}^T(t+\tau)\right]$ is given by the stationary component of $\mathbb{E}\left[z_{01}(t)z_{01}^T(t+\tau)\right]$ where $z_{01}(t)$ is governed by (5.13). This equation is very similar to (5.4) hence we concluded that for evaluating (5.12) we can still use the existing noise simulation algorithms. However we need the following modifications:

- We need to add another noise source to the noise equations corresponding to the phase to wide-band amplitude noise conversion of the input signal phase noise by the nonlinear system. For this we first need to perform noise analysis of the oscillator to determine the phase noise performance of the input signal.

- We only need to consider the stationary component of the cyclostationary noise statis-

tics computed by the algorithm.

We now briefly outline two noise simulation algorithms, one in time domain [TKW96] and one in frequency domain [RFL98] which are suited for this purpose. For both these analyses we assume that the equations governing the unperturbed (noiseless) circuit response are given by

$$\frac{\mathrm{d}q(x)}{\mathrm{d}t} + f(x) + b_0(t) = 0$$

The periodic steady-state solution of this system of equations is $x_s(t)$. The equations governing the circuit response with perturbation (noise) are given by

$$\frac{\mathrm{d}q(x)}{\mathrm{d}t} + f(x) + b_0(t) + D(x)b(t) = 0 \tag{5.15}$$

where $q(\cdot), f(\cdot) : \mathbb{R}^n \to \mathbb{R}^n$ and $b_0(t)$, $D(x)$ are $b(t)$ are as defined in Section 5.1. The solution of (5.15) is of the form $x_s(t) + y(t)$ where $y(t)$, as usual, is the small deviation of the solution around the large unperturbed steady-state solution. Substituting this in (5.15), linearizing around the $x_s(t)$ and using the fact that $x_s(t)$ satisfies the unperturbed system of equations we obtain the following linear periodic time varying (LPTV) system of equations for $y(t)$:

$$\frac{\mathrm{d}}{\mathrm{d}t}\left(\left.\frac{\mathrm{d}q(x)}{\mathrm{d}x}\right|_{x_s(t)} y(t)\right) + \left.\frac{\mathrm{d}f(x)}{\mathrm{d}x}\right|_{x_s(t)} y(t) + D(x_s(t))b(t) = 0 \tag{5.16}$$

For periodic deterministic perturbation $b(t)$ (of angular frequency ω), it follows from the theory of LPTV system of equations that the response $y(t)$ will be of the form

$$y(t) = \sum_{k=-\infty}^{\infty} Y_k \exp(\jmath(\omega + k\omega_0)t)$$

where $\omega_0 = 1/T$. This implies that

$$y(t+T) = y(t)\exp(\jmath\omega T)$$

For white noise perturbation $b(t) = \xi(t)$, the output $y(t)$ will be stochastic process whose statistics vary periodically with time. To solve (5.16), we need to find the LPTV transfer function and compute the output noise power.

5.6.1 Time-Domain Technique

The approach described in [TKW96] solves (5.16) in time domain. For one period T, time is discretized in m steps and (5.16) is solved using a linear multi-step method, such as Backward Euler. At the i^{th} Backward Euler step, the equation for $\tilde{y}(t_i)$, the approximation to $y(t)$ at time t_i is given by

$$\left(\frac{1}{h_i}\left.\frac{\mathrm{d}q}{\mathrm{d}x}\right|_{x_s(t_i)} + \left.\frac{\mathrm{d}f}{\mathrm{d}x}\right|_{x_s(t_i)}\right)\tilde{y}(t_i) - \frac{1}{h_i}\left.\frac{\mathrm{d}q}{\mathrm{d}x}\right|_{x_s(t_{i-1})}\tilde{y}(t_{i-1}) + D(x_s(t_i))b(t_i) = 0$$

where $h_i = t_i - t_{i-1}$. The above equation represents a sequence of m equations. These m equations are rewritten in matrix form as

$$\begin{bmatrix} \frac{C_1}{h_1}+G_1 & & -\frac{C_m\alpha(\omega)}{h_1} \\ -\frac{C_1}{h_1} & \frac{C_2}{h_2}+G_2 & \\ \ddots & \ddots & \\ & -\frac{C_{m-1}}{h_m} & \frac{C_m}{h_m}+G_m \end{bmatrix} \begin{bmatrix} \tilde{y}(t_1) \\ \tilde{y}(t_2) \\ \vdots \\ \tilde{y}(t_m) \end{bmatrix} = \begin{bmatrix} -D(x_s(t_1))b(t_1) \\ -D(x_s(t_2))b(t_2) \\ \vdots \\ -D(x_s(t_m))b(t_m) \end{bmatrix}$$

where $\alpha(\omega) = \exp(\jmath\omega T)$,

$$C_i = \left.\frac{\mathrm{d}q}{\mathrm{d}x}\right|_{x_s(t_i)}$$

and

$$G_i = \left.\frac{\mathrm{d}f}{\mathrm{d}x}\right|_{x_s(t_i)}$$

The coefficient matrix is written as a sum of two terms, as follows

$$\begin{bmatrix} \frac{C_1}{h_1}+G_1 & & -\frac{C_m\alpha(\omega)}{h_1} \\ -\frac{C_1}{h_1} & \frac{C_2}{h_2}+G_2 & \\ \ddots & \ddots & \\ & -\frac{C_{m-1}}{h_m} & \frac{C_m}{h_m}+G_m \end{bmatrix} = \underbrace{\begin{bmatrix} \frac{C_1}{h_1}+G_1 & & \\ -\frac{C_1}{h_1} & \frac{C_2}{h_2}+G_2 & \\ \ddots & \ddots & \\ & -\frac{C_{m-1}}{h_m} & \frac{C_m}{h_m}+G_m \end{bmatrix}}_{\triangleq L} + \underbrace{\begin{bmatrix} 0 & & -\frac{C_m}{h_1} \\ 0 & 0 & \\ & \ddots & \ddots \\ & 0 & 0 \end{bmatrix}}_{\triangleq B}\alpha(\omega)$$

and the matrix equation is rewritten as

$$(I + \alpha(\omega)L^{-1}B)\begin{bmatrix} \tilde{y}(t_1) \\ \tilde{y}(t_2) \\ \vdots \\ \tilde{y}(t_m) \end{bmatrix} = -L^{-1}\begin{bmatrix} D(x_s(t_1))b(t_1) \\ D(x_s(t_2))b(t_2) \\ \vdots \\ D(x_s(t_m))b(t_m) \end{bmatrix}$$

The above system of equation is efficiently solved using a preconditioned Krylov sub-space method with L^{-1} as a preconditioner. Since L is a block lower bi-diagonal matrix, and each of the blocks are sparse (they are derived from the circuit matrix), multiplication by L^{-1}, i.e., solution of $Lx = y$, can be performed very efficiently.

5.6.2 Frequency-Domain Technique

We now describe a harmonic balance based technique for solving (5.16) [RFL98]. This equation is rewritten in the following form

$$C(t)\dot{y} + G(t)y + A(t)b(t) = 0 \tag{5.17}$$

where

$$C(t) = \left.\frac{\mathrm{d}q}{\mathrm{d}x}\right|_{x_s(t)}$$

$$G(t) = \left.\frac{\mathrm{d}f}{\mathrm{d}x}\right|_{x_s(t)} + \frac{\mathrm{d}}{\mathrm{d}t}\left(\left.\frac{\mathrm{d}q}{\mathrm{d}x}\right|_{x_s(t)}\right)$$

and

$$A(t) = D(x_s(t))$$

Since (5.17) is linear in $y(t)$, let the corresponding linear time varying transfer function be $h(t_2, t_1)$. The output $y(t)$ is written in terms of input $b(t)$ as

$$y(t_2) = \int_{-\infty}^{\infty} h(t_2, t_1)b(t_1)\mathrm{d}t_1 \tag{5.18}$$

5.6.2.1 Noise Propagation Through Linear Time-Varying System

We first computer the output noise power spectral density in terms of input noise power spectral density when noise propagates through a linear periodically time varying (LPTV) system.

Since $C(t)$ and $G(t)$ are T-periodic, the linear time varying transfer function $h(t_2, t_1)$ can be expressed as (4.38) and (4.39) which are repeated here:

$$h(t_2, t_1) = \sum_{i=-\infty}^{\infty} h_i(t_2 - t_1)\exp(\jmath i\omega_0 t_2)$$

and

$$H_i(\omega) = \int_{-\infty}^{\infty} h_i(t) \exp(-\jmath\omega t)\mathrm{d}t$$

Using (4.38) and (4.39) it follows that the transfer function $h(t_2, t_1)$ can be written as

$$h(t_2, t_1) = \frac{1}{2\pi} \sum_{i=-\infty}^{\infty} \int_{-\infty}^{\infty} H_i(\omega) \exp[\jmath\omega(t_2 - t_1)] \exp(\jmath i\omega_0 t_2)\mathrm{d}\omega$$

Since $y(t)$ and $b(t)$ are, in general, stochastic processes whose statistics vary with time, the autocorrelation function for these processes is defined as

$$R_{pp}(t_1, t_2) = \mathbb{E}\left[p(t_1)p^T(t_2)\right]$$

and the power spectral density is defined as the two-dimensional Fourier transform of the autocorrelation function as

$$S_{pp}(\omega_1, \omega_2) = \int_{-\infty}^{\infty}\int_{-\infty}^{\infty} R_{pp} \exp[-\jmath(\omega_1 t_1 + \omega_2 t_2)]\mathrm{d}t_1\mathrm{d}t_2 \tag{5.19}$$

From (5.18) it follows that the autocorrelation function of the output noise process is related to the input noise process as

$$\begin{aligned} R_{yy}(t_1, t_2) &= \mathbb{E}\left[y(t_1)y^T(t_2)\right] \\ &= \mathbb{E}\left[\int_{-\infty}^{\infty}\int_{-\infty}^{\infty} h(t_1, s_1)b(s_1)b^T(s_2)h^T(t_2, s_2)\mathrm{d}s_1\mathrm{d}s_2\right] \\ &= \int_{-\infty}^{\infty}\int_{-\infty}^{\infty} h(t_1, s_1)R_{bb}(s_1, s_2)h^T(t_2, s_2)\mathrm{d}s_1\mathrm{d}s_2 \end{aligned} \tag{5.20}$$

Combining (5.19), (5.18), (4.38) and (4.39) we have

$$\begin{aligned} S_{yy}(\omega_1, \omega_2) &= \int_{-\infty}^{\infty}\iiint h(t_1, s_1)R_{bb}(s_1, s_2)h^T(t_2, s_2) \exp[-\jmath(\omega_1 t_1 + \omega_2 t_2)]\mathrm{d}t_1\mathrm{d}t_2\mathrm{d}s_1\mathrm{d}s_2 \\ &= \frac{1}{16\pi^4} \int_{-\infty}^{\infty}\iiint\iiint\iiint \sum_{i=-\infty}^{\infty}\sum_{k=-\infty}^{\infty} H_i(\omega_3) \exp[\jmath\omega_3(t_1 - s_1)] \exp(\jmath i\omega_0 t_1)S_{bb}(\omega_5, \omega_6) \\ &\qquad \exp[\jmath(\omega_5 s_1 + \omega_6 s_2)]H_k^T(\omega_4) \exp[\jmath\omega_4(t_2 - s_2)] \\ &\qquad \exp(\jmath k\omega_0 t_2) \exp[-\jmath(\omega_1 t_1 + \omega_2 t_2)]\mathrm{d}t_1\mathrm{d}t_2\mathrm{d}s_1\mathrm{d}s_2 \\ &\qquad \mathrm{d}\omega_3\mathrm{d}\omega_4\mathrm{d}\omega_5\mathrm{d}\omega_6 \\ &= \frac{1}{16\pi^4} \int_{-\infty}^{\infty}\iiint\iiint\iiint \sum_{i=-\infty}^{\infty}\sum_{k=-\infty}^{\infty} H_i(\omega_3)S_{bb}(\omega_5, \omega_6)H_k^T(\omega_4) \exp[\jmath(\omega_5 - \omega_3)s_1] \\ &\qquad \exp[\jmath(\omega_3 + i\omega_0 - \omega_1)t_1 + \jmath(\omega_4 + k\omega_0 - \omega_2)t_2] \\ &\qquad \exp[\jmath(\omega_6 - \omega_4)s_2]\mathrm{d}t_1\mathrm{d}t_2\mathrm{d}s_1\mathrm{d}s_2\mathrm{d}\omega_3\mathrm{d}\omega_4\mathrm{d}\omega_5\mathrm{d}\omega_6 \end{aligned}$$

Using the identity

$$\frac{1}{2\pi}\int_{-\infty}^{\infty}\exp(\jmath\omega t)\mathrm{d}t = \delta(\omega)$$

we have

$$\begin{aligned}
S_{yy}(\omega_1,\omega_2) &= \iiiint_{-\infty}^{\infty}\sum_{i=-\infty}^{\infty}\sum_{k=-\infty}^{\infty} H_i(\omega_3)S_{bb}(\omega_5,\omega_6)H_k^T(\omega_4)\delta(\omega_3+i\omega_0-\omega_1)\delta(\omega_5-\omega_3) \\
&\qquad\qquad \delta(\omega_4+k\omega_0-\omega_2)\delta(\omega_6-\omega_4)\mathrm{d}t_1\mathrm{d}t_2\mathrm{d}s_1\mathrm{d}s_2 \\
&= \sum_{i=-\infty}^{\infty}\sum_{k=-\infty}^{\infty} H_i(\omega_1-i\omega_0)S_{bb}(\omega_1-i\omega_0,\omega_2-k\omega_0)H_k^T(\omega_2-k\omega_0)
\end{aligned} \tag{5.21}$$

Since both input and output noise are assumed to be cyclostationary, the autocorrelation $R_{yy}(t_1,t_2)$ can be expressed as a Fourier series as

$$R_{yy}(t_1,t_2) = \sum_{i=-\infty}^{\infty} R_{yy,i}(t_2-t_1)\exp(\jmath i\omega_0 t_2)$$

The one-dimensional Fourier transform of $R_{yy,i}(t)$ is referred to the harmonic power spectral density (HSPD) [RFL98] and is defined as

$$S_{yy,i}(\omega) = \int_{-\infty}^{\infty} R_{yy,i}(t)\exp(-\jmath\omega t)\mathrm{d}t$$

The original two-dimensional power spectral density $S_{pp}(\omega_1,\omega_2)$ can be related to the harmonic power spectral density as follows:

$$\begin{aligned}
S_{pp}(\omega_1,\omega_2) &= \int_{-\infty}^{\infty}\int_{-\infty}^{\infty} R_{pp}(t_1,t_2)\exp[-\jmath(\omega_1 t_1+\omega_2 t_2)]\mathrm{d}t_1\mathrm{d}t_2 \\
&= \int_{-\infty}^{\infty}\int_{-\infty}^{\infty}\sum_{i=-\infty}^{\infty} R_{pp_i}(t_2-t_1)\exp(\jmath i\omega_0 t_2)\exp[-\jmath(\omega_1 t_1+\omega_2 t_2)]\mathrm{d}\omega\mathrm{d}t_1\mathrm{d}t_2 \\
&= \frac{1}{2\pi}\iiint_{-\infty}^{\infty}\sum_{i=-\infty}^{\infty} S_{pp_i}(\omega)\exp[\jmath(\omega+i\omega_0-\omega_2)t_2]\exp[-\jmath(\omega+\omega_1)t_1]\mathrm{d}\omega\mathrm{d}t_1\mathrm{d}t_2 \\
&= 2\pi\int_{-\infty}^{\infty}\sum_{i=-\infty}^{\infty} S_{pp_i}(\omega)\delta(\omega+i\omega_0-\omega_2)\delta(-\omega-\omega_1)\mathrm{d}\omega \\
&= 2\pi\sum_{i=-\infty}^{\infty} S_{pp_i}(-\omega_1)\delta(-\omega_1+i\omega_0-\omega_2)
\end{aligned} \tag{5.22}$$

From (5.21) and (5.22) the output noise HSPD's can be related to the input noise HSPD's as follows:

$$S_{yy_l}(-\omega) = \sum_{i=-\infty}^{\infty} \sum_{k=-\infty}^{\infty} H_i(\omega - i\omega_0) S_{bb_k}(-\omega + i\omega_0) H^T_{l-(i+k)}[-\omega + (i+k)\omega_0]$$

(see Section 4.5.2). The above relation is rewritten in matrix form as [RFL98]

$$\mathcal{S}_{yy}(\omega) = \mathcal{H}(\omega)\mathcal{S}_{bb}(\omega)\mathcal{H}^*(\omega) \tag{5.23}$$

where $\mathcal{H}$ is the *harmonic balance conversion matrix* (see Definition 4.3 in Section 4.5.2),

$$\mathcal{S}_{bb}(\omega) = \begin{bmatrix}
 & \vdots & \vdots & \vdots & \vdots & \vdots & \\
\cdots & S_{bb,0}(-\omega+2\omega_0) & S_{bb,1}(-\omega+2\omega_0) & S_{bb,2}(-\omega+2\omega_0) & S_{bb,3}(-\omega+2\omega_0) & S_{bb,4}(-\omega+2\omega_0) & \cdots \\
\cdots & S_{bb,0}(-\omega+\omega_0) & S_{bb,1}(-\omega+\omega_0) & S_{bb,2}(-\omega+\omega_0) & S_{bb,3}(-\omega+\omega_0) & S_{bb,4}(-\omega+\omega_0) & \cdots \\
\cdots & S_{bb,0}(-\omega) & S_{bb,1}(-\omega) & S_{bb,2}(-\omega) & S_{bb,3}(-\omega) & S_{bb,4}(-\omega) & \cdots \\
\cdots & S_{bb,0}(-\omega-\omega_0) & S_{bb,1}(-\omega-\omega_0) & S_{bb,2}(-\omega-\omega_0) & S_{bb,3}(-\omega-\omega_0) & S_{bb,4}(-\omega-\omega_0) & \cdots \\
\cdots & S_{bb,0}(-\omega-2\omega_0) & S_{bb,1}(-\omega-2\omega_0) & S_{bb,2}(-\omega-2\omega_0) & S_{bb,3}(-\omega-2\omega_0) & S_{bb,4}(-\omega-2\omega_0) & \cdots \\
 & \vdots & \vdots & \vdots & \vdots & \vdots &
\end{bmatrix}$$

and similarly

$$\mathcal{S}_{yy}(\omega) = \begin{bmatrix}
 & \vdots & \vdots & \vdots & \vdots & \vdots & \\
\cdots & S_{yy,0}(-\omega+2\omega_0) & S_{yy,1}(-\omega+2\omega_0) & S_{yy,2}(-\omega+2\omega_0) & S_{yy,3}(-\omega+2\omega_0) & S_{yy,4}(-\omega+2\omega_0) & \cdots \\
\cdots & S_{yy,0}(-\omega+\omega_0) & S_{yy,1}(-\omega+\omega_0) & S_{yy,2}(-\omega+\omega_0) & S_{yy,3}(-\omega+\omega_0) & S_{yy,4}(-\omega+\omega_0) & \cdots \\
\cdots & S_{yy,0}(-\omega) & S_{yy,1}(-\omega) & S_{yy,2}(-\omega) & S_{yy,3}(-\omega) & S_{yy,4}(-\omega) & \cdots \\
\cdots & S_{yy,0}(-\omega-\omega_0) & S_{yy,1}(-\omega-\omega_0) & S_{yy,2}(-\omega-\omega_0) & S_{yy,3}(-\omega-\omega_0) & S_{yy,4}(-\omega-\omega_0) & \cdots \\
\cdots & S_{yy,0}(-\omega-2\omega_0) & S_{yy,1}(-\omega-2\omega_0) & S_{yy,2}(-\omega-2\omega_0) & S_{yy,3}(-\omega-2\omega_0) & S_{yy,4}(-\omega-2\omega_0) & \cdots \\
 & \vdots & \vdots & \vdots & \vdots & \vdots &
\end{bmatrix}$$

The output PSD's evaluated at ω are given by the central block row of $\mathcal{S}_{yy}$. The HSPD's of the self- and cross-powers of the p^{th} output are available in the p^{th} row of this block. This can be obtained by post-multiplying the transpose of (5.23) by a unit block vector E_0 followed by the p^{th} unit vector e_p as

$$\bar{\mathcal{H}}(\omega)\mathcal{S}^T_{bb}(\omega)\mathcal{H}^T(\omega)E_0 e_p$$

5.6.2.2 Evaluation of System Transfer Function

We now express the LPTV transfer function $h(t_2, t_1)$ in terms of parameters of (5.17).

Since $C(t)$ and $G(t)$ in (5.17) are T-periodic, they can be expanded in Fourier series as

$$C(t) = \sum_{i=-\infty}^{\infty} C_i \exp(\jmath i\omega_0 t)$$

and

$$G(t) = \sum_{i=-\infty}^{\infty} G_i \exp(\jmath i\omega_0 t)$$

For the purpose of this analysis we assume that $b(t)$ is a deterministic signal whose Fourier Transform $B(\omega)$ exists and is given by

$$B(\omega) = \int_{-\infty}^{\infty} b(t) \exp(-\jmath\omega t)\mathrm{d}t$$

Since $h(t_2, t_1)$ is the linear transfer function corresponding to (5.17), we have

$$\begin{aligned}
y(t_2) &= \int_{-\infty}^{\infty} h(t_2, t_1) b(t_1)\mathrm{d}t_1 \\
&= \frac{1}{4\pi^2} \iiint_{-\infty}^{\infty} \sum_{i=-\infty}^{\infty} H_i(\omega_1) \exp[\jmath\omega_1(t_2 - t_1)] \exp(\jmath i\omega_0 t_2) B(\omega_2) \exp(\jmath\omega_2 t_1)\mathrm{d}\omega_1\mathrm{d}\omega_2\mathrm{d}t_1 \\
&= \frac{1}{2\pi} \int_{-\infty}^{\infty}\int_{-\infty}^{\infty} \sum_{i=-\infty}^{\infty} H_i(\omega_1) \exp[\jmath(\omega_1 + i\omega_0)t_2] B(\omega_2)\delta(\omega_2 - \omega_1)\mathrm{d}\omega_1\mathrm{d}\omega_2 \\
&= \frac{1}{2\pi} \sum_{i=-\infty}^{\infty} \int_{-\infty}^{\infty} H_i(\omega) B(\omega) \exp[\jmath(\omega + i\omega_0)t_2]\mathrm{d}\omega
\end{aligned}$$

This implies that the Fourier transform of $y(t)$ is given by

$$Y(\omega) = \sum_{i=-\infty}^{\infty} H_i(\omega - i\omega_0) B(\omega - i\omega_0) \tag{5.24}$$

(5.17) is rewritten as

$$\begin{aligned}
&\frac{1}{2\pi} \int_{-\infty}^{\infty} \sum_{i=-\infty}^{\infty} C_i \exp(\jmath i\omega_0 t)\jmath\omega Y(\omega) \exp(\jmath\omega t)\mathrm{d}\omega \\
+&\frac{1}{2\pi} \int_{-\infty}^{\infty} \sum_{i=-\infty}^{\infty} G_i \exp(\jmath i\omega_0 t) Y(\omega) \exp(\jmath\omega t)\mathrm{d}\omega + \frac{1}{2\pi} \int_{-\infty}^{\infty} AB(\omega) \exp(\jmath\omega t)\mathrm{d}\omega = 0
\end{aligned}$$

Fourier transform of the above expression is given by

$$\sum_{i=-\infty}^{\infty} C_i \jmath(\omega - i\omega_0) Y(\omega - i\omega_0) + \sum_{i=-\infty}^{\infty} G_i Y(\omega - i\omega_0) + AB(\omega) = 0$$

Substituting the value of $Y(\omega)$ from (5.24) in the above expression we have

$$\sum_{i=-\infty}^{\infty} \sum_{k=-\infty}^{\infty} C_i \jmath(\omega - i\omega_0) H_k(\omega - (i+k)\omega_0) B(\omega - (i+k)\omega_0)$$
$$+ \sum_{i=-\infty}^{\infty} \sum_{k=-\infty}^{\infty} G_i H_k(\omega - (i+k)\omega_0) B(\omega - (i+k)\omega_0) + AB(\omega) = 0$$

Since the above expression is valid for every $B(\omega)$, it must be necessary that for $i + k = 0$

$$\sum_{i=-\infty}^{\infty} \jmath(\omega - i\omega_0) C_i H_{-i}(\omega) + \sum_{i=-\infty}^{\infty} G_i H_{-i}(\omega) + A = 0 \tag{5.25}$$

and for $i + k = l \neq 0$ we have

$$\sum_{i=-\infty}^{\infty} \jmath(\omega - i\omega_0) C_i H_{l-i}(\omega - l\omega_0) + \sum_{i=-\infty}^{\infty} G_i H_{l-i}(\omega - l\omega_0) = 0 \tag{5.26}$$

Collocating the terms in (5.25) at frequencies $\omega - l\omega_0$ for $l \in \mathbb{Z}$ we have

$$\sum_{i=-\infty}^{\infty} \jmath[\omega - (i+l)\omega_0] C_i H_{-i}(\omega - l\omega_0) + \sum_{i=-\infty}^{\infty} G_i H_{-i}(\omega - l\omega_0) + A = 0 \tag{5.27}$$

(5.27) and (5.26) can written compactly as

$$\mathcal{J}(\omega)\mathcal{H} = -\mathcal{A}$$

where

$$\mathcal{J}(\omega) = \mathcal{G} + \jmath\Omega(\omega)\mathcal{C}$$

$$\mathcal{G} = \begin{bmatrix} & \vdots & \vdots & \vdots & \vdots & \vdots & \\ \cdots & G_0 & G_{-1} & G_{-2} & G_{-3} & G_{-4} & \cdots \\ \cdots & G_1 & G_0 & G_{-1} & G_{-2} & G_{-3} & \cdots \\ \cdots & G_2 & G_1 & G_0 & G_{-1} & G_{-2} & \cdots \\ \cdots & G_3 & G_2 & G_1 & G_0 & G_{-1} & \cdots \\ \cdots & G_4 & G_3 & G_2 & G_1 & G_0 & \cdots \\ & \vdots & \vdots & \vdots & \vdots & \vdots & \end{bmatrix}$$

$$\mathcal{C} = \begin{bmatrix} & \vdots & \vdots & \vdots & \vdots & \vdots & \\ \cdots & C_0 & C_{-1} & C_{-2} & C_{-3} & C_{-4} & \cdots \\ \cdots & C_1 & C_0 & C_{-1} & C_{-2} & C_{-3} & \cdots \\ \cdots & C_2 & C_1 & C_0 & C_{-1} & C_{-2} & \cdots \\ \cdots & C_3 & C_2 & C_1 & C_0 & C_{-1} & \cdots \\ \cdots & C_4 & C_3 & C_2 & C_1 & C_0 & \cdots \\ & \vdots & \vdots & \vdots & \vdots & \vdots & \end{bmatrix}$$

$$\mathcal{A} = \begin{bmatrix} & \vdots & \vdots & \vdots & \vdots & \vdots & \\ \cdots & A_0 & A_{-1} & A_{-2} & A_{-3} & A_{-4} & \cdots \\ \cdots & A_1 & A_0 & A_{-1} & A_{-2} & A_{-3} & \cdots \\ \cdots & A_2 & A_1 & A_0 & A_{-1} & A_{-2} & \cdots \\ \cdots & A_3 & A_2 & A_1 & A_0 & A_{-1} & \cdots \\ \cdots & A_4 & A_3 & A_2 & A_1 & A_0 & \cdots \\ & \vdots & \vdots & \vdots & \vdots & \vdots & \end{bmatrix}$$

$$\Omega(\omega) = \begin{bmatrix} \ddots & & & & \\ & (\omega - \omega_0)I & & & \\ & & \omega I & & \\ & & & (\omega + \omega_0)I & \\ & & & & \ddots \end{bmatrix}$$

and $\mathcal{H}(\omega)$ is the harmonic balance conversion matrix as in Definition 4.3.

In an actual calculation, the infinite matrices need to be truncated to a finite number of harmonics. [RFL98] make the observation that, in order to compute the output noise statistics in (5.23) the (finite) block Toeplitz structure of $\mathcal{C}$ and $\mathcal{G}$ can be approximated by a block circulant structure without loss of accuracy. Then the circulant matrix can be expressed as products of sparse block diagonal matrices, permutations and Fourier transforms. Hence matrix vector product can be computed very efficiently ($O(mn \log n)$ m: number of harmonics and n: circuit size) and iterative linear algebra techniques with appropriate preconditioning can be used to compute expressions of the type $\mathcal{H}(\omega)x = \mathcal{J}^{-1}(\omega)\mathcal{A}x$ in an efficient manner.

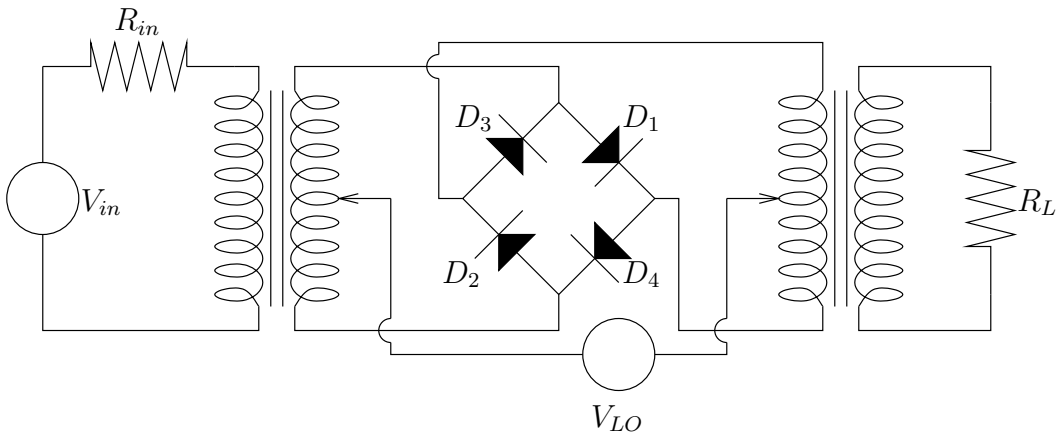

Figure 5.2: Four Diode Mixer

5.7 Examples

The noise simulation algorithm is implemented in MATLAB. We use the time domain technique presented in Section 4.5.1 for performing noise simulation for oscillators and the harmonic balance based technique presented in [RFL98] to perform the noise analysis of the nonautonomous portions of the circuit. The steady-state response of the circuit and the Jacobians are computed by performing transient simulations in SPICE and later handed over to MATLAB.

We illustrate our technique using a passive mixer and an active mixer. Consider the oscillator shown in Figure 4.5. The basic configuration is a Colpitt's oscillator. The circuit oscillates at 2.2 GHz. This circuit has 11 state variables and 8 noise sources. c was computed to be 3.19×10^{-19} sec which corresponds to relative noise power of 98.1 dBc/Hz below the carrier at an offset frequency of 100 kHz. We use this oscillator to generate the 2.2 GHz local oscillator (LO) signal for both the mixers.

5.7.1 Passive Mixer

The schematic of the four-diode passive mixer is shown in Figure 5.2. For the purpose of this analysis the chokes are assumed to be ideal. The mixer circuit has 21 state variables along with 10 noise sources (excluding the one added for the oscillator noise contribution). The RF signal is assumed to come from a 50 Ω port at 2.4 GHz. The noise figure of this mixer at the IF port at 200 MHz, without the contribution of the LO

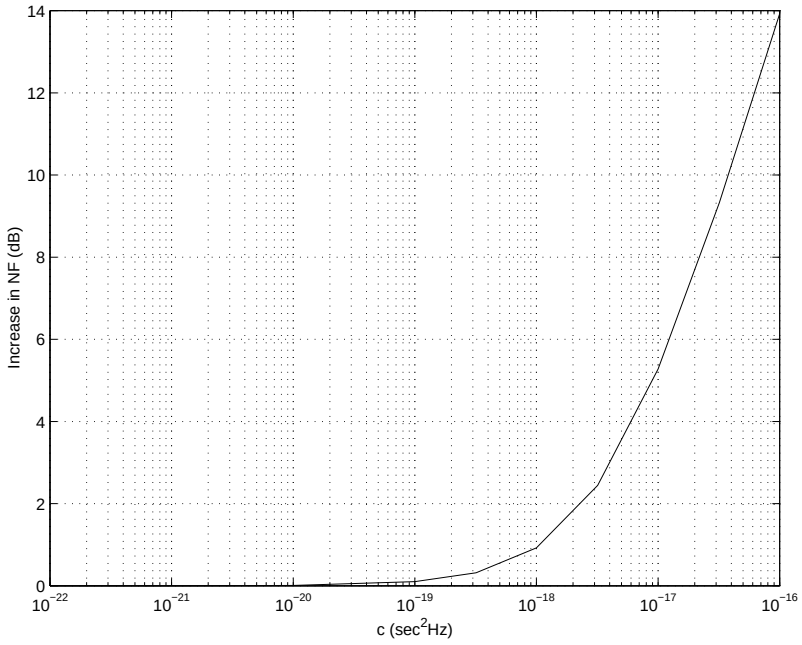

Figure 5.3: Increase of mixer noise figure with phase noise of the local oscillator (LO) signal for the passive mixer with 2% offset in the center tap of the output inductor

phase noise, was computed to be 13.3 dB. In this analysis, fifteen significant harmonics were considered. Including the effect of LO phase noise, the noise figure remains unchanged. The MATLAB implementation of the noise analysis took ten seconds on a 600 MHz Digital Alpha workstation.

It is observed that as the input signal phase noise is increased, the noise at the output node is not affected. This is explained by the perfect symmetry of the circuit. Since the circuit is symmetric, the white noise source due to input signal phase noise appears as a common mode signal to the output of this circuit and hence does not affect the noise at the output node of the circuit. It should be noted that input signal phase noise does affect the noise at other nodes of the circuit. However, in a realistic scenario, perfect symmetry cannot be achieved. To simulate the real scenario, a 2% offset in the center tap of the output transformer was artificially introduced.

Figure 5.3 shows the increase in noise figure (from the noiseless oscillator case) as a function of c for the passive mixer with a 2% offset in the center tap of the output transformer. This increase is negligible for $c < 1 \times 10^{-19}$ sec but as c increases beyond this value, the noise figure degrades rapidly. This cross-over point is the value of c where the

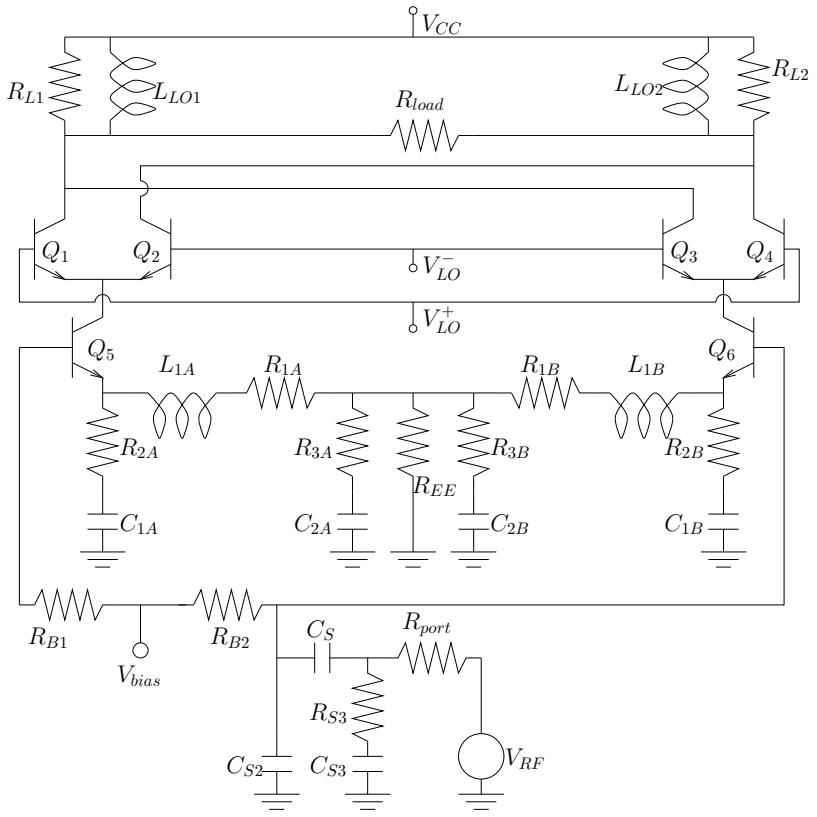

Figure 5.4: Gilbert cell based mixer

input signal phase noise starts dominating over the circuit noise. This also suggests that for this particular mixer, it is an overkill for the LO to have phase noise performance better than 113.2 dBc/Hz at 100 kHz offset.

5.7.2 Active Mixer

The schematic of the active mixer is shown in Figure 5.4. The inductors are implemented on chip and hence contain significant number of parasitic elements. The mixer circuit has 53 state variables along with 46 noise sources (excluding the one added for the oscillator noise contribution). The RF signal is assumed to come from a 50 Ω port at 2.4 GHz. The noise figure of this mixer at the IF port at 200MHz, without the contribution of the LO phase, noise was computed to be 7 dB. In this analysis, fifteen significant harmonics were considered. Including the effect of LO phase noise, the noise figure stays almost the same. The noise analysis for this circuit took thirty seconds on a 600 MHz DEC alpha

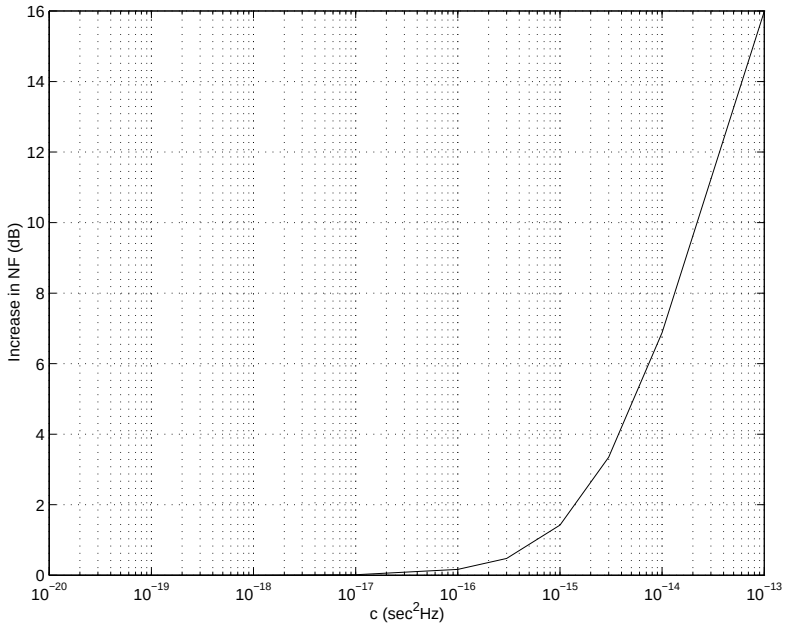

Figure 5.5: Increase of mixer noise figure with phase noise of the local oscillator (LO) signal for the Gilbert cell mixer

station.

Figure 5.5 shows the increase in noise figure (from the noiseless oscillator case) as a function of c for this circuit. This increase is negligible for $c < 1 \times 10^{-17}$ sec but as c increases beyond this value, the noise figure degrades rapidly. This cross-over point is the value of c where the input signal phase noise starts dominating over the circuit noise. This also suggests that for this particular mixer, it is an overkill for the LO to have phase noise performance better than 83 dBc/Hz at 100 kHz offset. We observe that using an active mixer instead of a passive mixer not only reduces the overall noise figure but also is less sensitive to the LO phase noise. Using an active mixer eases the noise specifications of the oscillator which generates the LO.

This technique, as presented here can only handle white noise sources. However for noise with long-term correlations, i.e., flicker noise, the steps outlines above are not rigorously justified. [DLSV96] used the modulated stationary noise model to analyze flicker noise. However, the asymptotic arguments in this formulation need to be carefully examined before these results can be carried over to the flicker noise case as well.

Chapter 6

Noise Analysis of Circuits with Multitone Inputs

In the previous chapter, we developed a noise simulation algorithm for nonautonomous circuits which takes into account the effect of input signal phase noise as well. We showed that, for a nonautonomous circuit driven by a large periodic input signal corrupted by Brownian motion phase deviation, output noise is stationary. We also showed exactly how input signal phase noise contributed to wide band amplitude noise at the output. In this chapter we extend the analysis to the case when the nonautonomous circuit is subjected to more than one large periodic excitations. In this case, the circuit response is *quasi-periodic*.

This analysis is desirable in many RF circuits. For the mixer shown in Figure 5.1 let the signal at the RF port to be a sum to two periodic signals of frequency f_{RF} and f_{BLOCK}, where f_{RF} is the frequency of the desired signal that is downconverted to f_{IF} and f_{BLOCK} is the frequency of a signal that occupies an adjacent band (this signal is typically called *blocker* or *jammer*). In an ideal mixer, f_{BLOCK} would be downconverted to $|f_{BLOCK} - f_{LO}|$ which would be out of the frequency band to interest and hence would be filtered out[1]. However, for a nonideal mixer, the inband noise performance is affected by the blocker in the following ways:

- If the blocker signal is large, it can drive the small-signal preamplifier stages and the

[1]This would not be the case if $f_{BLOCK} = 2f_{LO} - f_{RF}$, i.e., the blocker is at the *image* frequency for this mixer. There are mixers which are specifically designed to suppress this image signal (called *image reject mixers*). For simplicity we assume that the blocker is far away from the image frequency.

mixer into gain compression. This results in a drop in receiver conversion gain and hence a decrease in the overall signal to noise ratio.

- The blocker acts as a second LO to the nonlinear circuit and therefore translates additional low frequency circuit noise to IF at the output. For instance, a blocker 10 MHz away from the f_{RF} mixes with circuit noise at 10 MHz which appears as additional noise at f_{IF} at the output [FHM97].

- Due to phase noise in blocker, there is finite noise power at frequency f_{RF} due to the presence of the blocker. This increases the output noise.

- Additionally finite noise power of the local oscillator at the blocker frequency gets downconverted to base band.

In this chapter we attempt to quantify this increase in output noise power due to the presence of a blocker. We first derive the spectrum of the output of a memoryless nonlinearity driven by two large periodic signals with uncorrelated phase noise. We also review existing techniques for simulating nonlinear circuits driven by multitone excitations on which we will base our noise analysis technique. We present numerical techniques for efficiently computing this noise response and conclude this chapter by applying our numerical techniques to compute the noise performance of the two mixers described in Section 5.7 in presence of blockers.

6.1 Mathematical Preliminaries

The dynamics of a unperturbed nonautonomous system can be described by the following system of differential equations

$$\dot{x} = f(x) + b_1(t) + b_2(t) \tag{6.1}$$

where $x \in \mathbb{R}^n$ is a vector of state variables, $f(x) : \mathbb{R}^n \to \mathbb{R}^n$ and $b_1(t), b_2(t) : \mathbb{R} \to \mathbb{R}^n$ are deterministic periodic inputs with periods T_1 and T_2 respectively. We present our analysis for the case where the nonautonomous circuit is driven by two large periodic signals. This allows to introduce our technique for noise simulation of nonautonomous circuits driven by multitone excitations while keeping the notation simple. The two-tone case is also of more practical interest than the general multitone case. The extension to the general multitone

case is tedious but straight forward. We assume that this equation satisfies the Cauchy-Peano existence and uniqueness theorem for the initial value problem [Gri90]. We further assume that the system is stable in the sense that in the absence of $b_1(t)$ and $b_2(t)$, the steady-state solution of this equation is 0. We assume that the steady-state solution of this system (in presence of $b_1(t)$ and $b_2(t)$) is given by $x_s(t)$.

As before we are interested in the response of this system in the presence of noise, both in the form of circuit intrinsic noise $D(x)\xi(t)$ and phase noise in the input signals of the form $b_1(t+\alpha_1(t))$ and $b_2(t+\alpha_2(t))$. $D(\cdot) : \mathbb{R}^n \to \mathbb{R}^{n\times p}$ describes the connectivity and modulation of the circuit noise sources, $\xi(\cdot) : \mathbb{R} \to \mathbb{R}^p$ are circuit white noise sources and $\alpha_1(\cdot), \alpha_2(\cdot) : \mathbb{R} \to \mathbb{R}$ are the phase deviation process of the input signal which are scaled Brownian motion processes, i.e., of the form $\sqrt{c_1}B_1(t)$ and $\sqrt{c_2}B_2(t)$ where c_1 and c_2 are the respective rates of increase of the variance (see Section 4.4 and (4.33)). Hence the behaviour of the nonautonomous circuit along with noise is governed by the following differential equation.

$$\dot{x} = f(x) + b_1(t+\alpha_1(t)) + b_2(t+\alpha_2(t)) + D(x)\xi(t)$$

Since $\alpha_1(t)$, $\alpha_2(t)$ and $\xi(t)$ are stochastic processes, $x(t)$ in general will also be a stochastic process and the above equation should be treated as a stochastic differential equation. We rewrite this in the following form

$$\mathrm{d}x = f(x)\mathrm{d}t + b_1(t+\alpha_1(t))\mathrm{d}t + b_2(t+\alpha_2(t))\mathrm{d}t + D(x)\mathrm{d}B_p(t) \tag{6.2}$$

where $B_p(t)$ is a p-dimensional Brownian motion independent of $\alpha_1(t)$ and $\alpha_2(t)$.

6.2 Spectrum of Nonlinear Mixing of Two Tones

In this section we derive the spectrum of the output of a memoryless nonlinearity with two large signal periodic inputs corrupted by Brownian motion phase noise. Let the memoryless nonlinearity be of the form

$$f(t) = f(x_1(t), x_2(t))$$

We rewrite $f(t)$ in its bivariate form [BWLBG96, Roy97, BWL97] as

$$\hat{f}(t_1, t_2) = f(x_1(t_1), x_2(t_2))$$

$f(t)$ and $\hat{f}(t_1, t_2)$ satisfy the following relation

$$\hat{f}(t,t) = f(t)$$

For noiseless inputs $x_1(t_1) = b_1(t_1)$ and $x_2(t_2) = b_2(t_2)$, let the bivariate form of the output be given by

$$\hat{f}(t_1,t_2) = \sum_{i=-\infty}^{\infty} \sum_{k=-\infty}^{\infty} F(i,k) \exp(\jmath\omega_1 i t_1) \exp(\jmath\omega_2 k t_2)$$

where

$$\omega_1 = \frac{2\pi}{T_1} \quad \text{and} \quad \omega_2 = \frac{2\pi}{T_2}$$

In general $F(i,k)$ will be functions of ω_1 and ω_2. The bivariate form of the output in presence of input signal phase noise is given by

$$\hat{f}(t_1,t_2) = \sum_{i=-\infty}^{\infty} \sum_{k=-\infty}^{\infty} F(i,k) \exp\big(\jmath\omega_1 i(t_1 + \alpha_1(t_1))\big) \exp\big(\jmath\omega_2 k(t_2 + \alpha_2(t_2))\big)$$

The output is now a stochastic process since $\alpha_1(t)$ and $\alpha_2(t)$ are stochastic processes. The autocorrelation function of $f(t)$ is given by

$$\begin{aligned}
R_{ff}(t,\tau) &= \mathbb{E}\left[f(t) f^*(t+\tau)\right] \\
&= \mathbb{E}\Bigg[\sum_{i,k,l,m=-\infty}^{\infty} F(i,k)F^*(l,m) \exp\big(\jmath\omega_1 i(t+\alpha_1(t))\big) \exp\big(\jmath\omega_2 k(t+\alpha_2(t))\big) \\
&\qquad \exp\big(-\jmath\omega_1 l(t+\tau+\alpha_1(t+\tau))\big) \exp\big(-\jmath\omega_2 m(t+\tau+\alpha_2(t+\tau))\big) \Bigg] \\
&= \sum_{i,k,l,m=-\infty}^{\infty} F(i,k)F^*(l,m) \exp\big(\jmath\omega_1(it_1 - l(t+\tau))\big) \exp\big(\jmath\omega_1(kt_1 - m(t+\tau))\big) \\
&\qquad \mathbb{E}\Big[\exp\big(\jmath\omega_1(i\alpha_1(t) - l\alpha_1(t+\tau))\big) \exp\big(\jmath\omega_2(k\alpha_2(t) - m\alpha_2(t+\tau))\big)\Big]
\end{aligned}$$

Since $\alpha_1(t)$ and $\alpha_2(t)$ are independent processes, we have

$$\begin{aligned}
R_{ff}(t,\tau) = \sum_{i,k,l,m=-\infty}^{\infty} & F(i,k)F^*(l,m) \exp\big(\jmath\omega_1(it_1 - l(t+\tau))\big) \exp\big(\jmath\omega_1(kt_1 - m(t+\tau))\big) \\
& \mathbb{E}\left[\exp\big(\jmath\omega_1(i\alpha_1(t) - l\alpha_1(t+\tau))\big)\right] \mathbb{E}\left[\exp\big(\jmath\omega_2(k\alpha_2(t) - m\alpha_2(t+\tau))\big)\right]
\end{aligned}$$

Using similar arguments as in Section 4.2 we can conclude that since $\alpha_1(t)$ and $\alpha_2(t)$ are Brownian motion processes, $R_{ff}(t,\tau)$ has a nontrivial value only for $i = l$ and $k = m$ and

asymptomatically

$$R_{ff}(t,\tau) = \sum_{i=-\infty}^{\infty}\sum_{k=-\infty}^{\infty} F(i,k)F^*(i,k)\exp(-\jmath\omega_1 i\tau)\exp(-\jmath\omega_2 k\tau)\exp\left(-\frac{1}{2}\omega_1^2 i^2 c_1|\tau|\right) \exp\left(-\frac{1}{2}\omega_2^2 k^2 c_2|\tau|\right)$$

The autocorrelation function $R_{ff}(t,\tau)$ is independent of t hence the output process is wide-sense stationary. The power spectral density of the output process, which is Fourier transform of this autocorrelation functions is given by

$$S_{ff}(\omega) = \sum_{i=-\infty}^{\infty}\sum_{k=-\infty}^{\infty} F(i,k)F^*(i,k)\frac{\omega_1^2 i^2 c_1 + \omega_2^2 k^2 c_2}{\frac{1}{4}(\omega_1^2 i^2 c_1 + \omega_2^2 k^2 c_2)^2 + (\omega + i\omega_1 + k\omega_2)^2} \tag{6.3}$$

From the above expression we conclude that the spectrum of the output consists of a series of Lorentzian spectra centered around frequencies $i\omega_1 + k\omega_2$, $i,k \in \mathbb{Z}$.

6.3 Multirate Analysis of Circuits with Multitone Excitations

In this section we briefly review simulation techniques for computing the steady-state response of a nonautonomous circuit driven by two-tone excitations. A naïve method of computing the steady-state response of the circuit would be to use shooting or harmonic balance method directly. This would imply that the circuit would be simulated for a time which is of the order of the slowly varying signal while the time-steps need to be small enough so as to follow the fast waveform. If the two signal frequencies are widely separated, the simulation is very expensive. Multirate methods described in [BWLBG96, Roy97, BWL97] circumvent this problem by constructing a partial differential equation with multiple time-scales corresponding to the circuit equations. This partial differential equation can be efficiently solved and the circuit response can be easily derived from the multirate solution. We now give a brief review of these techniques. In the following we assume that the system of nonlinear ordinary differential-algebraic equations governing the behaviour of the circuit is given by

$$\frac{\mathrm{d}q(x)}{\mathrm{d}t} + f(x) + b_1(t) + b_2(t) = 0 \tag{6.4}$$

where $x(\cdot) : \mathbb{R} \to \mathbb{R}^n$ is the vector of node voltages and some branch currents, $q(\cdot) : \mathbb{R}^n \to \mathbb{R}^n$ is the vector of charges and fluxes and $f(\cdot) : \mathbb{R}^n \to \mathbb{R}^n$ is the vector of sums of currents

entering each node and branch voltages, both depending on $x(t)$. Furthermore, $b_1(\cdot), b_2(\cdot) : \mathbb{R} \to \mathbb{R}^n$ are the vector of input sources which are periodic with period T_1 and T_2 respectively and, as before

$$\omega_1 = \frac{2\pi}{T_1} \quad \text{and} \quad \omega_2 = \frac{2\pi}{T_2}$$

We also assume that ω_1 and ω_2 are incommensurable, i.e., for all $i, k \in \mathbb{Z}$ we have

$$i\omega_1 + k\omega_2 = 0 \text{ iff } i = 0 \text{ and } k = 0$$

This implies that functions of the kind

$$\exp(\jmath(i\omega_1 + k\omega_2)t)$$

are linearly independent for all $i, k \in \mathbb{Z}$.

Since the circuit is nonautonomous, we can assume that the steady-state response $x_s(t)$ is quasi-periodic and can be expressed as

$$x_s(t) = \sum_{i=-\infty}^{\infty} \sum_{k=-\infty}^{\infty} X_s(i,k) \exp(\jmath(i\omega_1 + k\omega_2)t) \tag{6.5}$$

Let $\hat{x}_s(t_1, t_2)$ be the bivariate form of $x_s(t)$, where, as before, $\hat{x}_s$ and x_s satisfy the following relation

$$\hat{x}_s(t,t) = x_s(t)$$

and let

$$\hat{b}(t_1, t_2) = b_1(t_1) + b_2(t_2)$$

As a suitable generalization of (6.4) for two dimensional functions we consider the following partial differential equation.

$$\frac{\partial q(\hat{x}(t_1,t_2))}{\partial t_1} + \frac{\partial q(\hat{x}(t_1,t_2))}{\partial t_2} + f(\hat{x}(t_1,t_2)) + \hat{b}(t_1,t_2) = 0 \tag{6.6}$$

Considering this partial DAE only for solutions of the form (6.5) implicitly imposes the following boundary conditions

$$\hat{x}(0,t_2) = \hat{x}(T_1,t_2) \tag{6.7}$$

$$\hat{x}(t_1,0) = \hat{x}(t_1,T_2) \tag{6.8}$$

The following theorem, due to [BWLBG96, Roy97], relates the solution $\hat{x}_s(t_1, t_2)$ of (6.6) to the solution $x_s(t)$ of (6.4):

Theorem 6.1 ([BWLBG96, Roy97]) *The DAE (6.4) has a quasi-periodic solution $x_s(t)$ iff the partial DAE (6.6) has a solution $\hat{x}_s(t_1, t_2)$ of the form (6.5). The two solutions are related by*

$$x_s(t) = \hat{x}_s(t, t)$$

for all $t \in \mathbb{R}$.

(6.6) can be solved by the following three different classes of techniques

1. Equations in both time scales t_1 and t_2 can be solved in time domain [Roy97] either by using *multivariate finite difference time domain method* or *hierarchal shooting*.

   - In the multivariate finite difference time domain method the t_1, t_2 plane is suitably gridded on the rectangle $[0, T_1] \times [0, T_2]$ resulting in a grid of size $m_1 \times m_2$. The partial differential operators of (6.6) are discretized using a linear multistep method and (6.6) is collocated on the grid. This leads to a set of nonlinear algebraic equations in the unknowns which is solved using a Newton-Raphson method. The collocation leads to a system of $m = m_1 \times m_2$ equations. The $m_1 + m_2$ extra unknowns which result from the discretization of the differential operators at $t_1 = 0$ and $t_2 = 0$ are eliminated using the bi-periodic boundary conditions (6.7) and (6.7). The resulting nonlinear system of equations is solved using Newton-Raphson technique. The Jacobian of size $(nm_1m_2) \times (nm_1m_2)$ for the linearized system is of the following p-cyclic form [Roy97]

$$\begin{bmatrix} D_1 & & & & -L_{m_1} \\ -L_1 & D_2 & & & \\ & -L_2 & D_3 & & \\ & & \ddots & \ddots & \\ & & & -L_{n_1-1} & D_{n_1} \end{bmatrix}$$

     Each block (of size $(nm_2) \times (nm_2)$) is itself an $m_2 \times m_2$ block matrix with p-cyclic or diagonal structure. Each block is in turn a sparse matrix of size n, consisting of circuit conductance and capacitance matrices. Hence the overall Jacobian is extremely sparse and diagonally dominant hence easily amenable to solving using iterative linear algebra techniques.

- A hierarchal extension of the classical shooting algorithm can also be used for solving (6.6). The bivariate functions $\hat{x}$, $\hat{b}$, q and f can be viewed as functions of the single argument t_1 that return values that are vector valued functions, i.e., the multivariate functions are maps from $\mathbb{R} \rightarrow \{h(\cdot) : \mathbb{R} \rightarrow \mathbb{R}^n\}$ [Roy97]. Let these maps be $Q(t_1)$, $X(t_1)$, $F(t_1)$ and $B(t_1)$; in other words, $Q(t_1)$ equals the entire function $q(t_1, \cdot)$ for fixed t_1. (6.6) can then be written formally as a DAE in function-valued variables as

$$\frac{\mathrm{d}Q(X)}{\mathrm{d}t_1} + \mathcal{D}_{t_2}[Q(X)] + F(X) + B(t_1) = 0$$

  where $\mathcal{D}_{t_2}$ is an operator that differentiates the function that it operates on. The above equation can be discretized using Backward Euler (say) as

$$\frac{Q\left(X(t_{1_i})\right) - Q\left(X(t_{1_i})\right)}{t_{1_i} - t_{1_{i-1}}} + \mathcal{D}_{t_2}[Q(X)] + F(X) + B(t_1) = 0$$

  This equation can be solved for $X\left(t_{1_i}\right)$ which represents the function $\hat{x}\left(t_{1_i}, \cdot\right)$ at a fixed t_1 value. This equation is also a DAE and can be solved using shooting. This inner loop DAE is solved for each time step of outer loop.

2. In the multivariate mixed frequency time method [BWL97, Roy97], $\hat{x}(t_1, t_2)$ and $\hat{b}(t_1, t_2)$ are expanded as Fourier series in either one of the time scales, say t_1. (6.6) then reduces to

$$\begin{aligned} 0 = &\sum_{i=-M}^{M} \jmath i\omega_1 Q_i(t_2) \exp(\jmath i\omega_1 t_1) + \sum_{i=-M}^{M} \jmath i\omega_1 \frac{\partial Q_i(t_2)}{\partial t_2} \exp(\jmath i\omega_1 t_1) \\ &+ \sum_{i=-M}^{M} F_i(t_2) \exp(\jmath i\omega_1 t_1) + \sum_{i=-M}^{M} B_i(t_2) \exp(\jmath i\omega_1 t_1) \end{aligned}$$

   Since $\exp(\jmath i\omega_1 t_1)$ are linearly independent, the Fourier components in the above equation can be separated leading to [BWL97]

$$\frac{\mathrm{d}\bar{Q}(t_2)}{\mathrm{d}t_2} + \jmath\Omega_1 \bar{Q}(t_2) + \bar{F}(t_2) + \bar{B}(t_2) = 0 \tag{6.9}$$

   where

$$\Omega_1 = \omega_1 \begin{bmatrix} M & & & & \\ & M-1 & & & \\ & & \ddots & & \\ & & & -M+1 & \\ & & & & -M \end{bmatrix}$$

$$\bar{Q} = \begin{bmatrix} Q_M \\ Q_{M-1} \\ \vdots \\ Q_{-M+1} \\ Q_{-M} \end{bmatrix}$$

$$\bar{F} = \begin{bmatrix} F_M \\ F_{M-1} \\ \vdots \\ F_{-M+1} \\ F_{-M} \end{bmatrix}$$

and

$$\bar{B} = \begin{bmatrix} B_M \\ B_{M-1} \\ \vdots \\ B_{-M+1} \\ B_{-M} \end{bmatrix}$$

(6.9) being a vector DAE can be solved in time domain using either finite difference method or shooting.

3. Yet another method for solving (6.6) is to assume that $\hat{x}_s(t_1, t_2)$ is of the form

$$\hat{x}_s(t_1, t_2) = \sum_{i=-\infty}^{\infty} \sum_{k=-\infty}^{\infty} \hat{X}_s(i,k) \exp(\jmath(i\omega_1 t_1 + k\omega_2 t_2))$$

and solve for $\hat{X}_s(i,k)$ directly [BWLBG96]. To this end we assume that the bivariate versions of the waveforms $x(t)$, $f(x(t))$ and $q(x(t))$ are of the form

$$\hat{y}(t_1, t_2) = \sum_{i=-I}^{I} \sum_{k=-K}^{K} \hat{Y}(i,k) \exp(\jmath(i\omega_1 t_1 + k\omega_2 t_2))$$

where I and K are chosen such that the truncation error is sufficiently small. Now $\hat{y}(t_1, t_2)$ is restricted to the line [BWLBG96]

$$\tilde{y}(t) = \hat{y}\left(t_1 = t, t_2 = \frac{\omega_1}{\omega_2} \frac{1}{2K+1} t\right) \tag{6.10}$$

Along this line

$$t_2 = \frac{\omega_1}{\omega_2}\frac{1}{2K+1}t_1$$

the function $\tilde{y}$ is periodic with period $T_0 = (2K+1)T_1$ and angular frequency $\omega_0 = \frac{2\pi}{T_0}$. Therefore

$$\begin{aligned}\tilde{y}(t) &= \sum_{i=-I}^{I}\sum_{k=-K}^{K}\hat{Y}(i,k)\exp\left(\jmath\left(i\omega_1 t + k\omega_1\frac{1}{2K+1}t\right)\right)\\ &= \sum_{i=-I}^{I}\sum_{k=-K}^{K}\hat{Y}(i,k)\exp\big(\jmath(i(2K+1)+k)\omega_0 t\big) \qquad (6.11)\\ &= \sum_{l=-L}^{L}\tilde{Y}(l)\exp(\jmath l\omega_0 t)\end{aligned}$$

The two sets of coefficients $\hat{Y}(i,k)$ and $\tilde{Y}(l)$ are related one-to-one by the following mapping

$$\hat{Y}(i,k) = \tilde{Y}(i(2K+1)+k) \qquad (6.12)$$

and

$$\tilde{Y} = \hat{Y}\left(i = \frac{(l+K)-(l+K) \mod (2K+1)}{2K+1}, k = l - i(2K+1)\right) \qquad (6.13)$$

The artificial spectrum is dense and equally spaced hence optimal for FFT operation.

This method transforms the quasi-periodic waveform $\hat{x}(t_1,t_2)$ into the periodic waveform $\tilde{x}(t)$ using (6.13). The nonlinear relations $f(\hat{x}(t_1,t_2))$ and $q(\hat{x}(t_1,t_2))$ and its partial derivatives are now evaluated along the line

$$\left(t_1 = t, t_2 = \frac{\omega_1}{\omega_2}\frac{1}{2K+1}t\right)$$

and transformed into the frequency domain by a 1-dimensional FFT of size $(2I+1)\times(2K+1)$.

Figure 6.1 shows the output of the four diode mixer described in Section 5.7.1 with a 2.5 GHz 10 dBm RF tone and a 2.2 GHz LO signal. The output corresponds to the following representation

$$x(t) = \sum_{i=-I}^{I}\sum_{k=-K}^{K}X(i,k)\exp[\jmath(i\omega_1 + k\omega_2)t]$$

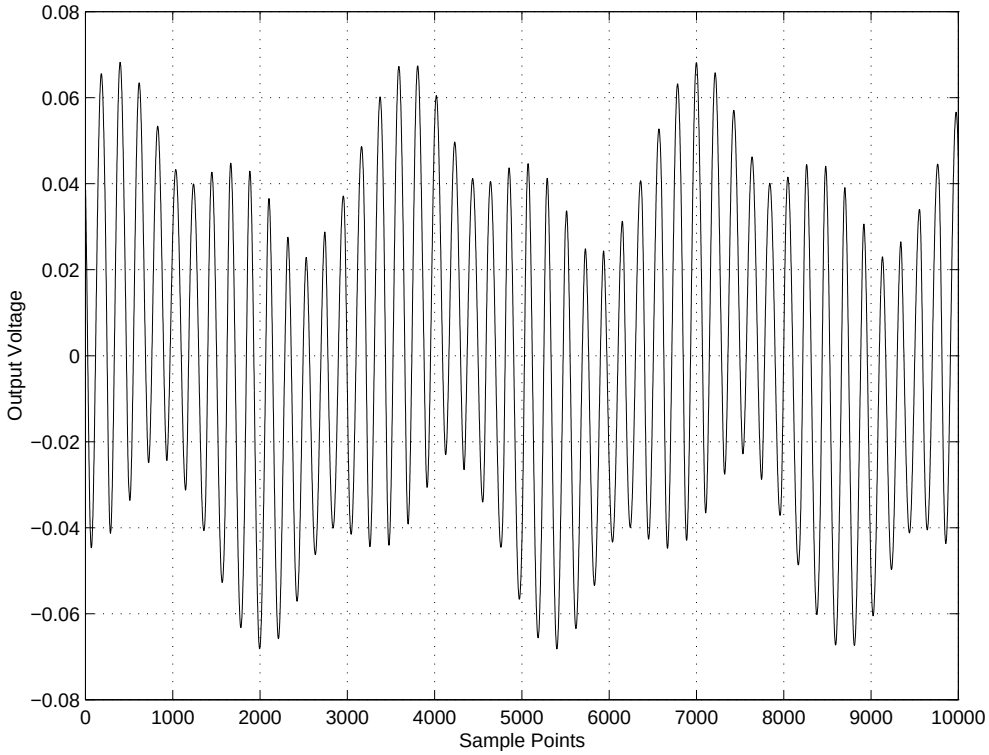

Figure 6.1: $x(t)$ representation of the output of a four diode mixer

It consists of signals of various frequency mixes of the two large tones and requires 10000 sample points to represent it. Figure 6.2 shows the same output in the representation $\tilde{x}(t)$ described by (6.10). This requires only 225 points for representation. Even though the resemblance to $x(t)$ is minimal, this waveform captures all the harmonic information of $x(t)$. Moreover, $\tilde{x}(t)$ is periodic allowing conventional harmonic balance analysis to be used. If the frequency separation between the two tones is very large or very small then the savings by using the quasi-periodic formulation are even more dramatic.

6.4 Noise Analysis of Circuits Driven by Multitone Excitations

We now describe our noise analysis technique for nonautonomous circuits driven by two large signals with phase noise. We again assume that the noiseless steady-state

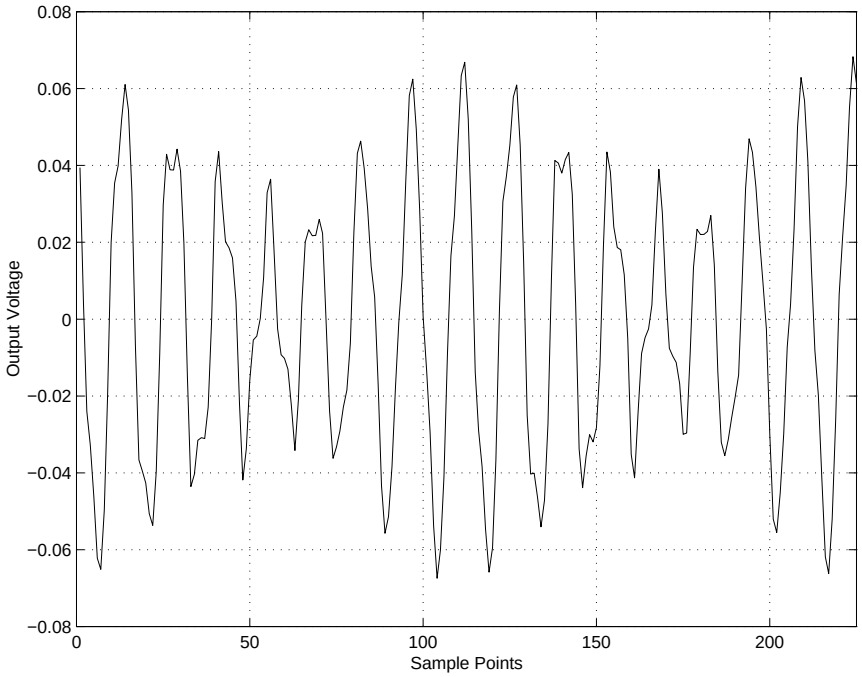

Figure 6.2: $\tilde{x}(t)$ representation of the output of a four diode mixer

solution of the circuit x_s is of the form

$$x_s(t) = \sum_{i=-\infty}^{\infty} \sum_{k=-\infty}^{\infty} X_s(i,k) \exp(\jmath i\omega_1 t) \exp(\jmath k\omega_2 t)$$

The corresponding bivariate form [BWLBG96, BWL97, Roy97] of $x_s(t)$ is given by

$$\hat{x}_s(t_1,t_2) = \sum_{i=-\infty}^{\infty} \sum_{k=-\infty}^{\infty} X_s(i,k) \exp(\jmath i\omega_1 t_1) \exp(\jmath k\omega_2 t_2)$$

Appealing to the above bivariate form and using arguments similar to those in Section 5.3 we assume that when the input signals are corrupted by Brownian motion phase errors, i.e., are of the form $b_1(t+\alpha_1(t))$ and $b_2(t+\alpha_2(t))$, the solution of (6.2) is of the form

$$x_{two\ tone} = x_n(t) + y(t) \tag{6.14}$$

where

$$x_n(t) = \sum_{i=-\infty}^{\infty} \sum_{k=-\infty}^{\infty} X_s(i,k) \exp\big(\jmath i\omega_1(t+\alpha_1(t))\big) \exp\big(\jmath k\omega_2(t+\alpha_2(t))\big)$$

From Section 6.2 the spectrum of $x_n(t)$ consists of a series of Lorentzians centered around frequencies $i\omega_1 + k\omega_2$, $i, k \in \mathbb{Z}$. $y(t)$ consists of a wide band noise term (among possibly other terms). However for the multitone case, the spectrum due to $x_n(t)$ is non-negligible at the output frequency of interest (f_{IF}). The large blocker signal mixes with the local oscillator signal to result in a large signal close to (but not *exactly at*) the intermediate frequency. The Lorentzian centered at $|f_{LO} - f_{BLOCKER}|$ causes a nonnegligible noise power at the intermediate frequency.

We need to substitute the form of the solution (6.14) in (6.2). Similar to Section 5.3, we first assume that the circuit itself is noiseless, i.e., $D(x) = 0$. We first make the following useful observations:

Definition 6.1 *Let*

$$s(t) = \begin{bmatrix} s_1(t) \\ s_2(t) \end{bmatrix} = \begin{bmatrix} 1 \\ 1 \end{bmatrix} \mathrm{d}t + \begin{bmatrix} \sqrt{c_1} & 0 \\ 0 & \sqrt{c_2} \end{bmatrix} \begin{bmatrix} \mathrm{d}B_1(t) \\ \mathrm{d}B_2(t) \end{bmatrix} \tag{6.15}$$

Lemma 6.2 *$s(t)$ as defined in (6.15) is a 2-dimensional Itô process.*

Hence we can use the following generalization of Lemma 5.2 to evaluate $\mathrm{d}x_{two\ tone}$.

Lemma 6.3 (The general Itô formula [Øks98]) *Let*

$$\mathrm{d}X = u\mathrm{d}t + v\mathrm{d}B$$

be an n-dimensional Itô process. Let

$$g(t,x) = \begin{bmatrix} g_1(t,x) \\ \vdots \\ g_p(t,x) \end{bmatrix}$$

be a twice continuously differentiable map $\mathbb{R}_+ \times \mathbb{R}^n \to \mathbb{R}^p$. Then the process

$$Y(t) = g(t, X(t))$$

is also p-dimensional Itô process whose k^{th} component is given by

$$\mathrm{d}Y_k = \frac{\partial g_k}{\partial t}(t, X(t))\mathrm{d}t + \sum_i \frac{\partial g_k}{\partial x_i}(t, X(t))\mathrm{d}X_i + \frac{1}{2}\sum_i \sum_j \frac{\partial^2 g_k}{\partial x_1 \partial x_2}(t, X(t))\mathrm{d}X_i \mathrm{d}X_j$$

where

$$\mathrm{d}B_i \mathrm{d}B_j = \delta_{i,j}\mathrm{d}t$$

Using the result of Lemma 6.3, we can evaluate $\mathrm{d}x_n(t)$ as:

$$\begin{aligned}
\mathrm{d}x_n(t) = &\sum_{i=-\infty}^{\infty}\sum_{k=-\infty}^{\infty} X_s(i,k)\jmath i\omega_1 \exp\big[\jmath i\omega_1(t+\alpha_1(t))\big]\exp\big[\jmath k\omega_2(t+\alpha_2(t))\big](\mathrm{d}t+\sqrt{c_1}\mathrm{d}B_1(t))\\
&+\sum_{i=-\infty}^{\infty}\sum_{k=-\infty}^{\infty} X_s(i,k)\jmath k\omega_2 \exp\big[\jmath i\omega_1(t+\alpha_1(t))\big]\exp\big[\jmath k\omega_2(t+\alpha_2(t))\big](\mathrm{d}t+\sqrt{c_2}\mathrm{d}B_2(t))\\
&-\frac{1}{2}\sum_{i=-\infty}^{\infty}\sum_{k=-\infty}^{\infty} X_s(i,k)i^2\omega_1^2 \exp\big(\jmath i\omega_1(t+\alpha_1(t))\big)\exp\big(\jmath k\omega_2(t+\alpha_2(t))\big)c_1\mathrm{d}t\\
&-\frac{1}{2}\sum_{i=-\infty}^{\infty}\sum_{k=-\infty}^{\infty} X_s(i,k)k^2\omega_2^2 \exp\big(\jmath i\omega_1(t+\alpha_1(t))\big)\exp\big(\jmath k\omega_2(t+\alpha_2(t))\big)c_2\mathrm{d}t\\
=&\sum_{i=-\infty}^{\infty}\sum_{k=-\infty}^{\infty} X_s(i,k)\left(\jmath i\omega_1+\jmath k\omega_2-\frac{1}{2}c_1i^2\omega_1^2-\frac{1}{2}c_2k^2\omega_2^2\right)\exp\big(\jmath i\omega_1(t+\alpha_1(t))\big)\\
&\qquad\exp\big(\jmath k\omega_2(t+\alpha_2(t))\big)\mathrm{d}t\\
&+\sum_{i=-\infty}^{\infty}\sum_{k=-\infty}^{\infty} X_s(i,k)\jmath i\omega_1\sqrt{c_1}\exp\big(\jmath i\omega_1(t+\alpha_1(t))\big)\exp\big(\jmath k\omega_2(t+\alpha_2(t))\big)\mathrm{d}B_1(t)\\
&+\sum_{i=-\infty}^{\infty}\sum_{k=-\infty}^{\infty} X_s(i,k)\jmath\jmath\omega_2\sqrt{c_2}\exp\big(\jmath i\omega_1(t+\alpha_1(t))\big)\exp\big(\jmath k\omega_2(t+\alpha_2(t))\big)\mathrm{d}B_2(t)
\end{aligned}$$

The noiseless circuit equation driven by input signals with phase noise is given by

$$\mathrm{d}x(t) = f(x)\mathrm{d}t + b_1(t+\alpha_1(t))\mathrm{d}t + b_2(t+\alpha_2(t))\mathrm{d}t \tag{6.16}$$

We assume that the solution of this equation is of the form $x_n(t)+y_1(t)$. Since $y_1(t)$ is assumed to be small compared to $x_n(t)$, $f(x)$ in (6.16) can be linearized around $x_n(t)$. Then (6.16) can be rewritten as

$$\mathrm{d}x_n(t)+\mathrm{d}y_1(t) = f(x_n(t))\mathrm{d}t + \left.\frac{\partial f(x)}{\partial x}\right|_{x_n(t)} y_1(t)\mathrm{d}t + b_1(t+\alpha_1(t))\mathrm{d}t + b_2(t+\alpha_2(t))\mathrm{d}t$$

Also since $\hat{x}_s(t_1,t_2)$ is bi-periodic, $f(\hat{x}_s(t_1,t_2))$ can be written in bivariate form as

$$f(\hat{x}_s(t_1,t_2)) = \sum_{i=-\infty}^{\infty}\sum_{k=-\infty}^{\infty} F(i,k)\exp(\jmath(i\omega_1t_1+k\omega_2t_2)) \tag{6.17}$$

Similarly

$$\left.\frac{\partial f(x)}{\partial x}\right|_{\hat{x}_s(t_1,t_2)} = \sum_{i=-\infty}^{\infty}\sum_{k=-\infty}^{\infty} J(i,k)\exp(\jmath(i\omega_1t_1+k\omega_2t_2)) \tag{6.18}$$

We know that $x_s(t)$ is a solution of (6.1) iff $\hat{x}_s(t_1,t_2)$ of the form

$$\hat{x}_s(t_1,t_2) = \sum_{i=-\infty}^{\infty}\sum_{k=-\infty}^{\infty} X_s(i,k)\exp(\jmath(i\omega_1t_1+k\omega_2t_2)) \tag{6.19}$$

is the solution of

$$\frac{\partial \hat{x}(t_1,t_2)}{\partial t_1} + \frac{\partial \hat{x}(t_1,t_2)}{\partial t_2} = f(\hat{x}(t_1,t_2)) + b_1(t_1) + b_2(t_2) \tag{6.20}$$

and $x_s(t) = \hat{x}_s(t,t)$. Substituting (6.19) and (6.17) in (6.20) we have

$$\begin{aligned}
&\sum_{i=-\infty}^{\infty}\sum_{k=-\infty}^{\infty} X_s(i,k)\jmath i\omega_1 \exp(\jmath(i\omega_1 t_1 + k\omega_2 t_2)) \\
&+ \sum_{i=-\infty}^{\infty}\sum_{k=-\infty}^{\infty} X_s(i,k)\jmath k\omega_2 \exp(\jmath(i\omega_1 t_1 + k\omega_2 t_2)) \\
&= \sum_{i=-\infty}^{\infty}\sum_{k=-\infty}^{\infty} F(i,k)\exp(\jmath(i\omega_1 t_1 + k\omega_2 t_2)) + b_1(t_1) + b_2(t_2)
\end{aligned}$$

This expression is valid for all t_1 and t_2, in particular $t_1+\alpha_1(t_1)$ and $t_2+\alpha_2(t_2)$. Therefore,

$$\begin{aligned}
&\sum_{i=-\infty}^{\infty}\sum_{k=-\infty}^{\infty} X_s(i,k)\jmath i\omega_1 \exp\Big[\jmath\big[i\omega_1(t_1+\alpha_1(t_1)) + k\omega_2(t_2+\alpha_2(t_2))\big]\Big] \\
&+ \sum_{i=-\infty}^{\infty}\sum_{k=-\infty}^{\infty} X_s(i,k)\jmath k\omega_2 \exp\Big[\jmath\big[i\omega_1(t_1+\alpha_1(t_1)) + k\omega_2(t_2+\alpha_2(t_2))\big]\Big] \\
&= \sum_{i=-\infty}^{\infty}\sum_{k=-\infty}^{\infty} F(i,k)\exp\Big[\jmath\big[i\omega_1(t_1+\alpha_1(t_1)) + k\omega_2(t_2+\alpha_2(t_2))\big]\Big] \\
&+ b_1(t_1+\alpha_1(t_1)) + b_2(t_2+\alpha_2(t_2))
\end{aligned} \tag{6.21}$$

The corresponding expression in one time scale is obtained by substituting $t_1 = t_2 = t$ in the above expression. (6.16) can be written as

$$\begin{aligned}
&\sum_{i=-\infty}^{\infty}\sum_{k=-\infty}^{\infty} X_s(i,k)\Big[\jmath i\omega_1 + \jmath k\omega_2 - \frac{c_1 i^2\omega_1^2 + c_2 k^2\omega_2^2}{2}\Big]\exp\big[\jmath i\omega_1(t+\alpha_1(t)) + \jmath k\omega_2(t+\alpha_2(t))\big]\mathrm{d}t \\
&\quad + \sum_{i=-\infty}^{\infty}\sum_{k=-\infty}^{\infty} X_s(i,k)\jmath i\omega_1\sqrt{c_1}\exp\big(\jmath i\omega_1(t+\alpha_1(t))\big)\exp\big(\jmath k\omega_2(t+\alpha_2(t))\big)\mathrm{d}B_1(t) \\
&\quad + \sum_{i=-\infty}^{\infty}\sum_{k=-\infty}^{\infty} X_s(i,k)\jmath\jmath\omega_2\sqrt{c_2}\exp\big(\jmath i\omega_1(t+\alpha_1(t))\big)\exp\big(\jmath k\omega_2(t+\alpha_2(t))\big)\mathrm{d}B_2(t) + \mathrm{d}y_1(t) \\
&= \sum_{i=-\infty}^{\infty}\sum_{k=-\infty}^{\infty} F(i,k)\exp\Big[\jmath\big[i\omega_1(t+\alpha_1(t)) + k\omega_2(t+\alpha_2(t))\big]\Big]\mathrm{d}t \\
&\quad + \sum_{i=-\infty}^{\infty}\sum_{k=-\infty}^{\infty} J(i,k)\exp\Big[\jmath\big[i\omega_1(t+\alpha_1(t)) + k\omega_2(t+\alpha_2(t))\big]\Big]y_1(t)\mathrm{d}t + b_1(t+\alpha_1(t))\mathrm{d}t \\
&\quad + b_2(t+\alpha_2(t))\mathrm{d}t
\end{aligned} \tag{6.22}$$

Using the equality (6.21), (6.22) becomes

$$\begin{aligned}
\mathrm{d}y_1(t) &= \sum_{i=-\infty}^{\infty}\sum_{k=-\infty}^{\infty} J(i,k)\exp\Big[\jmath\big[i\omega_1(t+\alpha_1(t))+k\omega_2(t+\alpha_2(t))\big]\Big]y_1(t)\mathrm{d}t \\
&+ \sum_{i=-\infty}^{\infty}\sum_{k=-\infty}^{\infty} X_s(i,k)\frac{c_1 i^2\omega_1^2+c_2k^2\omega_2^2}{2}\exp\big(\jmath i\omega_1(t+\alpha_1(t))\big)\exp\big(\jmath k\omega_2(t+\alpha_2(t))\big)\mathrm{d}t \\
&- \sum_{i=-\infty}^{\infty}\sum_{k=-\infty}^{\infty} X_s(i,k)\jmath i\omega_1\sqrt{c_1}\exp\big(\jmath i\omega_1(t+\alpha_1(t))\big)\exp\big(\jmath k\omega_2(t+\alpha_2(t))\big)\mathrm{d}B_1(t) \\
&- \sum_{i=-\infty}^{\infty}\sum_{k=-\infty}^{\infty} X_s(i,k)\jmath k\omega_2\sqrt{c_2}\exp\big(\jmath i\omega_1(t+\alpha_1(t))\big)\exp\big(\jmath k\omega_2(t+\alpha_2(t))\big)\mathrm{d}B_2(t)
\end{aligned} \tag{6.23}$$

The above stochastic differential equation is linear in $y_1(t)$. This means that $y_1(t)$ can be viewed as $y_1(t) = y_{11}(t) + y_{12}(t)$ where $y_{11}(t)$ satisfies the following stochastic differential equation

$$\begin{aligned}
\mathrm{d}y_{11}(t) &= \sum_{i=-\infty}^{\infty}\sum_{k=-\infty}^{\infty} J(i,k)\exp\Big[\jmath\big[i\omega_1(t+\alpha_1(t))+k\omega_2(t+\alpha_2(t))\big]\Big]y_{11}(t)\mathrm{d}t \\
&- \sum_{i=-\infty}^{\infty}\sum_{k=-\infty}^{\infty} X_s(i,k)\jmath i\omega_1\sqrt{c_1}\exp\big(\jmath i\omega_1(t+\alpha_1(t))\big)\exp\big(\jmath k\omega_2(t+\alpha_2(t))\big)\mathrm{d}B_1(t) \\
&- \sum_{i=-\infty}^{\infty}\sum_{k=-\infty}^{\infty} X_s(i,k)\jmath k\omega_2\sqrt{c_2}\exp\big(\jmath i\omega_1(t+\alpha_1(t))\big)\exp\big(\jmath k\omega_2(t+\alpha_2(t))\big)\mathrm{d}B_2(t)
\end{aligned} \tag{6.24}$$

and $y_{12}(t)$ satisfies the following stochastic differential equation

$$\begin{aligned}
\mathrm{d}y_{12}(t) &= \sum_{i=-\infty}^{\infty}\sum_{k=-\infty}^{\infty} J(i,k)\exp\Big[\jmath\big[i\omega_1(t+\alpha_1(t))+k\omega_2(t+\alpha_2(t))\big]\Big]y_{12}(t)\mathrm{d}t \\
&+ \sum_{i=-\infty}^{\infty}\sum_{k=-\infty}^{\infty} X_s(i,k)\frac{c_1 i^2\omega_1^2+c_2k^2\omega_2^2}{2}\exp\big(\jmath i\omega_1(t+\alpha_1(t))\big)\exp\big(\jmath k\omega_2(t+\alpha_2(t))\big)\mathrm{d}t
\end{aligned} \tag{6.25}$$

The input terms in (6.24) correspond to two independent white noise sources which are modulated by

$$-\sqrt{c_1}\left.\frac{\partial\hat{x}_s(t_1,t_2)}{\partial t_1}\right|_{t_1=t+\alpha_1(t),t_2=t+\alpha_2(t)}$$

and

$$-\sqrt{c_2}\left.\frac{\partial\hat{x}_s(t_1,t_2)}{\partial t_2}\right|_{t_1=t+\alpha_1(t),t_2=t+\alpha_2(t)}$$

Using similar arguments as in Section 5.3, we can conclude that $y_{11}(t)$ is the stationary component of $z_{11}(t)$ where $z_{11}(t)$ is governed by the following linear stochastic differential equation

$$\begin{aligned} \mathrm{d}z_{11}(t) = &\sum_{i=-\infty}^{\infty}\sum_{k=-\infty}^{\infty} J(i,k)\exp\big[\jmath(i\omega_1 + k\omega_2)t\big] z_{11}(t)\mathrm{d}t \\ &- \sqrt{c_1}\,\frac{\partial \hat{x}_s(t_1,t_2)}{\partial t_1}\bigg|_{t_1=t_2=t} \mathrm{d}B_1(t) - \sqrt{c_2}\,\frac{\partial \hat{x}_s(t_1,t_2)}{\partial t_2}\bigg|_{t_1=t_2=t} \mathrm{d}B_2(t) \end{aligned} \tag{6.26}$$

Using similar arguments as in Section 5.3 it also follows that $y_{12}(t)$ in (6.25) is a deterministic bi-periodic signal except that it is corrupted by phase deviation terms $\alpha_1(t)$ and $\alpha_2(t)$ of the two input signals $b_1(t+\alpha_1(t))$ and $b_2(t+\alpha_2(t))$. Since the original system is nonautonomous, it follows that for small c_1 and c_2, i.e., small input signal phase noise, $y_{12}(t)$ is small compared to $x_n(t)$. The spectrum of $y_{12}(t)$ is similar to the spectrum of $x_n(t)$ except that it is of *much smaller* amplitude. Hence the effect of adding $y_{12}(t)$ to the output is to change the amplitude of the spectrum of the original signal $x_n(t)$ without altering its frequency content.

It is easy to argue that when circuit noise sources are also included, i.e., $D(x) \neq 0$, the output process can be expressed as $x_n(t) + y_0(t)$ and

$$y_0(t) = y_{01}(t) + y_{12}(t)$$

Here $y_{12}(t)$ is the same as defined in (6.25) and $y_{01}(t)$ is the stationary component of $z_{01}(t)$ where $z_{01}(t)$ is governed by

$$\begin{aligned} \mathrm{d}z_{01}(t) = &\sum_{i=-\infty}^{\infty}\sum_{k=-\infty}^{\infty} J(i,k)\exp\big[\jmath(i\omega_1 + k\omega_2)t\big] z_{01}(t)\mathrm{d}t - \sqrt{c_1}\,\frac{\partial \hat{x}_s(t_1,t_2)}{\partial t_1}\bigg|_{t_1=t_2=t} \mathrm{d}B_1(t) \\ &- \sqrt{c_2}\,\frac{\partial \hat{x}_s(t_1,t_2)}{\partial t_2}\bigg|_{t_1=t_2=t} \mathrm{d}B_2(t) + D(x_s(t))\mathrm{d}B_p(t) \end{aligned} \tag{6.27}$$

This equation is very similar to the one obtained using conventional two tone noise analysis. The only difference is the addition to *two* white noise sources, appropriately modulated and the fact that we only need to consider the stationary component of output noise. This result can be generalized to the case when l large input signals are present. It can be shown that l additional white noise terms of the form

$$-\sqrt{c_i}\,\frac{\partial \hat{x}_s(t_1,\ldots,t_l)}{\partial t_i}\bigg|_{t_1=\ldots=t_l=t} \qquad 1 \le i \le l$$

are added to the circuit noise equations. In the next section we describe how to compute the statistics of the output noise $z_{01}(t)$ for the bi-periodic case.

6.5 Numerical Techniques

We begin by describing the conventional small signal and noise analysis of a nonautonomous circuit driven by two large incommensurable tones. We will derive expressions for the output noise statistics in terms of the input noise statistics and the linear transfer function. We use the property that a bi-periodic signal, when approximated by a truncated two dimensional Fourier series and its time axis suitably warped, is in fact a periodic signal for an appropriate frequency. The bi-periodic noise analysis problem reduces to a periodic noise analysis problem and we can use techniques described in Section 5.6. In particular, the frequency domain technique can be easily extended for the bi-periodic case. Therefore, we only discuss the frequency domain technique here.

Consider (6.1) with a steady-state solution of the form (6.5). We consider the case when the large input signals $b_1(t)$ and $b_2(t)$ are noiseless and the system of equations is perturbed by additive noise as $D(x(t))\xi(t)$ and is given by

$$\frac{\mathrm{d}x}{\mathrm{d}t} = f(x(t)) + b_1(t) + b_2(t) + D(x(t))\xi(t) \tag{6.28}$$

and the solution is assumed to be of the form

$$x(t) = x_s(t) + y(t)$$

and $y(t)$ is assumed to be small for small perturbation $D(x(t))\xi(t)$. Substituting this in (6.28) we have

$$\frac{\mathrm{d}x_s}{\mathrm{d}t} + \frac{\mathrm{d}y}{\mathrm{d}t} = f(x_s(t) + y(t)) + b_1(t) + b_2(t) + D(x_s(t) + y(t))\xi(t)$$

Linearizing the nonlinear function $f(x_s(t)+y(t))$ around the large unperturbed steady-state solution $x_s(t)$ and ignoring $y(t)$ in the argument of $D(x)$ in the above equations we have

$$\frac{\mathrm{d}x_s}{\mathrm{d}t} + \frac{\mathrm{d}y}{\mathrm{d}t} = f(x_s(t)) + J(x_s(t))y(t) + b_1(t) + b_2(t) + D(x_s(t))\xi(t) \tag{6.29}$$

where

$$J(x_s(t)) = \left.\frac{\partial f(x)}{\partial x}\right|_{x_s(t)}$$

Since $x_s(t)$ is the solution of (6.1), (6.29) reduces to

$$\frac{\mathrm{d}y}{\mathrm{d}t} = J(x_s(t))y(t) + D(x_s(t))\xi(t) \tag{6.30}$$

The above differential equation is linear in $y(t)$. Since $x_s(t)$ is bi-periodic, the coefficient matrix $J(x_s(t))$ is bi-periodic. Hence this equation represents as linear bi-periodic time varying transfer function. We now describe propagation of noise through a linear bi-periodic time varying system. The derivation is along the lines of that described in Section 5.6 for periodic case. The extension to general quasi-periodic case is immediate.

6.5.1 Propagation of Noise Through a Liner Quasi-Periodic Time Varying System

(6.30) is a linear differential equation (in $y(t)$) with bi-periodic coefficient matrix. This equation represents a linear bi-periodic transfer function $h(t_2, t_1)$ which implies that this transfer function is periodic with respect to displacements of T_1 and T_2 in both its arguments, i.e., $h(t_2 + T_1, t_1 + T_1) = h(t_2, t_1)$ and $h(t_2 + T_2, t_1 + T_2) = h(t_2, t_1)$. The bi-periodicity of h implies that it can be expanded as

$$h(t_2, t_1) = \sum_{i=-\infty}^{\infty} \sum_{k=-\infty}^{\infty} h_{i,k}(t_2 - t_1) \exp(\jmath(i\omega_1 + k\omega_2)t) \tag{6.31}$$

$h_{i,k}(\cdot)$ are called *bi-harmonic impulse responses* of the linear bi-periodic time varying system. Their Fourier transforms $H_{i,k}(\omega)$ are called *bi-harmonic transfer functions* of the system, i.e.,

$$H_{i,k}(\omega) = \int_{-\infty}^{\infty} h_{i,k}(t) \exp(-\jmath\omega t)\mathrm{d}t \tag{6.32}$$

Since circuit noise are in general nonstationary stochastic processes, their covariance matrix is defined as $R_{uu}(t_1, t_2) = \mathbb{E}\left[u(t_1)u^T(t_2)\right]$ where u is the input noise source. The output noise x is related to the input noise as

$$\begin{aligned} R_{xx}(t_1, t_2) &= \mathbb{E}\left[x(t_1)x^T(t_2)\right] \\ &= \mathbb{E}\left[\int_{-\infty}^{\infty}\int_{-\infty}^{\infty} h(t_1, s_1)u(s_1)u^T(s_2)h^T(s_2, t_1)\mathrm{d}s_1\mathrm{d}s_2\right] \\ &= \int_{-\infty}^{\infty}\int_{-\infty}^{\infty} h(t_1, s_1)R_{uu}(s_1, s_2)h^T(t_2, s_2)\mathrm{d}s_1\mathrm{d}s_2 \end{aligned}$$

The two dimensional Fourier transform of $R_{xx}(t_1, t_2)$ is defined as

$$S_{xx}(\omega_3, \omega_4) = \int_{-\infty}^{\infty}\int_{-\infty}^{\infty} R_{xx}(t_1, t_2) \exp\big(-\jmath(\omega_3 t_1 + \omega_4 t_2)\big)\mathrm{d}t_1\mathrm{d}t_2$$

Substituting (6.31) and (6.32) in the above expression of $S_{xx}(\omega_3, \omega_4)$ we have

$$
\begin{aligned}
S_{xx}(\omega_3,\omega_4) &= \int_{-\infty}^{\infty}\!\!\int\!\!\int\!\!\int h(t_1,s_1)R_{uu}(t_1,t_2)h(t_2,s_2)\exp\big(-\jmath(\omega_3 t_1+\omega_4 t_2)\big)\mathrm{d}s_1\mathrm{d}s_2\mathrm{d}t_1\mathrm{d}t_2 \\
&= \frac{1}{16\pi^4}\int_{-\infty}^{\infty}\!\!\int\!\!\int\!\!\int\!\!\int\!\!\int\!\!\int\!\!\int\!\!\int \sum_{i,k,l,m=-\infty}^{\infty} H_{i,k}(\omega_7)\exp\Big(\jmath\big(\omega_7(t_1-s_1)+(i\omega_1+k\omega_2)t_1\big)\Big) \\
&\qquad S_{uu}(\omega_5,\omega_6)\exp\big(\jmath(\omega_5 s_1+\omega_6 s_2)\big)H^T_{l,m}(\omega_8) \\
&\qquad \exp\Big(\jmath\big(\omega_8(t_2-s_2)+(l\omega_1+m\omega_2)t_2\big)\Big) \\
&\qquad \exp\big(-\jmath(\omega_3 t_1+\omega_4 t_2)\big)\mathrm{d}s_1\mathrm{d}s_2\mathrm{d}t_1\mathrm{d}t_2\mathrm{d}\omega_5\mathrm{d}\omega_6 \\
&\qquad \mathrm{d}\omega_7\mathrm{d}\omega_8 \\
&= \frac{1}{16\pi^4}\int_{-\infty}^{\infty}\!\!\int\!\!\int\!\!\int\!\!\int\!\!\int\!\!\int\!\!\int\!\!\int \sum_{i,k,l,m=-\infty}^{\infty} H_{i,k}(\omega_7)S_{uu}(\omega_5,\omega_6)H^T_{l,m}(\omega_8)\exp\big(\jmath(\omega_5-\omega_7)s_1\big) \\
&\qquad \exp\big(\jmath(\omega_6-\omega_8)s_2\big)\exp\big(\jmath(\omega_7+i\omega_1+k\omega_2-\omega_3)t_1\big) \\
&\qquad \exp\big(\jmath(\omega_8+l\omega_1+m\omega_2-\omega_4)t_2\big)\mathrm{d}s_1\mathrm{d}s_2\mathrm{d}t_1\mathrm{d}t_2\mathrm{d}\omega_5 \\
&\qquad \mathrm{d}\omega_6\mathrm{d}\omega_7\mathrm{d}\omega_8 \\
&= \int_{-\infty}^{\infty}\!\!\int\!\!\int\!\!\int\!\!\int \sum_{i,k,l,m=-\infty}^{\infty} H_{i,k}(\omega_7)S_{uu}(\omega_5,\omega_6)H^T_{l,m}(\omega_8)\delta(\omega_5-\omega_7)\delta(\omega_6-\omega_8) \\
&\qquad \delta(\omega_7+i\omega_1+k\omega_2-\omega_3)\delta(\omega_8+l\omega_1+m\omega_2-\omega_4) \\
&\qquad \mathrm{d}\omega_5\mathrm{d}\omega_6\mathrm{d}\omega_7\mathrm{d}\omega_8 \\
&= \int_{-\infty}^{\infty}\int_{-\infty}^{\infty} \sum_{i,k,l,m=-\infty}^{\infty} H_{i,k}(\omega_5)S_{uu}(\omega_5,\omega_6)H^T_{l,m}(\omega_6)\delta(\omega_5+i\omega_1+k\omega_2-\omega_3) \\
&\qquad \delta(\omega_6+l\omega_1+m\omega_2-\omega_4)\mathrm{d}\omega_5\mathrm{d}\omega_6 \\
&= \sum_{i,k,l,m=-\infty}^{\infty} H_{i,k}(\omega_3-i\omega_1-k\omega_2)S_{uu}(\omega_3-i\omega_1-k\omega_2,\omega_4-l\omega_1-m\omega_2) \\
&\qquad H^T_{l,m}(\omega_4-l\omega_1-m\omega_2)
\end{aligned}
\tag{6.33}
$$

Here we have used the fact that

$$\frac{1}{2\pi}\int_{-\infty}^{\infty}\exp(\jmath\omega t)\mathrm{d}t = \delta(\omega)$$

Since $x_s(t)$ is bi-periodic, the coefficient matrix $D(x_s(t))$ in (6.29) is also bi-periodic. Hence the statistics of circuit noise sources are also bi-periodic. This implies that R_{xx} and R_{uu} do not change if T_1 or T_2 are added to both their arguments, i.e.,

$$R_{pp}(t_1 + T_1, t_2 + T_1) = R_{pp}(t_1 + T_2, t_2 + T_2) = R_{pp}(t_1, t_2)$$

Hence both can be expanded in Fourier series as

$$R_{pp}(t_1, t_2) = \sum_{i=-\infty}^{\infty} \sum_{k=-\infty}^{\infty} R_{pp_{i,k}}(t_2 - t_1) \exp\big(\jmath(i\omega_1 + k\omega_2)t\big)$$

$R_{xx_{i,k}}$ and $R_{uu_{i,k}}$ are known as *bi-harmonic covariances* of the input and output noise respectively. Their Fourier transform is referred to as *bi-harmonic power spectral density* and is given by

$$S_{pp_{i,k}}(\omega) = \int_{-\infty}^{\infty} R_{pp_{i,k}} \exp(-\jmath\omega t)\mathrm{d}t$$

With the assumption that input and output noise autocorrelations are bi-periodic with respect to T_1 and T_2, the two-dimensional power spectral densities of input and output noise are given by

$$\begin{aligned}
S_{pp}(\omega_3, \omega_4) &= \int_{-\infty}^{\infty}\int_{-\infty}^{\infty} R_{pp} \exp\big(-\jmath(\omega_3 t_1 + \omega_4 t_2)\big)\mathrm{d}t_1\mathrm{d}t_2 \\
&= \int_{-\infty}^{\infty}\int_{-\infty}^{\infty} \sum_{i=-\infty}^{\infty}\sum_{k=-\infty}^{\infty} R_{pp_{i,k}}(t_2 - t_1) \exp\big(\jmath(i\omega_1 + k\omega_2 - \omega_4)t_2 - \omega_3 t_1)\big)\mathrm{d}t_1\mathrm{d}t_2 \\
&= \frac{1}{2\pi}\iiint_{-\infty}^{\infty} \sum_{i=-\infty}^{\infty}\sum_{k=-\infty}^{\infty} S_{pp_{i,k}}(\omega) \exp\big(\jmath(i\omega_1 + k\omega_2 - \omega_4)t_2 - \omega_3 t_1)\big) \\
&\qquad\qquad \exp\big(\jmath\omega(t_2 - t_1)\big)\mathrm{d}\omega\mathrm{d}t_1\mathrm{d}t_2 \\
&= 2\pi \int_{-\infty}^{\infty} \sum_{i=-\infty}^{\infty}\sum_{k=-\infty}^{\infty} S_{pp_{i,k}}(\omega)\delta(-\omega_3 - \omega)\delta(i\omega_1 + k\omega_2 - \omega_4 + \omega)\mathrm{d}\omega \\
&= 2\pi \sum_{i=-\infty}^{\infty}\sum_{k=-\infty}^{\infty} S_{pp_{i,k}}(-\omega_3)\delta(\omega_4 + \omega_3 - i\omega_1 - k\omega_2)
\end{aligned}$$

Using the above form in (6.33) we have

$$\begin{aligned}
&2\pi \sum_{i=-\infty}^{\infty}\sum_{k=-\infty}^{\infty} S_{xx_{i,k}}(-\omega_3)\delta(\omega_3 + \omega_4 - i\omega_1 - k\omega_2) \\
=&2\pi \sum_{l,m,n,p,q,r=-\infty}^{\infty} H_{l,m}(\omega_3 - l\omega_1 - m\omega_2) S_{uu_{n,p}}(-\omega_3 + l\omega_1 + m\omega_2) \\
&\qquad \delta\big(\omega_3 + \omega_4 - (l + n + q)\omega_1 - (p + m + r)\omega_2\big) H^T_{q,r}(\omega_4 - q\omega_1 - r\omega_2)
\end{aligned}$$

Therefore

$$S_{xx_{i,k}}(-\omega) = \sum_{l,m,n,p=-\infty}^{\infty} H_{l,m}(\omega - l\omega_1 - m\omega_2) S_{uu_{n,p}}(-\omega + l\omega_1 + m\omega_2) \\ H^T_{i-(l+n),k-(m+p)}\big(-\omega - (l+n)\omega_1 - (m+p)\omega_2\big) \tag{6.34}$$

In an actual RF circuit, the signal bandwidth is limited and hence a finite number harmonics of signals are present. Hence the infinite summations in all the above expressions are truncated. We assume that harmonics corresponding to ω_1 are truncated to $\pm I$ and the harmonics corresponding to ω_2 are truncated to $\pm K$. Hence a bi-periodic waveform $z(t)$ in this system is given by

$$z(t) = \sum_{i=-I}^{I} \sum_{k=-K}^{K} Z(i,k) \exp\big(\jmath(i\omega_1 + k\omega_2)t\big)$$

The bivariate form of this signal is given by

$$\hat{z}(t_1, t_2) = \sum_{i=-I}^{I} \sum_{k=-K}^{K} Z(i,k) \exp\big(\jmath(i\omega_1 t_1 + k\omega_2 t_2)\big)$$

Consider the waveform $\tilde{z}(t)$ which obtained from $\hat{z}(t_1, t_2)$ by constraining it on the line (6.10). $\tilde{z}(t)$ is periodic with a period $T_0 = (2K+1)T_1$ and can be written as

$$\tilde{z}(t) = \sum_{i=-L}^{L} \tilde{Z}(l) \exp(\jmath l\omega_0 t)$$

where

$$\omega_0 = \frac{2\pi}{(2K+1)T_1}$$

and

$$L = \frac{(2I+1)(2K+1) - 1}{2} = 2IK + I + K$$

The one-to-one mapping between the harmonics present in the circuit and the artificial spectrum [Kun89] is given by (6.12) and (6.13) and is depicted in Figure 6.3. Note that $\tilde{z}(t)$ is derived from $z(t)$ by suitably distorting the time axis. If $z(t)$ is not required in the intermediate calculation, then the entire analysis can be carried out using the artificial

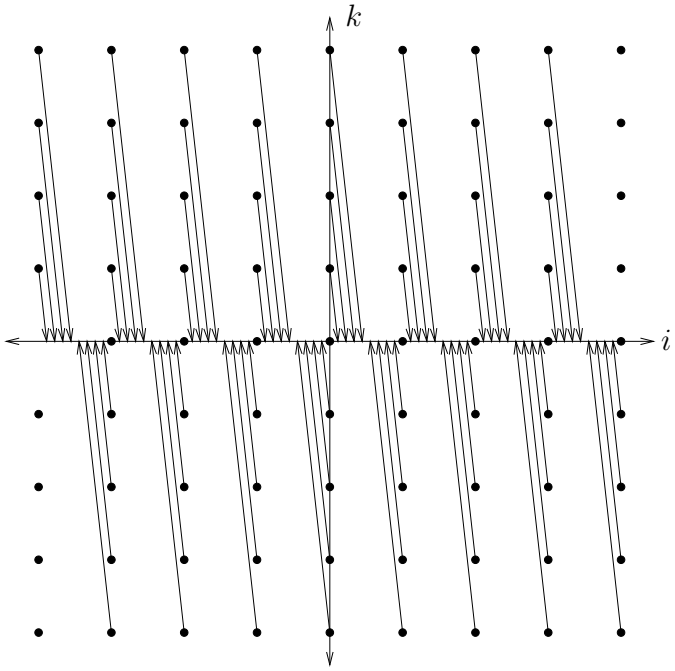

Figure 6.3: Illustration of the AFM method for a box truncation scheme with two incommensurable frequencies

spectrum. The advantage is that we can reuse the analysis developed previously for the periodic case. For instance, if the summations in (6.34) are truncated then

$$S_{xx_{i,k}}(-\omega) = \sum_{l,n=-I}^{I} \sum_{m,p=-K}^{K} H_{l,m}(\omega - l\omega_1 - m\omega_2) S_{uu_{n,p}}(-\omega + l\omega_1 + m\omega_2) \\ H^T_{i-(l+n),k-(m+p)}\big(-\omega - (l+n)\omega_1 - (m+p)\omega_2\big) \tag{6.35}$$

for $-I \leq i \leq I$ and $-K \leq k \leq K$. (6.35) can be written in terms of $\tilde{S}$ and $\tilde{H}$ as

$$\tilde{S}_{xx_{\tilde{i}}} = \sum_{\tilde{l}=-L}^{L} \sum_{\tilde{n}=-L}^{L} \tilde{H}_{\tilde{l}}(\omega - \tilde{l}\omega_0) \tilde{S}_{uu_{\tilde{n}}}(-\omega + \tilde{l}\omega_0) \tilde{H}_{\tilde{i}-\tilde{l}-\tilde{n}}\big(-\omega + (\tilde{l}+\tilde{n})\omega_0\big)$$

This expression is exactly the same as the one derived for the periodic case in Section 5.6.2.1.

6.5.2 Derivation of the Form of Transfer Function

Consider (5.17) which is repeated here for convenience

$$C(t)\dot{y} + G(t)y + Ab(t) = 0$$

where $G(t)$ and $C(t)$ are assumed to be bi-periodic with periods T_1 and T_2. We further assume that system of equations is nonautonomous. Since (5.17) is linear in $y(t)$, the corresponding linear bi-periodic time varying transfer function $h(t_2, t_1)$ can be written as

$$\begin{aligned} h(t_2,t_1) &= \sum_{i=-\infty}^{\infty}\sum_{k=-\infty}^{\infty} h_i(t_2-t_1)\exp[\jmath(i\omega_1+k\omega_2)t_2] \\ &= \frac{1}{2\pi}\int_{-\infty}^{\infty}\sum_{i=-\infty}^{\infty}\sum_{k=-\infty}^{\infty} H_{i,k}(\omega)\exp[\jmath\omega(t_2-t_1)]\exp[\jmath(i\omega_1+k\omega_2)t_2]\mathrm{d}\omega \end{aligned}$$

For the purpose of this analysis we assume that $b(t)$ is deterministic and its Fourier transform is given by

$$B(\omega) = \int_{-\infty}^{\infty} b(t)\exp(-\jmath\omega t)\mathrm{d}t$$

Since $h(t_2, t_1)$ is the linear transfer function corresponding to (5.17), we have

$$\begin{aligned} y(t_2) &= \int_{-\infty}^{\infty} h(t_2,t_1)b(t_1)\mathrm{d}t_1 \\ &= \frac{1}{4\pi^2}\iiint_{-\infty}^{\infty}\sum_{i=-\infty}^{\infty}\sum_{k=-\infty}^{\infty} H_{i,k}(\omega_3)\exp[\jmath\omega_3(t_2-t_1)]\exp[\jmath(i\omega_1+k\omega_2)t_2]B(\omega_4)\exp(\jmath\omega_4 t_1) \\ &\qquad\qquad \mathrm{d}\omega_3\mathrm{d}\omega_4\mathrm{d}t_1 \\ &= \frac{1}{2\pi}\int_{-\infty}^{\infty}\int_{-\infty}^{\infty}\sum_{i=-\infty}^{\infty}\sum_{k=-\infty}^{\infty} H_{i,k}(\omega_3)\exp[\jmath(\omega_3+i\omega_1+k\omega_2)t_2]B(\omega_4)\delta(\omega_4-\omega_3)\mathrm{d}\omega_3\mathrm{d}\omega_3 \\ &= \frac{1}{2\pi}\sum_{i=-\infty}^{\infty}\sum_{k=-\infty}^{\infty}\int_{-\infty}^{\infty} H_{i,k}(\omega)B(\omega)\exp[\jmath(\omega+i\omega_1+k\omega_2)t_2]\mathrm{d}\omega \end{aligned}$$

This implies that the Fourier transform of $x(t)$ is given by

$$Y(\omega) = \sum_{i=-\infty}^{\infty}\sum_{k=-\infty}^{\infty} H_{i,k}(\omega-i\omega_1-k\omega_2)B(\omega-i\omega_1-2\omega_2)$$

(5.17) is rewritten as

$$\begin{aligned} 0 &= \frac{1}{2\pi}\int_{-\infty}^{\infty}\sum_{i=-\infty}^{\infty}\sum_{k=-\infty}^{\infty} C_{i,k}\exp[\jmath(i\omega_1+k\omega_2)t]\jmath\omega Y(\omega)\exp(\jmath\omega t)\mathrm{d}\omega \\ &+ \frac{1}{2\pi}\int_{-\infty}^{\infty}\sum_{i=-\infty}^{\infty}\sum_{k=-\infty}^{\infty} G_{i,k}\exp[\jmath(i\omega_1+k\omega_2)t]Y(\omega)\exp(\jmath\omega t)\mathrm{d}\omega \\ &+ \frac{1}{2\pi}\int_{-\infty}^{\infty} AB(\omega)\exp(\jmath\omega t)\mathrm{d}\omega \end{aligned}$$

Fourier transform of the above expression is given by

$$\sum_{i=-\infty}^{\infty}\sum_{k=-\infty}^{\infty} C_{i,k}\jmath(\omega - i\omega_1 - k\omega_2)Y(\omega - i\omega_1 - k\omega_2) + \sum_{i=-\infty}^{\infty}\sum_{k=-\infty}^{\infty} G_{i,k}Y(\omega - i\omega_1 - k\omega_2) + AB(\omega) = 0$$

Substituting the value of $Y(\omega)$ in the above expression we have

$$\begin{aligned}&\sum_{i,k,l,m=-\infty}^{\infty} C_{i,k}\jmath[\omega - i\omega_1 - k\omega_2]H_{l,m}[\omega - (i+l)\omega_1 - (k+m)\omega_2] \\ &\qquad B[\omega - (i+l)\omega_1 - (k+m)\omega_2] \\ &+ \sum_{i,k,l,m=-\infty}^{\infty} G_{i,k}H_{l,m}[\omega - (i+l)\omega_1 - (k+m)\omega_2]B[\omega - (i+l)\omega_1 - (k+m)\omega_2] \\ &+AB(\omega) = 0\end{aligned}$$

Since the above expression is valid for every $B(\omega)$, it must be necessary that for $i + l = 0$ and $k + m = 0$

$$\sum_{i=-\infty}^{\infty}\sum_{k=-\infty}^{\infty} \jmath(\omega - i\omega_1 - k\omega_2)C_{i,k}H_{-i,-k}(\omega) + \sum_{i=-\infty}^{\infty}\sum_{k=-\infty}^{\infty} G_{i,k}H_{-i,-k}(\omega) + A = 0 \tag{6.36}$$

and for $i + l = n \neq 0$ or $k + m = p \neq 0$ we have

$$\begin{aligned}&\sum_{i=-\infty}^{\infty}\sum_{k=-\infty}^{\infty} \jmath(\omega - i\omega_1 - k\omega_2)C_{i,k}H_{n-i,p-k}(\omega - n\omega_1 - p\omega_2) \\ &+ \sum_{i=-\infty}^{\infty}\sum_{k=-\infty}^{\infty} C_{i,k}H_{n-i,p-k}(\omega - n\omega_1 - p\omega_2) = 0\end{aligned} \tag{6.37}$$

Collocating (6.36) the terms at frequencies $\omega - n\omega_1 - p\omega_2$ for all $n, p \in \mathbb{Z}$ we have

$$\begin{aligned}&\sum_{i=-\infty}^{\infty}\sum_{k=-\infty}^{\infty} \jmath[\omega - (i+n)\omega_1 - (k+p)\omega_2]C_{i,k}H_{-i,-k}(\omega - n\omega_1 - p\omega_2) \\ &+ \sum_{i=-\infty}^{\infty}\sum_{k=-\infty}^{\infty} C_{i,k}H_{-i,-k}(\omega - n\omega_1 - p\omega_2) + A = 0\end{aligned} \tag{6.38}$$

To evaluate (6.37) and (6.38) we again appeal to the AFM technique introduced in Section 6.5.1. If the infinite summations in these equations are truncated to $\pm I$ and $\pm K$ respectively and an artificial frequency map constructed as in Section 6.5.1, (6.37) and (6.38) can be written as

$$\sum_{\tilde{i}=-L}^{L} \jmath(\omega - \tilde{i}\omega_0)C_{\tilde{i}}H_{\tilde{n}-\tilde{i}}(\omega - \tilde{n}\omega_0) + \sum_{\tilde{i}=-L}^{L} C_{\tilde{i}}H_{\tilde{n}-\tilde{i}}(\omega - \tilde{n}\omega_0) = 0$$

and for all $\tilde{n} \in \mathbb{Z}$

$$\sum_{\tilde{i}=-L}^{L} \jmath[\omega - (\tilde{i} + \tilde{n})\omega_0] C_{\tilde{i}} H_{-\tilde{i}}(\omega - \tilde{n}\omega_0) + \sum_{\tilde{i}=-L}^{L} C_{\tilde{i}} H_{-\tilde{i}}(\omega - \tilde{n}\omega_0) + A = 0$$

These equations are very similar to (5.26) and (5.27) and hence the technique outlined in Section 5.6.2 for the periodic case can be used to perform noise analysis.

6.6 Examples

We carried out a two tone analysis of the two mixers described in Section 5.7. In addition to the 2.2 GHz LO signal, a large blocker signal at 2.5 GHz was applied at the RF port. For the active mixer, the RF signal power was set to -10 dBm while for the passive mixer, it was set to 10 dBm. The noise figure for the active mixer increased by 2.1 dB in presence of the blocker signal. The corresponding increase in the noise of passive mixer was computed to be 4.1 dB. The LO and blocker signals were assumed to be noiseless for this analysis. This increase in NF in entirely due the fact that the large blocker signals drive the linear signal path of these mixers into gain compression which decreases the signal power and decreases the overall SNR.

The analysis was carried out using 225 frequency mixes and took approximately six minutes for the passive mixer and 9.5 minutes for the active mixer on a 600 MHz Digital Alpha workstation. In our implementation, since SPICE3 was used for transient simulation, the circuit waveforms and Jacobian matrices were converted to the bi-periodic representation. This conversion required an additional (30%) overhead. Since in an actual multitone implementation, this overhead will not be present, it is not reported in the above run times.

The blocker signal gets downconverted to a frequency which is at 300 MHz, i.e, 100 MHz away from the IF signal. If either the blocker or LO signal have phase noise, then according to (6.3) the output spectrum consists of a Lorentzian centered at 300 MHz. The noise contributed to the output by this can be significant specially if the blocker frequency is very close to the RF signal frequency. In addition, the wide band noise due to the phase noise of the two large tones also increases the overall output noise of the mixer. Figures 6.4 and 6.5 plot the increase in noise figure due to phase noise in the two large tones.

We observe that the presence of a large blocker signal *increases* the sensitivity of the circuit to input signal phase noise. Comparing these figures to Figures 5.3 and 5.5 we

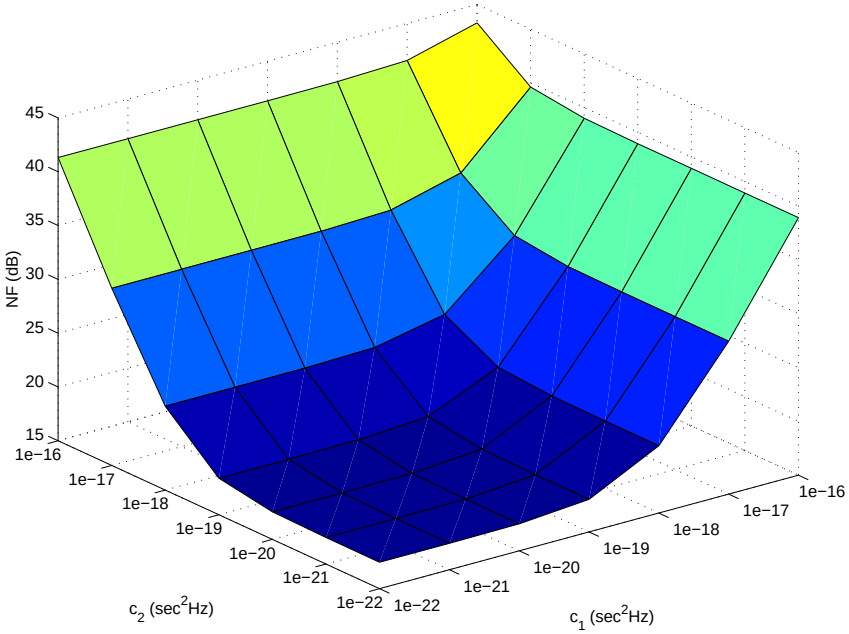

Figure 6.4: Increase in noise figure due to phase noise in the two input signal for the four diode mixer

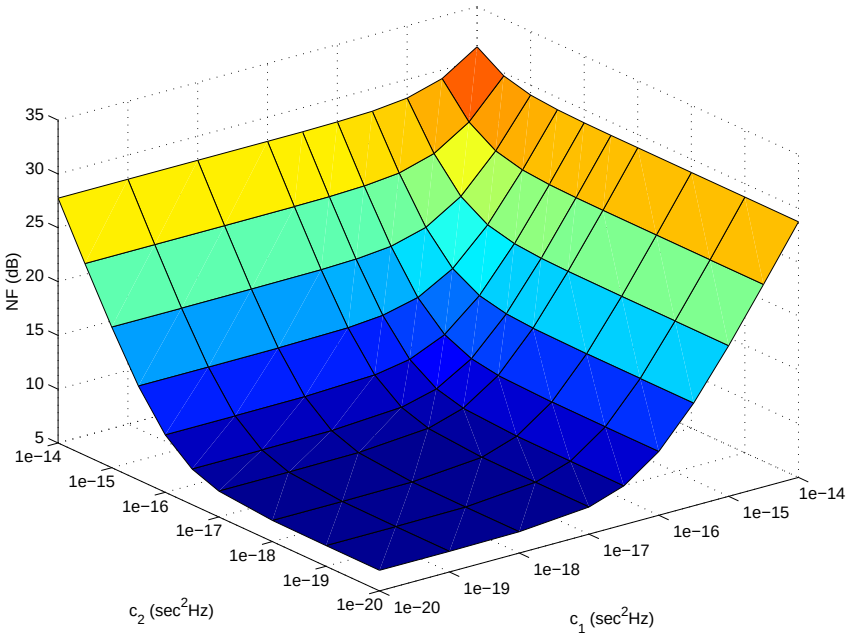

Figure 6.5: Increase in noise figure due to phase noise in the two input signal for the Gilbert cell mixer

find that the crossover point where the mixer noise figure starts increasing with c_i is reduced by about an order of magnitude. For the four diode mixer, we observed in Section 5.7 that due to perfectly symmetry, the output node was insensitive to LO signal phase noise. The presence of a large blocker destroys this symmetry and makes the output node susceptible to phase noise from both RF and LO signals. Therefore, blocker performance constraint poses much stricter constraints on the noise performance of input signal than just the one tone noise performance constraint.

Chapter 7

Conclusions and Future Directions

In this chapter we summarize our contributions and point out to some future directions where this research can proceed.

7.1 Conclusions

In this work we have investigated noise analysis and modelling problem for RF circuits. We first concentrated on noise analysis of autonomous circuits and then turned our attention to noise analysis of nonautonomous circuits which are driven by oscillators which have phase noise. We summarize our contributions below:

- We showed that linear perturbation analysis is not valid for oscillatory circuits. This analysis predicts that the deviation away from the unperturbed steady-state solution keeps increasing unbounded even for the smallest of perturbations. It was shown that noise analysis techniques for oscillators which are based on linear perturbation analysis predict nonphysical effects such as infinite total integrated noise power density.

- We developed a new perturbation analysis technique which is valid for oscillators. We showed that the perturbed oscillator response can be viewed as a sum of two signals: periodic steady-state unperturbed oscillator response time shifted by an amount $\alpha(t)$ and a small and bounded deviation away from the limit cycle. We derived a nonlinear differential equation for $\alpha(t)$, found the component of perturbation term that causes deviation only along the limit cycle of the form $x_s(t+\alpha(t))$ and showed that when we add in the rest of the perturbation term, it causes only small and bounded deviations

away from the limit cycle for all times. In terms of this phase plane interpretation we precisely defined the notion of phase error, phase deviation and amplitude deviation.

- For white noise perturbations, the nonlinear differential equation for phase error $\alpha(t)$ becomes a stochastic differential equation and we used techniques from stochastic calculus to obtain a second order characterization of phase error and oscillator response. We showed that oscillator response, as a stochastic process, is wide-sense stationary. We gave arguments for the physical interpretation of this result.

- We then addressed the noise analysis problem of nonautonomous circuits driven by a single large periodic signal which has phase noise. We argued that since a nonautonomous circuit, along with the driving oscillator, can be viewed as a composite oscillator, the output noise process will be stationary and not cyclostationary, as would be predicted by classical noise analysis for such circuits. We also derived this result mathematically. We showed that the effect of input signal phase noise is to add another white noise source to the circuit noise sources which is modulated by the time derivative of the noiseless steady-state response of the circuit.

- We extended this analysis for nonautonomous circuits driven by multi-tone excitations. We first reviewed some techniques in time domain, frequency domain and mixed time frequency domain techniques for simulating circuits driven by two large incommensurable frequency signals. We then discussed noise analysis techniques for these circuits.

7.2 Noise Models for Circuits Driven by Multitone Excitations

A byproduct of oscillator phase noise analysis presented in Chapter 4 was a compact and accurate noise model for oscillator output. We showed that a single scalar constant c is sufficient for modelling a noisy oscillator output. We later used this model in Chapters 5 and 6 for noise analysis of nonautonomous circuits. We also gave a noise model for nonautonomous circuit driven by an input signal with phase noise in terms of a stochastic differential equation. A similar model can be developed of the output of a nonautonomous circuit driven by two or more large periodic signals with phase noise. One possible choice

of the model would be the stochastic differential equation similar to the one we developed in Chapter 5.

7.3 Extensions to Non-White Noise Sources

Other than thermal and shot noise sources, there are other circuit noise sources that cannot be modelled as a white noise source. The most important of them is flicker noise which has a power spectral density inversely proportional to frequency. This represents a problem since total integrated noise power in any finite bandwidth around DC is infinite. This noise source cannot be modelled as a well defined stochastic process and hence is not amenable to be handled using stochastic differential equation theory. The approximation of replacing the flicker noise source with a series of white noise sources can be used. However, the asymptotic arguments that were presented throughout this exposition need not be valid and need to be revisited. Consider the oscillator phase noise equation (4.1) (which is repeated here)

$$\frac{\mathrm{d}\alpha(t)}{\mathrm{d}t} = v^T(t+\alpha(t))\xi(t)$$

where v is small, i.e., of the order ϵ. Let $t' = t\epsilon$ and let us rewrite the above equation as

$$\frac{\mathrm{d}\alpha(t)}{\mathrm{d}t} = v^T\left(t+\alpha\left(\frac{t'}{\epsilon}\right)\right)\xi\left(\frac{t'}{\epsilon}\right)$$

The averaging principle [FW84] states that at time $t' = O(1)$, α would be governed by [Zei98]

$$\frac{\mathrm{d}\alpha}{\mathrm{d}t} = \bar{g}\xi\left(\frac{t'}{\epsilon}\right)$$

For white noise sources $\xi(t)$, it immediately follows that α is a Brownian motion process. Now consider a low pass filtered white noise source. The low pass filter can be absorbed in the circuit equations and we can conclude that asymptotically α is still a Brownian motion. If the correlation time is sufficiently small, then at time $O(1/\epsilon)$, the noise source would appear *almost* white and the asymptotic argument will be valid. However, if the correlation time is comparable to $O(1/\epsilon)$, then the noise source does not appear white and the asymptotic argument is not valid. This is certainly the case for flicker noise where the correlation time is comparable, if not larger than the measurement time. Even though flicker noise is a low frequency phenomenon, in nonlinear circuits, it can mix with periodic signals and get shifted to frequencies of interest. Extending this analysis to handle the flicker noise case in a consistent manner is a very important problem.

7.4 Behavioural Level Noise Simulation

Once noise model for nonautonomous circuits driven by multitone excitation is in place, behavioural level noise analysis techniques for RF circuits need to be developed which utilize these models for nonautonomous and autonomous circuits. These techniques would also be based on the solution of appropriate stochastic differential equations. The behavioural level noise analysis would enable a system designer to quickly evaluate different choices of architectures for RF front-ends for noise performance and investigate various design trade-offs. This would possibly also enable the use of techniques in the digital domain to recover some noise performance, given the particular characterization of noise from the RF front end.

In conjunction with component level models and system level simulation techniques for distortion and other nonidealities in the system, this effort will hopefully enable efficient design of high performance RF systems. We believe that a more thorough understanding of how noise and other nonidealities affect the overall circuit response will be crucial in minimizing overdesign which exists in current RF design practices. Specifically for RF mobile systems, this would result in lower power and hence higher battery life. Equivalently, extra functionality can be incorporated in those parts of an RF system where lower power dissipation is not an important issue (such as base stations of RF communication systems).

Bibliography

[ABR76] J Robert Ashley, Thomas A Barley, and Gustaf J Rast, Jr. Automated spectral analysis of microwave oscillator noise. In *1976 IEEE MTT-S International Microwave Symposium*, pages 227–229, 1976. 2.3.1

[AKR94] Werner Anzill, Franz X Kärtner, and Peter Russer. Simulation of the phase noise of oscillators in the frequency domain. *Archiv für Elektronik und Übertragungstechnik*, 48(1):45–50, January 1994. 2.3.1

[AM83] Asad A Abidi and Robert G Meyer. Noise in relaxation oscillators. *IEEE Journal of Solid-State Circuits*, SC–18(6):794–802, December 1983. 2.3.2, 4.6.4, 4.6.4

[AM97] Krzysztof Antoszkiewicz and Janusz Markowski. Computer aided noise analysis of an oscillator. *Bulletin of the Polish Academy of Sciences, Technical Sciences*, 45(1):183–195, 1997. 2.3.1

[Arn74] Ludwig Arnold. *Stochastische Differentialgleichungen: Theorie und Anwendung*. John Wiley & Sons, 1974. 4.1, 4.1.2, 4.1.2

[AT72a] Thomas J Aprille, Jr. and Timothy N Trick. A computer algorithm to determine the steady-state response of nonlinear oscillators. *IEEE Transactions on Circuit Theory*, CT19(4):354–360, July 1972. 4.5.1

[AT72b] Thomas J Aprille, Jr. and Timothy N Trick. Steady-state analysis of nonlinear circuits with periodic inputs. *Proceedings of the IEEE*, 60(1):108–114, January 1972. 4.5.1

[Ber84] Jeremy Bernstein. *Three degrees above zero : Bell Labs in the information age*. New York : C. Scribner's, 1984. (document)

[BWL97] Hans-Georg Brachtendorf, Günther Welsch, and Rainer Laur. A novel time-frequency method for the simulation of the steady state of circuits driven by multi-tone signals. In *Proceedings of the 1997 IEEE International Symposium on Circuits and Systems*, volume 3, pages 1508–1511, 1997. 6.2, 6.3, 2, 2, 6.4

[BWLBG96] Hans-Georg Brachtendorf, Günther Welsch, Rainer Laur, and Angelika Bunse-Gerstner. Numerical steady state analysis of electronic circuits driven by multi-tone signals. *Electrical Engineering*, 79:103–112, 1996. 6.2, 6.3, 6.3, 6.1, 3, 3, 6.4

[Che91] Jonathan Y C Cheah. Analysis of phase noise in oscillators. *RF Design*, 14(12):99–100, 1991. 2.3.1

[CHG95] Chang-Li Chen, Xing-Nan Hong, and Bao-Xin Gao. A new and efficient approach to the accurate simulation of phase noise in microwave MESFET oscillators. In *1995 SBMO/IEEE MTT-S International Microwave and Optoelectronics Conference Proceedings*, pages 230–234, 1995. 2.3.1

[Dek87] Astrid P Dekker. Approximate noise analysis of a feedback oscillator using a nonlinear differential amplifier. *Archiv für Elektronik und Übertragungstechnik*, 41(3):129–132, 1987. 2.3.4

[DLSV96] Alper Demir, Edward Liu, and Alberto Sangiovanni-Vincentelli. Time-domain non Monte-Carlo noise simulation for nonlinear dynamic circuits with arbitrary excitations. *IEEE Transactions for Computer-Aided Design*, 15:493–505, May 1996. 2.2.2, 2.3.3, 5.7.2

[Dob93] Janusz A Dobrowolski. CAD oriented method for noise analysis of microwave circuits described by the nodal admittance matrix. *IEE Proceedings H Microwaves, Antennas and Propagation*, 140(4):321–325, August 1993. 2.2.2

[DSG97] Bart De Smedth and George Gielen. Accurate simulation of phase noise in oscillators. In *Proceedings of the 23rd European Solid-State Circuits Conference*, pages 208–211, 1997. 2.3.1

[DSV96] Alper Demir and Alberto Sangiovanni-Vincentelli. Simulation and modeling of

phase noise in open-loop oscillators. In *Proceedings of the IEEE 1996 Custom Integrated Circuits Conference*, pages 453–456, 1996. 2.3.3

[DTS98a] Aleksander Dec, László Tóth, and Ken Suyama. Noise analysis of a class of oscillators. *IEEE Transactions on Circuits and Systems II: Analog and Digital Signal Processing*, 45(6):757–60, June 1998. 2.3.1, 4.6.1, 4.4(b), 4.6.1

[DTS98b] Aleksander Dec, László Tóth, and Ken Suyama. Noise analysis of an oscillator with an M^{th}-order filter and comparator-type nonlinearity. In *Proceedings of the 1998 IEEE International Symposium on Circuits and Systems*, volume 1, pages 225–228, 1998. 2.3.1

[FAOR95] Tilman Felgentreff, Werner Anzill, Gerhard Olbrich, and Peter Russer. Analysis of g-r noise upconversion in oscillators. In *1995 IEEE MTT-S International Microwave Symposium Digest*, pages 947–950, 1995. 2.3.1

[Far94] Miklos Farkas. *Periodic Motions*. Applied mathematical sciences. Springer–Verlag, New York, 1994. 1, 1, 3.2, 3.1, 3.5

[FHM97] Keng L Fong, Christopher D Hull, and Robert G Meyer. A class AB monolithic mixer for 900-MHz applications. *IEEE Journal of Solid-State Circuits*, 32(8):1166–1172, August 1997. 3

[FM99] Keng L Fong and Robert G Meyer. Monolithic RF active mixer design. *IEEE Transactions on Circuits and Systems–II: Analog and Digital Signal Processing*, 46(3):231–239, March 1999. 1.1

[FV88] Gerard J Foschini and Giovanni Vannucci. Characterizing filtered light waves corrupted by phase noise. *IEEE Transactions on Information Theory*, 34(6):1437–1448, November 1988. 2.3.4

[FW84] Mark I Freidlin and Alexander D Wentzell. *Random Perturbations of Dynamical Systems*. Springer–Verlag, 1984. 7.3

[Gar83] Crispin W Gardiner. *Handbook of stochastic methods for physics, chemistry, and the natural sciences*, volume 13 of *Springer series in synergetics*. Springer–Verlag, Berlin, Heidelberg, New York, Tokyo, second edition, 1983. 4.1, 4.1, 4.1.2, 4.1.2

[Gar90] William A Gardner. *Introduction to Random Processes : with Applications to Signals and systems*. McGraw–Hill, New York, second edition, 1990. 4.2, 4.3.2

[Gha96] Ranjit Gharpurey. *Modeling and analysis of substrate coupling in integrated circuits*. PhD thesis, University of California at Berkeley, 1996. 1.2.1, 1.2.1

[GM93] Paul R Gray and Robert G Meyer. *Analysis and design of Analog Integrated Circuits*. Wiley, New York, third edition, 1993. 4.6.4

[GM95] Paul R Gray and Robert G Meyer. Future directions in silicon ICs for RF personal communications. In *Proceedings of the IEEE 1995 Custom Integrated Circuits Conference*, pages 83–90, 1995. 1.1, 1.1

[Gol89] Jules Goldberg. Nonlinear analysis of high Q oscillator phase noise. In *Proceedings of the 43rd Annual Symposium on Frequency Control 1989*, pages 63–74, 1989. 2.3.4

[Gri90] Roger Grimshaw. *Nonlinear ordinary differential equations*. Applied mathematics and engineering science texts. Blackwell Scientific Publications, Oxford, Boston, 1990. 3.2, 3.4.3, 3.4.3, 5.1, 6.1

[GS92] Geoffrey R Grimmett and David R Stirzaker. *Probability and random processes*. Oxford University Press, New York, second edition, 1992. 4.1, 1, 4.1.2, 4.1.2, 4.2

[Haf66] Erich Hafner. The effect of noise in oscillators. *Proceedings of the IEEE*, 54(2):179–198, February 1966. 2.3.1

[Hag81] Peter Hagedorn. *Nichtlineare Schwingungen*. Oxford University Press, 1981. 3.4.1

[HK77] Daniel N Held and Anthony R Kerr. Analysis of noise in room-temperature millimeter-wave mixers. In *1977 International Microwave Symposium Digest*, pages 483–486, 1977. 2.2.1

[HKK98] Robert L Howald, Stan Kesler, and Moshe Kam. BER performance analysis of OFDM-QAM in phase noise. In *Proceedings. 1998 IEEE International Symposium on Information Theory*, page 256, 1998. 1.2.2

[HKW91] Stefan Heinen, Jürgen Kunisch, and Ingo Wolff. A unified framework for computer-aided noise analysis of linear and nonlinear microwave circuits. *IEEE Transactions on Microwave Theory and Techniques*, 39(12):2170–2175, December 1991. 2.2.1

[HL98] Ali Hajimiri and Thomas H Lee. A general theory of phase noise in electrical oscillators. *IEEE Journal of Solid-State Circuits*, 33(2):179–94, February 1998. 2.3.1

[HM93] Christopher D Hull and Robert G Meyer. A systematic approach to the analysis of noise in mixers. *IEEE Transactions on Circuits and Systems I: Fundamental Theory and Applications*, 40(12):909–919, December 1993. 2.2.1

[Hud92] Premysl Hudec. Procedures for exact noise analysis of microwave circuits. *Microwave Journal*, 35(9):165–170, September 1992. 2.2.1

[Hul92] Christopher D Hull. *Analysis and Optimization of Monolithic RF Downconversion Receivers*. PhD thesis, University of California, Berkeley, 1992. 2.2.1

[Kär90] Franz X Kärtner. Analysis of white and $f^{-\alpha}$ noise in oscillators. *International Journal of Circuit Theory and Applications*, 18(5):485–519, October 1990. 2.3.4

[Kin98] Peter Kinget. A fully integrated 2.7 V 0.35 μm CMOS VCO for 5 GHz wireless applications. In *Digest of Technical Papers IEEE International Solid-State Circuits Conference*, pages 226–227, 1998. 4.6.2, 4.6.2

[Kun89] Kenneth S Kundert. *Steady state methods for simulating analog circuits*. PhD thesis, University of California at Berkeley, 1989. 6.5.1

[Kur68] Kaneyuki Kurokawa. Noise in synchronized oscillators. *IEEE Transactions on Microwave Theory and Techniques*, MTT-16(4):234–40, 1968. 2.3.1

[KWSV90] Kenneth S Kundert, Jacob K White, and Alberto L Sangiovanni-Vincentelli. *Steady-state methods for simulating analog and microwave circuits*. Kluwer Academic Publishers, Boston ; Dordrecht, 1990. 1, 4.5.1

[Lax67] Melvin Lax. Classical noise. v. noise in self-sustained oscillators. *Physical Review*, CAS–160:290–307, 1967. 2.3.4

[Lee66] David B Leeson. A simple model of feedback oscillator noise spectrum. *Proceedings of the IEEE*, 54(2):329–330, February 1966. 2.3.1

[McN97] John A McNeill. Jitter in ring oscillators. *IEEE Journal of Solid-State Circuits*, 32(6):177–193, June 1997. 2.3.2, 4.3.4, 4.6.3, 4.6.3, 4.6.3, 4.6.3, 4.6.3

[MK82] Kohji Motoishi and Tosiro Koga. Simulation of a noise source with 1/f spectrum by means of an RC circuit. *Electronics and Communications in Japan*, 65-A(3):19–27, March 1982. 1.2.1

[Nez98] Mohammad K Nezami. Phase noise analysis. 1. evaluate the impact of phase noise on receiver performance. *Microwaves & RF*, 37(5):165–166, May 1998. 1.2.2

[NM79] Ali Hasan Nayfeh and Dean T Mook. *Nonlinear Oscillations*. John Wiley & Sons, 1979. 3.4.1

[Ohi93] Takashi Ohira. Higher-order analysis on phase noise generation in varactor-tuned oscillators-baseband noise upconversion in GaAs MESFET oscillators. *IEICE Transactions on Electronics*, E76-C(12):1851–1854, December 1993. 2.3.1

[Øks98] Bernt K Øksendal. *Stochastic differential equations: an introduction with applications*. Springer–Verlag, 1998. 2.2, 2.2, 4.1, 4.1.1, 4.1.2, 4.1.2, 5.2, 5.2, 6.3, A

[OT97] Makiko Okumura and Hiroshi Tanimoto. A time-domain method for numerical noise analysis of oscillators. In *Proceedings of the Asia South Pacific Design Automation Conference*, pages 477–82, January 1997. 2.3.1

[OTS91] Makiko Okumura, Hiroshi Tanimoto, and Tsutomu Sugawara. Noise analysis method for nonlinear circuits with two frequency excitations using the computer. *Electronics and Communications in Japan Part 3*, 74(4):41–50, 1991. 2.2.1

[Pap91] Athanasios Papoulis. *Probability, Random Variables and Stochastic Processes*. McGraw Hill, third edition, 1991. 5.3

[Pat96] Andrew Patterson. Computer aided analysis of noise effects in GSM. *Electronic Engineering*, 68(838):53–54, 1996. 1.2

[Poo97] Rick Poore. Accurate simulation of mixer noise and oscillator phase noise in large RFICs. In *1997 Asia-Pacific Microwave Conference Proceedings APMC '97*, pages 357–360, 1997. 2.3.1

[Raz96] Behzad Razavi. A study of phase noise in CMOS oscillators. *IEEE Journal of Solid-State Circuits*, 31(3):331–43, March 1996. 2.3.1, 2.3.1

[RC95] Ulrich L Rohde and Chao-Ren Cheng. Analysis and optimization of oscillators for low phase noise and low power consumption. *RF Design*, 18(3):70–79, March 1995. 2.3.1

[RCMC94] Vittorio Rizzoli, Alessandra Costanzo, Franco Mastri, and Claudio Cecchetti. Harmonic-balance optimization of microwave oscillators for electrical performance, steady-state stability, and near-carrier phase noise. In *Proceedings of IEEE/MTT-S International Microwave Symposium*, pages 1401–4, May 1994. 2.3.1

[RFL98] Jaijeet S Roychowdhury, Peter Feldmann, and David E Long. Cyclostationary noise analysis of large RF circuits with multi-tone excitations. *IEEE Journal of Solid-State Circuits*, 33(3):324–36, March 1998. 2.2.1, 2.2.1, 4.5.2, 4.3, 4.5.2, 5.2, 5.6, 5.6.2, 5.6.2.1, 5.6.2.1, 5.6.2.2, 5.7

[Ris96] Hannes Risken. *The Fokker-Planck equation : methods of solution and applications*, volume 18 of *Springer series in synergetics*. Springer–Verlag, Berlin ; New York, second edition, 1996. 4.1

[RM92] Peter Russer and Stefan Müller. Noise analysis of microwave circuits with general topology. In *1992 IEEE MTT-S International Microwave Symposium Digest*, volume 3, pages 1481–1484, 1992. 2.2.1

[RMC89] Vittorio Rizzoli, Franco Mastri, and Claudio Cecchetti. Computer-aided noise analysis of MESFET and HEMT mixers. *IEEE Transactions on Microwave Theory and Techniques*, 37(9):1401–1410, September 1989. 2.2.1

[RMC98] Vittorio Rizzoli, Franco Mastri, and Claudio Cecchetti. Signal and noise analysis of large microwave front-ends by the inexact-newton harmonic-balance technique. In *1998 IEEE MTT-S International Microwave Symposium Digest*, volume 3, pages 1599–1602, 1998. 2.2.1

[RMM92a] Vittorio Rizzoli, Diego Masotti, and Franco Mastri. Advanced piecewise-harmonic-balance noise analysis of nonlinear microwave circuits with application to schottky-barrier diodes. In *1992 IEEE MTT-S International Microwave Symposium Digest*, pages 247–250, 1992. 2.2.1

[RMM92b] Vittorio Rizzoli, Diego Masotti, and Franco Mastri. General-purpose noise analysis of forced nonlinear microwave circuits. In *Conference Proceedings MM 92*, pages 293–298, 1992. 2.2.1

[RMM94a] Vittorio Rizzoli, Diego Masotti, and Franco Mastri. Full nonlinear noise analysis of microwave mixers. In *1994 IEEE MTT-S International Microwave Symposium Digest*, volume 2, pages 961–964, 1994. 2.2.1, 2.2.1

[RMM94b] Vittorio Rizzoli, Franco Mastri, and Diego Masotti. General noise analysis of nonlinear microwave circuits by the piecewise harmonic-balance techniques. *IEEE Transactions on Microwave Theory and Techniques*, 42:807–819, May 1994. 2.2.1, 2.2.1

[RMM95] Vittorio Rizzoli, Diego Masotti, and Franco Mastri. Computer-aided noise analysis of integrated microwave front-ends. In *1995 IEEE MTT-S International Microwave Symposium Digest*, volume 3, pages 1561–1564, 1995. 2.2.1

[RMMN92] Vittorio Rizzoli, Diego Masotti, Franco Mastri, and Andrea Neri. Noise analysis of a nonlinear microwave circuit driven by a noise sinusoidal source. *Microwave and Optical Technology Letters*, 5(10):534–537, September 1992. 2.2.1

[RMMN93] Vittorio Rizzoli, Diego Masotti, Franco Mastri, and Andrea Neri. Full nonlinear analysis of near-carrier noise in discriminator-stabilized microwave oscillators. *Microwave and Optical Technology Letters*, 6(16):907–911, 1993. 2.3.1

[Rob82] William P Robins. *Phase noise in signal sources : theory and applications*,

volume 9 of *IEE telecommunications series*. Peter Peregrinus on behalf of the Institution of Electrical Engineers, London, 1982. 1.2.2, 2.3.1

[ROC+97] Jacques C Rudell, Jia-Jiunn Ou, Thomas B Cho, George Chien, Francesco Brianit, Jeffrey A Weldon, and Paul R Gray. A 1.9-GHz wide-band IF double conversion CMOS receiver for cordless telephone applications. *IEEE Journal of Solid-State Circuits*, 32(12):2071–2088, December 1997. 1.1

[RON+98] Jacques C Rudell, Jia-Jiunn Ou, R Sekhar Narayanaswami, George Chien, Jeffrey A Weldon, Li Lin, King-Chun Tsai, Luns Tee, Kelvin Khoo, Danelle Au, Troy Robinson, Danilo Gerna, Masanori Otsuka, and Paul R Gray. Recent developments in high integration multi-standard CMOS transceivers for personal communication systems. In *Proceedings 1998 International Symposium on Low Power Electronics and Design*, pages 149–154, 1998. 1.1

[Roy97] Jaijeet S Roychowdhury. Efficient methods for simulating highly nonlinear multi-rate circuits. In *Proceedings of the 34th Design Automation Conference*, pages 269–274, 1997. 6.2, 6.3, 6.3, 6.1, 1, 1, 1, 2, 6.4

[RPP88] Ulrich L Rohde, Anthony M Pavio, and Robert A Pucel. Accurate noise simulation of microwave amplifiers using CAD. *Microwave Journal*, 31(12):130–141, December 1988. 2.2.1

[Sau77] Gérard Sauvage. Phase noise in oscillators: a mathematical analysis of Leeson's model. *IEEE Transactions on Instrumentation and Measurement*, IM-26(4):408–410, December 1977. 2.3.1

[SD98] Oliver Schein and Georg Denk. Numerical solution of stochastic differential-algebraic equations with applications to transient noise simulation of microelectronic circuits. *Journal of Computational and Applied Mathematics*, 100(1):77–92, 1998. 2.2.2

[Sjö72] Anders Sjölund. Analysis of large-signal noise in Read oscillators. *Solid-State Electronics*, 15(9):971–978, September 1972. 2.3.1

[SS85] Heinz J Siweris and Burkhard Schiek. Analysis of noise upconversion in mi-

crowave FET oscillators. *IEEE Transactions on Microwave Theory and Techniques*, MTT-33(3):233–242, March 1985. 2.3.1

[Swe72] Allen A Sweet. A general analysis of noise in Gunn oscillators. *Proceedings of the IEEE*, 60(8):999–1000, August 1972. 2.3.1

[TKW96] Ricardo Telichevesky, Kenneth S Kundert, and Jacob K White. Efficient AC and noise analysis for two-tone RF circuits. In *Proceedings of the 33rd Design Automation Conference*, pages 292–297, 1996. 2.2.1, 5.2, 5.6, 5.6.1

[Tom98] Luciano Tomba. Analysis of the effect of phase noise in OFDM systems. *European Transactions on Telecommunications*, 9(3):279–287, 1998. 1.2.2

[vdP22] Balthasar van der Pol. On oscillation hysteresis in a simple triode generator. *Philosophical Magazine*, 43:177–193, 1922. 3.4

[VLPG96] Jacques Verdier, Olivier Llopis, Robert Plana, and Jacques Graffeuil. Analysis of noise upconversion in microwave field-effect transistor oscillators. *IEEE Transactions on Microwave Theory and Techniques*, 44(8):1478–1483, August 1996. 2.3.1

[VV83] Vincent C Vannicola and Pramod K Varshney. Spectral dispersion of modulated signals due to oscillator phase instability: White and random walk phase model. *IEEE Transactions on Communications*, COM-31(7):886–895, July 1983. 1.2.2, 2.3.4

[Wei93] Guo Wei. Flicker noise process analysis. In *Proceedings of the 1993 IEEE International Frequency Control Symposium*, pages 321–325, 1993. 1.2.1

[WKG94] Todd C Weigandt, Beomsup Kim, and Paul R Gray. Analysis of timing jitter in CMOS ring oscillators. In *Proceedings of IEEE International Symposium on Circuits and Systems*, pages 27–30, 1994. 2.3.2, 4.6.3, 4.6.3, 4.6.3, 4.6.3

[YL97] Jiang Yilin and Xiao Lizhi. Analysis on phase noise for phase-lock radar frequency synthesizer. In *1997 IEEE International Conference on Intelligent Processing Systems*, volume 1, pages 28–31, 1997. 2.3.1

[Zei98] Ofer Zeitouni. personal communication, 1998. 7.3

Appendix A

Definitions and Solution Techniques of SDEs

Here we summarize the mathematical machinery we needed in Chapter 5. This material is from [Øks98].

A.1 Mathematical Preliminaries

Definition A.1 *If Ω is a given set, then a σ-algebra $\mathcal{F}$ on Ω is a family $\mathcal{F}$ of the subsets of Ω with the following properties*

1. $\emptyset \in \mathcal{F}$
2. $F \in \mathcal{F} \Rightarrow F^C \in \mathcal{F}$, *where* $F^C = \Omega \setminus F$ *is the complement of* F *in* Ω
3. $A_1, A_2, \ldots \in \mathcal{F} \Rightarrow A = \bigcup_{i=1}^{\infty} A_i \in \mathcal{F}$

The pair $(\Omega, \mathcal{F})$ is called a measurable space. *A* probability measure $\mathbb{P}$ *on a measurable space $(\Omega, \mathcal{F})$ is a function $\mathbb{P} : \mathcal{F} \to [0,1]$ such that*

1. $\mathbb{P}[\emptyset] = 0$, $\mathbb{P}[\Omega] = 1$
2. *if $A_1, A_2, \ldots \in \mathcal{F}$ and $\{A_i\}_{i=1}^{\infty}$ is disjoint then*

$$\mathbb{P}\left[\bigcup_{i=1}^{\infty} A_i\right] = \sum_{i=1}^{\infty} \mathbb{P}[A_i]$$

The triple $(\Omega, \mathcal{F}, \mathbb{P})$ *is called the* probability space.

The subsets F of Ω which belong to $\mathcal{F}$ are called $\mathcal{F}$*-measurable* sets. In a probability context these sets are called *events* and we use the interpretation

$$\mathbb{P}[F] = \text{“the probability that the event } F \text{ occurs”}$$

In particular, if $\mathbb{P}[F] = 1$ we say that F occurs with probability 1, or almost surely (a.s.).

Given any family $\mathcal{U}$ of subsets of Ω there is a smallest σ-algebra $\mathcal{H}_{\mathcal{U}}$ containing $\mathcal{U}$ namely

$$\mathcal{H}_{\mathcal{U}} = \bigcap \{\mathcal{H} : \mathcal{H} \ \sigma\text{-algebra of } \Omega, \ \mathcal{U} \in \mathcal{H}\}$$

$\mathcal{H}_{\mathcal{U}}$ is called the σ-algebra generated by $\mathcal{U}$.

For instance, if $\mathcal{U}$ is the collection of all open subsets of a topological space Ω (e.g. $\Omega = \mathbb{R}^n$), then $\mathcal{B} = \mathcal{H}_{\mathcal{U}}$ is called the *Borel* σ*-algebra* on Ω and the elements $B \in \mathcal{B}$ are called *Borel sets*. $\mathcal{B}$ contains all open sets, all closed sets, all countable unions of closed sets, all countable intersections of such countable unions etc.

If $(\Omega, \mathcal{F}, \mathbb{P})$ is a given probability space, then a function $Y : \Omega \to \mathbb{R}^n$ is called $\mathcal{F}$-measurable if

$$Y^{-1}(U) = \{\omega \in \Omega : Y(\omega) \in U\} \in \mathcal{F}$$

for all open sets $U \in \mathbb{R}^n$ (or, equivalently, for all Borel sets $U \subset \mathbb{R}^n$).

If $X : \Omega \to \mathbb{R}^n$ is any function, then *the* σ*-algebra* $\mathcal{H}_X$ *generated by* X is the smallest σ-algebra on Ω containing all the sets

$$X^{-1}(U) \quad U \subset \mathbb{R}^n \quad \text{open}$$

It can be shown that

$$\mathcal{H}_X = \{X^{-1}(B) : B \in \mathcal{B}\}$$

where $\mathcal{B}$ is the Borel σ-algebra on $\mathbb{R}^n$. Clearly X will then be $\mathcal{H}_X$-measurable and $\mathcal{H}_X$ is the smallest σ-algebra with this property.

A.2 Itô Integrals

The following integral is defined as the Itô integral

$$\int_S^T f(t,\omega)\mathrm{d}B_t(\omega)$$

where $B_t(\omega)$ is a 1-dimensional Brownian motion. We need the following definitions to describe the class of function $f(t,\omega)$ for which the Itô integral will be defined.

Definition A.2 *Let $B_t(\omega)$ be an n-dimensional Brownian motion. Then $\mathcal{F}_t = \mathcal{F}_t^{(n)}$ is defined to be the σ-algebra generated by the random variables $B_s(\cdot)$, $s \leq t$. In other words, $\mathcal{F}_t$ is the smallest σ-algebra containing all sets of the form*

$$\{\omega : B_{t_1}(\omega) \in F_1, \ldots, B_{t_k}(\omega) \in F_k\}$$

where $k = 1, 2 \ldots$, $t_j > 0$ and $F_j \subset \mathbb{R}^n$ are Borel sets. (All sets of measure zero are assumed to be included in $\mathcal{F}_t$.)

Definition A.3 *Let $\{\mathcal{N}_t\}_{t\geq 0}$ be a nondecreasing family of σ-algebras of subsets of Ω. A process $g(t,\omega) : \mathbb{R}_+ \times \Omega \to \mathbb{R}^n$ is called $\mathcal{N}_t$-adapted if for each $t \geq 0$ the function*

$$\omega \to g(t,\omega)$$

is $\mathcal{N}_t$-measurable.

Itô integral can be defined for the following class of functions:

Definition A.4 *Let $\mathcal{V} = \mathcal{V}(S,T)$ be the class of functions*

$$f(t,\omega) : \mathbb{R}_+ \times \Omega \to \mathbb{R}$$

such that

1. *$(t,\omega) \to f(t,\omega)$ is $\mathcal{B} \times \mathcal{F}$-measurable where $\mathcal{B}$ denotes the Borel σ-algebra on $\mathbb{R}_+$*
2. *$f(t,\omega)$ is $\mathcal{F}_t$ adapted*
3. *$\mathbb{E}\left[\int_S^T f(t,\omega)^2\mathrm{d}t\right] < \infty$*

Definition A.5 *A functions $\phi \in \mathcal{V}$ is called* elementary *if it has the form*

$$\phi(t,\omega) = \sum_j e_j(\omega)\mathcal{X}_{[t_j,t_{j+1})}(t) \tag{A.1}$$

where $\mathcal{X}$ denotes the characteristic (indicator) function.

Since $\phi \in \mathcal{V}$ each function e_j must be $\mathcal{F}_t$-measurable.

Definition A.6 (The Itô integral) *Let $f \in \mathcal{V}(S,t)$. Then the Itô integral of f (from S to T) is defined by*

$$\int_S^T f(t,\omega)\mathrm{d}B_t(\omega) = \lim_{n\to\infty}\int_S^T \phi_n(t,\omega)\mathrm{d}B_t(\omega) \quad (\textit{limit in } L^2(P)) \tag{A.2}$$

where $\{\phi_n\}$ is a sequence of elementary functions such that

$$\mathbb{E}\left[\int_S^T (f(t,\omega)-\phi_n(t,\omega))^2\mathrm{d}t\right] \to 0 \quad \textit{as } n\to\infty \tag{A.3}$$

An important property of the Itô integral is that it is a *martingale*.

Definition A.7 *A* filtration *(on $(\Omega,\mathcal{F})$) is a family $\{\mathcal{M}_t\}_{t\geq 0}$ of σ-algebras $\mathcal{M}_t \subset \mathcal{F}$ such that*

$$0 \leq s < t \Rightarrow \mathcal{M}_s \subset \mathcal{M}_t$$

(i.e., $\{\mathcal{M}_t\}$ is increasing). An n-dimensional stochastic process $\{M_t\}_{t\geq 0}$ on $(\Omega,\mathcal{F},\mathbb{P})$ is called a martingale *with respect to a filtration $\{\mathcal{M}_t\}_{t\geq 0}$ (and with respect to P^0) if*

1. *M_t is $\mathcal{M}_t$-measurable for all t*
2. *$\mathbb{E}[|M_t|] < \infty$ for all t*
3. *$\mathbb{E}[M_s|\mathcal{M}_t] = M_t$ for all $s \geq t$*

Here the expectation and the conditional expectation are taken with respect to P^0.

For continuous martingales we have the following important inequality due to Doob:

Theorem A.1 (Doob's martingale inequality) *If M_t is a martingale such that $t \to M_t(\omega)$ is continuous a.s., then for all $p \geq 1$, $T \geq 0$ and all $\lambda > 0$*

$$\mathbb{P}\left[\sup_{0\leq t\leq T}|M_t| \geq \lambda\right] \leq \frac{1}{\lambda^p}\mathbb{E}\left[|M_T|^p\right]$$

This inequality can be used to prove that the Itô integral

$$\int_0^t f(s,\omega)\mathrm{d}B_s$$

can be chosen to depend continuously on t.

Theorem A.2 *Let $f \in (0,T)$. Then there exists a t-*continuous version *of*

$$\int_0^t f(s,\omega)\mathrm{d}B_s(\omega) \quad 0 \le t \le T$$

i.e., there exists a t-continuous stochastic process J_t on $(\Omega, \mathcal{F}, \mathbb{P})$ such that

$$\mathbb{P}\left[J_t = \int_0^t f(s,\omega)\mathrm{d}B_s(\omega)\right] = 1 \quad \forall t \quad 0 \le t \le T \tag{A.4}$$

Corollary A.3 *Let $f(s,\omega) \in \mathcal{V}(0,T)$ for all T. Then*

$$M_t(\omega) = \int_0^t f(s,\omega)\mathrm{d}B_s$$

is a martingale with respect to $\mathcal{F}_t$ and

$$\mathbb{P}\left[\sup_{0\le t\le T}|M_t| > \lambda\right] \le \frac{1}{\lambda^2}\mathbb{E}\left[\int_0^T f(s,\omega)^2\mathrm{d}s\right] \quad \lambda, T > 0 \tag{A.5}$$

The Itô integral $\int f\mathrm{d}B$ can be defined for a larger class of integrands f than $\mathcal{V}$. First, the measurability condition (2) of Definition A.4 can be relaxed to the following:

2': There exists an increasing family of σ-algebras $\mathcal{H}_t$ $t \ge 0$ such that

1. B_t is a martingale with respect to $\mathcal{H}_t$
2. f_t is $\mathcal{H}_t$-adapted

Condition 1 implies that $\mathcal{F}_t \subset \mathcal{H}_t$. The essence of this extension is that we can allow f_t to depend on more than $\mathcal{F}_t$ as long as the B_t remains a martingale with respect to the "history" of f_s $s \le t$. If the above conditions hold then $\mathbb{E}\left[B_s - B_t|\mathcal{H}_t\right] = 0$ for all $s > t$ and this is sufficient to carry out the construction of Itô integral.

Condition (3) of Definition A.4 can also be weakened to

$$3' \qquad \mathbb{P}\left[\int_0^t f(s,\omega)^2\mathrm{d}s < \infty \text{ for all } t \ge 0\right] = 1$$

Definition A.8 *$\mathcal{W}$ denotes a class of stochastic processes satisfying 1 of Definition A.4 and 2' and 3' above.*

A.3 Stochastic Differential Equations

Theorem A.4 (Existence and uniqueness theorem) *Let $T > 0$ and $b(\cdot,\cdot) : [0,T] \times \mathbb{R}^n \to \mathbb{R}^n$, $\sigma(\cdot,\cdot) : [0,T] \times \mathbb{R}^n \to \mathbb{R}^{n\times m}$ be measurable functions satisfying*

$$|b(t,x)| + |\sigma(t,x)| \leq C(1+|x|) \quad x \in \mathbb{R}^n \quad t \in [0,T] \tag{A.6}$$

for some constant C, where $|\sigma|^2 = \sum |\sigma_{ij}|^2$ and such that

$$|b(t,x) - b(t,y)| + |\sigma(t,x) - \sigma(t,y)| \leq D|x-y| \quad x,y \in \mathbb{R}^n \quad t \in [0,T] \tag{A.7}$$

for some constant D. Let Z be a random variation which is independent of the σ-algebra $\mathcal{F}_\infty$ generated by $B_s(\cdot)$, $s \geq 0$ and such that

$$\mathbb{E}\left[|Z|^2\right] < \infty \tag{A.8}$$

Then the stochastic differential equation

$$\mathrm{d}X_t = b(t,X_t)\mathrm{d}t + \sigma(t,X_t)\mathrm{d}B_t \quad 0 \leq t \leq T \quad X_0 = Z \tag{A.9}$$

has a unique t-continuous solution $X_t(\omega)$ each component of which belongs to $\mathcal{V}[0,T]$.

Remark A.1 *Conditions (A.6) and (A.7) are natural in view of the following two simple examples from deterministic differential equations (i.e., $\sigma = 0$):*

1. *The equation*

$$\frac{\mathrm{d}X_t}{\mathrm{d}t} = X_t^2 \quad X_0 = 1 \tag{A.10}$$

corresponding to $b(x) = x^2$ (which does not satisfy (A.6)) has the (unique) solution

$$X_t = \frac{1}{1-t} \quad 0 \leq t < 1$$

Thus it is impossible to find a global solution (defined for all t) in this case. More generally, condition (A.6) ensures that the solution $X_t(\omega)$ does not explode, *i.e., that $|X(\omega)|$ does not tend to ∞ in a finite time.*

2. *The equation*

$$\frac{\mathrm{d}X_t}{\mathrm{d}t} = 3X_t^{2/3} \quad X(0) = 0 \tag{A.11}$$

has more than one solution. In fact for any $a > 0$ *the function*

$$X_t = \begin{cases} 0 & t \leq a \\ (t-a)^3 & t > a \end{cases}$$

solves (A.11). In this case $b(x) = 3x^{2/3}$ *does not satisfy the Lipschitz condition (A.7) at* $x = 0$.

Thus condition (A.7) guarantees that equation (A.9) has a unique *solution. Here uniqueness means that if* $X_1(t,\omega)$ *and* $X_2(t,\omega)$ *are two* t*-continuous processes in* $\mathcal{V}[0,T]$ *satisfying (A.9) then*

$$X_1(t,\omega) = X_2(t,\omega) \text{ for all } t \geq T \text{ a.s.} \tag{A.12}$$

Index

σ-algebra, 92, 156
MATLAB, 74
SPICE, 74

additive noise, 88
amplitude deviation, 32, 36
amplitude noise, 50, 88, 98
asymptotic phase property, 21

Backward Euler method, 102
bit error rate, 6
block Toeplitz matrix, 76
blocker signal, 6, 114
Boltzmann's constant, 7
Borel σ-algebra, 157
Borel set, 157
Brownian motion, 56, 89, 95, 116, 158

characteristic multiplier, 44
cyclostationary process, 90, 95, 98

downconversion, 3

elementary function, 159
emitter-coupled multivibrator, 85
existence and uniqueness theorem
    Picard-Lindelőf, 20

flicker noise, 7
Floquet eigenvector, 27
Floquet theory, 23
Fokker-Planck equation, 52, 57, 90
forced oscillator circuit, 89
Fourier transform, 54

Gaussian process, 52, 65, 66
Gaussian random variable, 52, 59

harmonic balance, 75
    conversion matrix, 75, 106
harmonic impulse response, 75, 106
harmonic power spectral density, 75, 105

image frequency, 114
image reject mixer, 114
image-reject filter, 3
indicator function, 159
infrared system, 1
inverse Fourier transform, 54
Itô formula, 93
Itô integral, 158, 160
    martingale property of, 56, 159
Itô process, 92, 93

jammer signal, 114

Kramers-Moyal expansion, 52
    coefficient, 53

Lindstedt-Poincaré method, 37

linear analysis
time invariant, 67
time-varying, 67
Lipschitz condition, 162
Lorentzian spectrum, 64, 67, 81, 100, 118
low noise amplifier, 3
LPTV system of equations, 23, 88, 91, 101
characteristic multipliers, 24
Floquet exponents, 24, 74
fundamental matrix of, 23
principal, 23
state transition matrix, 23
LPTV transfer function, 75

martingale, 92, 159
measurable space, 156
memoryless nonlinearity, 115, 116
mixed differential-algebraic equation, 19, 89
modified nodal analysis, 89
Monte Carlo noise simulation, 83
multitone excitation, 116

noise, 2
coupling, 6
intrinsic, 7
noise analysis, 2
noise source figure of merit, 72
nonautonomous circuit, 88, 89, 116

orbital deviation, 32
orbital stability, 20
asymptotic, 20, 34, 45, 46, 77
oscillator
Colpitt's, 81
generic, 79
LC tank, 79, 81
relaxation, 79, 85
ring, 79, 83
van der Pol, 37
forced, 40, 42
voltage controlled, 85
oscillator perturbation analysis
linear, 19, 22
nonlinear, 30
oscillator phase noise
analysis
frequency domain, 75
time-domain, 73
spectrum, 64
dBc/Hz, 70
dBm/Hz, 70

perfect time reference, 68
periodic steady-state solution, 101
phase deviation, 31
phase lock loop, 3
phase noise, 50, 88
phase noise/timing jitter sensitivity, 72
Picard-Lindelőf Theorem, 23
power amplifier, 3
probability density function, 51
characteristic function, 53, 58
moments, 53
probability measure, 51, 156
probability space, 92, 157

quasi-periodic, 114

radio frequency system, 1
RF front end, 3
Riemann-Stieljes, 56

shooting method, 73, 74
shot noise, 7
signal to noise ratio, 6
singular matrix, 78
    null space of, 78
state transition matrix, 26, 73
stochastic differential equation, 14, 51, 90, 116, 129
    existence & uniqueness theorem, 161
stochastic integral, 56
    Itô's interpretation of, 56, 61, 64
    Stratonovich's interpretation of, 56
stochastic process, 7, 51
    autocorrelation, 7, 117
      cyclostationary component, 67
      stationary component, 67
    autocorrelation function, 64
    characteristic function, 66
    cumulant generating function, 64
    cumulants of, 64
    cyclostationary, 68
    ensemble, 51
    finite-dimensional distribution, 51
    power spectral density, 7
    sample path, 51
    stationary
      power spectral density, 64, 70
    wide-sense stationary, 7
substrate coupling, 6

thermal noise, 7
timing jitter, 71
    cycle-to-cycle, 72
Tow-Thomas filter, 79
transient simulation, 73

white noise, 7, 55
wide-sense stationary process, 67, 95, 97, 98
Wiener process, 59

zero-crossing, 71